

กลไกการตกผลึกและการตกตะกอน ไทเทเนียมออกไซด์ ภายใต้สภาวะโซลโวเทอร์มอล และผลของธาตุตัวที่สอง
บนผลิตภัณฑ์ไทเทเนียมออกไซด์



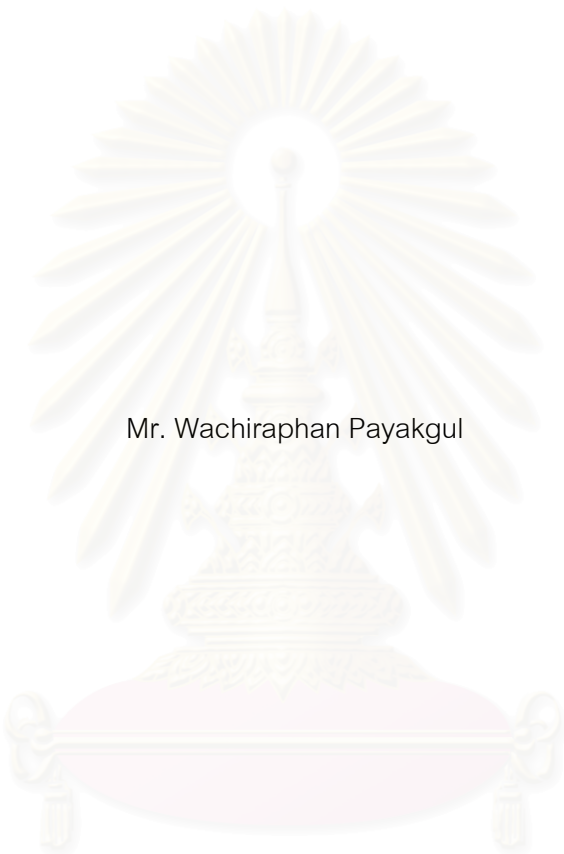
นายวชิรพันธ์ พยัคฆ์กุล

วิทยานิพนธ์นี้เป็นส่วนหนึ่งของการศึกษาตามหลักสูตรปริญญาวิศวกรรมศาสตรมหาบัณฑิต
สาขาวิชาวิศวกรรมเคมี ภาควิชาวิศวกรรมเคมี
คณะวิศวกรรมศาสตร์ จุฬาลงกรณ์มหาวิทยาลัย
ปีการศึกษา 2545

ISBN 974-17-2659-7

ลิขสิทธิ์ของจุฬาลงกรณ์มหาวิทยาลัย

CRYSTALLIZATION AND PRECIPITATION MECHANISM OF TITANIUM (IV)
OXIDE UNDER THE SOLVOTHERMAL CONDITION AND THE EFFECT OF
SECOND ELEMENT ON TITANIUM (IV) OXIDE PRODUCTS



Mr. Wachiraphan Payakgul

A Thesis Submitted in Partial Fulfillment of the Requirements
for the Degree of Master of Engineering in Chemical Engineering

Department of Chemical Engineering

Faculty of Engineering

Chulalongkorn University

Academic Year 2002

ISBN 974-17-2659-7

Thesis Title CRYSTALLIZATION AND PRECIPITATION MECHANISM
 OF TITANIUM (IV) OXIDE UNDER THE SOLVOTHERMAL
 CONDITION AND THE EFFECT OF SECOND ELEMENT
 ON TITANIUM (IV) OXIDE PRODUCTS

By Mr. Wachiraphan Payakgul

Field of Study Chemical Engineering

Thesis Advisor Professor Piyasan Praserthdam, Dr.Ing.

Thesis Co-advisor Dr. Waraporn Tanakulrungsank, D.Eng.

Accepted by the Faculty of Engineering, Chulalongkorn University in Partial
Fulfillment of the Requirements for the Master's Degree

..... Dean of Faculty of Engineering
(Professor Somsak Panyakeow, D.Eng.)

THESIS COMMITTEE

..... Chairman
(Associate Professor Ura Pancharoen, D.Eng.Sc.)

..... Thesis Advisor
(Professor Piyasan Praserthdam, Dr.Ing.)

..... Thesis Co-advisor
(Waraporn Tanakulrungsank, D.Eng.)

..... Member
(Associate Professor Paisan Kittisupakorn, Ph.D.)

..... Member
(Varong Pavarajarn, Ph.D.)

วชิรพันธ์ พัทย์ภักดิ์: กลไกการตกผลึกและการตกตะกอนของไทเทเนียมออกไซด์ ภายใต้สภาวะโซลโวเทอร์มอล และผลของธาตุตัวที่สองบนผลิตภัณฑ์ไทเทเนียมออกไซด์ (CRYSTALLIZATION AND PRECIPITATION MECHANISM OF TITANIUM (IV) OXIDE UNDER THE SOLVOTHERMAL CONDITION AND THE EFFECT OF SECOND ELEMENT ON TITANIUM (IV) OXIDE PRODUCTS) อ. ที่ปรึกษา: ศ.ดร.ปิยะสาร ประเสริฐธรรม, อ. ที่ปรึกษาร่วม: อ.ดร.วราภรณ์ ณะกุลรังสรรค์, 145หน้า, ISBN 974-17-2659-7

การศึกษากลไกการตกผลึกและตกตะกอนของไทเทเนียมออกไซด์ บนปฏิกิริยาโซลโวเทอร์มอลในตัวกลางอินทรีย์คือ 1,4 บิวเทนไดออล หรือ โทลูอิน ที่ 300 องศาเซลเซียส ภายใต้ความดันที่เกิดขึ้นเอง จะทำให้ผลึกแอนาเทสไทเทเนียมออกไซด์ ที่มีขนาดในระดับนาโนเมตร คุณสมบัติทางกายภาพและความเสถียรทางความร้อนจะขึ้นกับกลไกการเตรียม ไทเทเนียมออกไซด์ที่ทำการสังเคราะห์ โดยใช้ 1,4 บิวเทนไดออล จะให้ผลึกแอนาเทสซึ่งเกิดจากกลไกการตกผลึก ในขณะที่เดียวกัน ไทเทเนียมออกไซด์ที่เตรียมจากการสังเคราะห์โดยใช้สารละลายโทลูอินจะให้ผลิตภัณฑ์เป็นอัญฐานจากกลไกการตกตะกอน และเกิดเป็นผลึกแอนาเทสเมื่อทำการเปลี่ยนแปลงเวลาในการทำปฏิกิริยา ในการเตรียมจากสารละลายทั้งสองชนิด ขนาดผลึกจะมีขนาดเพิ่มขึ้นเมื่อเวลาการทำปฏิกิริยาเพิ่มขึ้น ไทเทเนียมออกไซด์ที่เตรียมขึ้นในสารละลายโทลูอิน จะมีพื้นที่ผิวสูงกว่าไทเทเนียมออกไซด์ที่สังเคราะห์จาก 1,4 บิวเทนไดออล ที่ขนาดผลึกเท่ากัน อย่างไรก็ตาม ไทเทเนียมออกไซด์ที่สังเคราะห์ใน 1,4 บิวเทนไดออล จะมีความเสถียรทางความร้อนสูง การเติมธาตุตัวที่สอง เช่น ซิลิกอน อลูมิเนียม หรือ ฟอสฟอรัส ในสารตั้งต้น จะเพิ่มความเสถียรทางความร้อน ขนาดผลึกของไทเทเนียมที่ถูกปรับปรุง จะมีขนาดเล็กกว่าไทเทเนียมที่ไม่ได้ปรับปรุง นอกจากนี้ โครงร่างของไทเทเนียมที่ถูกปรับปรุงจะขึ้นกับธาตุตัวที่สองที่ถูกเติมไปในสารตั้งต้น

ภาควิชา...วิศวกรรมเคมี..... ลายมือชื่อนิสิต.....
สาขาวิชา...วิศวกรรมเคมี..... ลายมือชื่ออาจารย์ที่ปรึกษา.....
ปีการศึกษา...2545..... ลายมือชื่ออาจารย์ที่ปรึกษาร่วม.....

จุฬาลงกรณ์มหาวิทยาลัย

##4470501021: MAJOR CHEMICAL ENGINEERING

KEY WORD: TITANIA / TITANIUM (IV) OXIDE / GLYCOTHERMAL / SOLVOTHERMAL /

SILICON-MODIFIED TITANIA / ALUMINIUM MODIFIED TITANIA / PHOSPHOROUS

MODIFIED TITANIA

WACHIRAPHAN PAYAKGUL: CRYSTALLIZATION AND PRECIPITATION MECHANISM OF TITANIUM (IV) OXIDE UNDER THE SOLVOTHERMAL CONDITION AND THE EFFECT OF SECOND ELEMENT ON TITANIUM (IV) OXIDE PRODUCTS. THESIS ADVISOR: PROFESSOR PIYASAN PRASERTHDAM, Dr.Ing, THESIS CO-ADVISOR: WARAPORN TANAKULRUNGSANK, D.Eng. 145 pp. ISBN 974-17-2659-7

The crystallization and precipitation mechanism of titanium (IV) oxide on the solvothermal reaction in organic media (1,4 butanediol, toluene) at 300°C under autogenous pressure was studied to yielded a nanocrystallite anatase titanium (IV) oxide. The physical properties and thermal stability of titanium (IV) oxide depended on the preparation mechanism. Titanium (IV) oxide synthesized in 1,4 butandiol yielded the anatase crystal due to the crystallization mechanism. On the other hand, titanium (IV) oxide synthesized in toluene yielded the amorphous phase due to the precipitation mechanism and transformed to anatase crystal with increasing the reaction time. For varying the reaction time, the crystallite size increases with an increasing the reaction time in both solvents. Titanium (IV) oxide synthesized in toluene showed a higher specific surface area than that synthesized in 1,4 butanediol with the same crystallite size. However, titanium (IV) oxide synthesized in 1,4 butanediol had a good thermal stability. Doping a second element, such as silicon, aluminium, phosphorous, in the starting material could improve the thermal stability. The crystallite size of modified titanium (IV) oxides were smaller than that of a pure titanium (IV) oxide. In addition, morphology of the modified titania depended on the doped second element.

Department...Chemical Engineering..... Student's signature.....

Field of study...Chemical Engineering.... Advisor's signature.....

Academic year...2002..... Co-Advisor's signature.....

ACKNOWLEDGEMENTS

The author would like to express his greatest gratitude to his advisor, Professor Dr. Piyasan Prasertthdam, for his invaluable guidance throughout this study. Special thanks to Dr. Waraporn Tanakulrungsank, his co-advisor, for her kind supervision this thesis. In addition, I would also grateful to thank to Associate Professor Dr. Ura Panchareon, as the chairman, Associate Professor Dr. Paisan Kittisupakorn and Dr. Varong Pavarajarn, members of the thesis committee for their kind cooperation.

Many thanks for kind suggestions and useful help to Dr. Choowong Chaisuk, Mr. Okorn Mekasuvandamrong, Miss Sirarat Kongwudthiti and many friends in the Research Center on Catalysis and Catalytic Reaction Engineering who always provide the encouragement and co-operate along the thesis study.

Finally, he also would like to dedicate this thesis to his parents who have always been the source of his support and encouragement.



สถาบันวิทยบริการ
จุฬาลงกรณ์มหาวิทยาลัย

CONTENTS

	Page
ABSTRACT (THAI).....	iv
ABSTRACT (ENGLISH).....	v
ACKNOWLEDGEMENT.....	vi
CONTENTS.....	vii
LIST OF TABLES.....	x
LIST OF FIGURES.....	xii
CHAPTER	
I INTRODUCTION.....	1
II LITERATURE REVIEWS.....	6
III THEORY.....	16
3.1 Titanium (Ti).....	16
Thermochemical data.....	16
3.2 Titanium (IV) oxide.....	17
Physical and chemical properties.....	17
3.3 Preparation procedure.....	21
3.3.1 Chemical vapor deposition (CVD) method.....	21
3.3.2 Chloride process.....	22
3.3.3 Precipitation method.....	23
3.3.4 Sol-gel method.....	23
3.3.5 Hydrothermal method.....	24
3.3.6 Glycothermal and solvothermal method.....	26
3.4 Single crystal.....	27
3.4.1 Growth techniques.....	27
3.4.2 Physical properties.....	27
IV EXPERIMENTAL.....	29
4.1 Chemicals.....	29
4.2 Equipment.....	30
4.2.1 Autoclave reactor.....	30
4.2.2 Temperature program controller.....	30

CONTENTS (cont.)

	Page
4.2.3 Electrical furnace (Heater).....	31
4.2.4 Gas controlling system.....	31
4.3 Preparation of titania.....	32
4.4 Characterization.....	33
4.4.1 X-ray diffraction spectroscopy (XRD).....	33
4.4.2 Scanning electron microscopy (SEM).....	33
4.4.3 Surface area measurement.....	34
4.4.5 Infrared Spectroscopy (IR).....	34
4.4.6 Thermogravimetric analysis (TGA).....	34
V RESULTS AND DISSCUSSION.....	35
5.1 Formation of Titanium (IV) oxide.....	35
5.1.1 Synthesis in 1,4-butanediol.....	35
5.1.1.1 The effect of reaction time.....	36
5.1.1.2 Effect of the starting material concentration	44
5.1.2 Synthesis in toluene.....	52
5.1.2.1 Effect of reaction time.....	52
5.1.2.2 Effect of reactant concentration.....	61
5.1.3 Comparison of titania products synthesized in both solvents.....	68
5.2 Effect of second element.....	72
5.2.1 Effect of silica on titania product.....	72
5.2.2 Effect of alumina on titania product.....	91
5.2.3 Effect of phosphorous on titania product.....	110
VI CONCLUSIONS AND RECOMMENDATION.....	131
6.1 Conclusions.....	131
6.2 Recommendation.....	131

CONTENTS (cont.)

	Page
REFERENCES.....	134
APPENDICES.....	139
APPENDIX A CALCULATION OF CATALYST PREPARATION.....	140
APPENDIX B CALCULATION OF THE CRYSTALLITE SIZE.....	141
APPENDIX C ISOTHERM PLOT OF NITROGEN	144
VITA.....	145



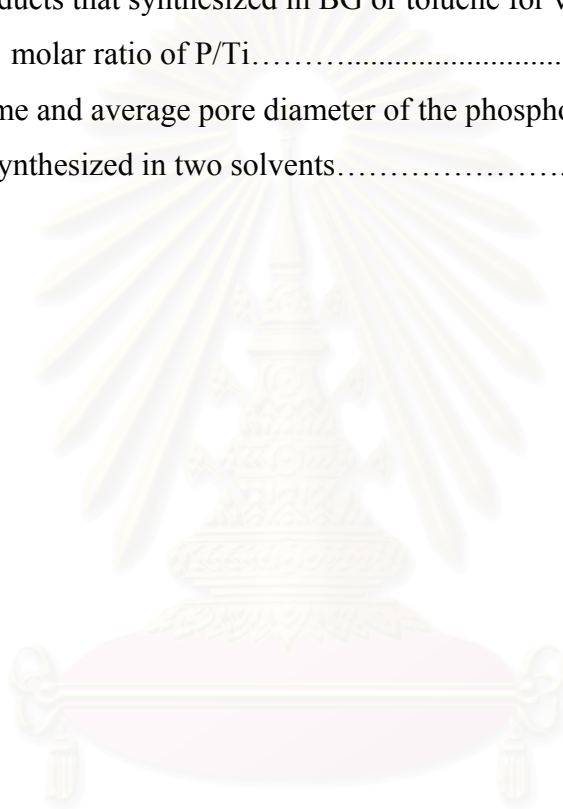
สถาบันวิทยบริการ
จุฬาลงกรณ์มหาวิทยาลัย

LIST OF TABLES

Table	Page
3.1 Thermal data for changes of state of titanium compounds.....	17
3.2 Thermochemical data for formation of titanium compounds.....	18
3.3 Crystallographic properties of anatase, brookite, and rutile.....	20
4.1 Reagents used for the synthesis of titania.....	29
4.1 (cont.) Reagents used for the synthesis of titania.....	30
5.1 Crystalline size and surface area of titania products synthesized in BG.....	39
5.2 Pore volume and average pore diameter of titania products synthesized in BG for various reaction time.....	40
5.3 Crystalline size and surface area of titania products synthesized for various reactant concentration.....	47
5.4 Pore volume and average pore diameter of titania products synthesized in BG for various concentrations.....	50
5.5 Crystalline size and surface area of titania products synthesized in toluene.....	55
5.6 Pore volume and average pore diameter of titania product synthesized in toluene.....	60
5.7 Crystalline size and surface area of titania products synthesized in toluene for various reactant concentration.....	61
5.8 Pore volume and average pore diameter of titania products synthesized in toluene for various concentrations.....	64
5.9 Dielectric constant of the two solvents.....	69
5.10 Crystalline size diameter and specific surface area of silicon modified titania product that synthesized in BG or toluene for various silicon content of molar ratio of Si/Ti.....	74
5.11 Pore volume and average pore diameter of the silica modified titania product synthesized in two solvents.....	82
5.12 Crystallite sizes diameter and specific surface areas of aluminium modified titania products that synthesized in BG or toluene for various aluminium contents of molar ratio of Al/Ti.....	94

LIST OF TABLES (cont.)

Table		Page
5.13	Pore volumes and average pore diameters of the aluminium modified titania products synthesized in two solvents.....	101
5.14	Crystallite size diameter and specific surface area of phosphorous modified titania products that synthesized in BG or toluene for various phosphorous content of molar ratio of P/Ti.....	113
5.15	Pore volume and average pore diameter of the phosphorous modified titania products synthesized in two solvents.....	120



สถาบันวิทยบริการ
จุฬาลงกรณ์มหาวิทยาลัย

LIST OF FIGURES

Figure	Page
2.1 Schematics of particle growth in the mixed solvent of alcohol and water.....	9
3.1 Crystal structure of TiO ₂	19
3.2 (a) Pressure-temperature relations for water at constant volume.....	26
3.2 (b) Schematic hydrothermal bomb used for crystal growth.....	26
4.1 Autoclave reactor.....	31
4.2 Diagram of the reaction equipment for the synthesis of titania.....	32
5.1 Mechanism of glycothermal reaction for the anatase formation.....	35
5.2 XRD patterns of titania product that synthesized in BG for various reaction time.....	37
5.3 SEM morphology of titania products synthesized in BG for various reaction times.....	38
5.4 Nitrogen adsorption-desorption isotherm of titania products synthesized in BG for various reaction times and crystallite sizes.....	41
5.4 (cont.) Nitrogen adsorption-desorption isotherm of titania products synthesized in BG for various reaction times and crystallite sizes.....	42
5.4 (cont.) Nitrogen adsorption-desorption isotherm of titania products synthesized in BG for various reaction times and crystallite sizes.....	43
5.5 Pore size distribution of titania products synthesized in BG for various reaction times.....	44
5.6 XRD pattern of titania products synthesized in BG for various concentrations of starting material.....	45
5.7 SEM image of titania product synthesized in BG for various concentrations of starting material.....	46
5.8 Nitrogen adsorption-desorption isotherm of titania products synthesized in BG for various concentrations of starting material and crystallite sizes.....	48

LIST OF FIGURES (cont.)

Figure	Page
5.8 (cont.) Nitrogen adsorption-desorption isotherm of titania products synthesized in BG for various concentrations of starting material and crystallite size.....	49
5.9 Pore size distribution of titania products synthesized in BG for various concentrations.....	51
5.10 Mechanism of reaction in toluene for the titania product.....	52
5.11 XRD patterns of titania products synthesized in toluene for various reaction times.....	53
5.12 SEM morphology of titania products synthesized with toluene for various reaction times.....	56
5.13 Nitrogen adsorption-desorption isotherm of titania products synthesized in toluene by various reaction times and crystallite sizes.....	57
5.13 (cont.) Nitrogen adsorption-desorption isotherm of titania products synthesized in toluene by various reaction times and crystallite sizes.....	58
5.13 (cont.) Nitrogen adsorption-desorption isotherm of titania products synthesized in toluene by various reaction times and crystallite sizes.....	59
5.14 Size distribution of titania products synthesized in toluene for various reaction times.....	60
5.15 XRD pattern of titania products synthesized in toluene for various reactant concentrations.....	62
5.16 SEM image of the as-synthesis products for various reactant concentrations.....	63
5.17 Nitrogen adsorption-desorption isotherm of titania products synthesized in toluene for various concentrations of starting material and crystallite sizes.....	65
5.17 (cont.) Nitrogen adsorption-desorption isotherm of titania products synthesized in toluene for various concentrations of starting material and crystallite sizes.....	66

LIST OF FIGURES (cont.)

Figure	Page
5.18 Pore size distribution of titania products synthesized in toluene for various concentrations.....	67
5.19 XRD pattern of titania products synthesized in two solvents at 250°C for non-reaction time.....	68
5.20 XRD pattern of titania products synthesized in 1,4 butanediol at 300°C for 2 hrs and calcined at various temperature.....	71
5.21 XRD pattern of titania products synthesized in toluene calcined at 300°C for 2 hrs and calcined at various temperature.....	71
5.22 XRD patterns of as-synthesized silicon modified titania product synthesized in BG for various silicon content in molar ratio of Si/Ti.....	73
5.23 XRD patterns of as-synthesized silicon modified titania product synthesized in toluene for various silicon content in molar ratio of Si/Ti.....	73
5.24 SEM morphology of silicon modified titania products which vary silicon content in molar ratio of Si/Ti, synthesized in two organic solvents.....	76
5.25 Relative pressure of N ₂ adsorption-desorption of silicon modified titania product synthesized in BG, from BET surface measurement, in molar ratio of Si/Ti and crystallite size.....	77
5.25 (cont.) Relative pressure of N ₂ adsorption-desorption of silicon modified titania product synthesized in BG, from BET surface measurement, in molar ratio of Si/Ti and crystallite size.....	78
5.25 (cont.) Relative pressure of N ₂ adsorption-desorption of silicon modified titania product synthesized in BG, from BET surface measurement, in molar ratio of Si/Ti and crystallite size.....	79
5.26 Relative pressure of N ₂ adsorption-desorption of silicon modified titania product synthesized in toluene, from BET surface measurement, in molar ratio of Si/Ti and crystallite size.....	79
5.26 (cont.) Relative pressure of N ₂ adsorption-desorption of silicon modified titania product synthesized in toluene, from BET surface measurement, in molar ratio of Si/Ti and crystallite size.....	80

LIST OF FIGURES (cont.)

Figure	Page
5.26 (cont.) Relative pressure of N ₂ adsorption-desorption of silicon modified titania product synthesized in toluene, from BET surface measurement, in molar ratio of Si/Ti and crystallite size.....	81
5.27 Pore size distribution of silica modified titania products synthesized in BG for various content of silica.....	83
5.28 Pore size distribution of silica modified titania products synthesized in toluene for various content of silica.....	83
5.29 Weight loss of silica modified titania products synthesized in BG for various ratio of Si/Ti and weight loss percentage.....	85
5.29 (cont.) Weight loss of silica modified titania products synthesized in BG for various ratio of Si/Ti and weight loss percentage.....	86
5.30 Weight loss of silica modified titania products synthesized in BG for various ratio of Si/Ti and weight loss percentage.....	87
5.30 (cont.) Weight loss of silica modified titania products synthesized in BG for various ratio of Si/Ti and weight loss percentage.....	88
5.31 XRD pattern of silica modified titania synthesized in BG at molar ratio of Si/Ti is 0.08 after calcined in various temperature.....	89
5.32 XRD pattern of silica modified titania synthesized in toluene at molar ratio of Si/Ti is 0.08 after calcined in various temperature.....	89
5.33 FT-IR spectra of silicon modified titania products synthesized in BG at molar ratio of Si/Ti is 0.08, at as-synthesized and after calcined.....	90
5.34 FT-IR spectra of silicon modified titania products synthesized in toluene at molar ratio of Si/Ti is 0.08, at as-synthesized and after calcined.....	90
5.35 XRD patterns of as-synthesized aluminium modified titania product synthesized in BG for various aluminium content in molar ratio of Al/Ti.....	92
5.36 XRD patterns of as-synthesized aluminium modified titania product synthesized in toluene for various aluminium content in molar ratio of Al/Ti.....	92

LIST OF FIGURES (cont.)

Figure	Page
5.37 SEM morphology of aluminium modified titania products which vary aluminium content in molar ratio of Al/Ti, synthesized in two organic solvents.....	93
5.38 Relative pressure of N ₂ adsorption-desorption of aluminium modified titania product synthesized in BG, from BET surface measurement, in molar ratio of Al/Ti and crystallite size.....	96
5.38 (cont.) Relative pressure of N ₂ adsorption-desorption of aluminium modified titania product synthesized in BG, from BET surface measurement, in molar ratio of Al/Ti and crystallite.....	97
5.38 (cont.) Relative pressure of N ₂ adsorption-desorption of aluminium modified titania product synthesized in BG, from BET surface measurement, in molar ratio of Al/Ti and crystallite size.....	98
5.39 Relative pressure of N ₂ adsorption-desorption of aluminium modified titania product synthesized in toluene, from BET surface measurement, in molar ratio of Al/Ti and crystallite size.....	98
5.39 (cont.) Relative pressure of N ₂ adsorption-desorption of aluminium modified titania product synthesized in toluene, from BET surface measurement, in molar ratio of Al/Ti and crystallite size.....	99
5.39 (cont.) Relative pressure of N ₂ adsorption-desorption of aluminium modified titania product synthesized in toluene, from BET surface measurement, in molar ratio of Al/Ti and crystallite size.....	100
5.40 Pore size distribution of alumina modified titania products synthesized in 1,4 BG for various content of alumina.....	102
5.41 Pore size distribution of alumina modified titania products synthesized in toluene for various content of alumina.....	102
5.42 Weight loss of aluminium modified titania products synthesized in BG for various ratio of Al/Ti and weight loss percentage.....	103
5.42 (cont.) Weight loss of aluminium modified titania products synthesized in BG for various ratio of Al/Ti and weight loss percentage.....	104

LIST OF FIGURES (cont.)

Figure	Page
5.43 Weight loss of aluminium modified titania products synthesized in BG for various ratio of Al/Ti and weight loss percentage.....	105
5.43 (cont.) Weight loss of aluminium modified titania products synthesized in BG for various ratio of Al/Ti and weight loss percentage.....	106
5.44 XRD pattern of aluminium modified titania synthesized in BG at molar ratio of Al/Ti is 0.08 after calcined in various temperatures.....	108
5.45 XRD pattern of aluminium modified titania synthesized in toluene at molar ratio of Al/Ti is 0.08 after calcined in various temperature.....	108
5.46 FT-IR spectra of aluminium modified titania products synthesized in BG at molar ratio of Al/Ti is 0.08, at as-synthesized and after calcined.....	109
5.47 FT-IR spectra of aluminium modified titania products synthesized in toluene at molar ratio of Al/Ti is 0.08, at as-synthesized and after calcined.....	109
5.48 XRD patterns of as-synthesized phosphorous modified titania products synthesized in BG for various phosphorous content in molar ratio of P/Ti.....	111
5.49 XRD patterns of as-synthesized phosphorous modified titania products synthesized in toluene for various phosphorous content in molar ratio of P/Ti.....	111
5.50 SEM morphology of phosphorous modified titania products which vary phosphorous content in molar ratio of P/Ti, synthesized in two organic solvents.....	112
5.51 Relative pressure of N ₂ adsorption-desorption of phosphorous modified titania products synthesized in BG, from BET surface measurement, in molar ratio of P/Ti and the crystallite sizes.....	115
5.51 (cont.) Relative pressure of N ₂ adsorption-desorption of phosphorous modified titania products synthesized in BG, from BET surface measurement, in molar ratio of P/Ti and crystallite sizes.....	116

LIST OF FIGURES (cont.)

Figure	Page
5.51 (cont.) Relative pressure of N ₂ adsorption-desorption of phosphorous modified titania product synthesized in BG, from BET surface measurement, in molar ratio of P/Ti and crystallite size.....	117
5.52 Relative pressure of N ₂ adsorption-desorption of phosphorous modified titania product synthesized in toluene, from BET surface measurement, in molar ratio of P/Ti and crystallite size.....	117
5.52 (cont.) Relative pressure of N ₂ adsorption-desorption of phosphorous modified titania products synthesized in toluene, from BET surface measurement, in molar ratio of P/Ti and crystallite sizes.....	118
5.52 (cont.) Relative pressure of N ₂ adsorption-desorption of phosphorous modified titania products synthesized in toluene, from BET surface measurement, in molar ratio of P/Ti and crystallite sizes.....	119
5.53 Pore size distribution of phosphorous modified titanias synthesized in BG for various content of phosphorous.....	121
5.54 Pore size distribution of phosphorous modified titanias synthesized in toluene for various content of phosphorous.....	121
5.55 Weight loss of phosphorous modified titania products synthesized in BG for various ratio of P/Ti and weight loss percentages.....	122
5.55 (cont.) Weight loss of phosphorous modified titania products synthesized in BG for various ratio of P/Ti and weight loss percentages.....	123
5.56 Weight loss of phosphorous modified titania products synthesized in toluene for various ratio of P/Ti and weight loss percentages.....	124
5.56 (cont.) Weight loss of phosphorous modified titania products synthesized in toluene for various ratio of P/Ti and weight loss percentages.....	125
5.57 XRD pattern of phosphorous modified titanias synthesized in BG at molar ration of P/Ti is 0.08 after calcined in various temperatures.....	127

LIST OF FIGURES (cont.)

Figure	Page
5.58 XRD pattern of phosphorous modified titanias synthesized in toluene at molar ratio of P/Ti is 0.08 after calcined in various temperatures.....	127
5.59 FT-IR spectra of phosphorous modified titania products synthesized in BG at molar ration of P/Ti is 0.08, at as-synthesized and after calcined.....	128
5.60 FT-IR spectra of phosphorous modified titania products synthesized in toluene at molar ratio of P/Ti is 0.08, at as-synthesized and after calcined.....	128



สถาบันวิทยบริการ
จุฬาลงกรณ์มหาวิทยาลัย

CHAPTER I

INTRODUCTION

Titanium (IV) oxide (TiO_2 or titania) has been known to be an excellent catalyst support in industrial process, (Matsuda and Kato, 1983; Inomata *et al.*, 1980; Luck., 1991) e.g., as a support in a commercial vanadium (V) oxide catalyst for selective catalytic reduction (SCR) of nitrogen oxides (NO_x) with ammonia. Due to stricter regulations, a higher level of removal of NO_x is now required and one of the most effective approaches to meet the new goals is to use a TiO_2 support having a larger surface area. Generally, large surface areas are required for catalyst. Since the catalyst is usually used at high temperature, high thermal stability, as well as large surface area, is also important (Kominami *et al.*, 1999).

Titania is commercially very important as a white pigment because of its maximum light scattering with virtually no absorption and because it is non toxic, chemically inert, and a dielectric ceramic material for its higher dielectric constant (Cheng *et al.*, 1995). Recently, it has been suggested that monodisperse oxide powders are preferable to ceramic raw materials (Ogihara *et al.*, 1991). Titania is known to have several natural polymorphs: Rutile is thermodynamically stable which tends to be more stable at high temperatures and thus is sometimes found in igneous rocks, but anatase is metastable at high temperatures (both belonging to the tetragonal crystal system), and brookite is formed only under hydrothermal conditions or usually found only in minerals and has a structure belonging to the orthorhombic crystal system (Keesmann, 1966). Anatase type titania has been used as a catalyst for photodecomposition and solar energy conversion, because of its high photoactivity (Lason and Falconer, 1994; Kamat and Dimitrijevic, 1990; Herrmann *et al.*, 1997; Fox and Dulay, 1993; Fujishima *et al.*, 1999). On the other hand, rutile-type titania has been used for white pigment materials, because of its good scattering effect, which protects materials from ultraviolet light. Anatase titania has been reported to be unstable at high temperature and its transformation temperatures to be scattered in a wide range (Zzandena *et al.*, 1958; Yoganarasimhan and Rao, 1962). Polymorphic transformation of ceramic materials generally depends on the grain size, impurities,

composition, nature of the dopant, amount of dopant, and processing (Hirano *et al.*, 2002).

There are a lot of methods for preparing TiO₂ (Kamal *et al.*, 1992; Tadafumi *et al.*, 1992; Jones *et al.*, 1992; Kutty *et al.*, 1988; Hu *et al.*, 1990). Titanium (IV) oxide is industrially produced generally by the so-called sulfate process and the so-called chloride process. In the latter, the requirements for equipment and materials are very harsh because of high reaction temperature (>1400 °C) and strong corrosiveness of Cl₂ at high temperature (Cheng *et al.*, 1995).

Titania for catalytic applications is usually prepared from titanium oxysulfate (TiO(SO₄)), sulfate (TiO(SO₄)₂), or chloride (TiCl₄) by the precipitation (or hydrolysis) method. However, it is known that the counter anion of the starting titanium salt remains in the product (Del Arco *et al.*, 1986) and affects the activity of the catalyst (Kurosaki *et al.*, 1976). To avoid the contamination of the counter anion, titanium alkoxide can be used as the starting material for catalysts, catalyst supports, and photocatalysts (Kominami *et al.*, 1999).

Nanocrystalline material and nano composites, characterized by an ultra fine grain size (<50 nm). Nanoclusters are subject of current interest because of their unusual magnetic, optical, electronic properties, which often differ from their bulk properties. Nanostructured metal-oxide thin films are receiving a growing attention for the realization of gas sensors (NO_x, CO, CO₂, CH₄ and aromatic hydrocarbon) with enhanced sensitivity and selectivity. Nanosize metallic powders have been used for the production of gas tight materials, dense parts and porous coating (Ahmed, 1999). Nanometer-size particles have different physical and chemical properties from bulk materials. When used as catalysts, their catalytic activity is expected to be enhanced not only because of their increased surface area, but also because of the change of surface properties such as surface defect (Popielarski, 1998).

The particle size of nanocrystalline titanium (IV) oxide plays an important role in the physical and chemical behavior of the material because the specific surface area, the chemical stability, and the chemical reactivity of the material are all highly correlated with particle size. It has been shown that the adsorption of organics onto

surface of nanocrystalline anatase is size-dependent and that the particle size is a crucial factor in photocatalytic decomposition of chloroform by nanocrystalline anatase titania (Zhang *et al.*, 2000).

Nano-sized TiO₂ have been prepared by several methods such as solvothermal method, hydrothermal method, thermal decomposition, vapor-phase hydrolysis laser-induced decomposition, sol-gel method, chemical vapor decomposition method (CVD) and molten salt method. Wet chemical routes (sol-gel, precipitation) seem to be more efficient in controlling the morphology and degree of agglomeration of nanocrystalline particles than the dry methods such as chemical vapor deposition (CVD). However, in the former methods, strong agglomerates can be easily formed among nanoparticles, because of their large specific surface area, which may lead to a degradation of properties. Titanium alkoxide and titanium chloride are usually used as precursors for TiO₂ (Bradley *et al.*, 1978). The precipitation of hard agglomerates often occurs during hydrolysis, because these reagents exhibit high reactivity with water (Yang *et al.*, 2001).

The sol-gel method, is one of the precipitation methods, affords titanias with extremely high surface area (Zaharescu *et al.*, 1997; Dagan and Tomkiewicz, 1994). The method basically consists of the hydrolysis of an alkoxide to form a sol, followed by gelling, ageing, drying and thermal stabilization. Each step can be controlled and modified in order to obtain specific material, narrow pore size distribution, and narrow particle size distribution (Montoya *et al.*, 1992). However, the thus-obtained titanias contained some amounts of the amorphous phase and their surface area decrease drastically in calcination to improve the crystallinity (Iwamoto *et al.*, 2001), moreover, several aqueous-based methods using metal salts as a precursor material, such as the hydrolysis method and homogeneous precipitation method have several problems; the concentration of reaction species should be low and the reaction time very long (Moon *et al.*, 1995).

Hydrothermal Methods have been widely applied for the synthesis of a variety of ceramic materials, while syntheses of metal oxides in organic solvents at temperature high than their boiling points (Solvothermal synthesis) have been experimented by only a few research groups (Bibby *et al.*, 1985; Cruickshack *et al.*,

1985; Fanelli *et al.*, 1989; Inoue *et al.*, 1991; Kominami *et al.*, 1999). Inoue *et al.* (1991) used organic media in place of water for hydrothermal method. They have explored the synthesis of inorganic materials in glycols at temperature higher than boiling point of the glycol, they call “Glycothermal Method”. By solvothermal method, nanocrystalline titanium (IV) oxide produced but mechanism of reaction occurred in several ways. At high temperature above supersaturation point, metal oxide was crystallized or precipitated which products was different in properties, morphology, crystalline etc.

Surface area is one of the important factors for the use of titania as catalyst materials. However, large-surface area materials have high tendency for sintering because of their surface energies. Thermal stability seriously affects the catalyst life, titania having large surface area with reasonable thermal stability has been sought. Thus, many studies having been devoted to improve the thermal stability of titania using additives such as Al (Martucci *et al.*, 1999; Reddy *et al.*, 2001), Si (Mahipal Reddy *et al.*, 1993; Jung *et al.*, 2000), P (Kohno *et al.*, 2001), La (Sibu *et al.*, 2002), Zr (Hirano *et al.*, 2002), Cr (Takeuchi *et al.*, 2000) and others. The effects of these additives are quite different by the procedures of the doping and the amount of the additives, and the mechanisms for the stabilization effects of these dopants are not yet fully elucidated (Iwamoto *et al.*, 2000).

In previous, synthesized titania used many solvent for preparation by the solvothermal method (Hydrothermal and Glycothermal method). But some work interested in effect in solvent used to synthesis. In addition, the effect of metal doped on titania synthesized in several solvent is less reported. In this work, the study will focus on the different mechanism of titania synthesize in different solvents such as 1,4 butanediol (glycothermal method) and toluene (solvothermal method). In addition, the effect of the second element modified titania is synthesized in the two solvents. After that, the physical properties of titania products are analyzed such as surface area, crystalline size, thermal stability and compare the properties of the product synthesized in the different solvents.

Objective of the thesis

1. Study of synthesis method of titanium (IV) oxide and the effective factors on synthesized titanium (IV) oxide properties.
2. Study of the effect of second element and synthesizing solvent on synthesized titanium (IV) oxide.

The present study is arranged as follows:

Chapter II presents literature reviews of the previous works related to this research.

Chapter III explains the basic theory about titania such as the general properties of titania, the various preparation methods to obtain the ultrafine titania.

Chapter IV shows the experimental equipment and systems, and the preparation method of titania by solvothermal method.

Chapter V exhibits the experimental results.

In the last chapter, the overall conclusions of this research are given.

Finally, the samples of calculation for the preparation of titania and crystallite size are included in appendices at the end of this thesis.

CHAPTER II

LITERATURE REVIEWS

There have been several studies on the synthesis of titania and improvement of titania properties. A researcher has been found the advantage and drawback which not only the synthesis method but also in titania properties. Their works are very useful to apply titania in several ways such as, the photocatalytic reaction, electronic equipment, industrial etc. and learn to develop technical for modify and apply in the future.

Montoya *et al.* (1992) studied the effects of the sol-gel synthesis parameters on textural and structure characteristics of TiO₂. They found that TiO₂ had been prepared by sol-gel method, variations in the synthesis conditions produced solids of different characteristics. It was found that parameters such as type of solvent, synthesis temperature, acid addition, alcohol/alkoxide and water/alkoxide molar ratios influence the texture, structure and morphology of the sample. When they calcined the samples at 500°C, its surface area decreased strongly. Microcrystalline anatase was obtained after drying at 80°C in most of the samples. Calcinations at 500°C of microcrystalline anatase brought about the coalescence of the fine material, producing larger size particles. Amorphous titania crystallized to anatase after calcinations at 400°C.

Inoue *et al.* (1992) studied reaction of aluminium alkoxides with various glycols and the layer structure of their products. They synthesized alumina products by hydrothermal reaction of aluminium isopropoxide (AIP) in various glycol solvents, instead of water for hydrothermal synthesis, such as 1,4 butanediol (1,4 1,4-BG), 1,3 propanediol (1,3 PG) and 1,6 hexanediol (1,6 HG), which the products were amorphous or boehmite depended on type of glycol. When they prepared alumina products by different starting materials in 1,4 1,4-BG, found that the product had identical structure. In various glycol, they reported that the crystallite sizes increased with increasing carbon number and the products had the glycol moieties incorporation. They concluded that the glycol moieties were incorporated between the

layers of boehmite resulting in enlargement of the basal spacing which the basal spacing of the product increased with increasing carbon number of the glycol. They found that a small amount of water may be present in the glycol sample and is possibly formed by thermal decomposition of glycol.

Inoue *et al.* (1992) studied thermal transformation of χ -alumina formed by thermal decomposition of aluminum alkoxide in organic solvent which they used of organic media in place of water for the hydrothermal method. They synthesized alumina by various aluminum alkoxide in toluene or other organic solvent such as benzene, xylene. They reported that the products were crystal and/or amorphous depend on starting material and solvent and reported that cleavage of C-O bonds was the prime factor for the decomposition of aluminum alkoxides. When aluminum *tert*-butoxide decomposed in toluene the product was amorphous, they explained that its low decomposition temperature, where the decomposed material dose not have sufficient thermal energy for crystallization of χ -alumina.

Yanggisawa *et al.* (1997) had synthesized anatase titanias were produced at low temperature below 350°C by hydrothermal hot-pressing of amorphous titania consisting of spherical particles prepared by hydrolysis of titanium tetraethoxide. They found that water included in the starting powder was released to produce hydrothermal conditions by heating and the hydrothermal treatment event at 100°C accelerated crystallization of the amorphous titania to anatase. In various temperature, the remarkable decrease in the surface area with the increase in reaction temperature from 100°C to 150°C indicated that a large amount of amorphous parts remained in the compacts produced at 100°C. In various reaction pressure, compressive pressure from outside the autoclave, the crystallite size did not change with varying reaction pressure, which suggested that the compression had no effect on the crystallization of anatase.

Kominami *et al.* (1997) used titanium (IV) tetra-*tert*-butoxide (TTB) to synthesized titania by thermal decomposition reaction in organic solvent at 573 K, the titania sample they prepared by this method will be called TD-TiO₂ (thermal decomposition). They found that TTB was completely decomposition at this condition

which yielded anatase without contamination of any other phase. When they changed solvent (toluene) in this reaction, they found that TTB was decomposed in toluene even at 473 K to give anatase having quite large surface area. Since the BET surface area of a sample synthesized at 523 K was larger than that calculated from its crystalline size (they assumed the density of anatase to be 3.84 g cm^{-3}), it suggested that the product synthesized at lower temperature were contaminated with the amorphous-like hydrated phase. In the effect of the structure of the alkyl group in the starting alkoxide, they found that primary and secondary alkoxides of titanium (IV) were not decomposed even at 573 K. This suggested that the process requires direct cleavage of the C-O bonds in alkoxides, and therefore the thermal stability of the C-O bond may be a decisive factor for the formation of TiO_2 lattice. When TiO_2 calcined the transformation had occurred to partly form rutile at 973 K and the loss of surface area by calcination was presumably because the as-prepared TiO_2 was well-crystallized having smaller tendency toward sintering and contained lesser amount of amorphous-like phase to be crystallized into anatase upon calcinations.

Yoshinaka *et al.* (1997) studied in a formation and sintering of TiO_2 (anatase) solid solution in system TiO_2 - SiO_2 . As-synthesized titania was prepared by hydrazine method, they had developed the new method using hydrazine monohydrate ($(\text{NH}_2)_2 \cdot \text{H}_2\text{O}$) in the hydrolysis reaction. The product was form anatase titania. When they added SiO_2 to synthesized titania, they found that transformation of anatase occurred at higher temperature with increased SiO_2 content and a linear decreased in specific surface area was due to the formation of tightly bound aggregated in the primary particles with in crease temperature. In the transformation of anatase to rutile they suggest that anatase by transformation decomposed into rutile and amorphous SiO_2 , no crystalline SiO_2 was recognized throughout the heating process.

Park *et al.* (1997) studied effect of solvent on titania particle formation and morphology in thermal hydrolysis of TiCl_4 . They synthesized titania powder by thermal hydrolysis of titanium tetrachloride in mixed solvent of *n*-propanol and water. They found that precipitates obtained with pure water were fine and highly agglomerated. They reported that a decrease in the dielectric constant of the solution promotes the precipitation of titania by reducing the solubility of the titania in the solvent and promotes the supersaturation of titania in the solvent. In addition, they

found that morphologies of titania depended on particle surface potential and the dielectric constant which the magnitude of the energy barrier and maximum repulsive force was determined mainly by them. In nucleation, they reported that the particle growth after nucleation can be also effect by the kinds of solvent, because the particle interaction potential is different in each solvent. They proposed the particle growth in three ways mechanism of agglomerate of secondary particles (Figure 2.1).

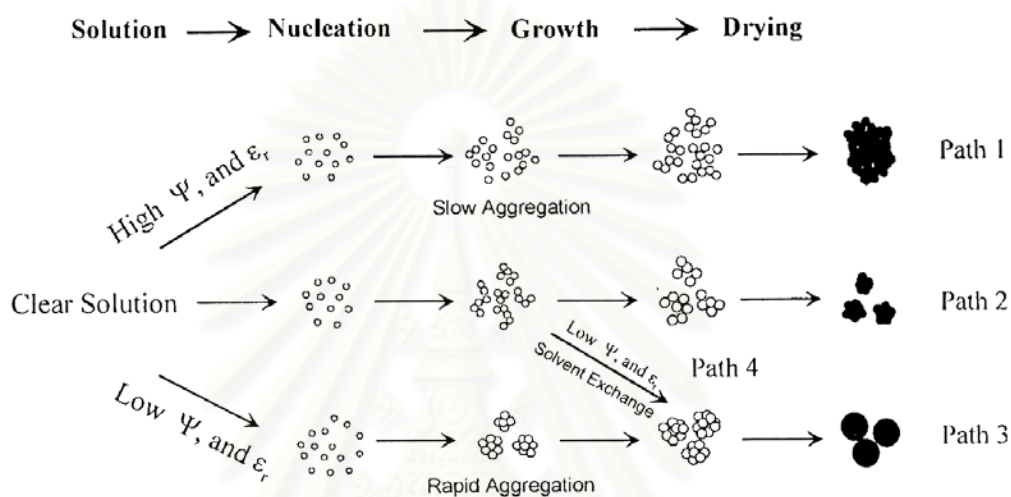


Figure 2.1 Schematics of particle growth in the mixed solvent of alcohol and water. (Park *et al.*, 1997)

In some previous work found that washing powder (starting material of ceramic material) with organic solvents is an effective way of avoiding the formation of hard agglomerates. It is proposed that agglomerate strength is determined by the extent to which water molecules, hydrogen-bonded to surface hydroxyl groups, are able bridges between adjacent particles. Organic solvents can remove hydroxyl groups and water and leads to reduction and/or elimination of hard agglomerates [Readey *et al.* (1990); Kaliszewaki *et al.* (1990)]. Yin *et al.* (1998) studied crystallization of titania in liquid media and photochemical propertied of crystallized titania. They prepared titania from titanium tetraisopropoxide in *i*-propanol that derived amorphous TiO_2 gel. When heat treatments of the gels in water, *n*-hexane and methanol crystallization occurred above 120 °C which the rate of crystallization was in the order in water > *n*-hexane > methanol. On the other hand, they studied in the crystallization behavior of the gels in methanol-water and *n*-hexane-water mixed

solutions found that the rate increased with increased water fraction. The results suggested that water is essential for crystallization of gel and that the crystallization proceeded via a dissolution-reprecipitation mechanism, where the gel dissolves as hydrated ions by reaction with water absorbed on the surface.

Inoue *et al.* (1998) studied glycothermal synthesis of rare earth iron garnets. They synthesized iron oxide products by glycothermal synthesis, the use of organic media in place of water for the hydrothermal method, in 1,4 butanediol. They reported that in the glycothermal reaction, thermal decomposition of the glycol moiety is directly connected with the crystallization of the products, and therefore starting materials with a high energy level provide a large driving force for the formation of the products. They explained that because of the large driving force available in the glycothermal reaction, crystal growth proceeds rapidly even though the lattice parameter of the grown crystals is much larger than that of the seed crystals. So that, the lattice strain caused by the epitaxial growth of a new crystal on a seed crystal having different lattice parameters is released by edge dislocations and the creation of a number of crystal defect is another characteristic of the glycothermal method. In the same year, Inoue *et al.* (1998) studied reactions of rare earth acetates with aluminum isopropoxide (AIP) in ethylene glycol. They found that modified-alumina had synthesized by glycothermal method derived amorphous and/or crystal. They reported that a formation of the amorphous product in the reaction can be interpreted by the difficulty in the cleavage of the C-O bond of the intermediate glycoxide formed by the reaction of AIP with ethylene glycol, where the ease in the cleavage of the C-O bond seems to be the prime factor for the formation of crystalline garnets by the reaction in 1,4 1,4-BG.

Kominami *et al.* (1999) has synthesized titania by hydrolyzed titanium alkoxide (titanium *n*-butoxide, TNB) in organic solvents at high temperatures and developed novel method, i.e., hydrolysis of titania alkoxides with water homogeneously formed from alcohols used as the solvent. The titania sample prepared by the novel method was called ThyCA (Transfer Hydrolytic Crystallization in Alcohols) TiO₂. the products prepared by this method was anatase with out contamination of any other phase such as rutile or brookite and the products contained a negligible amount of amorphous-like phase. In the effect of synthesis condition on

the physical properties of ThyCA-TiO₂, they prepared ThyCA-TiO₂ under various conditions such as vary alkoxide or vary alcohol. The reaction of TNB in 2-propanol, microcrystalline titania was formed at 548 K while reaction at 523 K gave no solid product, indicating that dehydration of 2-propanol required temperature higher than 523 K, when titanium isopropoxide (TIP) was dissolved in a mixed solvent of 2-propanol in toluene TIP was completely hydrolyzed to give anatase titania. When calcination on ThyCA-TiO₂ prepared in the TNB-2-propanol, phase transformation of anatase occurred at 1173 K which induced partial transformation onto the rutile. The high thermal stability of ThyCA-TiO₂, they assumed that the as-prepared ThyCA-TiO₂ consisted of single crystals and contained negligible amount of amorphous-like phase to be crystallized into anatase and to induced sintering of crystallites upon calcination. In the same year, Kominami *et al.* (1999) studied new synthesis method for nanosized by hydrolysis of titanium *n*-butoxide (TNB) in toluene and add water in the gap of autoclave. During the reaction, water in the gap was vaporized, dissolved in toluene from the gas phase, and hydrolyzed TNB. Titania was prepared in various conditions, found that anatase and amorphous formed in the reaction. When they calculate surface area in assumption that the particles were nonporous spheres for compared the specific surface area from BET measurement which test contaminate amorphous phase in the as-prepared titania. They found that when the reaction time was prolonged, the crystallite size was gradually increased and the effect of the combustion heat of the organic moieties locally raises the surface temperature of crystals, which can accelerate the crystallization and/or sintering of TiO₂ crystals (or particle) from the calcinations and the decrease in surface area from BET was probably due to sintering of single crystals.

Martucci *et al.* (1999) studied crystallization of Al₂O₃-TiO₂ sol-gel systems. They found that the presence of a large amount of Al₂O₃ in the system has an inhibitory effect on the crystallization of titania in both anatase and rutile structures which a shift in rutile crystallization temperature with increasing the Al₂O₃ content. In the other hand, they reported that the formation of titania rutile phase in the films may be attributed to be in great part due to the direct transformation amorphous-rutile, rather than anatase-rutile. They had discussed the effect of Al₂O₃ on the crystallization in two conclusions, first, Al₂O₃ could prevent the nucleation of anatase by interfering with the mutual contact between adjacent TiO₂ particles, second, the

presence in the film of nanometric TiO_2 clusters allow the formation of mixed Ti-O-Al bonds, localized at the surface of these clusters, which prevents the crystal growth and the anatase phase transformation. In more content Al, they found that sample was calcined at 1000°C the metastable $\beta\text{-Al}_2\text{TiO}_5$ and $\alpha\text{-Al}_2\text{O}_3$ were formed they reported that $\alpha\text{-Al}_2\text{O}_3$ was formed from amorphous Al_2O_3 and the metastable $\beta\text{-Al}_2\text{TiO}_5$ was form from both amorphous titania and alumina in the film.

Iwamoto *et al.* (2000) studied the synthesis of large-surface area silica-modified titania ultrafine particles by glycothermal method. They synthesized titania products from titanium tetraisopropoxide (TIP) and an appropriate amount of tetraethyl orthosilicate were added to 1,4 butanediol. They found that the titania products, were synthesized by this method, had quite large surface area and exhibited high thermal stabilities. In the product obtained by the reaction of TIP alone, its transformation temperature was much higher than that of the titania prepared by other method. When small amount of TEOS added to the reaction mixture caused the anatase-rutile phase transformation to shift markedly toward higher temperature and increase amount of TEOS the temperature transformation of titania increase. They reported that not only the temperature transformation increase but the specific surface area also increase when added TEOS in the reaction.

Kim *et al.* (1999) studied homogenous precipitation of titania ultrafine powder from aqueous TiOCl_2 solution. They found the as-precipitated hydroxide was amorphous at first and became crystalline as the heat-treatment temperature increased and found that the precipitation was not determined by the heating rate but by heating temperature and time. They reported that the homogenous precipitation method using simple heating produced nanosized crystalline powder. In agglomeration of primary particle, they found the increased agglomeration or growth of TiO_2 primary particle with increased in thermal energy in the reaction.

Jung *et al.* (2000) studied enhanced photocatalytivity of silica-embedded titania particles prepared by sol-gel process. They found that the major phase of the silica-titania particles prepared by sol-gel technique was pure anatase without other contamination phase and silica crystal. They reported that the added silicon formed segregated amorphous silica and embedded into anatase titania matrix which affect

the increase of thermal stability result in suppressing the phase transformation from anatase to rutile, in addition, the degree of aggregation of primary particles decreased with increasing the silica content.

Zhang *et al.* (2001) controlled the temperature of the hydrolysis of titanium ethoxide to synthesize nanocrystalline and amorphous titania. By heating the amorphous titania in air at 375 °C to 550 °C for 3 h, single-phase anatase powders were prepared. They had varied condition (synthesized at 0 °C for 3h, large amount batch at 0°C, at 50 °C for 3 h, at 70 °C for 3 h) for synthesize titania and found that at $T > 375$ °C for pure amorphous titania, single phase anatase can be generated from amorphous titania after heating for only 3 h or less. By heating various starting material at different temperature for 3 h, they found that the average size of anatase depends on the history of the starting material because the material history can effect the transformation kinetics and thus the average particle size. Anatase particle form by heating of the amorphous titania were spherical. They concluded that large anatase particles may have grown by one of three pathways, First, large anatase particles may form directly from aggregates of smaller amorphous titania particles. Second, large anatase particles may grow by atom-by-atom recrystallization of smaller anatase particles. Third, large anatase crystals may form by solid-state aggregation of adjacent small anatase particles as the crystals adopt appropriate crystallographic orientations.

Iwamoto *et al.* (2001) studied preparation of the xerogels of nanocrystalline titania by the removal of the glycol at the reaction temperature after the glycothermal method and their enhanced photocatalytic activities. They synthesized titania products by titanium tetraisopropoxide (TIP) and an appropriate amount of tetraethyl orthosilicate (TEOS) were added to 100 ml of 1,4 butanediol at 300°C and kept at that temperature for 2 h (glycothermal method), in the second method, after the glycothermal reaction, removed the organic vapor from the autoclave by flash evaporation while keeping at 300°C and its products formed anatase titania with non-contamination of other phase or amorphous phase. In second method, when increasing in the amount of the TEOS addition the crystallite size decrease which they reported that the crystallization mechanism was not effected by the removal of the glycol at the reaction temperature. In the other hand, the removal of the glycol at the reaction temperature, the titania product (without TEOS in the reaction) had improvement of

the thermal stabilities. In addition of TEOS in the reaction both of the method, the temperature transformation had shift, they reported that the silica-modification of titania had been improve thermal stability both of the methods. They found that the products, synthesized from second method, was the collapse of the coagulated structure indicated that coagulation during drying of wet gels due to the surface tension of the liquid.

Hirano *et al.* (2002) studied direct formation of zirconia-doped titania with stable anatase-type structure by thermal hydrolysis. They found that the ZrO_2 content in the starting solution increased, a shift of the diffraction peak of the as-precipitated anatase-type TiO_2 to lower diffraction angle was observed. In heat treatment, they found a small amount of tetragonal ZrO_2 was detected after heat treatment at $>950^\circ C$ and the anatase structure was fully maintained when ZrO_2 was doped in the titania, even after heat treatment at $1000^\circ C$. they reported that the hydrothermally precipitated anatase particles with nanosized crystallites can produce solid solution with large amount of ZrO_2 than those with high crystallinity and large crystallite size after heat treatment at $950^\circ - 1000^\circ C$.

Kominami *et al.* (2002) studied synthesis of perovskite-type lanthanum iron oxide by glycothermal reaction of a lanthanum-iron precursor. They prepared the precursor by reacted a mixture of lanthanum (III) isopropoxide (LIP) and iron (III) *n*-bitoxide (INB) in toluene, this process in toluene they call the solvothermal decomposition process and they used the precursor reacted in 1,4 butanediol (1,4-BG), this solvothermal process in 1,4-BG is called a glycothermal process. Formation of the amorphous phase that prepared by solvothermal decomposition of the mixture of LIP and INB in toluene, they found that it suggested a relatively strong interaction between two starting compounds and high homogeneity of lanthanum and iron species in the precursor. When they prepared the product by direct glycothermal reaction of a mixture of LIP and INB without preparation of the precursor using the solvothermal decomposition process they found that the starting materials, LIP and INB, reacted independently under glycothermal condition and yielded each related compound.

Kongwudthti *et al.* (2002) synthesized the large-surface area of silica-modified zirconia by the glycothermal method. They prepared the product from zirconium *n*-butoxide and amount of tetraethyl orthosilicate in 1,4 butanediol, they found that the tetragonal zirconia was formed for all the products and they reported that the crystallinity of sample prepared by the glycothermal method was not effected by increasing of the Si ratio. All the product were composed of spherical particle when TEOS was added to the reaction, the spherical particle formed agglomerates but the crystallite size of all product not different, they suggested that the nucleation frequency of product was scarcely affected by TEOS content added to the reaction. In thermal stability, the tetragonal to monoclinic phase transformation temperature shifted toward higher temperatures with the addition of TEOS.



สถาบันวิทยบริการ
จุฬาลงกรณ์มหาวิทยาลัย

CHAPTER III

THEORY

It is known that titanium (Ti) can form a large number of addition compounds by coordination with other substances such as hydrogen, nitrogen, boron, carbon, oxygen, and other systems. Titanium (IV) oxide (titania) is a titanium compound that is the most important commercial form. Physical and chemical properties of titania have been studied to include preparation procedure and its advantages.

3.1 Titanium (Ti) (Sornnarong Theinkeaw, 2000)

Titanium (atomic number 22; ionization potentials: first 6.83 eV, second 13.67 eV, third 27.47 eV, fourth 43.24 eV) is the first member of Group IVB of the periodic chart. It has four valence electrons, and Ti (IV) is its most stable valence state. The lower valence states Ti (II) and Ti (III) exist, but these are readily oxidized to the tetravalent state by air, water, and other oxidizing agents. The ionization potentials indicate that the Ti^{4++} ion would not be expected to exist and, indeed, Ti (IV) compounds are generally covalent. Titanium is able to expand its outer group of electrons and can form a large number of addition compounds by coordination with other substances having donor atoms, e.g., oxygen or sulfur. The most important commercial forms are titanium (IV) oxide and titanium metal.

Thermochemical data

Thermochemical data of titanium (IV) oxide and other titanium compounds are described. Data relating to changes of state of selected titanium compounds are listed in Table 3.1. Table 3.2 gives values for heat of formation, free energy of formation, and entropy of a number of titanium compounds at two temperatures, 298 K and 1300 K.

Table 3.1 Thermal data for changes of state of titanium compounds

Compound	Properties	Temperature,K	$\Delta H, \text{kJ/mol}$
TiCl ₄	melting point	249.05	9.966
	Boiling point	409	35.77
TiCl ₃	sublimation temperature	1104.1	166.15
TiCl ₂	sublimation temperature	1591.5	248.5
TiI ₄	melting point	428	19.23±0.63
	Boiling point	652.6	56.48±2.09
TiF ₄	sublimation temperature	558.6	97.78±0.42
TiBr ₄	melting point	311.4	12.89
	Boiling point	504.1	45.19
TiO ₂	phase change (anatase to rutile)		ca-12.6

3.2 Titanium (IV) oxide (Sornnarong Theinkeaw, 2000 and Fujishima *et al.*,1999)

Physical and chemical properties

Titanium (IV) oxide occurs naturally in three crystalline forms: anatase, which tends to be more stable at low temperature, brookite, which is usually found only in minerals, and rutile, which tends to be more stable at higher temperatures and thus is sometimes found in igneous rock. These crystals are substantially pure titanium (IV) oxide but usually amounts of impurities, e.g., iron, chromium, or vanadium, which darken them. A summary of the crystallographic properties of the three varieties is given in Table 3.3.

Although anatase and rutile are both tetragonal, they are not isomorphous (Figure 3.1). Anatase occurs usually in near-regular octahedral, and rutile forms slender prismatic crystal, which are frequently twinned. Rutile is the thermally stable form and is one of the two most important ores of titanium.

The three allotropic forms of titanium (IV) oxide have been prepared artificially but only rutile, the thermally stable form, has been obtained in the form of transparent large single crystal. The transformation from anatase to rutile is

Table 3.2 Thermochemical data for formation of titanium compounds

Compound	State	Heat formation		Free energy of formation		Entropy, S	
		ΔH_f° , kJ/mol	at 1300 K	ΔG_f° , kJ/mol	at 1300 K	J/(mol.K)	at 298 K
TiO	Crystal	-519.6	-515.9	-495.1	-417.1	50.2	127.0
TiO ₂							
Anatase	Crystal	-933.0	-930.0	-877.6	-697.4	49.9	150.6
Rutile	Crystal	-944.7	-942.4	-889.5	-707.9	50.3	149.0
TiC	Crystal	-184.1	-188.2	-180.5	-169.1	24.2	92.25
TiN	Crystal	-337.6	-337.6	-309.0	-215.0	30.2	100.8
TiCl ₂	Crystal	-515.5	-504.2	-465.5	-314.8	87.4	204.2
TiCl ₃	Crystal	-721.7	-698.2	-654.5	-445.9	139.7	290.9
TiCl ₄	Liquid	-804.2	-771.4	-737.3	-604.6	252.4	431.2
TiCl ₄	Gas	-763.2	-765.8	-726.8	-607.0	354.8	507.4
TiBr ₄	Crystal	-618.0	-654.5	-593.3	-347.2	243.6	440.6
TiBr ₃	Crystal	-550.2	-546.3	-525.6	-341.1	176.4	368.7
TiF ₄	Crystal	-1649.3	-1611.1	-1559.2	-1290.3	134.0	338.7
TiI ₄	Crystal	-413.4	-453.0	-370.7	-164.6	246.1	486.6
TiI ₃	Crystal	-322.2	-385.7	-318.5	-149.2	192.5	368.5
TiI ₂	Crystal	-266.1	-310.1	-258.9	-129.6	122.6	253.7

^a H_r and G_r refer to the formation of the named substance in the named states at 298 K and 1300 K from their elements in the standard states of those elements at these temperature.

accompanied by the evolution of ca. 12.6 kJ/mol (3.01 kcal/mol), but the rate of transformation is greatly affected by temperature and by the presence of other substance which may either catalyze or inhibit the reaction. The lowest temperature at which conversion of anatase to rutile takes place at a measurable rate is ca. 700°C, but this is not a transition temperature. The change is not reversible; ΔG for the change from anatase to rutile is always negative (see Table 3.1 and 3.2 for thermodynamic data)

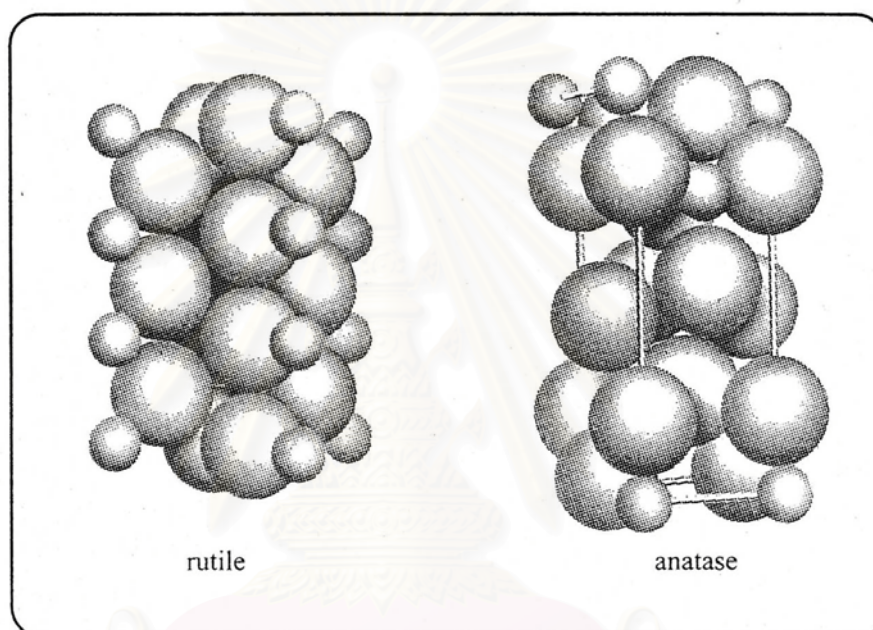


Figure 3.1 Crystal structure of TiO_2 . (Fujishima *et al.*, 1999)

Brookite has been produced by heating amorphous titanium (IV) oxide, prepared from an alkyl titanates of sodium titanate with sodium or potassium hydroxide in an autoclave at 200 to 600°C for several days. The important commercial forms of titanium (IV) oxide are anatase and rutile, and these can readily be distinguished by X-ray diffraction spectrometry.

Since both anatase and rutile are tetragonal, they are both anisotropic, and their physical properties, e.g. refractive index, vary according to the direction relative to the crystal axes. In most applications of these substances, the distinction between crystallographic direction is lost because of the random orientation of large numbers of small particles, and it is mean value of the property that is significant.

Table 3.3 Crystallographic properties of anatase, brookite, and rutile.

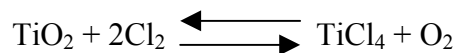
<i>Properties</i>	Anatase	Brookite	Rutile
Crystal structure	Tetragonal	Orthorhombic	Tetragonal
Optical	U n i a x i a l , negative	Biaxial, positive	U n i a x i a l , negative
Density, g/cm ³	3.9	4.0	4.23
Harness, Mohs scale	5 ^{1/2} – 6	5 ^{1/2} – 6	7 – 7 ^{1/2}
Unit cell	D _{4h} ¹⁹ .4TiO ₂	D _{2h} ¹⁵ .8TiO ₂	D _{4h} ¹² .3TiO ₂
Dimension, nm			
a	0.3758	0.9166	0.4584
b		0.5436	
c	0.9514	0.5135	2.953

Measurement of physical properties, in which the crystallographic directions are taken into account, may be made of both natural and synthetic rutile, natural anatase crystals, and natural brookite crystals. Measurements of the refractive index of titanium (IV) oxide must be made by using a crystal that is suitably orientated with respect to the crystallographic axis as a prism in a spectrometer. Crystals of suitable size of all three modifications occur naturally and have been studied. However, rutile is the only form that can be obtained in large artificial crystals from melts. The refractive index of rutile is 2.75. The dielectric constant of rutile varies with direction in the crystal and with any variation from the stoichiometric formula, TiO₂; an average value for rutile in powder form is 114. The dielectric constant of anatase powder is 48.

Titanium (IV) oxide is thermally stable (mp 1855°C) and very resistant to chemical attack. When it is heated strongly under vacuum, there is a slight loss of oxygen corresponding to a change in composition to TiO_{1.97}. The product is dark blue but reverts to the original white color when it is heated in air.

Hydrogen and carbon monoxide reduce it only partially at high temperatures, yielding lower oxides or mixtures of carbide and lower oxides. At ca. 2000°C and

under vacuum, carbon reduces it to titanium carbide. Reduction by metal, e.g., Na, K, Ca, and Mg, is not complete. Chlorination is only possible if a reducing agent is present; the position of equilibrium in the system is



The reactivity of titanium (IV) oxide towards acids is very dependant on the temperature to which it has been heated. For example, titanium (IV) oxide that has been prepared by precipitation from a titanium (IV) solution and gently heated to remove water is soluble in concentrated hydrochloric acid. If the titanium (IV) oxide is heated to ca. 900°C, then its solubility in acids is considerably reduced. It is slowly dissolved by hot concentrate sulfuric acid, the rate of salvation being increased by the addition of ammonium sulfate, which raises the boiling point of the acid. The only other acid in which it is soluble is hydrofluoric acid, which is used extensively in the analysis of titanium (IV) oxide for trace elements. Aqueous alkalies have virtually no effect, but molten sodium and potassium hydroxides, carbonates, and borates dissolve titanium (IV) oxide readily. An equimolar molten mixture of sodium carbonate and sodium borate is particularly effective as is molten potassium pyrosulfate.

3.3 Preparation procedure

large surface area titanium (IV) oxide powders have been prepared by several methods. The physical and chemical properties of titanium (IV) oxides are quite different by the process of preparation.

3.3.1 Chemical vapor deposition (CVD) method

Chemical vapor deposition (CVD) is a process to deposit solids in the form of a film or particles, using gaseous components. Extensive effort has been devoted to preparing ultrafine particles of metal, metal oxides and other inorganic compound. It is usual for the synthesis of particles by CVD method, to carry out the reaction at high-temperatures in order to avoid incomplete reaction. Attempts were made to use metal organic compounds as the starting material in CVD, which may lower the reaction temperature. One of the attractive features of the low temperature CVD is the

possibility of producing a material possessing a structure, which is unstable at high temperatures.

Ultrafine titanium (IV) oxide particles were prepared by chemical vapor deposition of titanium tetra isopropoxide. The particle formation reaction being catalyzed by titanium (IV) oxide deposit on the reaction wall, took place even at as low a temperature as 250°C, according to the stoichiometric relation as follows:



The titanium (IV) oxide particles were amorphous and porous, the specific surface area of which reached 300 m²g⁻¹.

3.3.2 Chloride process

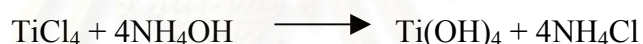
Ultrafine titanium (IV) oxide particles are produced routinely on a large scale by the oxidation of titanium tetrachloride (TiCl₄) vapor, it is so called “chloride process”. Reactions in the gas phase at the temperature range 700 to 1400°C, according to the stoichiometric relation of $\text{TiCl}_4 + \text{O}_2 \longrightarrow 2\text{Cl}_2$, result in the formation and growth of fine titanium (IV) oxide particles. Titanium (IV) oxide pigments that were produced by this method are used in coatings to provide maximum light scattering with actually no absorption.

Titanium (IV) oxide production from titanium tetrachloride vapor has been the force of experimental studies. Akntar et al. prepared titanium (IV) oxide particles from the oxidation of TiCl₄ in an aerosol reactor between 927 to 1450°C. The effect of process variables (reaction residence time, temperature and reactant concentration) on powder size and phase characteristics was investigated. They found that titanium particles were primarily anatase though the rutile weight fraction increase with increasing reaction temperature and the average particle size increased with increasing inlet TiCl₄ concentration, and residence time.

3.3.3 Precipitation method

Precipitation method involves the growth of crystals from a solvent of different composition to the crystal. The solvent may be one of the constituents of the desired crystals, e.g., crystallization of salt hydrate crystals using water as the solvent, or the solvent may be entirely separate liquid element or compound in which the crystals of interest are partially soluble, e.g., SiO₂ and various high melting silicates may be precipitated from low melting borate or halide melts. In these cases, the solvent melts are sometimes referred to as fluxed since they effectively reduce the melting point of the crystals by a considerable amount.

The method has recently been used to grow crystal of titanium (IV) oxide using titanium tetrachloride as starting material. Titanium (IV) oxide which, after washing and drying at 110°C, can be calcined at 800°C to remove combined water and chloride, according to the stoichiometric relation as follows:



This method used involves precipitation from titanium tetrachloride as hydrated titanium (IV) oxide conversion of the precipitate to the double oxalate, recrystallization of this from methanol and subsequent calcinations.

3.3.4 Sol-gel method

To prepare a solid using the sol-gel method, a sol is first prepared from a suitable reactants in a suitable liquid. Sol preparation can either be simply the dispersal of an insoluble solid or addition of a precursor which reacts with the solvent to form a colloid product. A typical example of the first is the dispersal of oxides or hydroxides in water with the pH adjusted so that the solid particles remain in suspension rather than precipitate out. A typical example of the second method is the addition of metal alkoxides to water. The alkoxides are hydrolyzed giving the oxide as a colloidal product. The sol is then either treated or simply left to form a gel. To obtain a final product, the gel is heated. This heating serves several purposes-it removes the solvent, it decomposes anions such as alkoxides or carbonates to give

oxides, it allows rearrangement of the structure of the solid and it allows crystallization to occur.

3.3.5 *Hydrothermal method* (West, 1999)

The method involves heating the reactants in water/steam at high pressures and temperatures. The water performs two roles, as a pressure-transmitting medium and as a solvent, in which the solubility of the reactants is P, T-dependent. In addition, some or all of the reactance are partially soluble in the water under pressure and this enables reaction to take place in, or with the aid of, liquid and/or vapor phases. Under these conditions, reactions may occur that, in the absence of water, would occur only at much high temperatures. The method is therefore particularly suited for the synthesis of phases that are unstable at higher temperatures. It is also a useful technique for growth of single crystals; by arranging for a suitable temperature gradient to be present in the reaction vessel, dissolution of the starting material may occur at the hot end and reprecipitation at the cooler end.

The design of hydrothermal equipment is basically a tube, usually of steel, closed at one end. The other end has a screw cap with a gasket of soft copper to provide a seal. Alternatively, the 'bomb' may be connected directly to an independent pressure source, such as a hydraulic ram; this is known as the 'cold seal' method. The reaction mixture and an appropriate amount of water are placed inside the bomb, which then sealed and placed inside an oven at the required temperature, usually at a temperature in the range 100-500°C. Pressure is controlled either externally or by the degree of filling in a sealed bomb. By making use of the P/T 'phase diagram', Figure 3.3(a); curve AB is the saturated steam curve and separates water (above) from steam (below); at temperatures above 374°C, point B, the water is in the supercritical condition and there is no distinction between liquid and vapor states.

The applications of the hydrothermal method is:

(a) Synthesis of new phases: calcium silicate hydrate.

Hydrothermal methods have been used successfully for the synthesis of many materials. A good example is the family of calcium silicate hydrates, many of which are important components of set cement and concrete. Typically, lime, CaO and quartz, SiO₂, are heated with water at temperatures in the range 150 to 500°C and pressure of 0.1 to 2 kbar. Each calcium silicate hydrate has, for its synthesis, optimum preferred conditions of composition of starting mix, temperature, pressure and time. For example, xonolite, Ca₆Si₆O₁₇(OH)₂, may be prepared by heating equimolar mixtures of CaO and SiO₂ at saturated steam pressures in the range 150 to 350°C.

(b) Growth of single crystals.

For the growth of single crystals by hydrothermal methods it is often necessary to add a mineralizer. A mineralizer is any compound added to the aqueous solution that speeds up its crystallization. It usually operates by increasing the solubility of the solute through the formation of soluble species that would not usually be present in the water. For instance, the solubility of quartz in water at 400°C and 2 kbar is too small to permit the recrystallization of quartz, in a temperature gradient, within a reasonable space of time. On addition of NaOH as a mineralizer, however, large quartz crystals may be readily grown. Using the following conditions, crystals of kilogram size have been grown: quartz and 1.0 M NaOH solution are held at 400°C and 1.7 kbar; at this temperature some of the quartz dissolves. A temperature gradient is arranged to exist in the reaction vessel and at 360°C the solution is supersaturated with respect to quartz, which precipitates onto a seed crystal. In summary, therefore, quartz dissolves in the hottest part of the reaction vessel, is transported throughout the vessel via convection currents and is precipitated in cooler parts of the vessel where its solubility in water is lower. Quartz single crystals are used in many devices in radar and sonar, as piezoelectric transducers, as monochromators in X-ray diffraction, etc. Annual world production of quartz single crystals, using hydrothermal and other methods, is currently a staggering 600 tons.

Using similar methods, many substances have been prepared as high quality single crystals, e.g. corundum (Al_2O_3) and ruby (Al_2O_3 doped with Cr^{3+}).

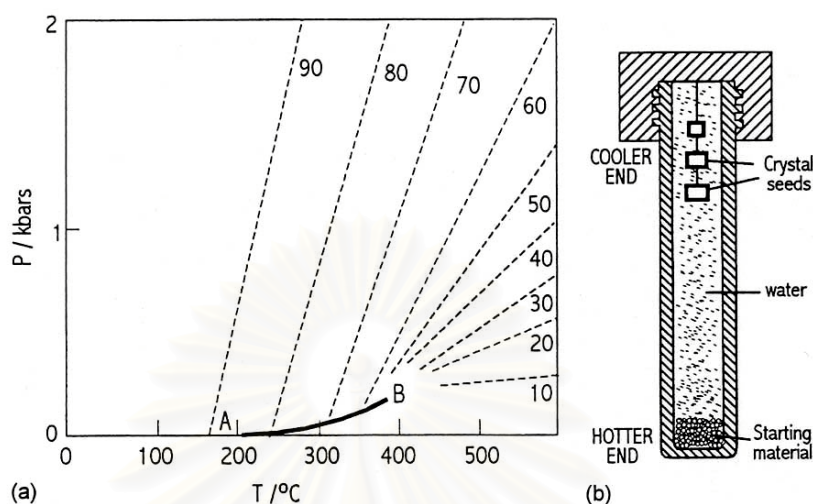


Figure 3.2 (a) Pressure-temperature relations for water at constant volume, dashed curves represent pressures developed inside a close vessel; numbers represent the percentage degree of filling of the vessel by water at ordinary P, T. (b) Schematic hydrothermal bomb used for crystal growth.

3.3.6 Glycothermal and solvothermal method

Glycothermal method and solvothermal method have been developed for synthesis of metal oxide and binary metal oxide by using glycol and solvent as the reaction medium, respectively. The use of glycol or solvent instead of water in the hydrothermal method produced the different form of intermediate phase and the stability of such intermediate phase was not strong. Instability of the intermediate phase gives a large driving force to the formation of product under quite mild condition. The preparation method is described in the experimental section, Chapter IV.

3.4 Single crystal (McGraw-Hill encyclopedia of science & technology, 1997)

In crystalline solids the atoms or molecules are stacked in a regular manner, forming a three-dimensional pattern, which may be obtained by a three-dimensional repetition of a certain pattern unit called a unit cell. When the periodicity of the pattern extends throughout the certain piece of material, one speaks of a single crystal. A single crystal is formed by the growth of a crystal nucleus without secondary nucleation or impingement on other crystal.

3.4.1 Growth techniques

Among the most common methods of growing single crystals are those of P. Bridgeman and J. Czochralski. In the Bridgeman method the material is melted in a vertical cylindrical vessel, which tapers conically to a point at the bottom. The vessel then is lowered slowly into a cold zone. Crystallization begins in the tip and continues usually by growth from the first formed nucleus. In the Czochralski method a small single crystal (seed) is introduced into the surface of the melt and then drawn slowly upward into a cold zone. Single crystals of ultrahigh purity have been grown by zone melting. Single crystals are also often grown by bathing a seed with a supersaturated solution, the supersaturation being kept lower than necessary for sensible nucleation.

When grown from a melt, single crystals usually take the form of their container. Crystals grown from solution (gas, liquid, or solid) often have a well-defined form, which reflects the symmetry of the unit cell. For example, rock salt or ammonium chloride crystals often grow from solutions in the form of cubes with faces parallel to the 100 planes of the crystal, or in the form of octahedrons with faces parallel to the 111 planes. The growth form of crystals is usually dictated by kinetic factors and does not correspond necessarily to the equilibrium form.

3.4.2 Physical properties

Ideally, single crystals are free from internal boundaries. They give rise to a characteristic x-ray diffraction pattern. For example, the Laue pattern of a single crystal consists of a single characteristic set of sharp intensity maxima.

Many types of single crystal exhibit anisotropy, that is, a variation of some of their physical properties according to the direction along which they are measured. For example, the electrical resistivity of a randomly oriented aggregate of graphite crystallites is the same in all directions. The resistivity of a graphite single crystal is different, however, when measured along crystal axes. This anisotropy exist both for structure-sensitive properties, which are strongly affected by crystal imperfections (such as cleavage and crystal growth rate), and structure-insensitive properties, which are not affected by imperfections (such as elastic coefficients).

Anisotropy of a structure-insensitive property is described by a characteristic set of coefficients, which can be combined to give the macroscopic property along any particular direction in the crystal. The number of necessary coefficients can often be reduced substantially by consideration of the crystal symmetry, whether anisotropy, with respect to a given property, exists depends on crystal symmetry. The structure-sensitive properties of crystals (for example, strength and diffusion coefficients) seem governed by internal defects, often on an atomic scale.



สถาบันวิทยบริการ
จุฬาลงกรณ์มหาวิทยาลัย

CHAPTER IV

EXPERIMENTAL

The synthesis of titania by using organic solvent is explained in this chapter. The chemicals and reaction apparatus are shown in sections 4.1 and 4.2, respectively. In sections 4.3 and 4.4, the catalyst preparation and characterization are explained.

4.1 Chemicals

This synthesis mixtures are prepared with the following reagent:

1. Titanium (IV) tert-butoxide (TNB, $\text{Ti}[\text{O}(\text{CH}_2)_3\text{CH}_3]_4$) available from Aldrich, 97%
2. Tetraethyl orthosilicate (TEOS, $\text{Si}(\text{OC}_2\text{H}_5)_4$) available from Aldrich, 98%
3. Aluminium isopropoxide (AIP, $[(\text{CH}_3)_2\text{CHO}]_3\text{Al}$) available from Aldrich, 98+%
4. Triethyl phosphate (TEPP, $\text{C}_6\text{H}_{15}\text{O}_4\text{P}$) available from Merck, >99%
5. 1,4 Butanediol (1,4-BG, $\text{HO}(\text{CH}_2)_4\text{OH}$) available from Aldrich, 99%
6. Toluene ($\text{C}_6\text{H}_5\text{CH}_3$) available from APS Finechem, 100%

Table 4.1 Reagents used for the synthesis of titania

Reagents	Weight/Volume
TNB (various starting material concentrations)	5, 7.5, 10, 15, 25 g
TEOS ^a (basis on TNB 15g)	
For Si/Ti = 0.005	0.0445 g
Si/Ti = 0.04	0.3635 g
Si/Ti = 0.06	0.5344 g
Si/Ti = 0.08	0.7270 g
AIP ^a (basis on TNB 15g)	
For Al/Ti = 0.005	0.0450 g
Al/Ti = 0.04	0.3601 g
Al/Ti = 0.06	0.5401 g
Al/Ti = 0.08	0.7201 g

^a Calculation of catalyst preparation, APPENDIX A

Table 4.1 (cont.) Reagents used for the synthesis of titania

Reagents	Weight/Volume
TEPP ^a (basis on TNB 15g)	
For P/Ti = 0.005	0.0393 g
P/Ti = 0.04	0.3146 g
P/Ti = 0.06	0.4720 g
P/Ti = 0.08	0.6293 g
Organic solvents (1,4-BG, toluene)	
In the synthesis mixtures	100 cm ³
In the gap	30 cm ³

^a Calculation of catalyst preparation, APPENDIX A

4.2 Equipment

The equipment for the synthesis of titania consisted of:

4.2.1 Autoclave reactor

- Made from stainless steel
- Volume of 1000 cm³
- 10 cm inside diameter
- Maximum temperature of 350°C
- Pressure gauge in the range of 0-140 bar
- Relief valve used to prevent runaway reaction
- Iron jacket was used to reduce the volume of autoclave to be 300 cm³
- Test tube was used to contain the reagent and glycol

The autoclave reactor is shown in Figure 4.1

4.2.2 Temperature program controller

A temperature program controller CHINO DB1000F was connected to a thermocouple with 0.5 mm diameter attached to the reagent in the autoclave.

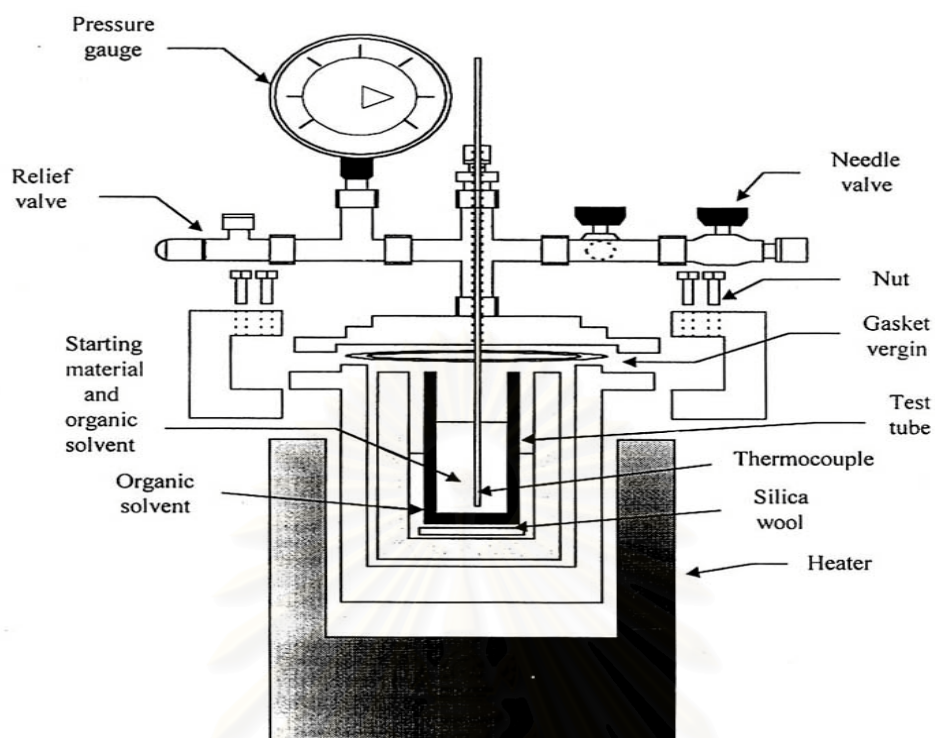


Figure 4.1 Autoclave reactor

4.2.3 Electrical furnace (Heater)

Electrical furnace supplied the required heat to the autoclave for the reaction.

4.2.4 Gas controlling system

Nitrogen was set with a pressure regulator (0-150 bar) and needle valves are used to release gas from autoclave.

The diagram of the reaction equipment for synthesis of zirconia is shown in Figure 4.2

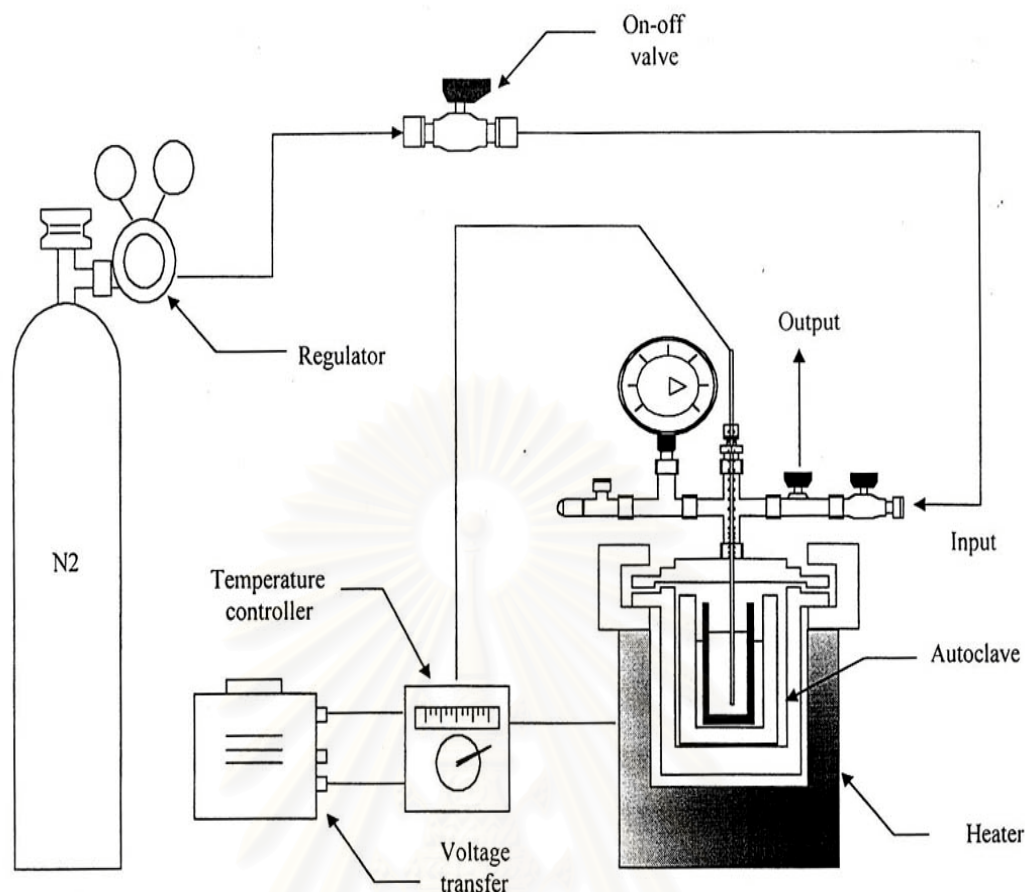


Figure 4.2 Diagram of the reaction equipment for the synthesis of titania

4.3 Preparation of titania

Titania was prepared by using TNB for various starting material. The starting material were suspended in 100 ml of solvent and in the test tube, and then set up in an autoclave. In the gap between the test tube and autoclave wall, 30 ml of solvent was added. After the autoclave was completely purged with nitrogen, the autoclave was heated to desired temperature (200°C - 300°C) at the rate of $2.5^{\circ}\text{C min}^{-1}$ and held at that temperature for 2 hours. In this study, beside the reaction temperature, the reaction time was also varied from 0-4 hours. Autogeneous pressure during the reaction gradually increased as the temperature was raised. After the reaction, the autoclave was cooled to room temperature. The resulting powders were collected after repeated washing with methanol by centrifugation. They were then air-dried.

For the synthesis of second element modified titania, the method are the same with that to obtain pure titania whereas the mixture of TNB 15 g and an amount of TEOS at Si/Ti molar ratio of 0.005-0.08 or AIP at Al/Ti molar ratio of 0.005-0.08 or TEPP at P/Ti molar ratio of 0.005-0.08 were used as the starting material (see Appendix A).

The calcination of the thus-obtained product was carried out in a box furnace. The product was heated at a rate of $10^{\circ}\text{C min}^{-1}$ to a desired temperature and held at that temperature for 1 hour.

4.4 Characterization

4.4.1 X-ray diffraction spectroscopy (XRD)

The X-ray diffraction (XRD) patterns of powder were performed by Siemens D5000 X-ray diffractometer at Center of Excellences on Catalysis and Catalytic Reaction Engineering, Chulalongkorn University. The experiments were carried out by using Ni-filtered $\text{CuK}\alpha$ radiation. The crystallite size was estimated from line broadening according to the Scherrer equation (see Appendix B) and $\alpha\text{-Al}_2\text{O}_3$ was used as standard.

4.4.2 Scanning electron microscopy (SEM)

The morphology and size of secondary particle of the samples were observed by Scanning electron microscopy (SEM). Model of SEM for experiments: JSM-5410LV at the Scientific and Technological Research Equipment Center, Chulalongkorn University (STREC).

4.4.3 Surface area measurement

The multipoint BET surface area of the samples were measured by a micromeritics model ASAP 2000 using nitrogen as the adsorbate at the Analysis Center of the Department of Chemical Engineering, Faculty of Engineering, Chulalongkorn University. The operating conditions are as follows:

Sample weight	~ 0.3 g
Degas temperature	200°C for as-synthesized sample 300°C for calcined sample
Vacuum pressure	< 10 μ mHg

4.4.5 Infrared Spectroscopy (IR)

The functional group in the samples was determined by using Infrared spectroscopy. Before measurement, the sample was mixed with KBr and then was formed into a thin wafer. Model of IR for experiments: Nicolet impact 400 at Center of Excellences on Catalysis and Catalytic Reaction Engineering, Chulalongkorn University

4.4.6 Thermalgravimetric analysis (TGA)

The weight loss pattern of the samples during heating up was analyzed by Shimadzu TGA model 50. The sample was loaded in a platinum pan located in a furnace. The purging gas were N₂ with flow rate 30 ml/min and Air with flow rate 100 ml/min. The furnace temperature was programmed to rise from room temperature to 600 °C at a constant rate of 10 °C/min. The data were displayed and record using a microcomputer.

CHAPTER V

RESULTS AND DISCUSSION

The nanocrystal titanium (IV) oxide (titania) obtained in this work were synthesized from Titanium tert-butoxide (TNB) mixed with organic solvents, 1,4 butanediol or toluene, in an autoclave under autogenous pressure. The procedure is the so-call solvothermal method. Titania prepared in each organic solvent have different physical properties and thermal stability (Sornnarong Theinkaew, 2000 : 70).

5.1 Formation of Titanium (IV) oxide

5.1.1 Synthesis in 1,4-butanediol

Titanium (IV) oxide has been synthesized in 1,4-BG at 300°C for various reaction times, Glycothermal Method. Under glycothermal conditions, titanium (IV) tert-butoxide (TNB) was easily converted to glycoxide. Thermal decomposition of the glycoxide molecule was occurred by intramolecular participation of the remaining hydroxyl group of glycol moiety and subsequently a $\equiv\text{Ti}-\text{O}^-$ anion was formed. The nucleophilic attack of this titanate ion on another ion and crystallization of titanium (IV) oxide were taken place. The mechanism of TNB in 1,4-BG can be depicted in Figure 5.1.

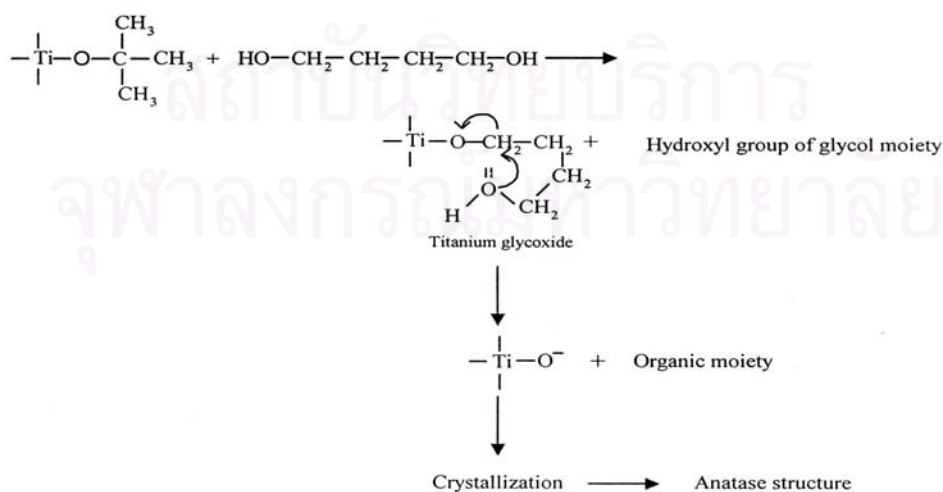


Figure 5.1 Mechanism of glycothermal reaction for the anatase formation (Sornnarong Theinkaew, 2000 : 70).

5.1.1.1 The effect of reaction time

The as-synthesized nanocrystallite titania products were synthesized by reaction in 1,4-BG at 300°C for various reaction times (0, 0.25, 0.5, 1, 2, or 4 h). XRD patterns indicated that the as-synthesized products were the anatase phase for all of the products as shown in Figure 5.2. These confirmed that the reaction yielded the anatase titania products and non-contaminate with other phases such as brookite or rutile. Although the reaction time at 300°C was not hold, the product was still the anatase titania. It was indicated that at this temperature the reaction decomposed completely and yielded certainly the titania product. Drop of water into the clear reacted solvent shown that the white fine particle not occurred. These confirmed absolutely that the reaction was complete at this temperature. Because if the metal alkoxide remains in the reacted solvent, it will react with water to form metal oxide (Sornnarong Theinkeaw, 2000 : 71).

The titania products were characterized by SEM for analyzing morphology of the products as shown in Figure 5.3. SEM results indicate that morphology of the secondary particle which a shape was irregular particle is not change with increasing the reaction time.

Table 5.1 shows the crystallite sizes calculated from XRD patterns at the 101 diffraction peak of anatase titania by Sherrer equation (Kominami *et al.*, 1997; Yang *et al.*, 2001; Iwamoto *et al.*, 2001) and the specific surface area of titania by BET measurement. For no holding the reaction time, the crystallite size and BET surface area of the as-synthesized product were 10 nm and 150 m²/g, respectively. When the reaction time was prolonged, the crystallite size was gradually increase. It should be noted that the growth of anatase crystal gradually proceeded in the reaction (Kominami *et al.*, 1997). Alternatively, the surface area which was calculated from diameter size of the crystal, became 142 m²/g. It was noted that the equation was used to calculate as $6/d_p$ on assumption that the crystal is nonporous spherical crystal (Kominami *et al.*, (1999). Interestingly, the obtained surface area was not different from BET surface area. These identify that the titania product is not contaminate with amorphous-like phase or organic phase as shown through ratio of S_1/S_2 in Table 5.1

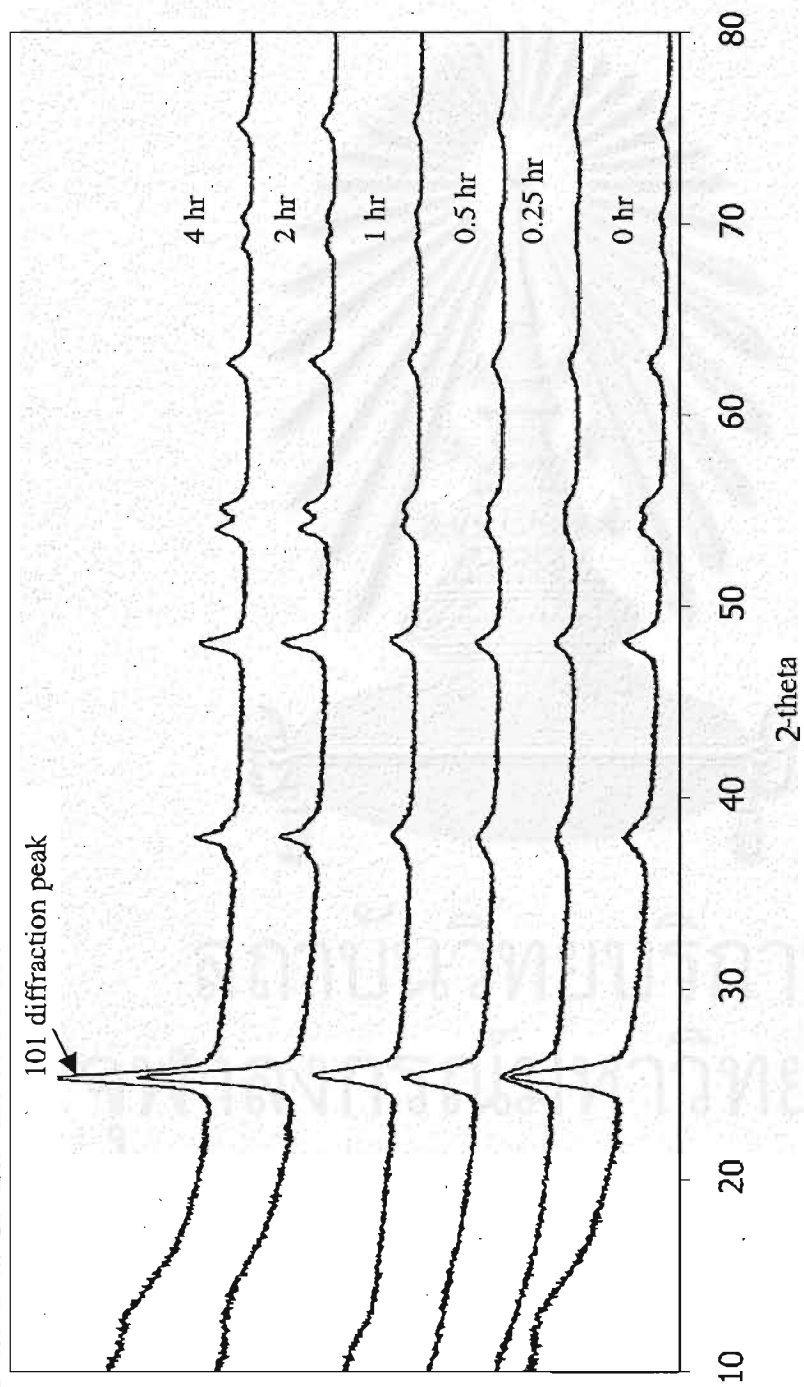


Figure 5.2 XRD patterns of titania product that synthesized in 1,4-BG for various reaction time. All of as-synthesized were anatase titania without contamination of other phase such as brookite or rutile.

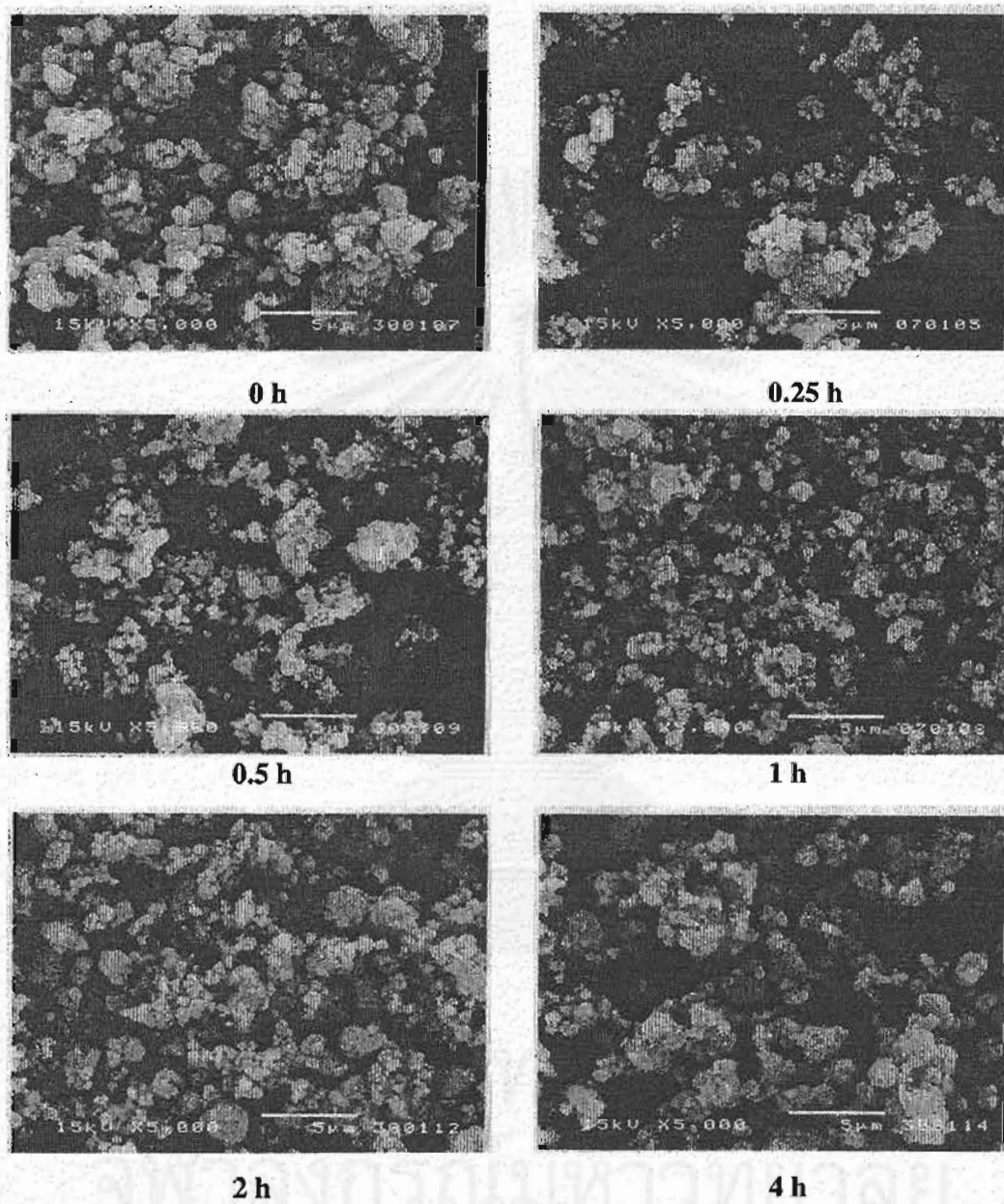


Figure 5.3 SEM morphology of titania products synthesized in 1,4-BG for various reaction times. The morphology of as-synthesized titania were irregular shape not depended on the reaction time.

(S_1 is BET surface area and S_2 is surface area calculated). Kominami *et al.* (1997) synthesized titania from the solvothermal method. They calculated the surface area from the crystallite size by assuming the density of anatase to be 3.84 g cm^{-3} . They found that the surface area obtained from BET measurement was larger than that calculated from the crystallite size and suggested that the product was contaminated with the amorphous-like phase.

For other reaction times, the approximate unity of S_1/S_2 ratio implied that the products were without the amorphous phase. When the reaction time was increased, the specific surface area decreased but the crystallite size increased slightly.

Table 5.1 Crystallite size and surface area of titania products synthesized in 1,4-BG.

Reaction time (hr)	Crystallite size (nm)	surface area (m^2/g)		S_1/S_2
		S_1^a	S_2^b	
0	10	150	154	1.0
0.25	9	170	171	1.0
0.5	9	166	171	1.0
1	11	128	140	0.9
2	13	110	118	0.9
4	15	100	103	1.0

^a Specific BET surface area from BET measurement.

^b Specific surface area calculated from equation of $6/d\rho$ on assumption that the crystal is spherical particle and the density of anatase titania is 3.9 g cm^{-3} .

Figure 5.4 shows the relative pressure of N_2 adsorption and desorption of the titania products from BET measurement. These titanias showed type IV isotherm, with hysteresis loop due to capillary condensation, which indicates that the secondary particle of titania are mesoporous materials. The isotherms afforded by these materials could be more precisely attributed to one of two subcategories in type IV isotherms: H2, usually found in materials with cross-link porous system, and H3, normally assigned to slit-shape pores (see APPENDIX C). Adsorption at low relative pressure increased weakly, suggesting the presence of a small amount of micropores (Mariscal *et al.*, 2000). So that, the relative pressure of N_2 adsorption and desorption showed

that the products consisted of mesopores and micropores and that the pore were open-end pore structure. For without holding the reaction time, the pore structure was mainly a ink bottle pore. However, the pore structure was arranged to form cylinder pore with increasing the reaction time (Gregg and Sing, 1982). These support that the reaction time affected to pore structure of titania products.

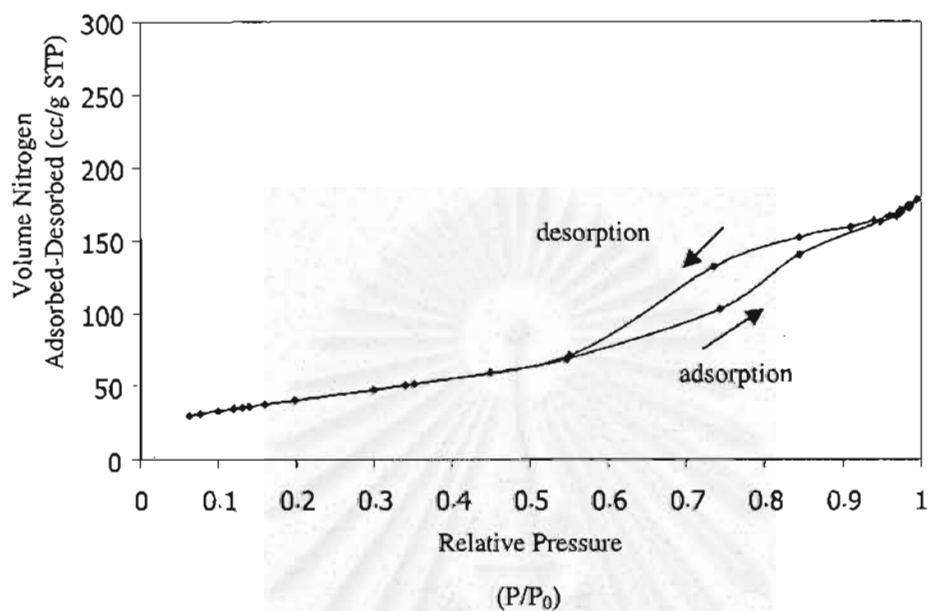
Table 5.2 shows pore volumes and average pore diameters of the titania products for various reaction times. When the reaction time was prolonged, the pores were expanded. From this table, the pore volumes were constant and independent on the reaction time. On the other hand, the average pore diameters slightly increased with increasing the reaction time. These results were in agreement with the relative pressure plots and the product was therefore arranged to be crystallite structure.

Table 5.2 Pore volume and average pore diameter of titania products synthesized in 1,4-BG for various reaction time.

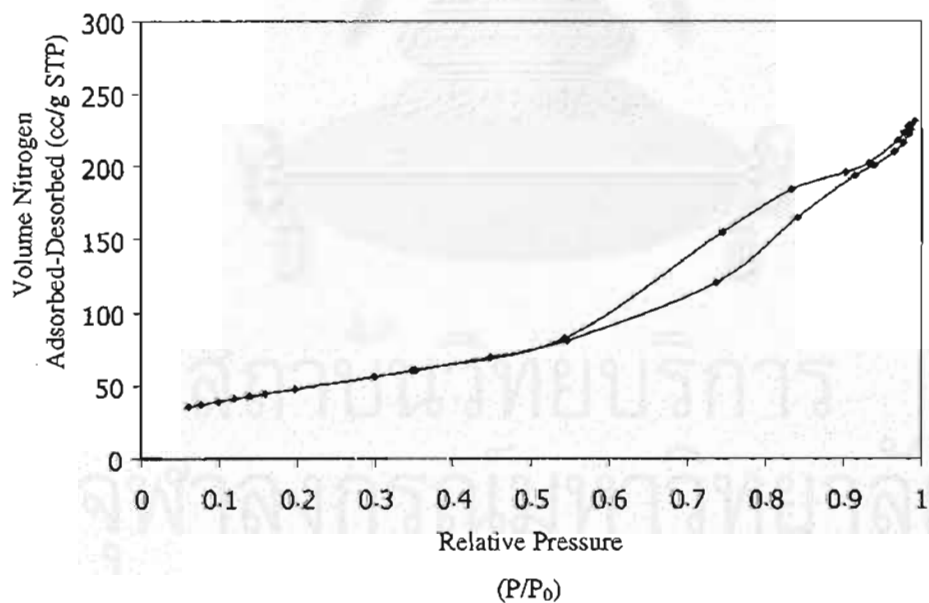
<i>Reaction time (hr)</i>	<i>Pore volume (cc/g)^a</i>	<i>Average pore diameter (nm)^b</i>
0	0.3	5
0.25	0.4	6
0.5	0.4	7
1	0.4	10
2	0.4	11
4	0.4	13

^a BJH cumulative desorption pore volume of pores

^b BJH desorption average pore diameter (4V/A)

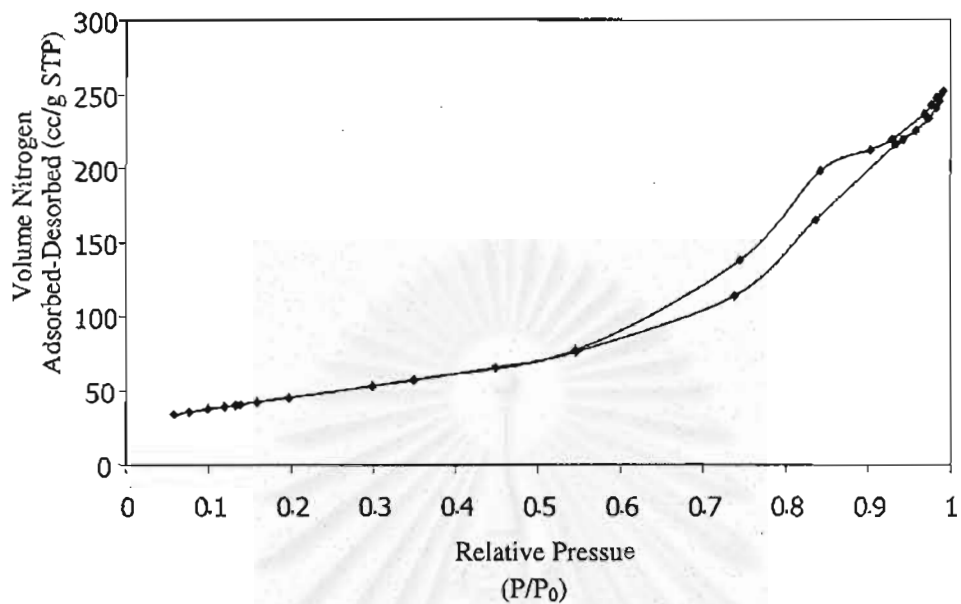


0 h, 10nm, the pore structure is ink bottle open-end pore structure.

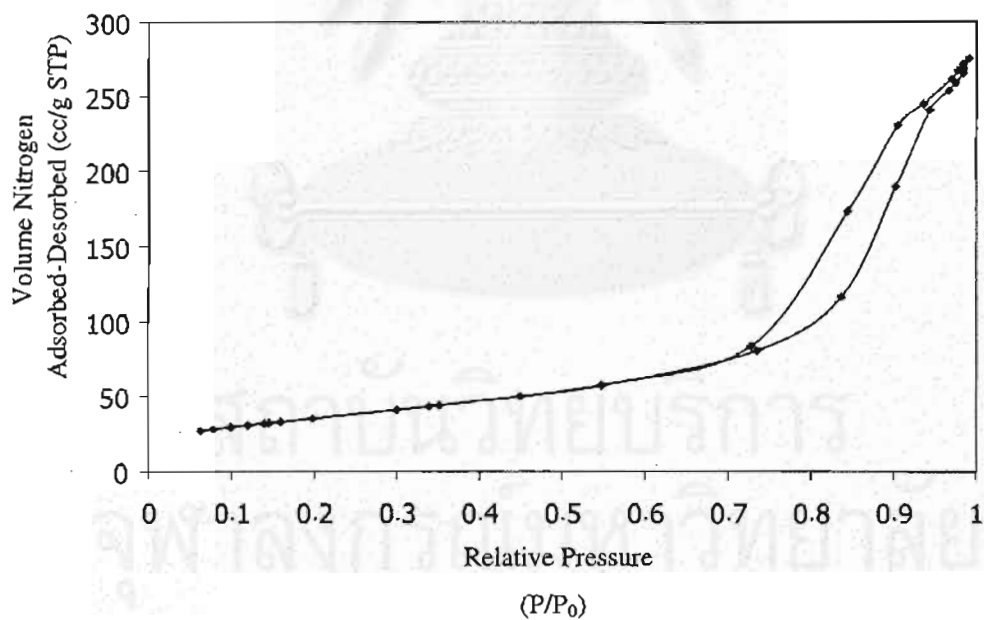


0.25 h, 9nm, the pore structure is the ink bottle open-end pore structure.

Figure 5.4 Nitrogen adsorption-desorption isotherm of titania products synthesized in 1,4-BG for various reaction times and crystallite sizes. (see APPENDIX C)

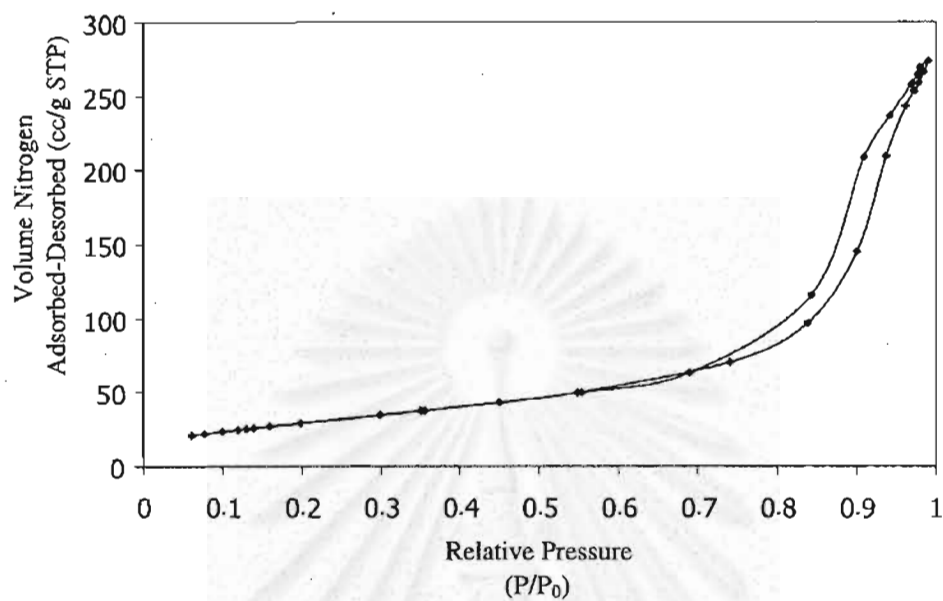


0.5 h, 9 nm, the pore structure is ink bottle open-end pore structure.

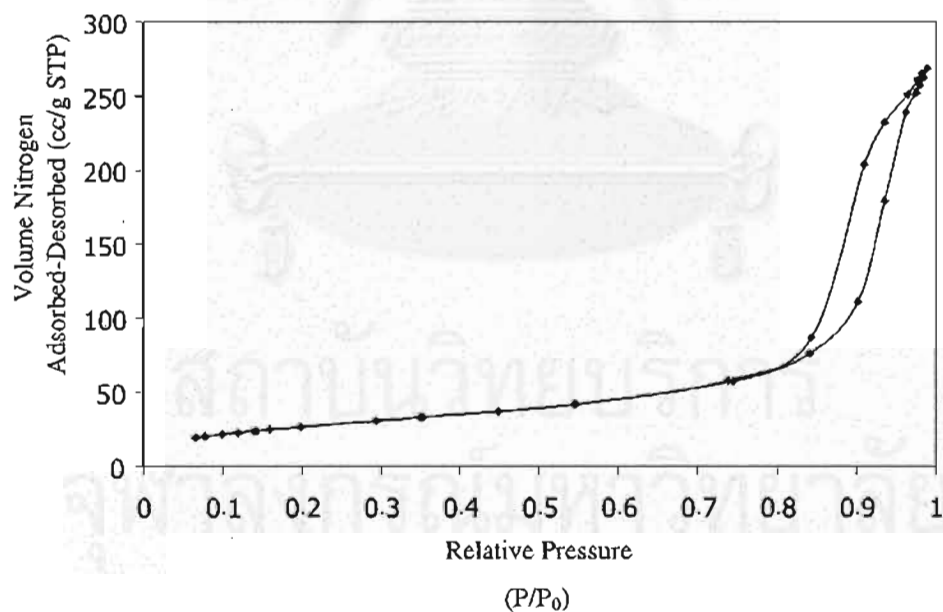


1 h, 11 nm, the pore structure is ink bottle open-end pore structure.

Figure 5.4 (cont.) Nitrogen adsorption-desorption isotherm of titania products synthesized in 1,4-BG for various reaction times and crystallite sizes.



2 h, 13 nm, the pore structure is cylindrical open-end pore structure.



4 h, 15 nm, the pore structure is cylindrical open-end pore structure.

Figure 5.4 (cont.) Nitrogen adsorption-desorption isotherm of titania products synthesized in 1,4-BG for various reaction times and crystallite sizes.

Figure 5.5 shows pore size distributions of titania products in 1,4-BG for various reaction times. When the reaction time was increased, the profile of pore size distribution was shifted to a wider pore diameter. However, the pattern of distribution curves were not changed. These results suggest that change of reaction time affected directly the arrangement of pore structure.

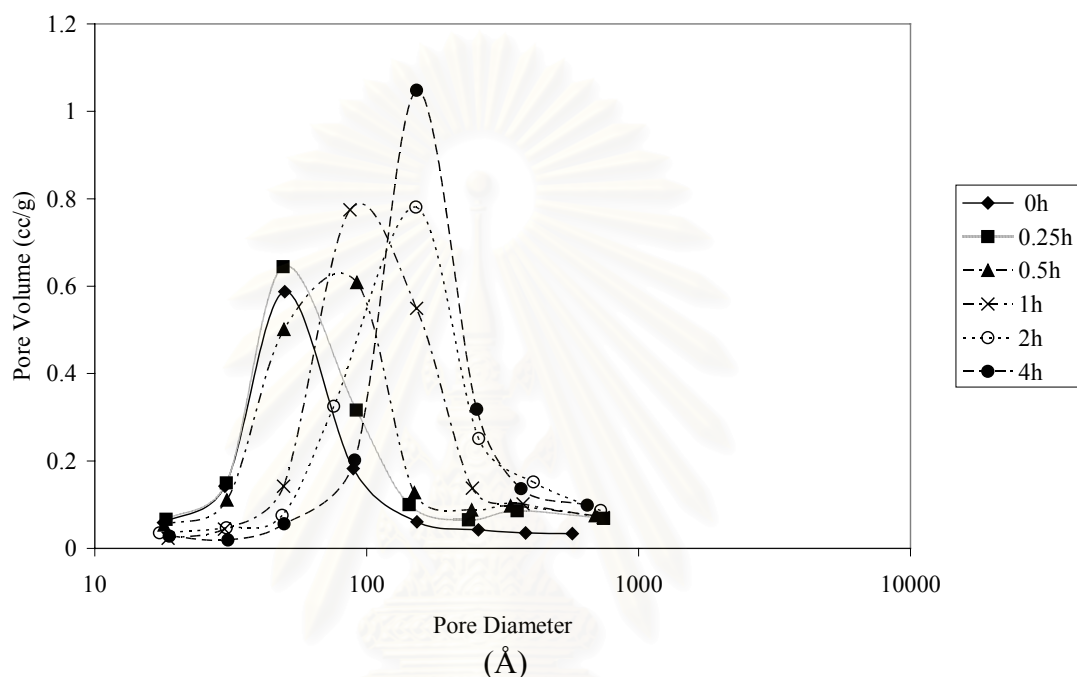


Figure 5.5 Pore size distribution of titania products synthesized in 1,4-BG for various reaction times.

5.1.1.2 Effect of the starting material concentration

In this part, various TNB concentrations was used to react with 100 ml of 1,4-BG at 300°C for 2 hrs. These concentrations were varied as 5, 7.5, 10, 15, and 25 g. All of the as-synthesized titanias yielded the anatase titania products. Evidence was obtained from XRD patterns of anatase phase without the other phases of titania as illustrated in Figure 5.6. SEM morphology show that the secondary particle size was not changed with increasing the TNB concentration as showed in Figure 5.7.

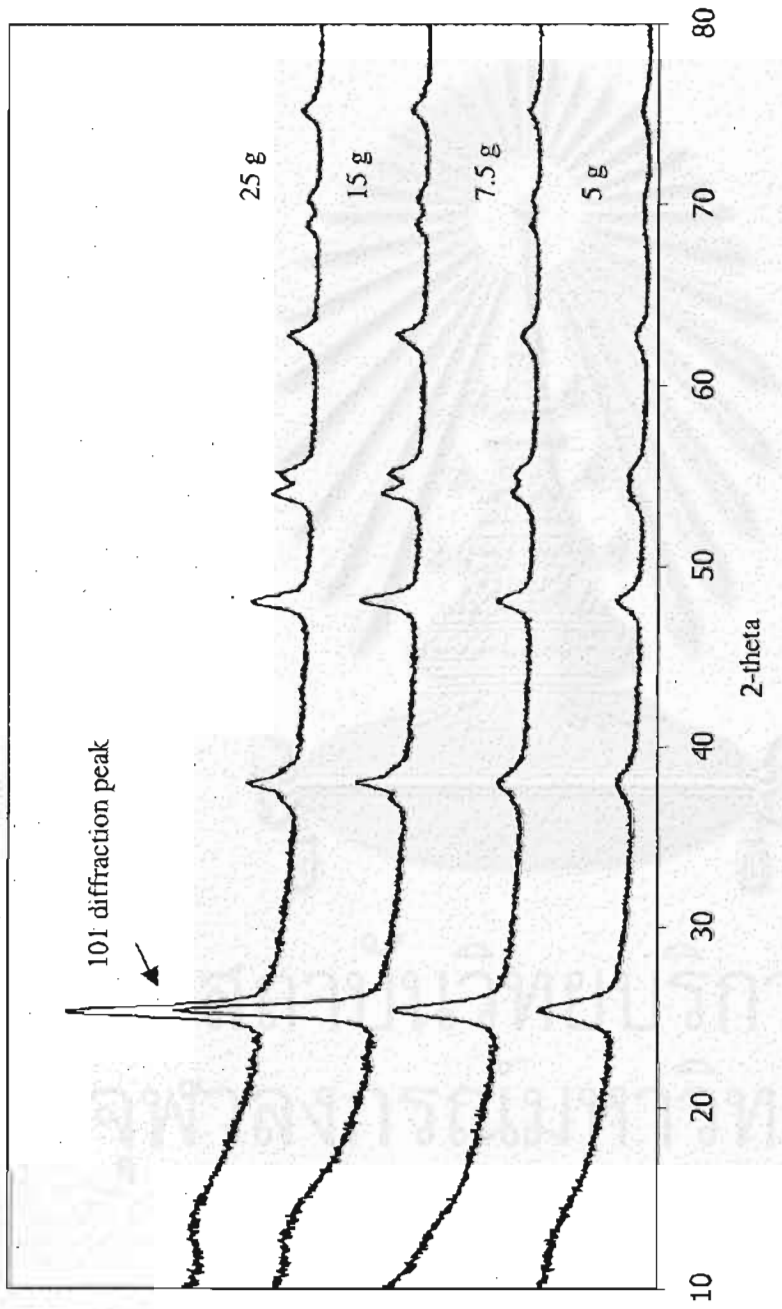


Figure 5.6 XRD pattern of titania products synthesized in 1,4-BG for various concentrations of starting material. All as-synthesized were the anatase titania phase without contamination of other phase.

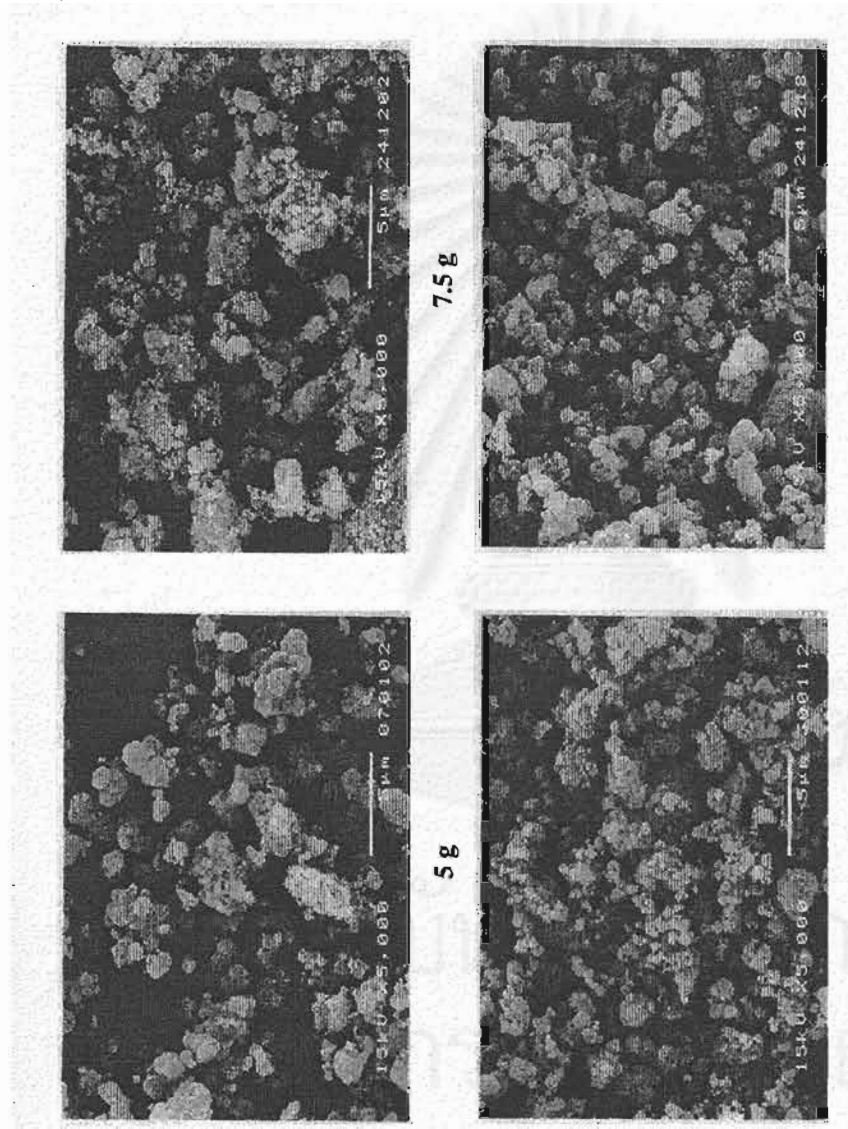


Figure 5.7 SEM image of titanium product synthesized in 1,4-BG for various concentrations of starting material. The morphology of all as-synthesized were irregular shape of secondary particle and not depended on the amount of the starting material.

Table 5.3 shows the crystallite size and the specific surface areas of the titania products. The crystallite size was increased with an increasing of the concentration of the starting material. Alternatively, at the concentration more than 15 g the crystallite size was constant as 13 nm. A little change of the BET surface area could confirm this as well.

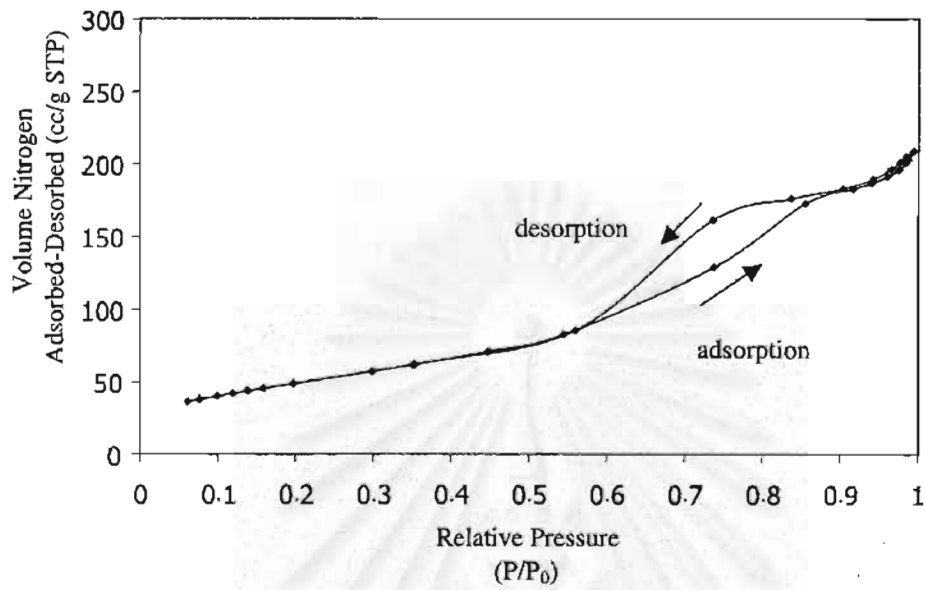
Table 5.3 Crystallite size and surface area of titania products synthesized for various reactant concentration

<i>R e a c t a n t</i> <i>concentration</i> <i>(g/100ml)</i>	<i>Crystallite</i> <i>size (nm)</i>	<i>surface area (m²/g)</i>		<i>S₁/S₂</i>
		<i>S₁^a</i>	<i>S₂^b</i>	
5	8	179	192	0.9
7.5	10	139	154	0.9
10	12	105	128	0.8
15	13	110	118	0.9
25	13	105	118	0.9

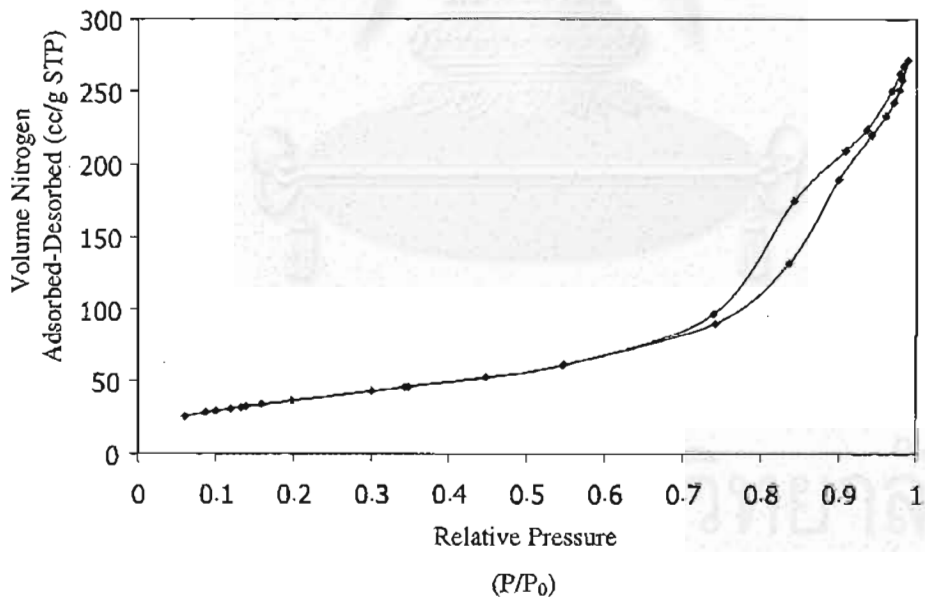
^a Specific BET surface area from BET measurement.

^b Specific surface area calculated from equation of $6/d\rho$ on assumption that the crystal is spherical particle and the density of anatase titania is 3.9 g cm^{-3} .

Figure 5.8 shows the relative pressure of N₂ adsorption and desorption in various concentrations. The synthesized products in various concentrations contained both mesopore and micropore, which their pore structure was open-end pore. However, at low concentration the pore structure was ink bottle pore but at high concentration it became cylinder pore. In addition, the lower concentration of starting material, the smaller pore size.

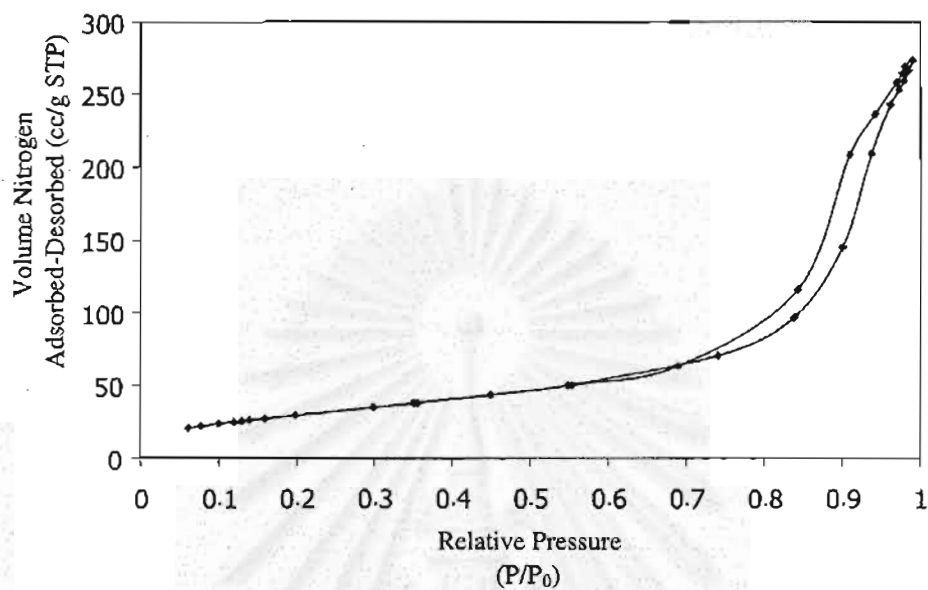


5 g, 8 nm, the pore structure is ink bottle open-end pore.

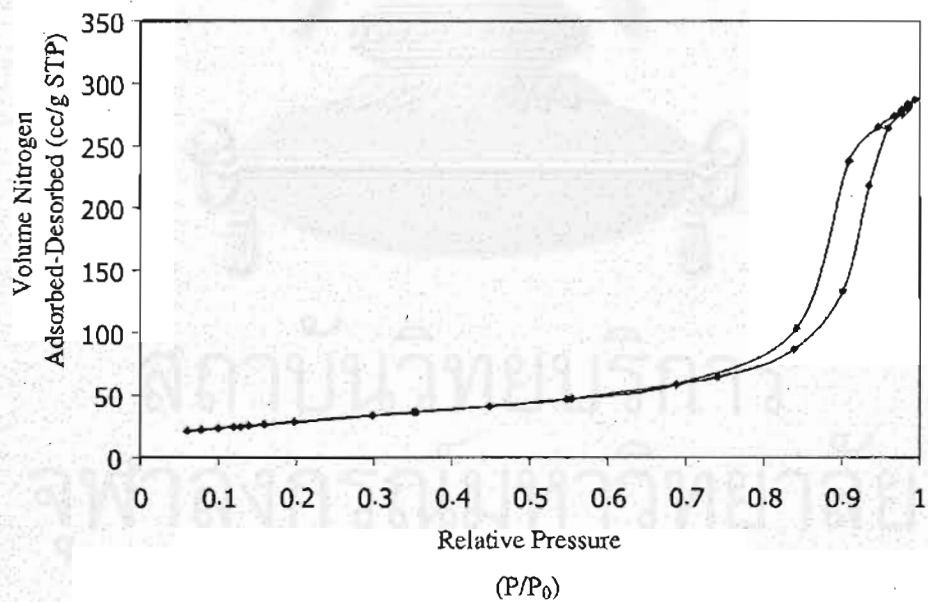


7.5 g, 10 nm, the pore structure is mainly ink bottle open-end pore.

Figure 5.8 Nitrogen adsorption-desorption isotherm of titania products synthesized in 1,4-BG for various concentrations of starting material and crystallite sizes. (see APPENDIX C)



15 g, 13 nm, the pore structure is cylindrical open-end pore.



25 g, 13 nm, the pore structure is cylindrical open-end pore.

Figure 5.8 (cont.) Nitrogen adsorption-desorption isotherm of titania products synthesized in 1,4-BG for various concentrations of starting material and crystallite sizes.

Table 5.4 shows pore volume and average pore diameter of titania products synthesized in 1,4-BG for various concentrations. When concentration of starting material was increased, the pore volume approach about 0.4 cc/g and was kept constant at this value. Thus, the pore volume does not depend on the TNB concentration. Alternatively, an increase of average pore diameter confirmed that the titania was formed to single crystal or the titania product was segregated.

Table 5.4 Pore volume and average pore diameter of titania products synthesized in 1,4-BG for various concentrations.

<i>R e a c t a n t concentration (g/100ml)</i>	<i>Pore volume (cc/g)^a</i>	<i>Average pore diameter (nm)^b</i>
5	0.3	5
7.5	0.4	9
10	0.4	12
15	0.4	11
25	0.4	12

^a BJH cumulative desorption pore volume of pores

^b BJH desorption average pore diameter (4V/A)

Figure 5.9 shows the pore size distribution of titania synthesized in 1,4-BG for various concentrations. When concentration of starting material was increased, pore size of the product was shifted to the higher pore diameter. Alternatively, the pattern of distribution curves did not change. An increase of average pore diameter suggested aggregation of the crystal.

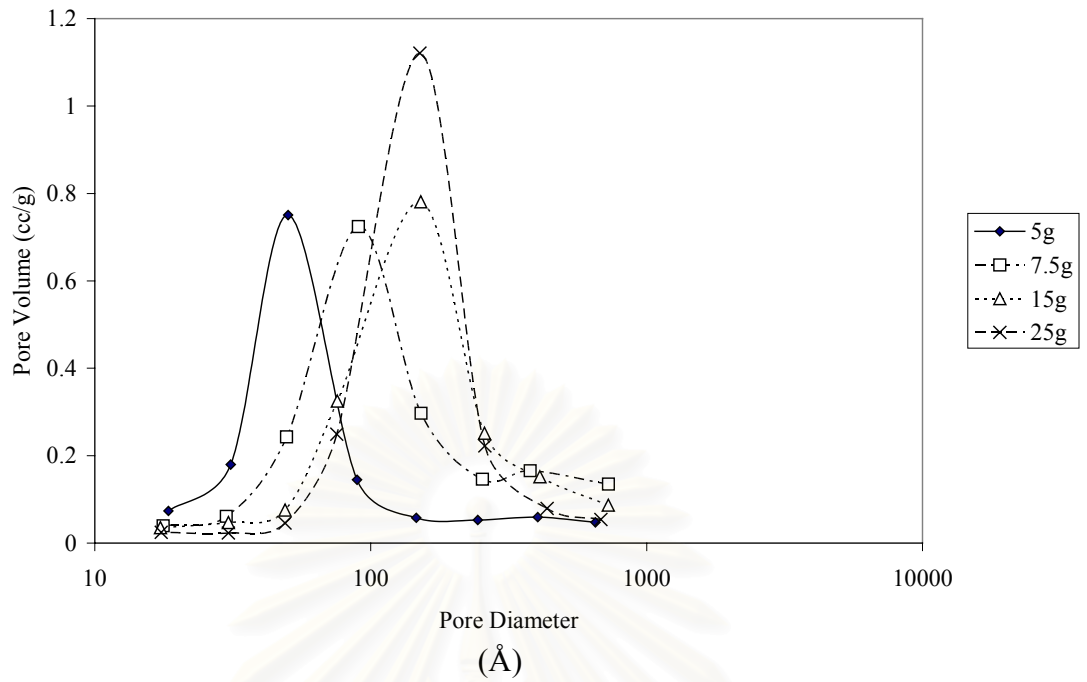


Figure 5.9 Pore size distribution of titania products synthesized in 1,4-BG for various concentrations.

5.1.2 Synthesis in toluene

Titanium (IV) oxide has been synthesized in toluene at 300°C for various reaction times (Solvothermal Method). In this work effect of reaction time and reactant concentration were investigated. Under inert organic solvent condition, thermal decomposition of TNB in toluene was occurred, yielding a $\equiv\text{Ti-O}^-$ anion. The nucleophilic attack of the titanate ion on another ion and crystallization was taken place, finally yielding the anatase titania. The mechanism of TNB in toluene can be depicted as shown in Figure 5.10.

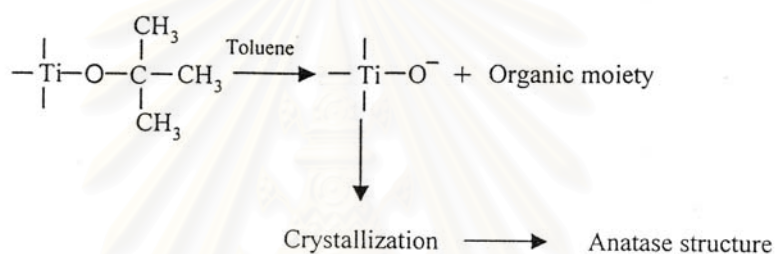


Figure 5.10 Mechanism of reaction in toluene for the titania product (Sornnarong Theinkeaw, 2000 : 71).

5.1.2.1 Effect of reaction time

Titania was synthesized for various reaction times (0, 0.25, 0.5, 1, 2, and 4 h). As shown in Figure 5.11, XRD pattern of the products obtained from the reaction at 300°C indicated that the synthesized titania product without reaction time appeared amorphous phase but for only 15 min of reaction time, titania product started to become anatase phase without contamination of other phases such as brookite and rutile, which denoted the anatase titania product was form at these temperature when the reaction time was prolonged.

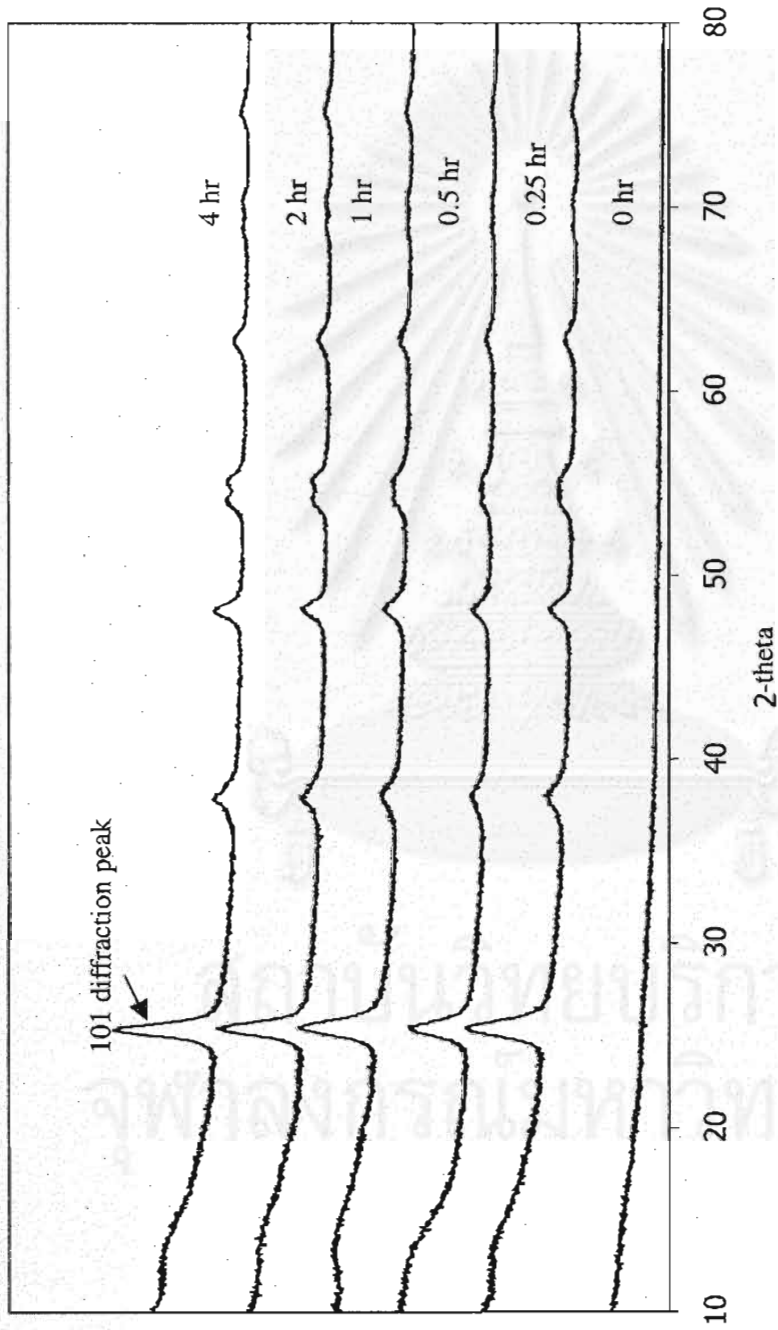


Figure 5.11 XRD patterns of titania products synthesized in toluene for various reaction times. For non holding time, the titania product was amorphous phase, but increasing the reaction time, the as-synthesized were formed the anatase phase without contamination of other phase.

Kondo *et al.* (1994) examined the hydrothermal treatment of alkoxide-derived amorphous TiO₂ particles and found that the crystallite size of anatase formed was increased to 25 nm by the treatment at 250°C. Inoue *et al.* (1996) synthesized χ -alumina from thermal decomposition of a mixture of aluminium isopropoxide and tetraethoxysilcane in toluene at 300°C. The as-synthesized product was amorphous. When thermal treatment of the as-synthesized product in various temperatures was prolonged, the χ -alumina was formed. Yanagisawa *et al.* (1997) synthesized titania from hydrothermal reaction by used titanium tetraethoxide and ethanol with water. The resultant precipitate was amorphous hydrous titania. When it was heated in air, a large weight loss was observed at 100°C and crystallization to anatase occurred at about 400°C. The as-synthesized product was used to be the starting material to study effect of a reaction pressure -compressive pressure from the outside the autoclave- on the anatase titania product. On the other hand, in this study, the anatase titania was formed due to the crystallization of amorphous under the reaction for holding time.

Addition of water to the supernatant after the reaction gave no precipitates indicate that TNB was completely decomposed in toluene (Kominami *et al.*, 1999). From XRD pattern, the crystallite size of the anatase samples was calculated from the half-height width of the 101 diffraction peak of anatase using the Scherrer equation. The crystallite size at 0.25 hr of the reaction time was 9 nm and approached 13 nm at 4 hrs as shown in Table 5.5.

Table 5.5 shows the crystallite size and specific surface area. The crystallite size increased slightly with increasing the reaction time. On the other hand, the specific surface areas obtained from both BET measurement and calculation by equation was decreased with increasing the reaction time. S_1/S_2 ratio increased. A decrease of the BET surface area with reaction time indicated that the amorphous was formed into titania crystal. These suggested that the titania product synthesized in toluene was crystallized from amorphous phase.

Table 5.5 Crystallite size and surface area of titania products synthesized in toluene

Reaction time (hr)	Crystallite size diameter (nm)	Crystalline surface area (m ² /g)		S ₁ /S ₂
		S ₁ ^a	S ₂ ^b	
0	amorphous	204	-	-
0.25	9	163	171	1.0
0.5	10	156	154	1.0
1	10	161	154	1.0
2	12	145	128	1.1
4	13	143	118	1.2

^a Specific BET surface area from BET measurement.

^b Specific surface area calculated from equation of $6/d\rho$ on assumption that the crystal is spherical particle and the density of anatase titania is 3.9 g cm⁻³.

As see in Figure 5.12, observation reveals that amorphous phase was changed to anatase phase by crystallization and then agglomerated to secondary particle. The secondary particle morphology from SEM showed the formation of spherical shape, not only being a large size but also agglomerating with increasing the reaction time.

Figure 5.13 shows the relative pressure of N₂ adsorption-desorption of titania products synthesized in toluene for various times. This indicate that the pore structures were mainly the ink bottle pore and reconstructed to form cylinder pore when reaction time was prolonged. This shows that the reaction time is affect on the pore structure of titania synthesized in toluene.

Table 5.6 shows the pore volume and the average pore diameter of titania products synthesized in toluene for various reaction times. The pore volumes were constant not depended on the reaction time, but the average pore diameter were slightly increased with increasing the reaction time. These confirm the relative pressure of N₂ volume adsorbed-desorbed was increased with prolonging the reaction times. Figure 5.14 shows the pore size distribution of titania products synthesized in toluene for various reaction times. The pore volume and the pore diameter were increased with increasing the reaction time. In addition, the wider distribution of pore diameter presented at the longer reaction time.

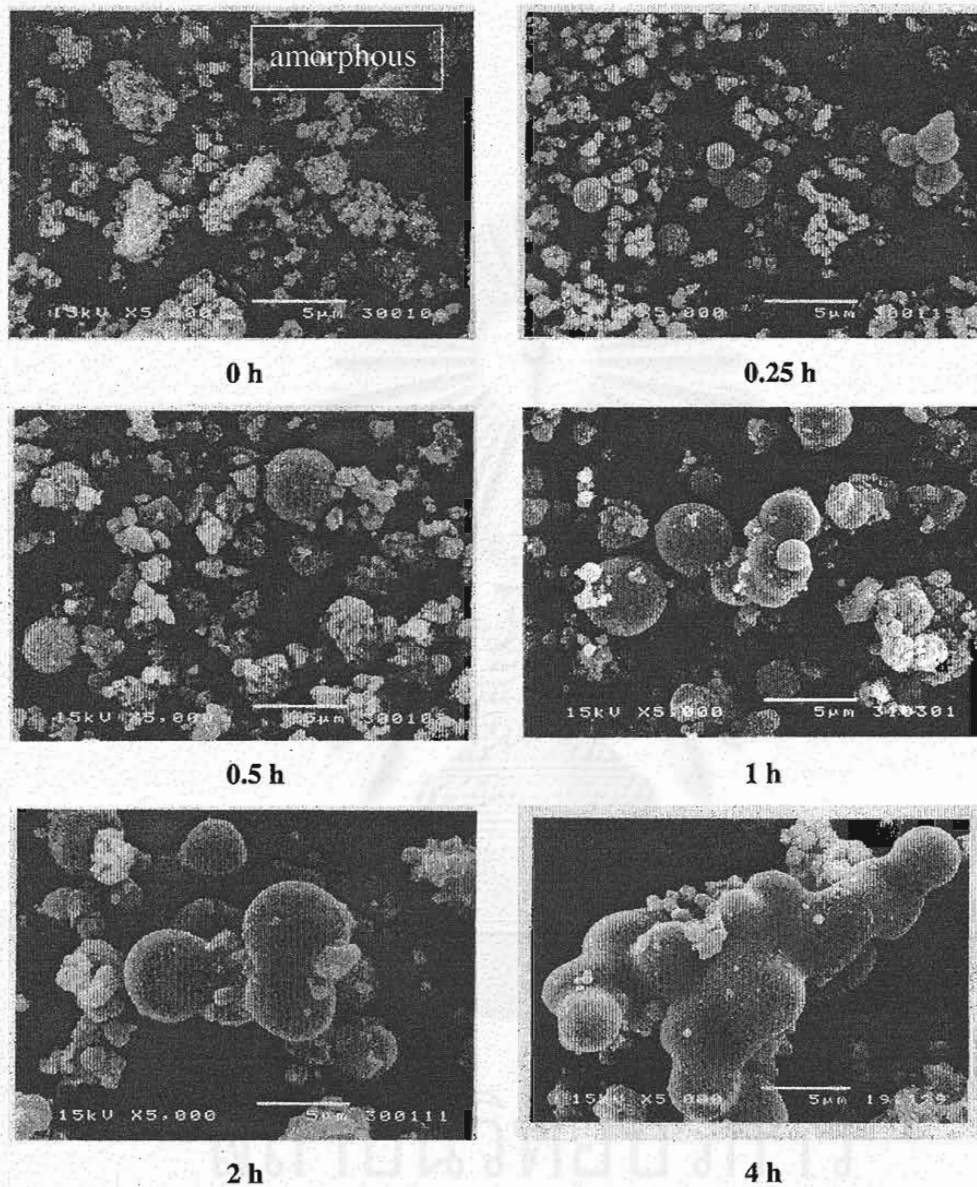
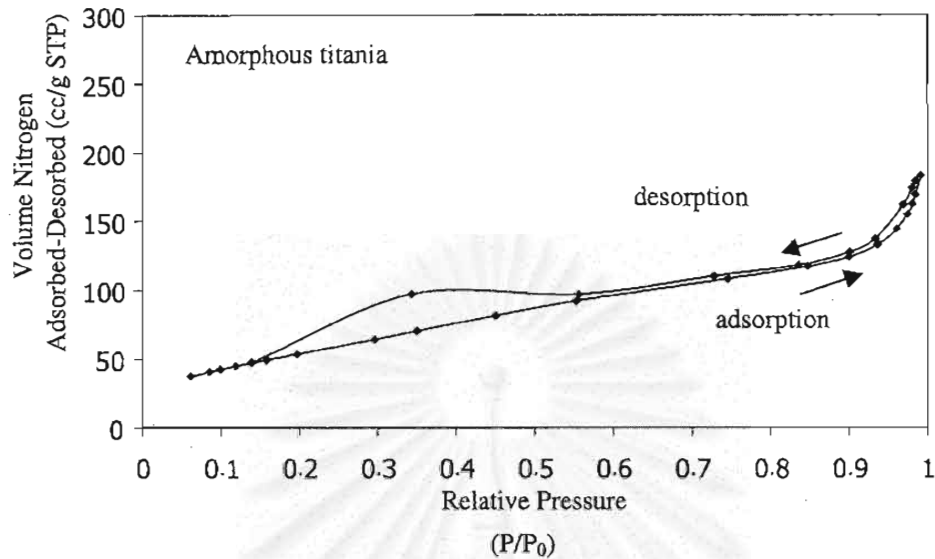
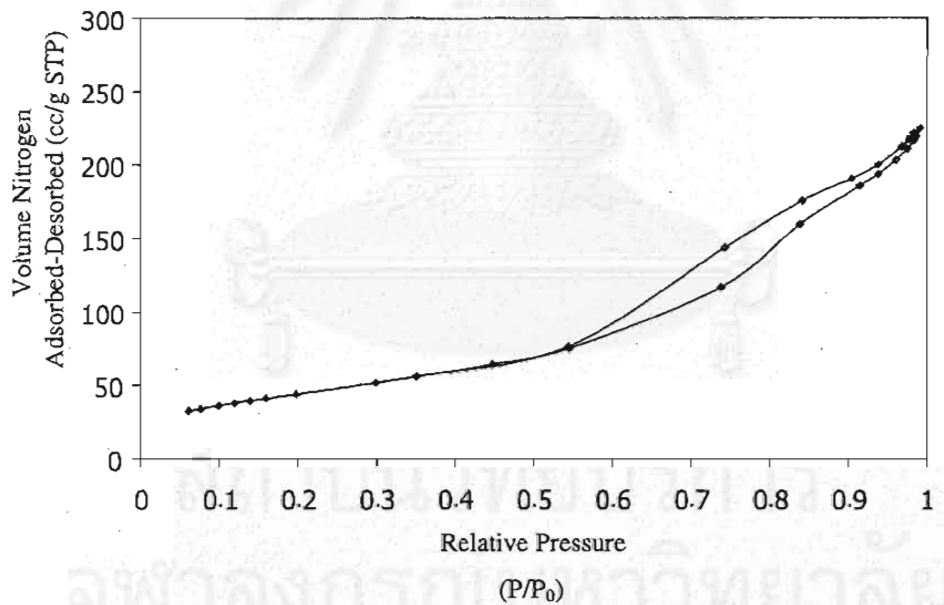


Figure 5.12 SEM morphology of titania products synthesized with toluene for various reaction times. The morphology of secondary particles were spherical and were agglomerated to form the large size particles with increasing the reaction time. At non holding reaction time, the as-synthesized was amorphous phase and the particle shape was irregular shape. When increasing the reaction time, the crystals were formed and the spherical shapes of secondary particles were formed due to the agglomeration.

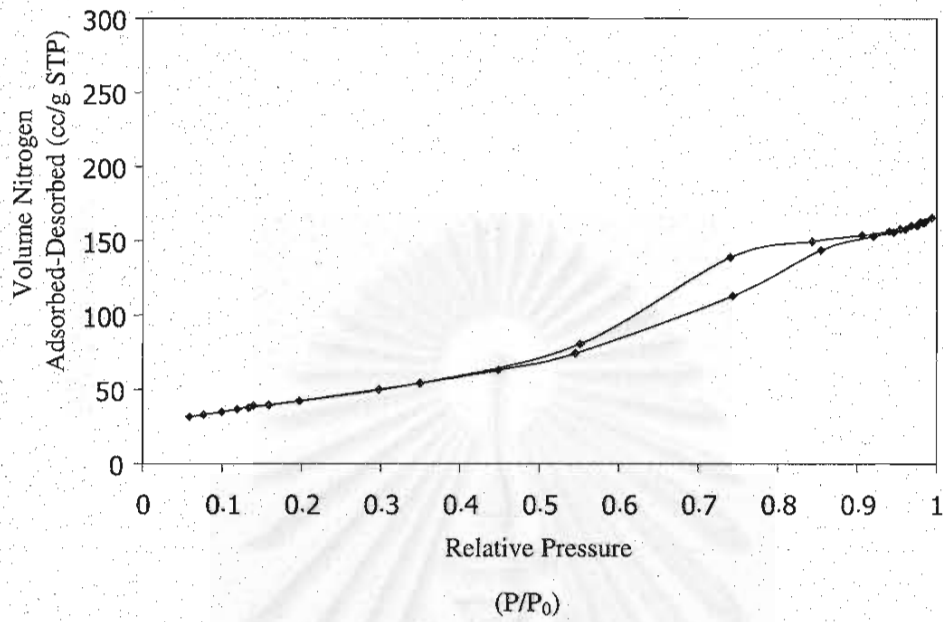


0 h, amorphous phase, the product has mesopore and micropore.

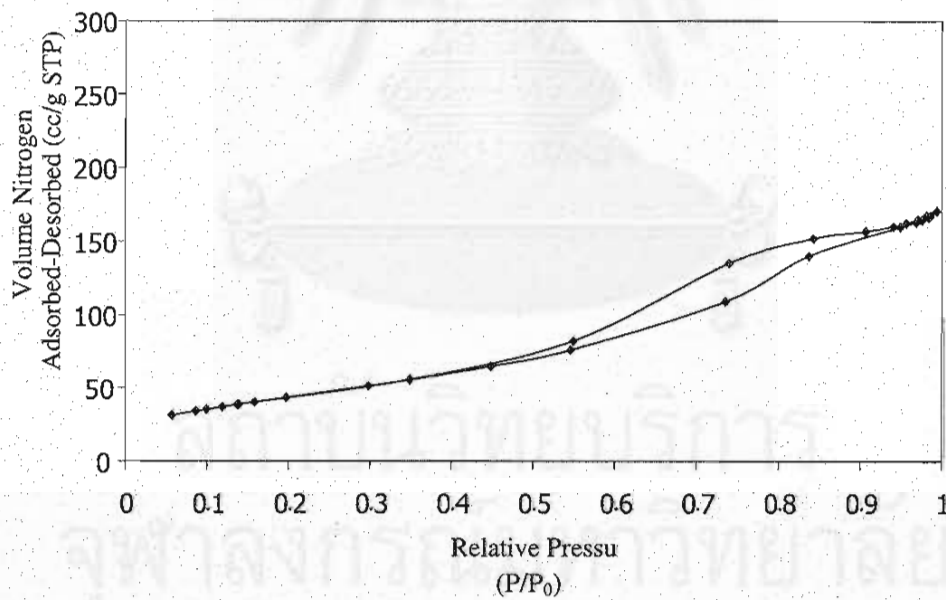


0.25 h, 9 nm, the pore structure is ink bottle open-end pore.

Figure 5.13 Nitrogen adsorption-desorption isotherm of titania products synthesized in toluene by various reaction times and crystallite sizes. At non holding time, the pore structure of amorphous can not identified but increasing the reaction time the pore was formed to the ink bottle pore. (see APPENDIX C)

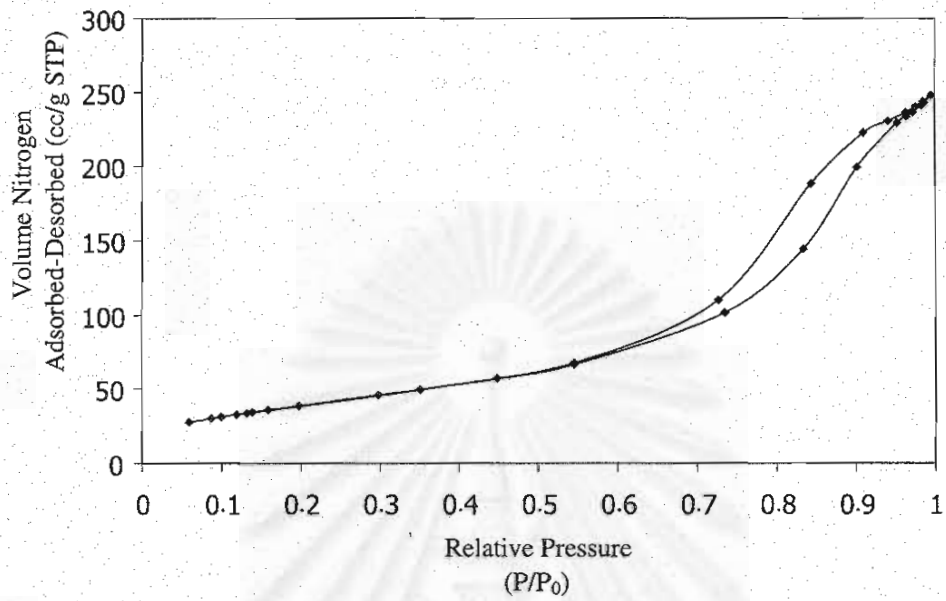


0.5 h, 10 nm, the pore structure is ink bottle open-end pore.

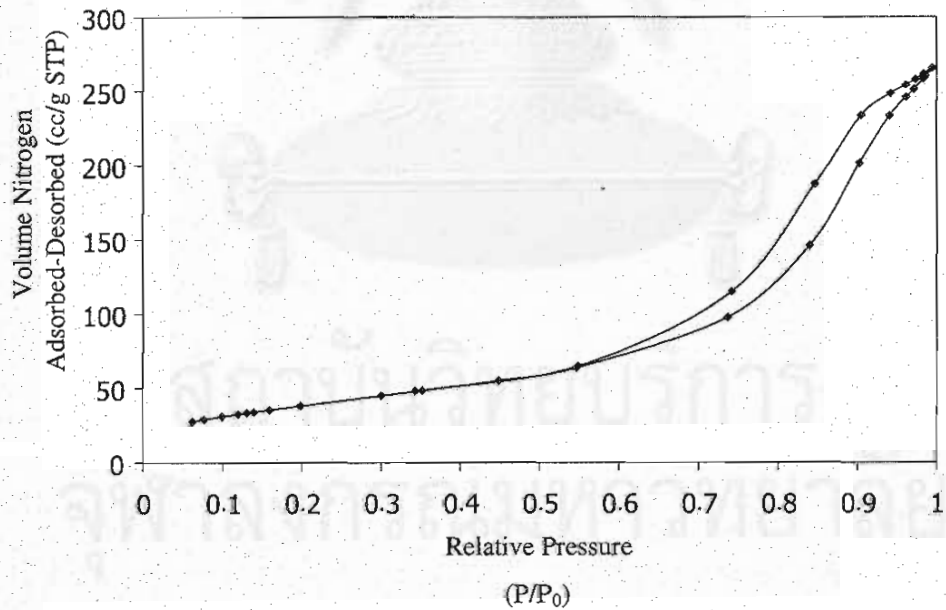


1 h, 10 nm, the pore structure is ink bottle open-end pore.

Figure 5.13 (cont.) Nitrogen adsorption-desorption isotherm of titania products synthesized in toluene by various reaction times and crystallite sizes.



2 h, 12 nm, the pore structure is ink bottle open-end pore.



4 h, 13 nm, the pore structure is cylindrical open-end pore.

Figure 5.13 (cont.) Nitrogen adsorption-desorption isotherm of titania products synthesized in toluene by various reaction times and crystallite sizes.

Table 5.6 Pore volume and average pore diameter of titania product synthesized in toluene.

<i>Reaction time (hr)</i>	<i>Pore volume (cc/g)^a</i>	<i>Average pore diameter (nm)^b</i>
0	0.3	4
0.25	0.4	6
0.5	0.3	4
1	0.4	5
2	0.4	7
4	0.4	8

^a BJH cumulative desorption pore volume of pores

^b BJH desorption average pore diameter (4V/A)

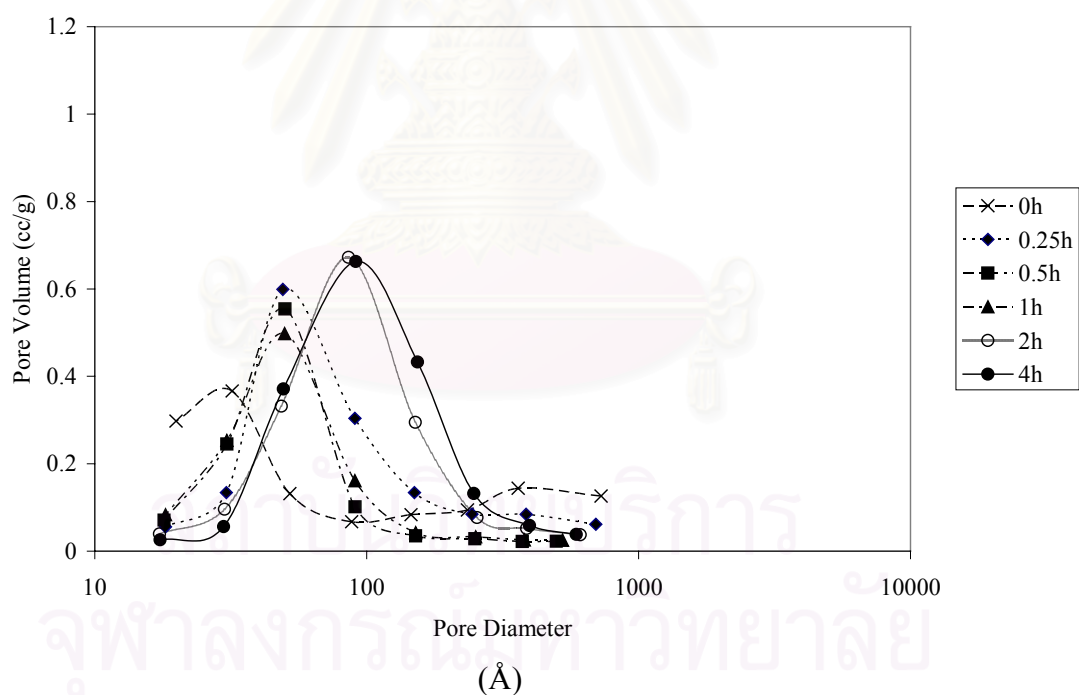


Figure 5.14 Size distributions of titania products synthesized in toluene for various reaction times.

5.1.2.2 Effect of reactant concentration

For all of concentrations of starting material synthesized in toluene at 300°C for 2 h, it was found that the as-synthesized product was formed to be anatase titania phase. The XRD patterns of the products prepared in different concentrations are given in Figure 5.15. The relevant SEM micrographs of products are shown in Figure 5.16. The secondary particle morphology was changed when concentration of starting material was increased. Concentration of starting material affected definitely the agglomeration of secondary particle, which was formed to be spherical shape. This should be proposed that the more amount of starting material may accelerated the agglomeration of the particle.

The crystallite size and the specific surface area are shown in Table 5.7. At a large amount of starting material, the crystallite size was rather large (12 nm) under this reaction condition. The BET surface area decreases with an increase of the reaction concentration. Consider the same crystallite size, a decrease of the surface area indicated that the product contaminated with amorphous phase and was formed to be crystal.

Table 5.7 Crystallite size and surface area of titania products synthesized in toluene for various reactant concentration.

<i>R e a c t a n t</i> <i>concentration</i> (g/100ml)	<i>Crystallite</i> <i>size (nm)</i>	<i>Crystalline surface area (m²/g)</i>		<i>S₁/S₂</i>
		<i>S₁^a</i>	<i>S₂^b</i>	
5	8	201	192	1.0
7.5	9	169	171	1.0
10	10	201	154	1.4
15	12	145	128	1.1
25	12	123	128	1.0

^a Specific BET surface area from BET measurement.

^b Specific surface area calculated from equation of $6/d\rho$ on assumption that the crystal is spherical particle and the density of anatase titania is 3.9 g cm⁻³.

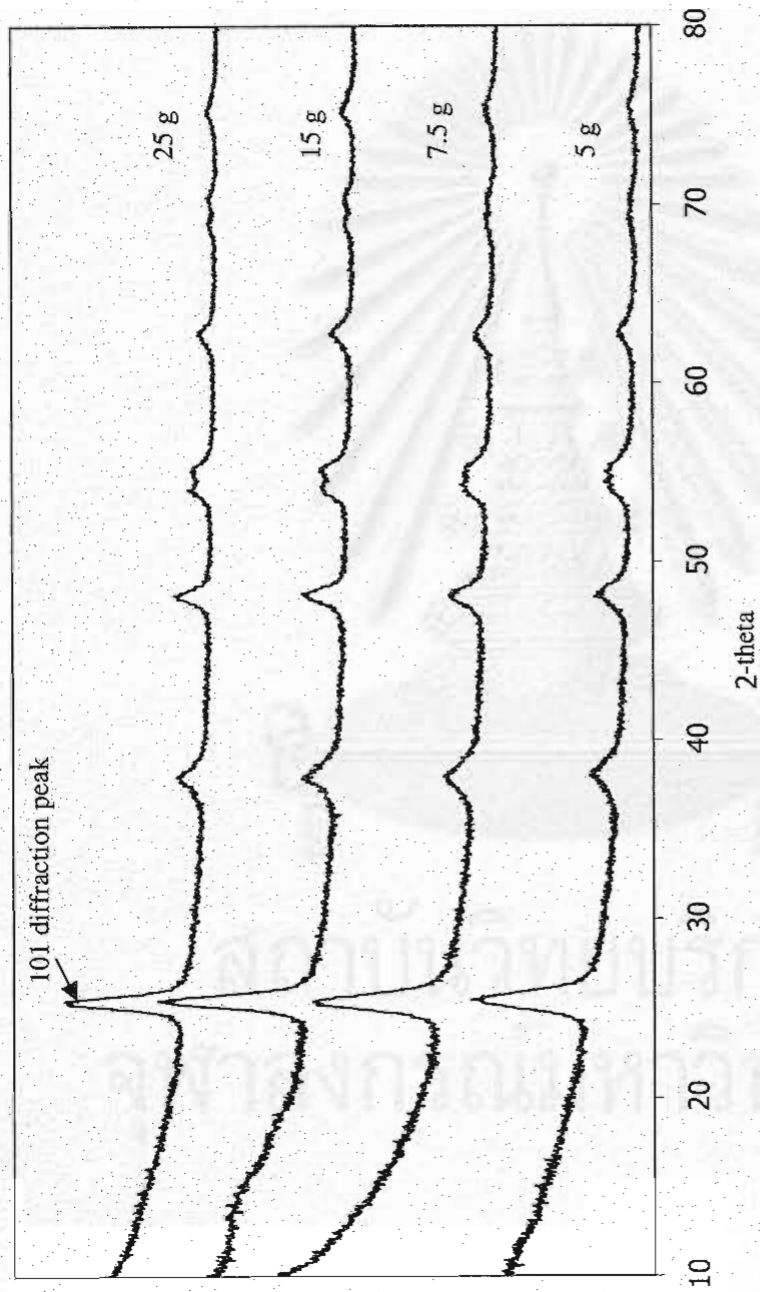


Figure 5.15 XRD pattern of titania products synthesized in toluene for various reactant concentrations (TNB). All as-synthesized were anatase phase without contamination of other phase.

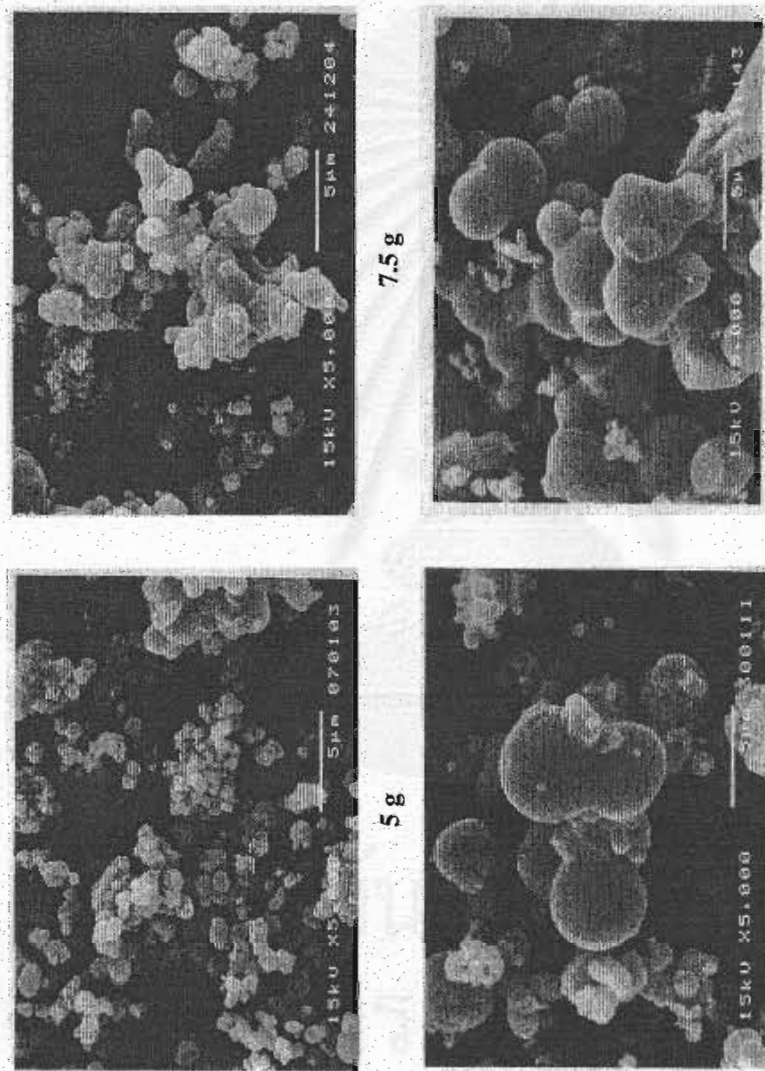


Figure 5.16 SEM images of the as-synthesis products for various reactant concentrations. At low amount of the starting material, the secondary particle was small irregular shape particle, but, for more content of TNB, the secondary particle was a large spherical secondary particle due to the agglomeration of small particles.

Figure 5.17 shows the relative pressure plot of titania products synthesized in toluene for various reactant concentrations. The pore structures were mainly ink bottle pores and consisted of both mesopores and micropores. The increase concentration of the starting material did not affect the pore structure.

Table 5.8 shows the pore volume and average pore diameter in various concentrations of starting material. The pore volume of products was independent on concentration of starting material. This confirms again that the pore structure was not changed for different concentrations. Average pore diameter increased slightly when concentration was increased and was approximately constant at a large amount of starting material. This is similar to the relationship between the crystallite size and reactant concentration.

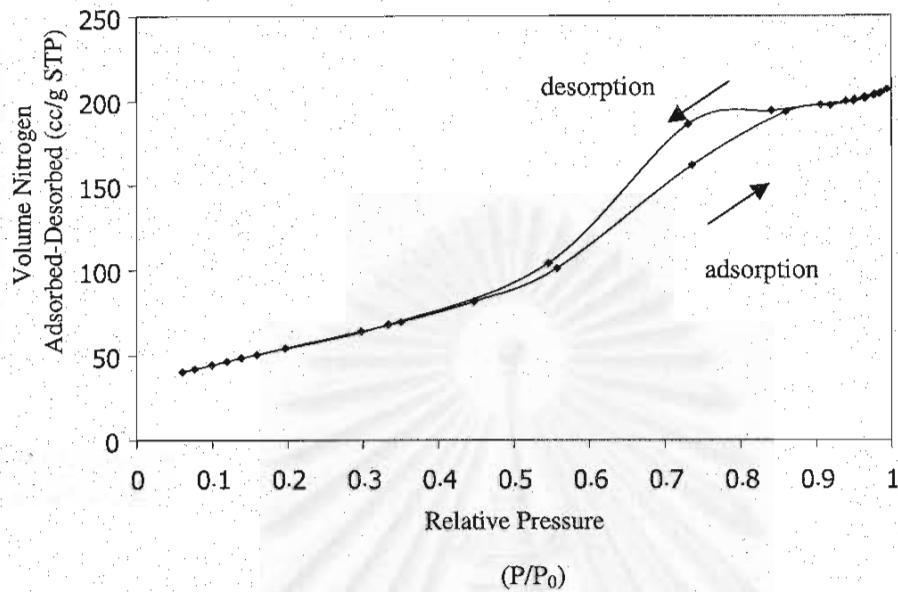
Table 5.8 Pore volume and average pore diameter of titania products synthesized in toluene for various concentrations.

<i>Reactant concentration (g/100ml)</i>	<i>Pore volume (cc/g)^a</i>	<i>Average pore diameter (nm)^b</i>
5	0.3	4
7.5	0.3	5
10	0.4	5
15	0.4	7
25	0.3	6

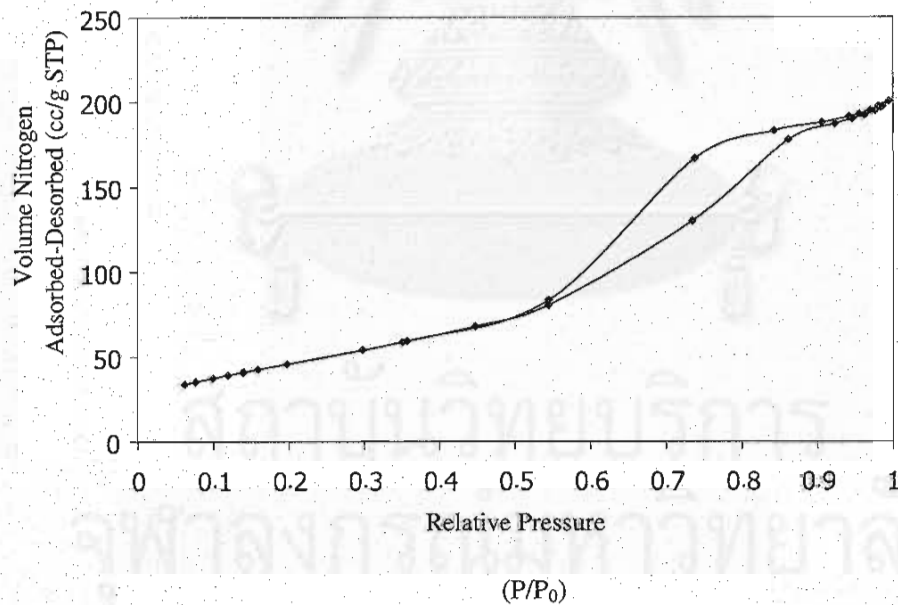
^a BJH cumulative desorption pore volume of pores

^b BJH desorption average pore diameter (4V/A)

Figure 5.18 shows the pore size distribution of titania products synthesized in toluene for various concentrations of starting material. When the reactant concentration was increased, the pore volume was decreased but the average pore diameter was increased. In addition, the distribution curve was wider with increasing the reactant concentration.

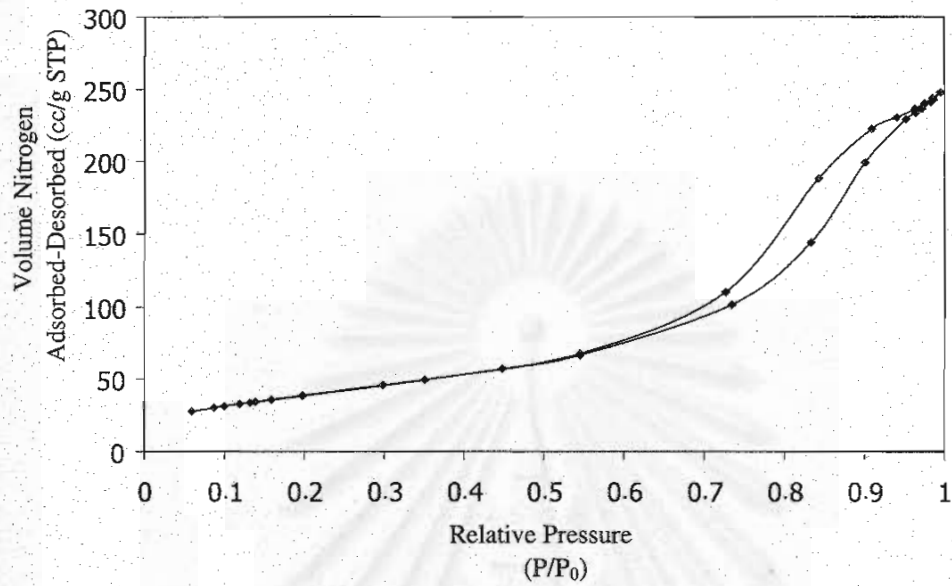


5 g, 8 nm, the pore structure is ink bottle open-end pore.

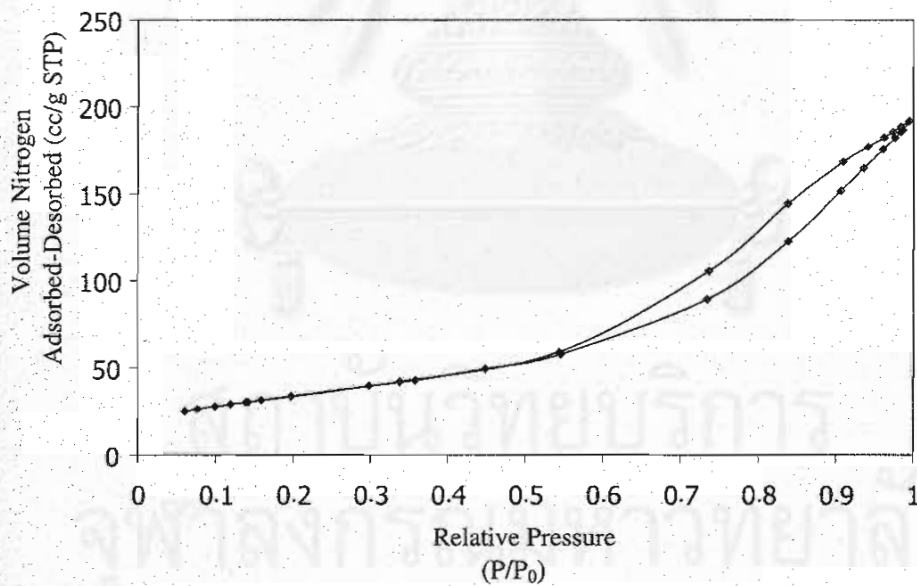


7.5 g, 9 nm, the pore structure is ink bottle open-end pore.

Figure 5.17 Nitrogen adsorption-desorption isotherm of titania products synthesized in toluene for various concentrations of starting material and crystallite sizes. For increasing the amount of TNB, the pore structure were not change which formed ink bottle pore. (see APPENDIX C)



15 g, 12 nm, the pore structure is ink bottle open-end pore.



25 g, 12 nm, the pore structure is ink bottle open-end pore.

Figure 5.17 (cont.) Nitrogen adsorption-desorption isotherm of titania products synthesized in toluene for various concentrations of starting material and crystallite sizes. The pore structure not depended on the amount of TNB.

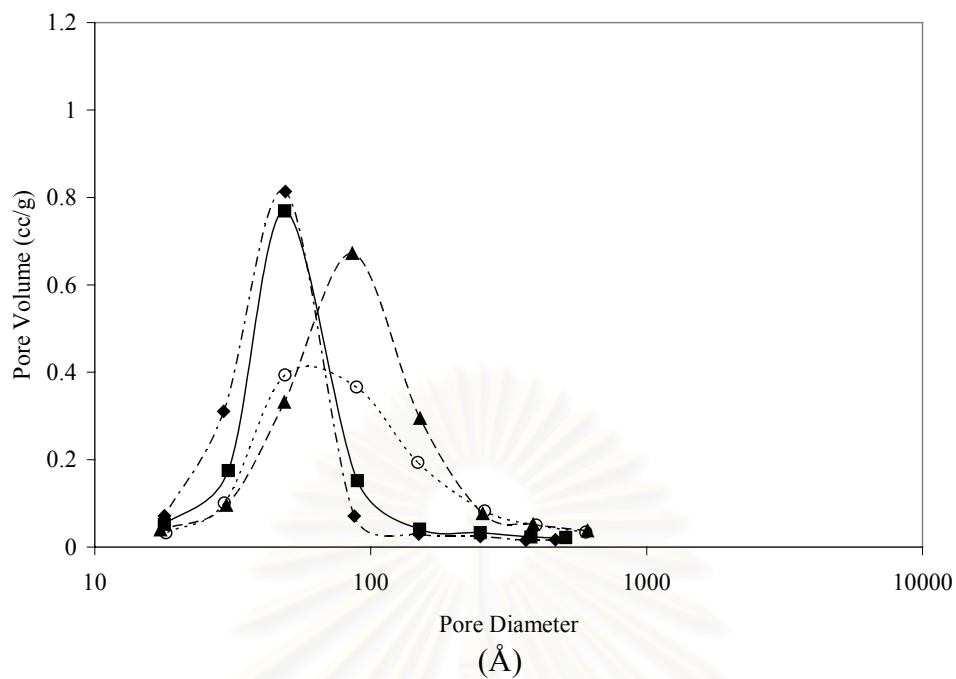


Figure 5.18 Pore size distribution of titania products synthesized in toluene for various concentrations.

สถาบันวิทยบริการ
จุฬาลงกรณ์มหาวิทยาลัย

5.1.3 Comparison of titania products synthesized in both solvents

In previous results, it was found that the as-synthesized titania products in two solvents was distinctly different. When the reaction time was not held, the titania product synthesized in 1,4-BG provided titania crystal having 10 nm of crystallite size but that synthesized in toluene became amorphous phase. It was necessary to held instantly reaction time for the crystal formation of titania synthesized in toluene. To test the mechanisms, synthesis at 220°C in two solvents the titania was not formed, on the other hand, titania products was synthesized at 250°C without reaction time. In 1,4-BG, the small amount product, which formed anatase titania, was fine particle in liquid solvent. But in toluene, the small amount product was amorphous mixing in reacted-solution. Figure 5.19 shows the XRD patterns of titania products synthesized in both solvents at 250°C without reaction time. This suggested that the mechanism of two reactions was different. It was proposed that the product synthesized in 1,4-BG could form crystal immediately after supersaturation point. On the other hand, the product synthesized in toluene formed amorphous titania, which formed was produced free radical in the solution and precipitated from the solution and crystallized to anatase. These should be propose that the mechanism of synthesized titania in 1,4BG was directly crystallization, but, the mechanism of synthesized titania in toluene proceeded via solid state reaction from precipitated amorphous.

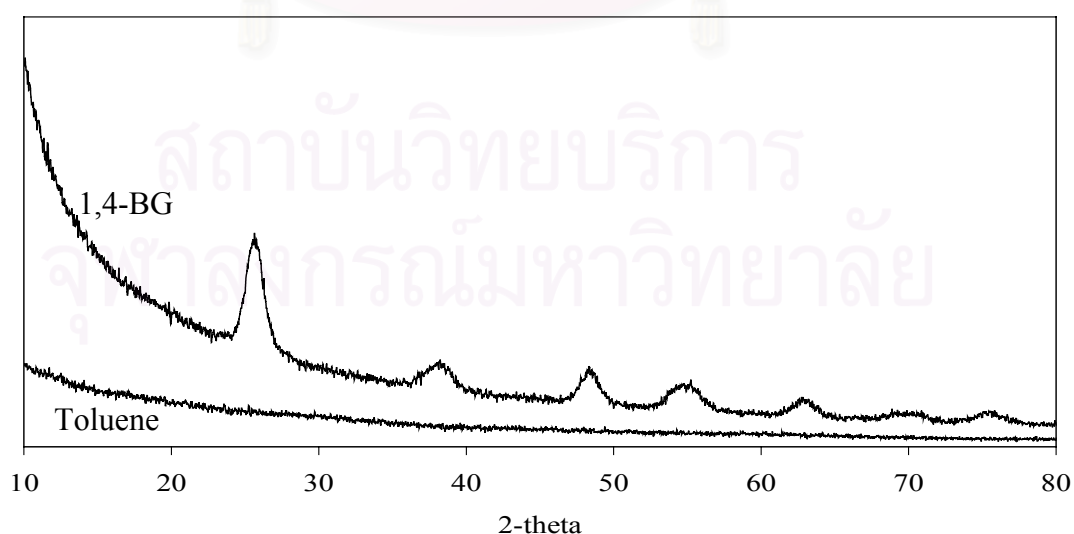


Figure 5.19 XRD pattern of titania products synthesized in two solvents at 250°C for non-reaction time.

Comparison of the growth of crystal, the titania synthesized in 1,4-BG was grown due to the crystal from the nucleation but the titania synthesized in toluene the crystal was grown due to crystallization of amorphous. So, the crystallite size of titania products synthesized in 1,4-BG have more significant effect on reaction time and concentration than that synthesized in toluene.

Comparing morphology of titania products synthesized in two solvents, it was found that the secondary particle of the titania synthesized in toluene was spherical particle but that synthesized in 1,4-BG was irregular fine particle. Park *et al.* (1997) synthesized titania in thermal hydrolysis of TiCl_4 . They found that the secondary particle shape depended on the dielectric constant of solvent and the particle potential. The secondary particle synthesized in low dielectric constant solvent was spherical shape, on the other hand, for high dielectric constant solvent, the secondary particle was irregular shape. Moreover, they proposed that the growth after nucleation can be also affected by the kind of solvents, because the particle interaction potential is different in each solvent. Table 5.9 shows the dielectric constant of two solvents. These results confirmed morphology of the titania products in the different solvents. The dielectric constant of 1,4-BG is higher than toluene so that secondary particle of titania was irregular shape. The dielectric constant is proportion of the surface energy. The titania synthesized in 1,4 BG have a high surface energy so the secondary particle was irregular shape (Park *et al.*, 1997).

Table 5.9 Dielectric constant of the two solvents (Dean, 1999).

Substances	Dielectric constant, ϵ (25° C)
1,4 Butanediol	32
Toluene	2.4

Considering S_1/S_2 values, which compared the BET surface areas with surface areas that calculated from crystallite size. If the values were more than the unity, it will be proposed in two assumptions; (1) the products were the single crystal and/or (2) the products contaminated with amorphous phase and/or organic moiety. In 1,4-

BG, the S_1/S_2 values were estimate a unit without depend on the reaction conditions such as the reaction time and concentration of starting material (Table 5.1 and 5.3). Alternatively, in toluene, the values were increased with increasing the reaction time, indicated that the products were possibly formed to the single crystal or free-flow crystal, a crystal formed by the growth of a crystal nucleus without secondary nucleation or impingement on other crystal (Table 5.5). However, titania synthesized in toluene that the concentration approached to 25 g, the crystal was not the single crystal so that the S_1/S_2 value is less than the value of the product that synthesized in toluene at 15 g of starting material (Table 5.7).

In the relative pressure of N_2 absorption-desorption volume, at the crystallite size was 9 nm of both solvents, for example, the relative pressure plot pattern of the titanias, synthesized in both 1,4-BG and toluene, were similar. These indicate that the pore structure of titania depended only on the crystallite size. For increased crystallite size the pore structure were formed to cylinder pore. For pore size distribution, the pore was shifted to higher pore diameter with increasing the reaction time or amount of the starting material. These proposed that the reaction time and amount of the starting material is affected on the pore structure of titania synthesized in solvothermal reaction.

The XRD patterns of titania synthesized in both solvents as shown in Figure 5.20 and 5.21. Phase transformation of titania that synthesized in toluene was beginning at 800°C, but in 1,4-BG, the phase transformation occurred at 900°C. These confirmed that the product synthesized in toluene was contaminated with amorphous-like phase so the phase transformation was occurred at low temperature (Kominami *et al.*, 1999).

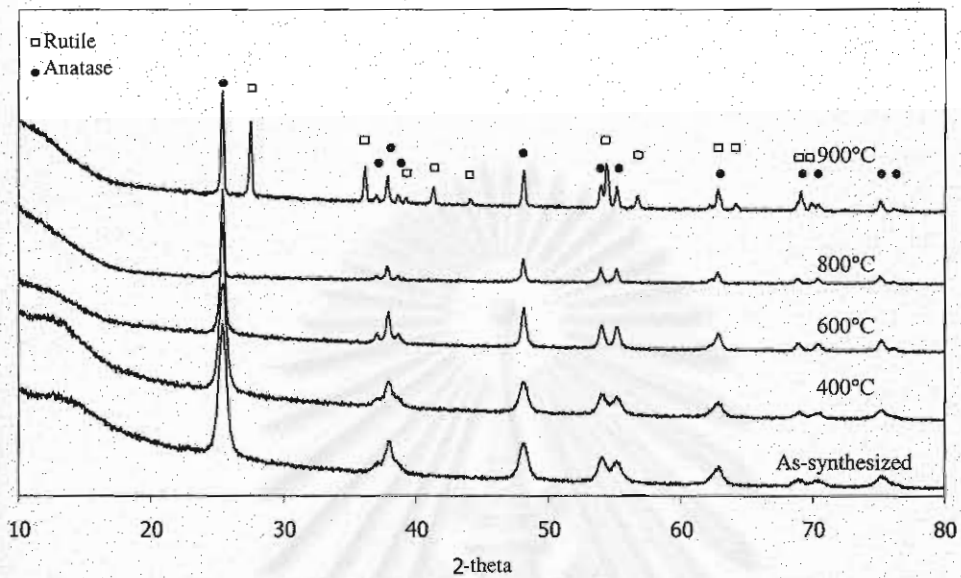


Figure 5.20 XRD pattern of titania products synthesized in 1,4 butanediol at 300°C for 2 hrs and calcined at various temperature. The phase transformation was starting at 900°C.

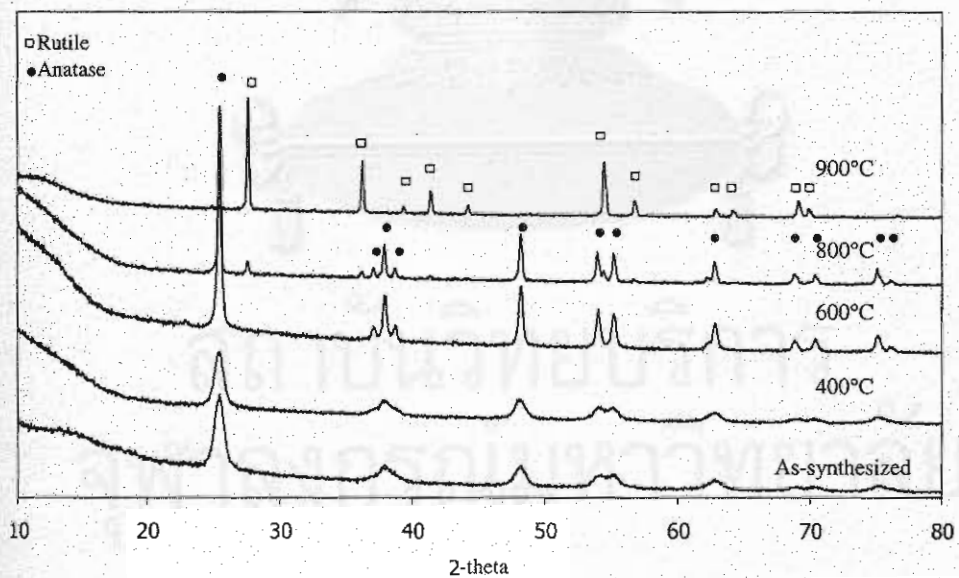


Figure 5.21 XRD pattern of titania products synthesized in toluene calcined at 300°C for 2 hrs and calcined at various temperature. The phase transformation was starting at 800°C.

5.2 Effect of the second element

5.2.1 Effect of silicon on titania product

Silicon modified titania products were synthesized from mixing various molar ratio of TEOS to TNB in 1,4-BG or toluene at 300°C for 2 hr. First, the TNB was decomposed completely in 1,4-BG or toluene under the reaction condition. XRD patterns of silicon modified titania products were shown in Figure 5.22 and 5.23. Those indicated that titania products were formed anatase phase without the contamination of other phase of titania and silica. This proposes that the silicon will form to amorphous phase.

Sornnarong Thiemkaew (2000) synthesized silica modified titania products with molar ratio of Si/Ti between 0.05 and 0.5 in either 1,4-BG or toluene. He found that the XRD pattern showed a decrease of the peak intensities of anatase with increasing silica content. This was due to transformation of the amorphous phase and the anatase-rutile phase to shift markedly toward higher temperature when the amount of TEOS was added to the reaction mixture.

Table 5.10 shows the crystallite size and the specific surface area of silicon modified titania products. In 1,4-BG, the crystallite size decreased with doping the silicon content, however, the crystallite size approximately constant in ratio of 0.04 – 0.08. In toluene, the crystallite size of silicon modified titania was smaller than the pure titania and the crystallite size was approximately constant in ratio 0.005 – 0.08. However, the specific surface areas of silicon modified titania synthesized in both solvents decreased with an increase of the Si/Ti ratio. For S_1/S_2 value, in 1,4-BG, the values estimate constant, but, in toluene, the values slightly increase with increasing the content of silicon in starting material. These indicated that in toluene, the crystal was formed to free-flow crystal when the silicon content was increased. On the other hand, the surface area of titania synthesized in toluene was higher than the titania that synthesized in 1,4-BG, at same crystallite size. these suggested that the products synthesized in toluene was occurred through contamination of amorphous phase or the products synthesized in 1,4-BG was formed by aggregation of crystal .

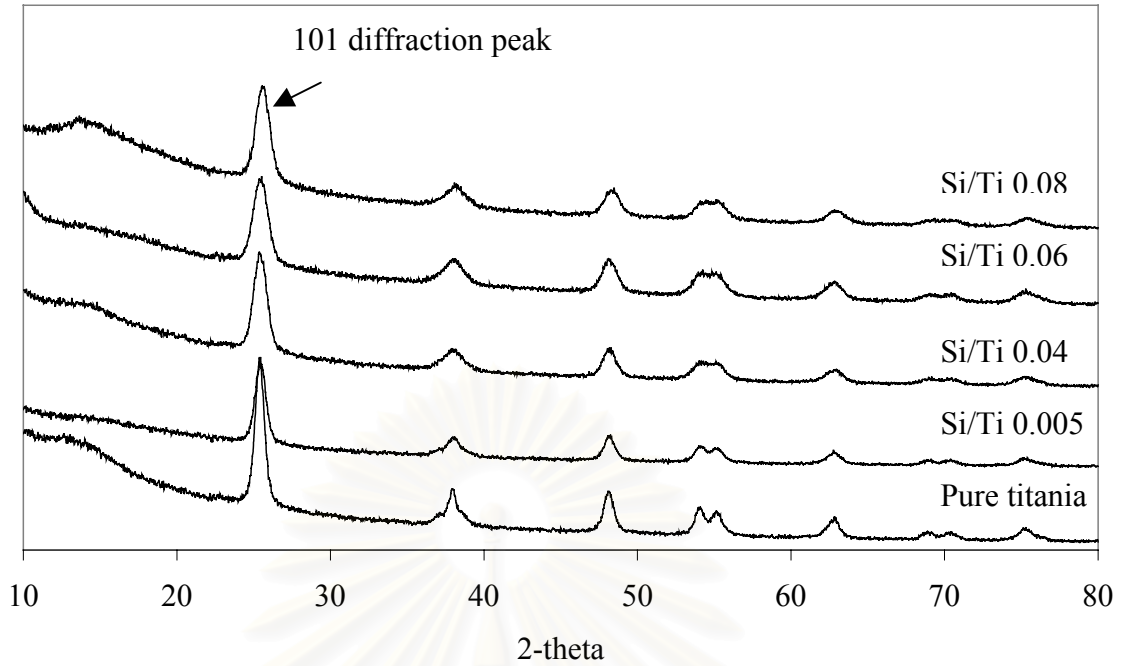


Figure 5.22 XRD patterns of as-synthesized silicon modified titania products synthesized in 1,4-BG for various silicon contents in molar ratio of Si/Ti. All as-synthesized were anatase titania without contamination of other phase of titania and silica phase.

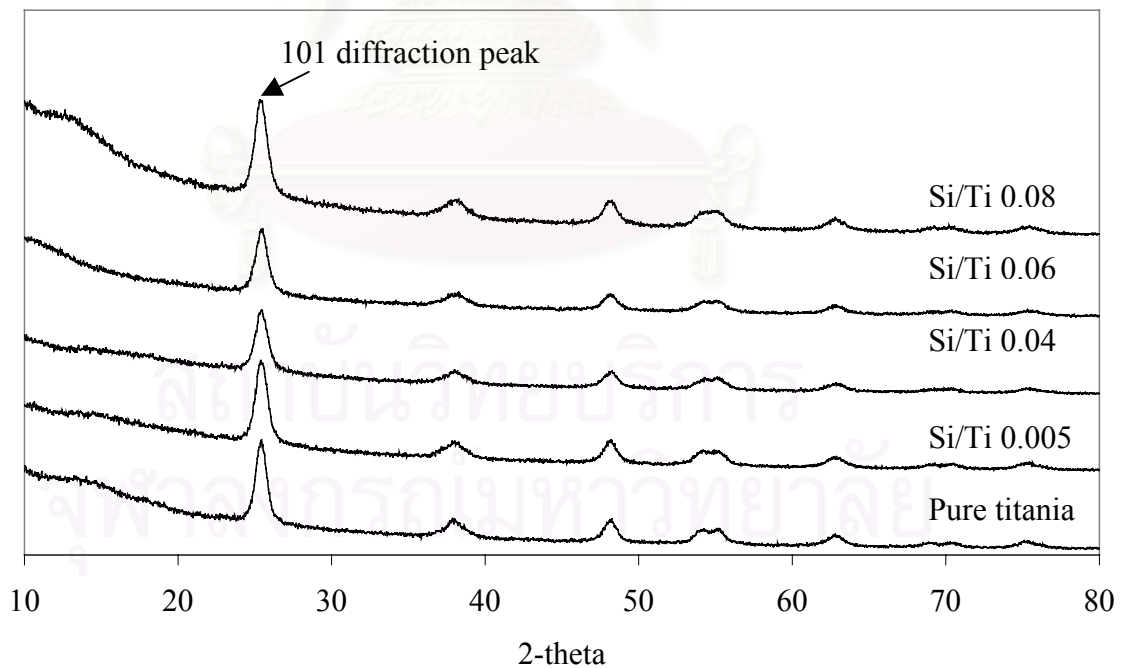


Figure 5.23 XRD patterns of as-synthesized silicon modified titania products synthesized in toluene for various silicon contents in molar ratio of Si/Ti. All as-synthesized were anatase titania without contamination of other phase of titania and silica phase.

Table 5.10 The crystallite size and the specific surface area of silicon modified titania products that were synthesized in 1,4-BG or toluene for various silicon contents of molar ratio of Si/Ti.

<i>Si/Ti in molar ratio^a</i>	<i>1,4-BG</i>				<i>Toluene</i>			
	<i>Crystallite size (nm)^b</i>	<i>Surface area (m²/g)</i>		<i>S₁/S₂</i>	<i>Crystallite size (nm)^b</i>	<i>Surface area (m²/g)</i>		<i>S₁/S₂</i>
		<i>S₁^c</i>	<i>S₂^d</i>			<i>S₁^c</i>	<i>S₂^d</i>	
0.000	13	110	118	0.9	12	145	128	1.1
0.005	12	112	128	0.9	11	155	140	1.1
0.04	9	155	171	0.9	10	187	154	1.2
0.06	8	173	192	0.9	11	201	140	1.4
0.08	9	175	171	1.0	10	199	154	1.3

^a The titania products synthesized from mixed-reactant (TEOS and TNB) in molar ratio (Si/Ti) at 300°C in organic solvents.

^b Crystallite size of anatase titania from the 101 diffraction peak by using Sherrer equation.

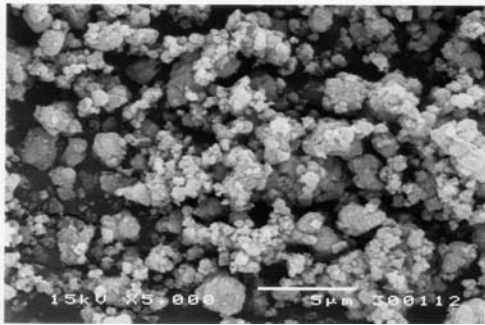
^c Specific BET surface area from BET measurement.

^d Specific surface area calculated from equation of $6/d\rho$ on assumption that the crystal is spherical particle and the density of anatase titania is 3.9 g cm⁻³.

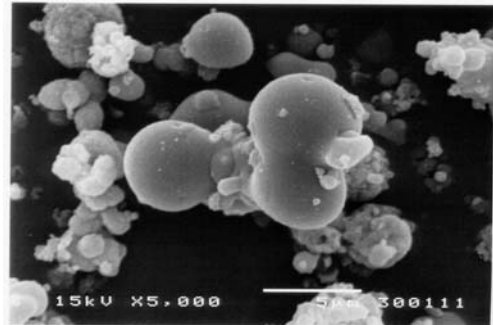
SEM morphologies show the secondary particle of titania products that synthesized in two solvents as shown in Figure 5.24. For 1,4-BG, the morphology of silicon modified titania did not change with increasing the content of silicon. The shape of the secondary particle was an irregular particle. On the other hand, the size of secondary particle of silicon modified titania products that was synthesized in toluene was spherical shape. It was increased and formed to large size with increasing the content of Si. For the morphology, in toluene, the agglomeration of the secondary particles was affected by the content of silicon in the starting material.

Figures 5.25 and 5.26 show the relative pressure of N₂ adsorption and desorption of the silica modified titania products synthesized in two solvents. For both synthetics, the pore structures were mesopore and micropore and formed the open-end pore. In 1,4-BG, the pores were mainly the cylinder pores and the pore structures did not depend on the content of silica doped in the synthesis. On the other hand, the pores of silica modified titania products synthesized in toluene were mainly the ink bottle pores with increasing the content of silica.

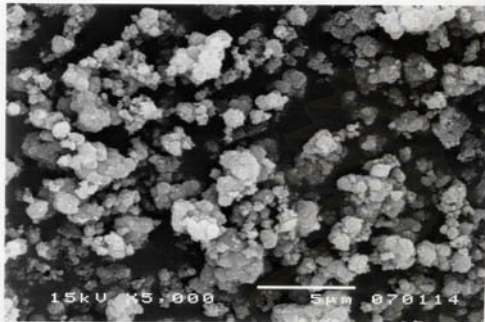
Table 5.11 shows the pore volume and the average pore diameter. The pore volumes were approximately constant and do not depend on the content of silicon and the solvents. The average pore diameter of silicon modified titania synthesized in both solvents were smaller than that of pure titania synthesized in the same condition. The average pore diameters were constant and independent on the silicon content because the crystallite sizes were so small that the pores between the particles were small and depended on the crystallite size. Figures 5.27 and 5.28 show the pore size distribution of silica modified titania. In 1,4-BG solvent, the pore size distribution was shifted to smaller pore size diameter with increasing the content of the silica. Alternatively, the pore size distribution of silica modified titania synthesized in toluene did not change with increasing the content of silica. These results confirm the changing of the surface area of silicon modified titanias that synthesized in both solvents, the surface area increased when the content of silicon increased. This indicated that the products were contaminated with amorphous depended on the content of silicon in the starting material.



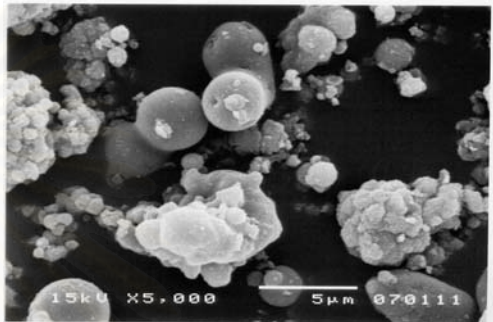
Pure titania, 1,4-BG



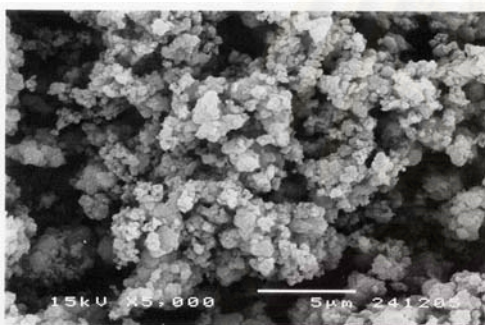
Pure titania, toluene



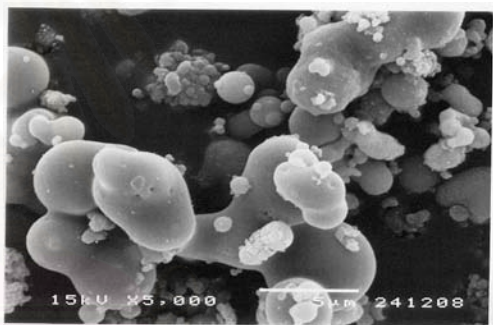
Si/Ti 0.005, 1,4-BG



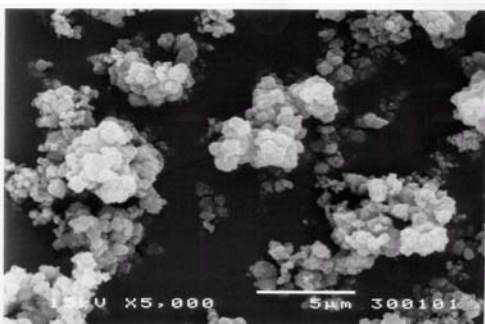
Si/Ti 0.005, toluene



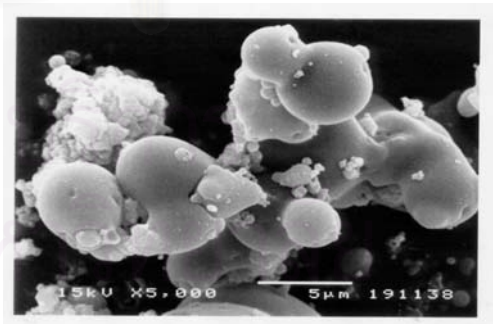
Si/Ti 0.04, 1,4-BG



Si/Ti 0.04, toluene

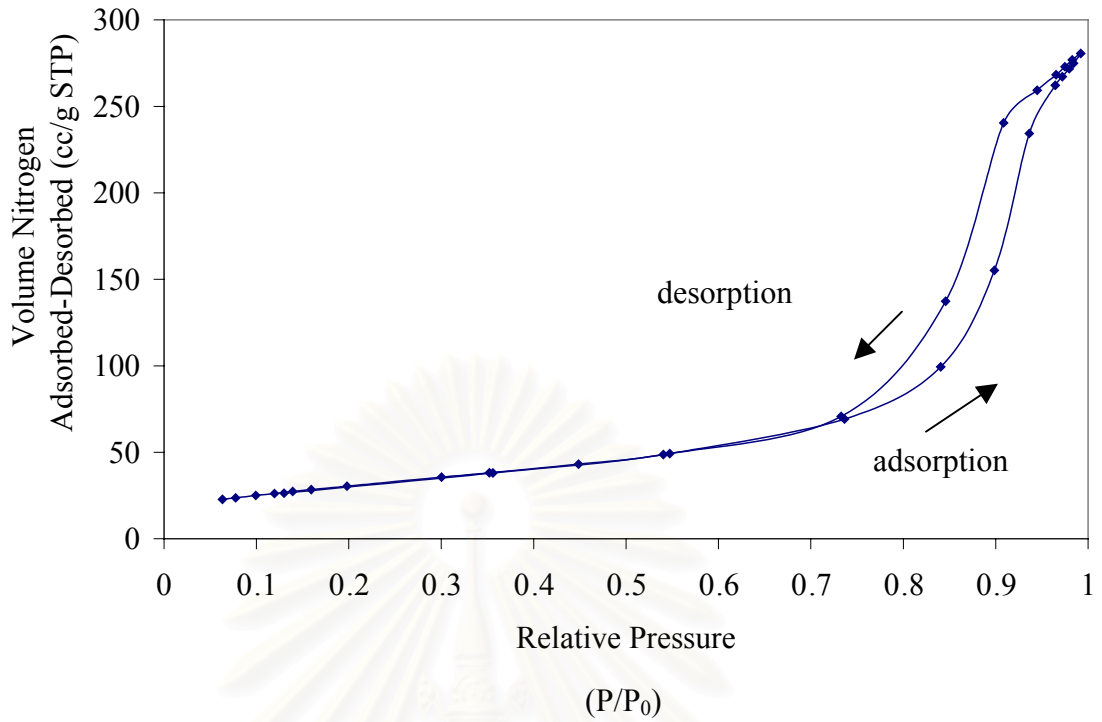


Si/Ti 0.08, 1,4-BG

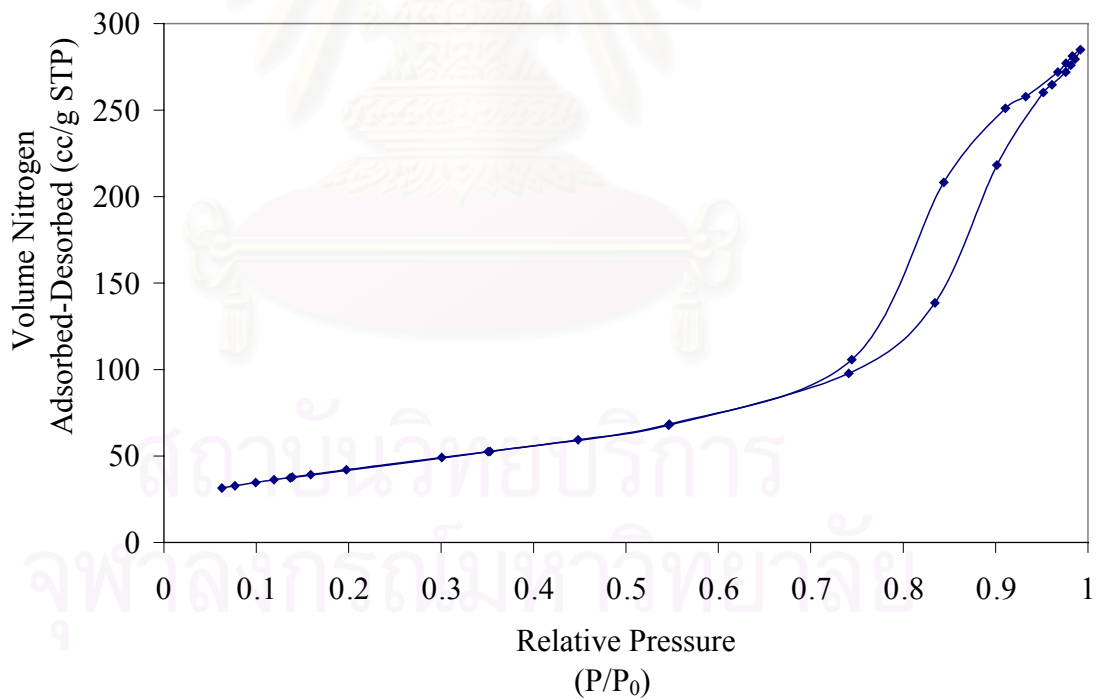


Si/Ti 0.08, toluene

Figure 5.24 SEM morphology of silicon modified titania products synthesized in two solvents of various silicon contents in molar ratio of Si/Ti. For synthesized in 1,4-BG, the secondary particle were irregular shape and not depended on the content of silicon. On the other hand, for synthesized in toluene, the secondary particles were spherical shape and agglomerated to large size with increasing the amount of silicon.

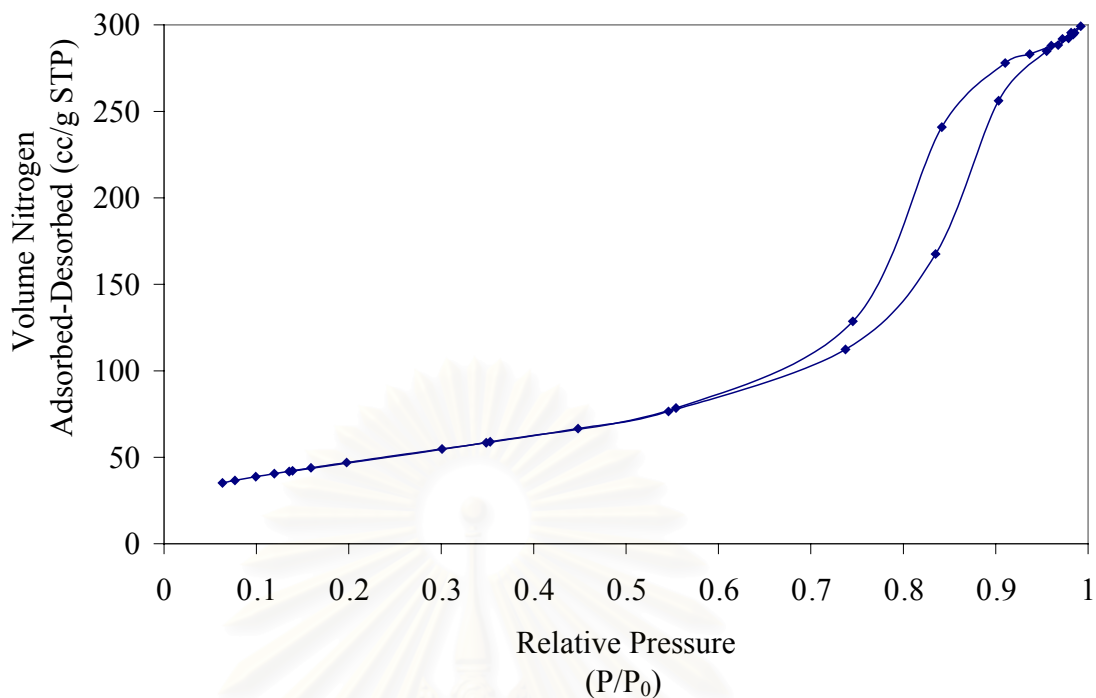


Pure titania, 13 nm, the pore structure is mainly cylindrical pore.

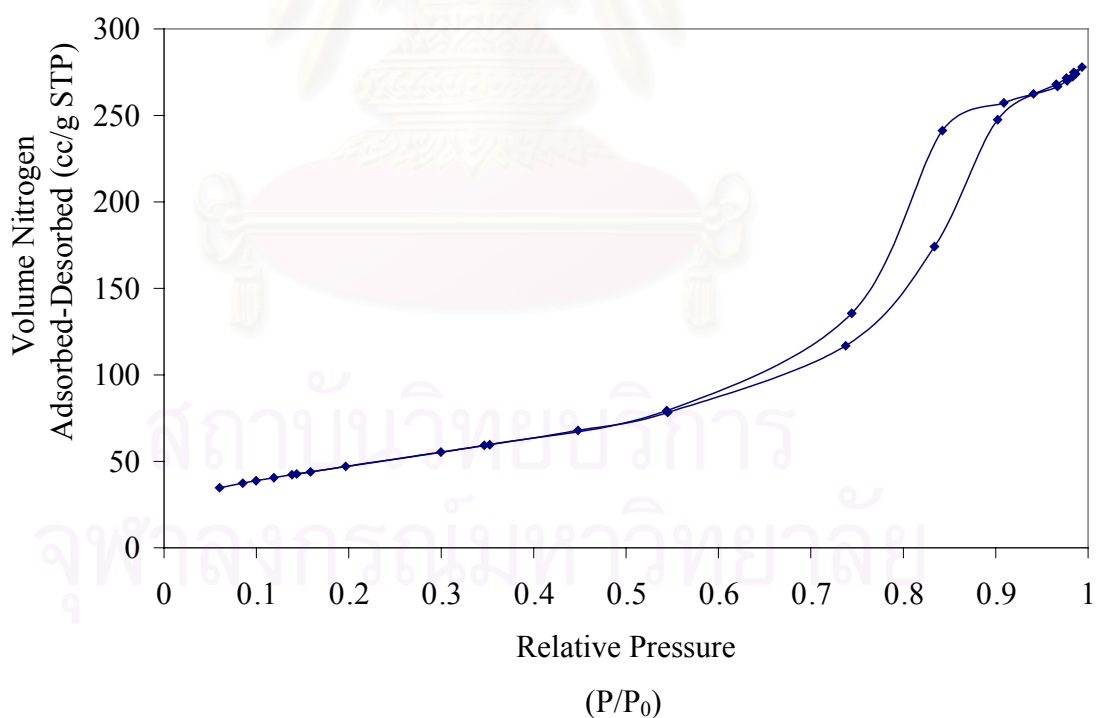


Si/Ti 0.005, 12 nm, the pore structure is mainly cylindrical pore.

Figure 5.25 Relative pressure of N₂ adsorption-desorption of silicon modified titania product synthesized in 1,4-BG for various molar ratios of Si/Ti and crystallite sizes, using BET surface measurement. (see APPENDIX C)

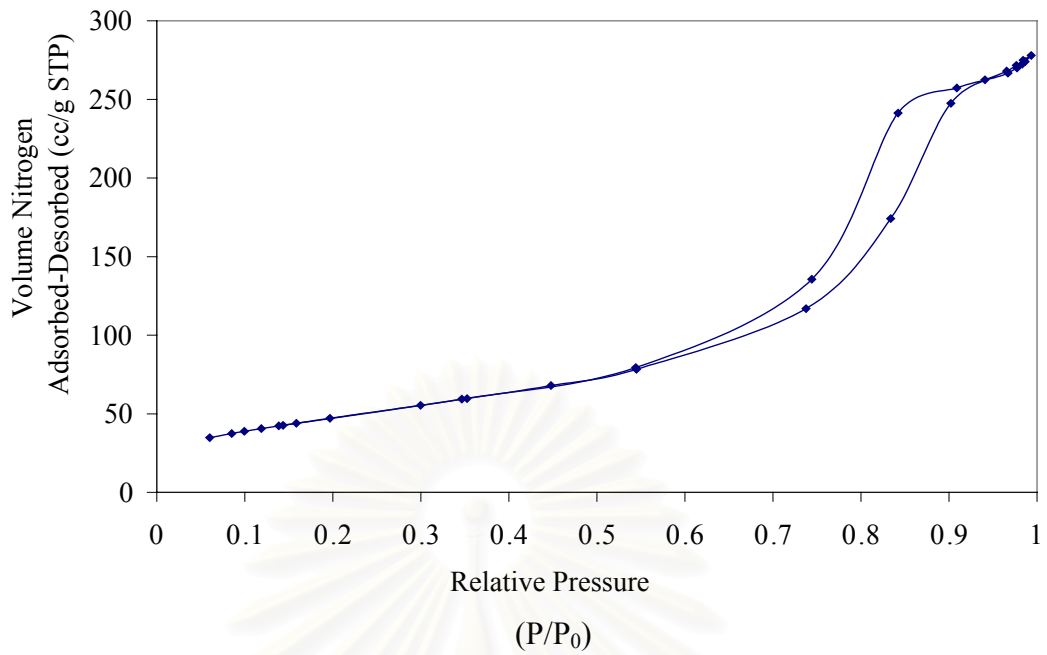


Si/Ti 0.04, 9 nm, the pore structure is mainly cylindrical pore.



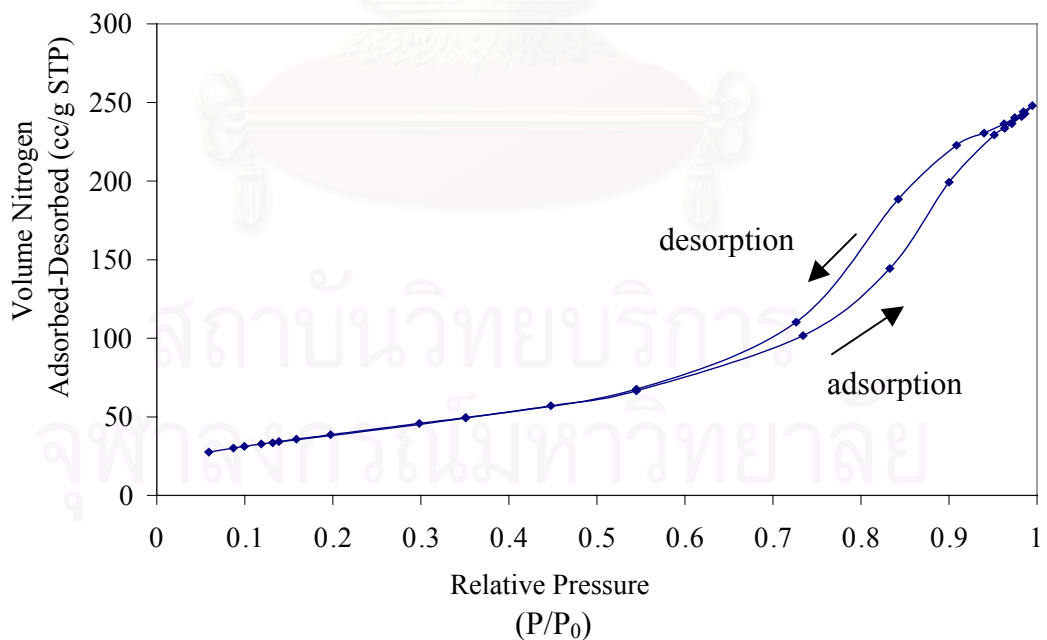
Si/Ti 0.06, 8 nm, the pore structure is mainly cylindrical pore.

Figure 5.25 (cont.) Relative pressure of N₂ adsorption-desorption of silicon modified titania product synthesized in 1,4-BG for various molar ratios of Si/Ti and crystallite sizes, using BET surface measurement.



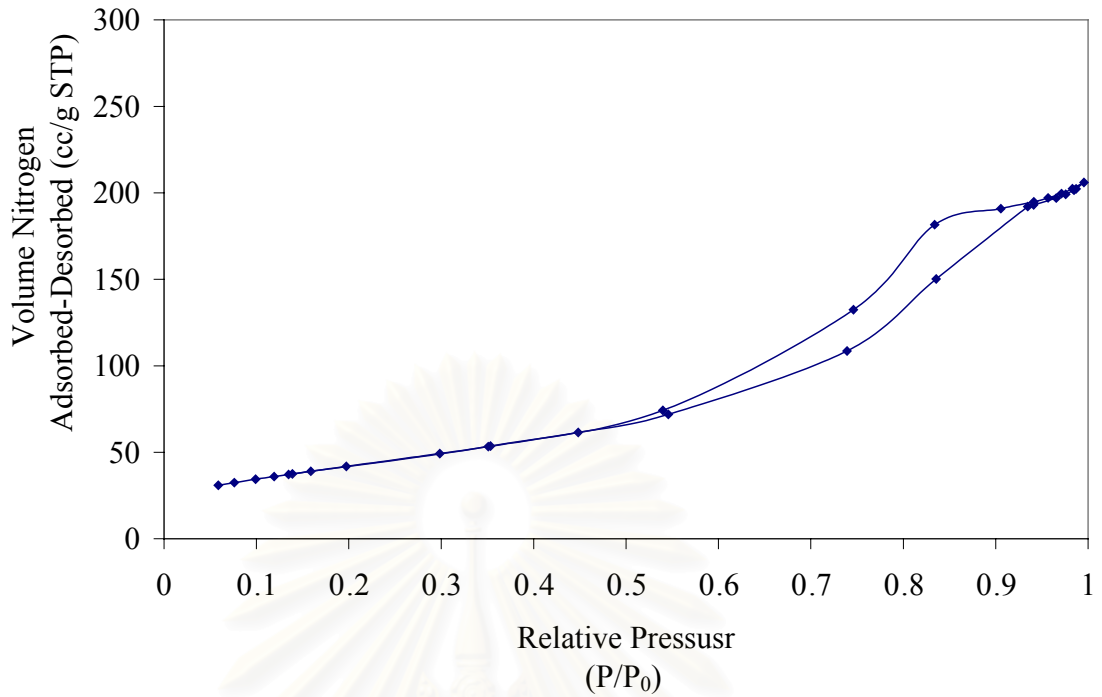
Si/Ti 0.08, 9 nm, the pore structure is mainly cylindrical pore.

Figure 5.25 (cont.) Relative pressure of N₂ adsorption-desorption of silicon modified titania product synthesized in 1,4-BG for various molar ratios of Si/Ti and crystallite sizes, using BET surface measurement.

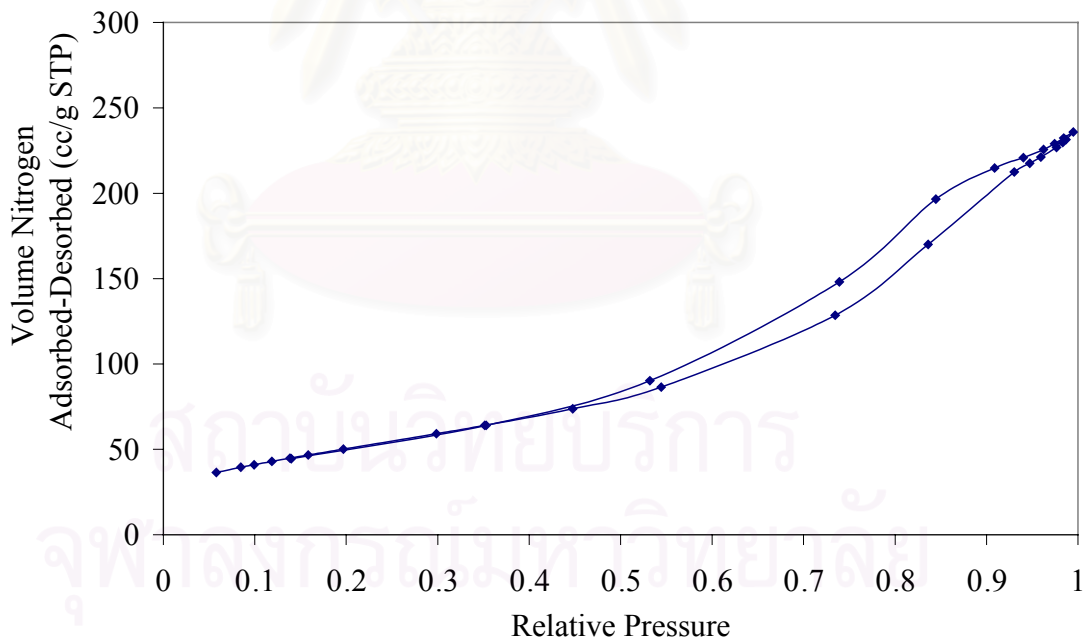


Pure titania, 12 nm, the pore structure is ink bottle pore.

Figure 5.26 Relative pressure of N₂ adsorption-desorption of silicon modified titania product synthesized in toluene for various molar ratios of Si/Ti and crystallite sizes, using BET surface measurement. (see APPENDIX C)

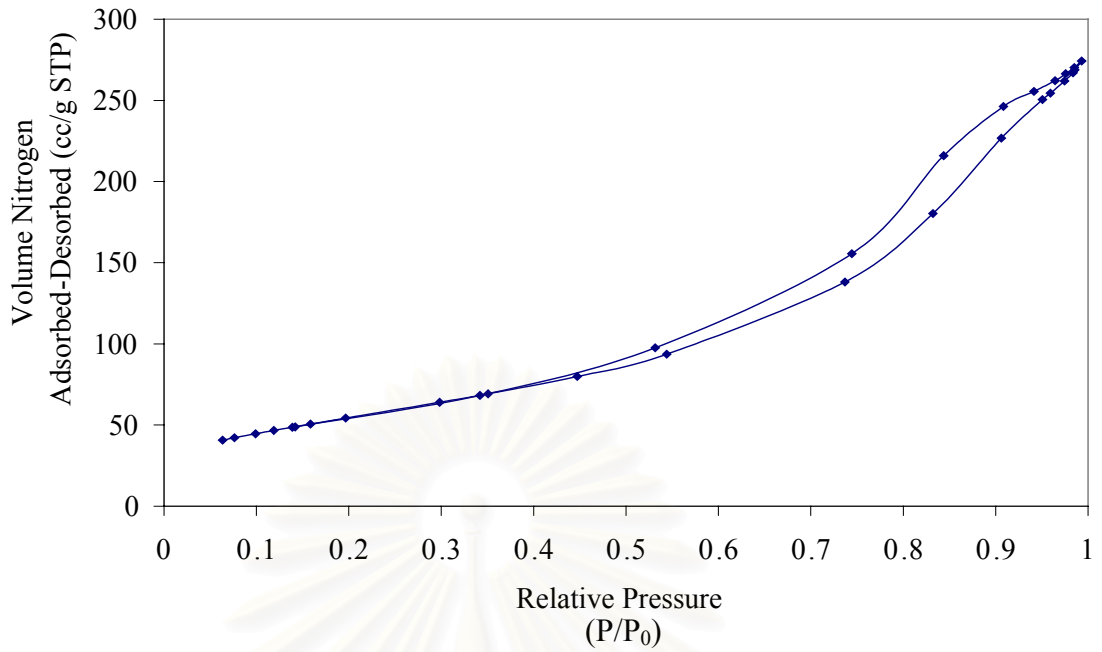


Si/Ti 0.005, 11 nm, the pore structure is ink bottle pore.

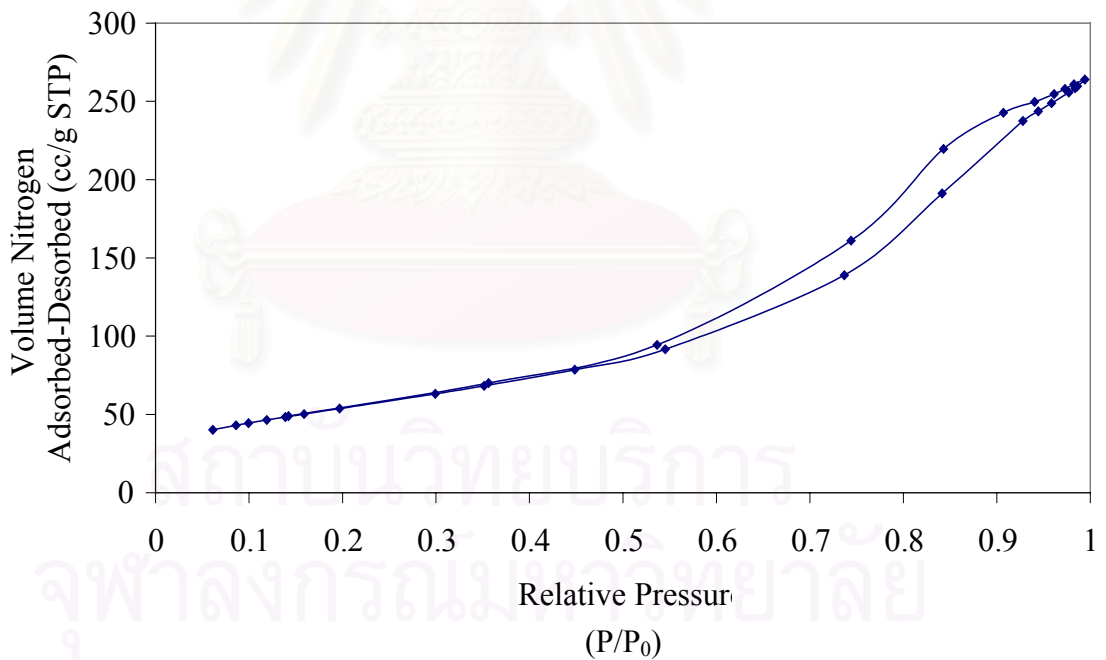


Si/Ti 0.04, 10 nm, the pore structure is ink bottle pore.

Figure 5.26 (cont.) Relative pressure of N₂ adsorption-desorption of silicon modified titania product synthesized in toluene for various molar ratios of Si/Ti and crystallite sizes, using BET surface measurement.



Si/Ti 0.06, 11 nm, the pore structure is ink bottle pore.



Si/Ti 0.08, 10 nm, the pore structure is ink bottle pore.

Figure 5.26 (cont.) Relative pressure of N₂ adsorption-desorption of silicon modified titania product synthesized in toluene for various molar ratios of Si/Ti and crystallite sizes, using BET surface measurement.

Table 5.11 Pore volume and average pore diameter of the silica modified titania products synthesized in two solvents.

<i>Si/Ti molar ratio</i>	<i>1,4 Butanediol</i>		<i>Toluene</i>	
	<i>Pore Volume (cc/g)^a</i>	<i>Average pore diameter^b (nm)</i>	<i>Pore Volume (cc/g)^a</i>	<i>Average pore diameter^b (nm)</i>
0.000	0.4	11	0.4	7
0.005	0.4	11	0.3	6
0.040	0.4	8	0.4	5
0.060	0.5	8	0.4	6
0.080	0.4	7	0.4	6

^a BJH cumulative desorption pore volume of pores

^b BJH desorption average pore diameter (4V/A)

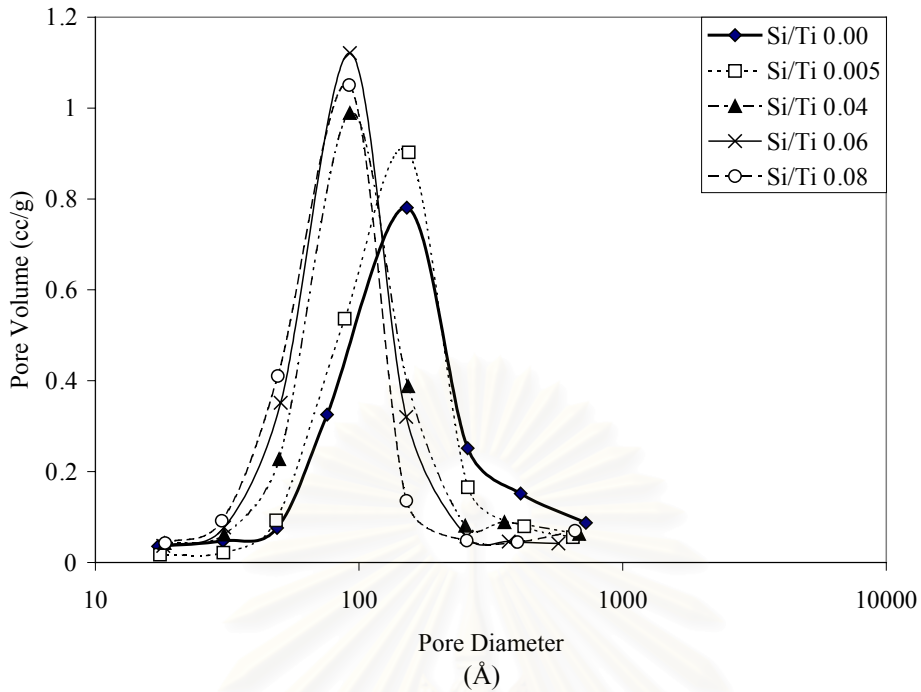


Figure 5.27 Pore size distribution of silica modified titania products synthesized in 1,4-BG for various contents of silica.

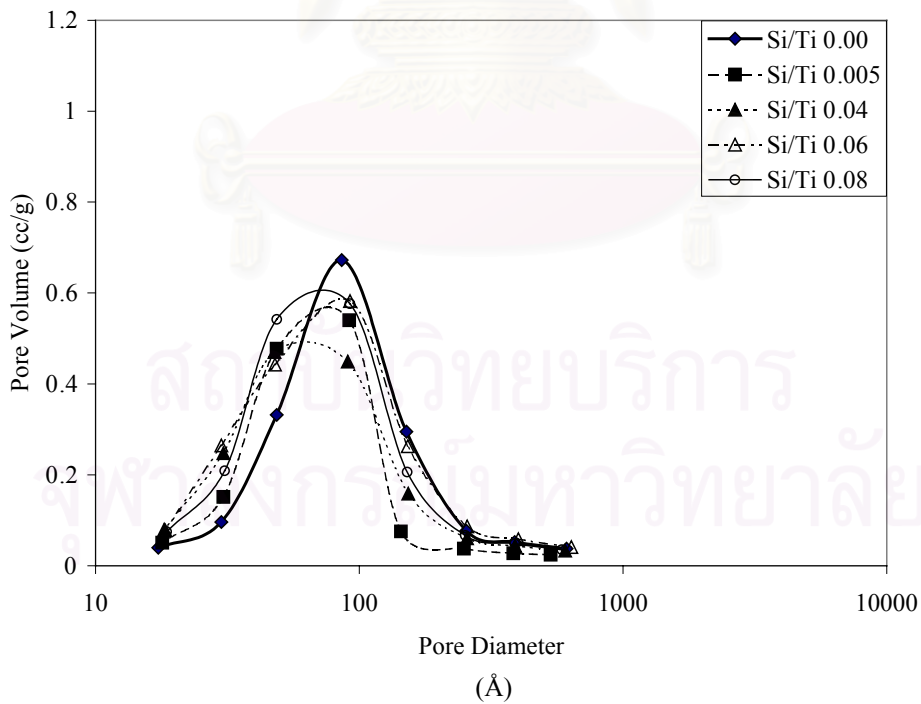
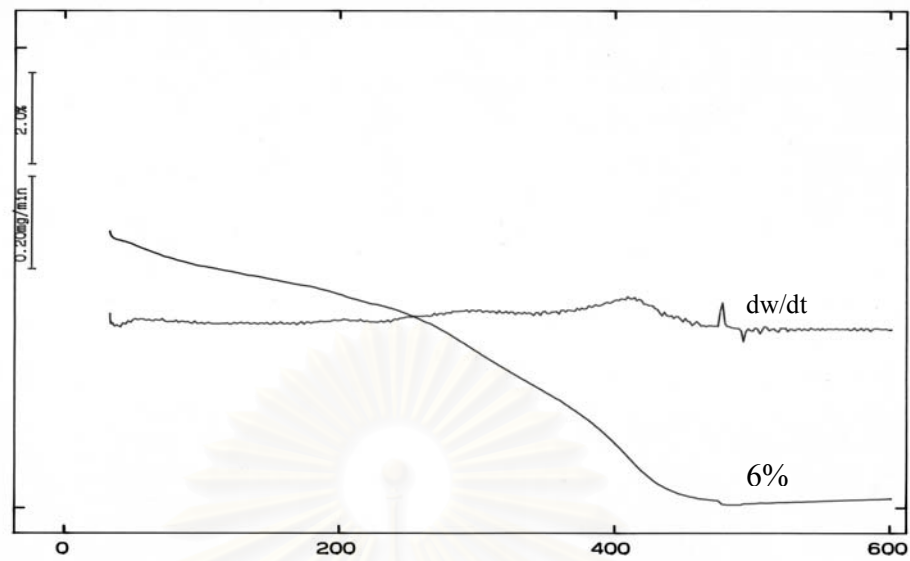


Figure 5.28 Pore size distribution of silica modified titania products synthesized in toluene for various contents of silica.

Figures 5.29 and 5.30 show weight loss of modified titania synthesized in two solvents during calcination in air from ambient temperature to 600°C. For both solvents, the weight losses were not different. These identify the contaminating of water and organic moiety on the product which were not different. Montoya *et al.* (1992) synthesized titania by sol-gel method. They found that the thermal gravimetric of the products had two main zone, the first range at 70 - 200°C was assigned to the elimination of the physically adsorbed water and alcohol, the second zone lied between 260 and 460°C and corresponded to the burning of the residual organic material and chemically adsorbed water. In the study, the thermal gravimetric shows the zone at 260 - 460°C.

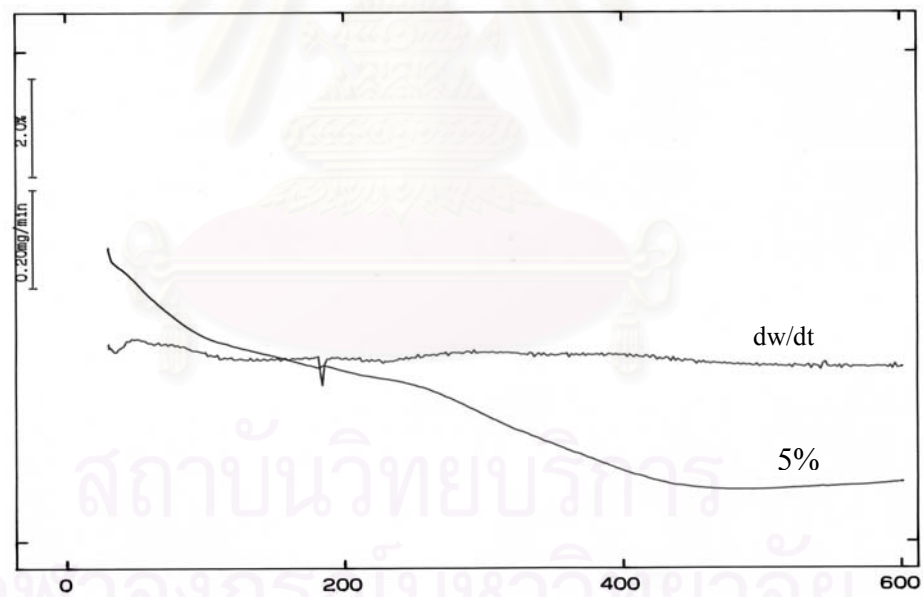
Figures 5.31 and 5.32 show XRD patterns of the silicon modified titania synthesized in 1,4-BG or toluene and calcinated at various temperatures. The phase transformation of anatase to rutile of the silicon modified titania synthesized in toluene began at 1000°C. On the other hand, the phase transformation of the silicon modified titania synthesized in 1,4-BG was not occurred at this temperature.

The FT-IR spectra of silicon modified titania synthesized in both solvents for various amount of silicon as shown in Figure 5.33 and 5.34. Transmittance band at ca. 1100 and 1200 cm^{-1} can be attributed to symmetric Si-O-Si stretching vibration while titania-silica mixed oxide are characterized by a typical band at ca. 950 cm^{-1} , assigned to the distorted Si-O tetrahedron due to the presence of Ti-O-Si bands. (Imai *et al.*, 1999; Dean, 1999; Mariscal *et al.*, 2000; Sornnarong Theinkeaw, 2000; Sibū *et al.*, 2002). Besides, the Ti-O-Ti bond are observed at 495-436 cm^{-1} (Musić *et al.*, 1997), but they were not observe in this modified titania. An increase of calcination temperature of silicon modified titania were not effect on bonding of Si and Ti but the organic bands were absent at high temperature. These results confirmed to the weight loss due to the organic moiety were calcined at 400 - 600°C.



Temperature (°C)

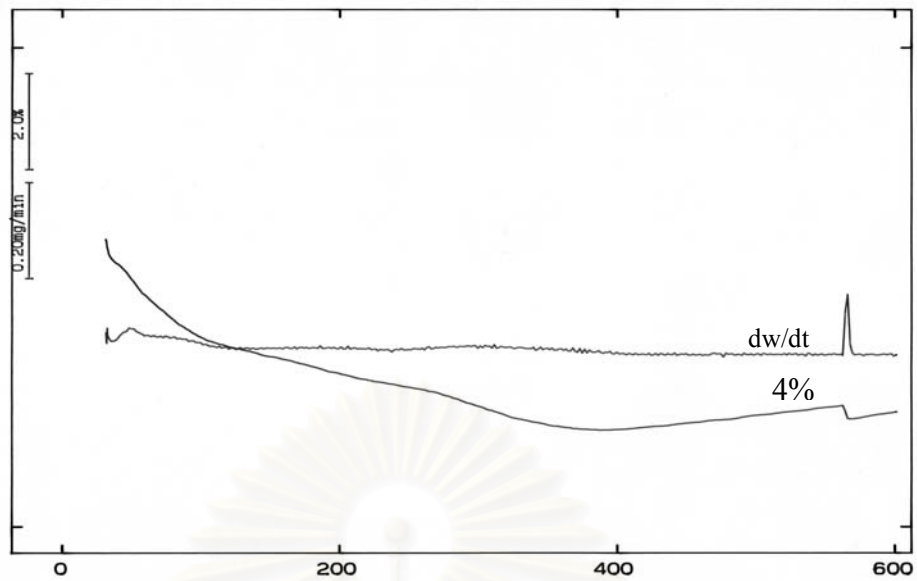
Pure titania



Temperature (°C)

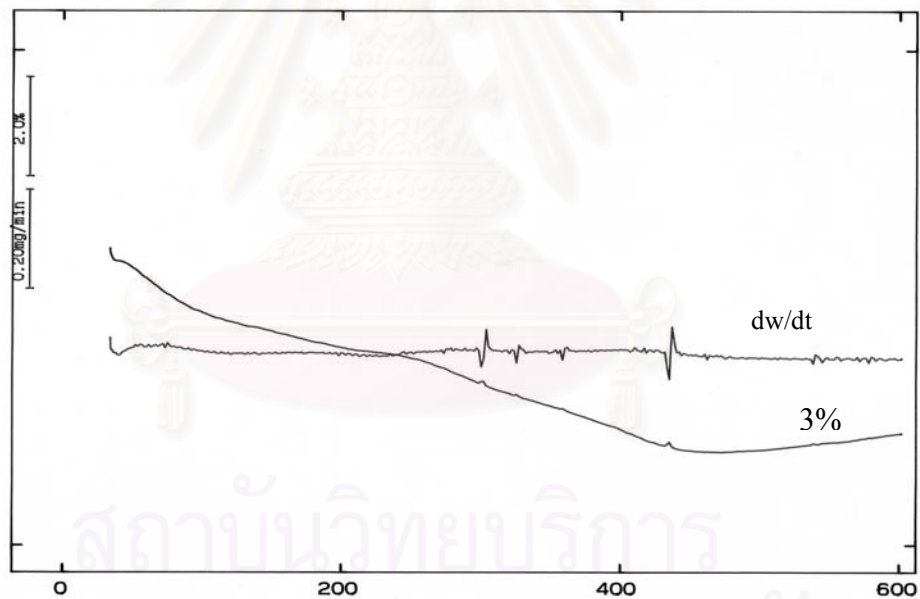
Si/Ti 0.04

Figure 5.29 Weight loss of silica modified titania products synthesized in 1,4-BG for various ratios of Si/Ti and weight loss percentages under the calcinations condition.



Temperature (°C)

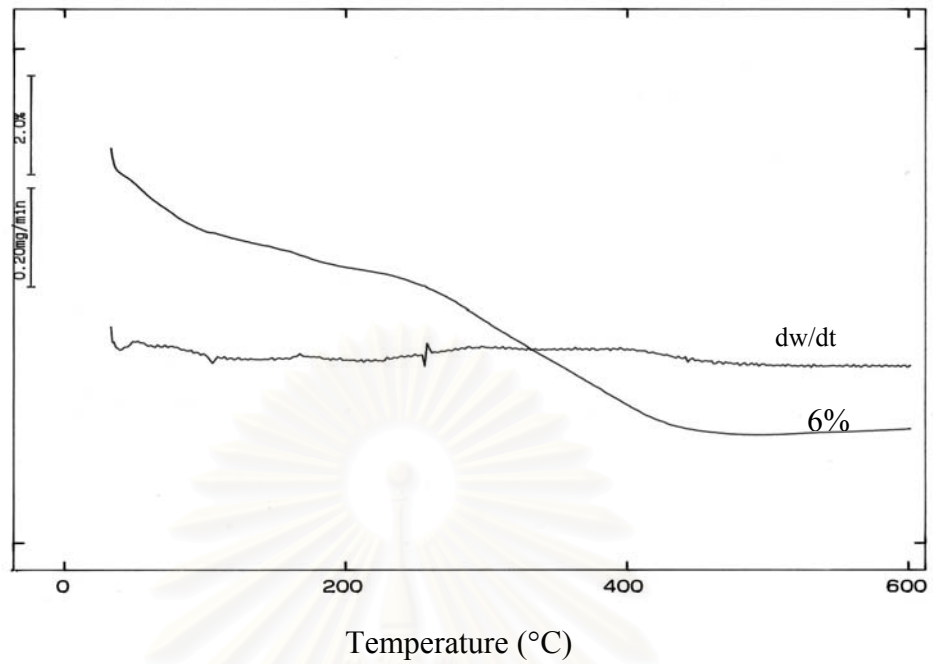
Si/Ti 0.06



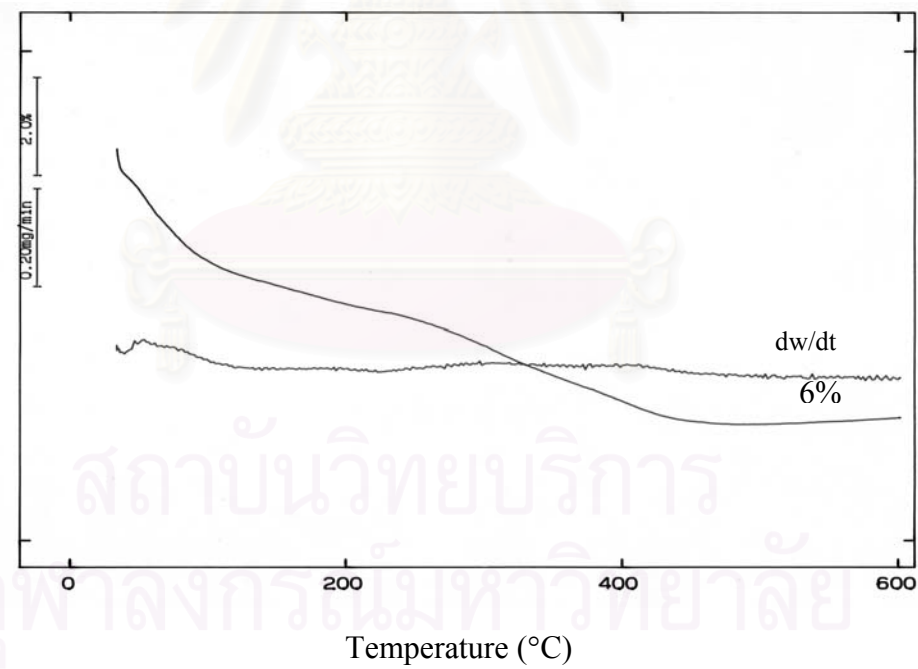
Temperature (°C)

Si/Ti 0.08

Figure 5.29 (cont.) Weight loss of silica modified titania products synthesized in 1,4-BG for various ratio of Si/Ti and weight loss percentage under the calcinations condition.

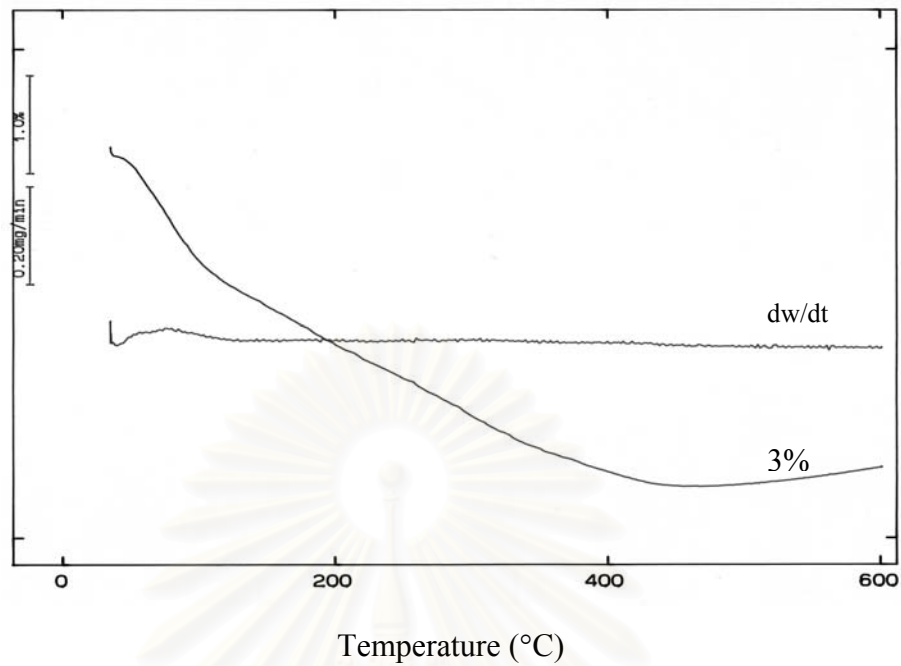


Pure titania

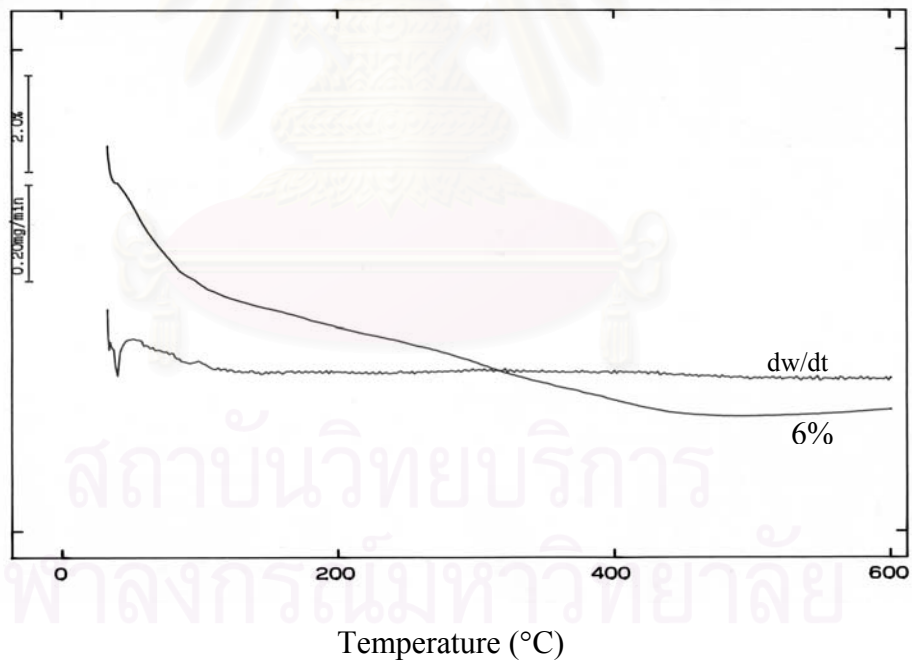


Si/Ti 0.04

Figure 5.30 Weight loss of silica modified titania products synthesized in toluene for various ratios of Si/Ti and weight loss percentages under the calcinations condition.



Temperature (°C)
Si/Ti 0.06



Temperature (°C)
Si/Ti 0.08

Figure 5.30 (cont.) Weight loss of silica modified titania products synthesized in toluene for various ratios of Si/Ti and weight loss percentages under the calcinations condition.

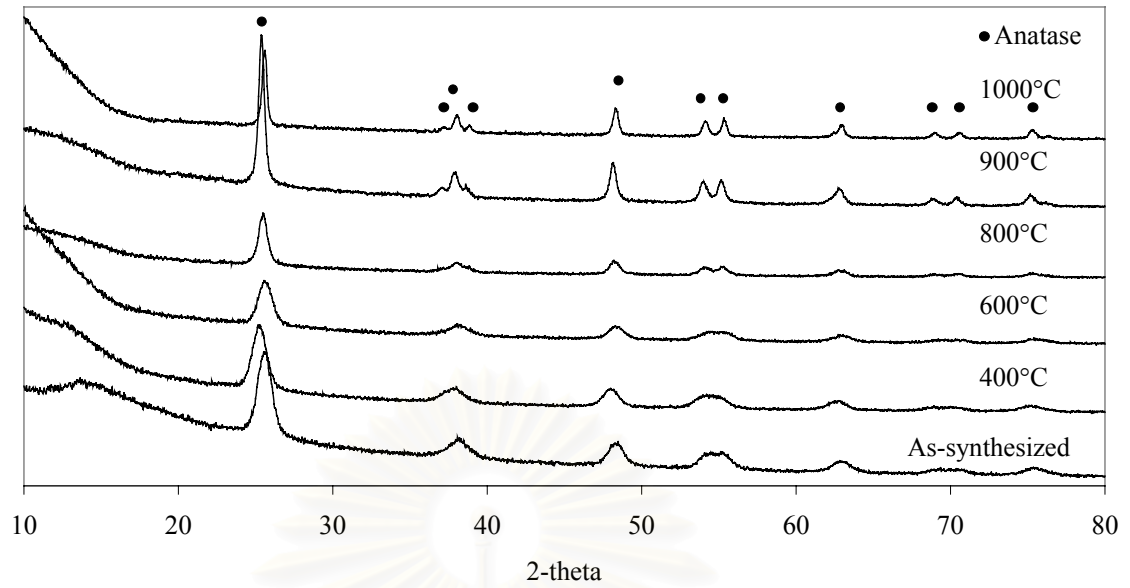


Figure 5.31 XRD pattern of silica modified titanias synthesized in 1,4-BG at molar ratio of Si/Ti as 0.08 after calcination in various temperatures.

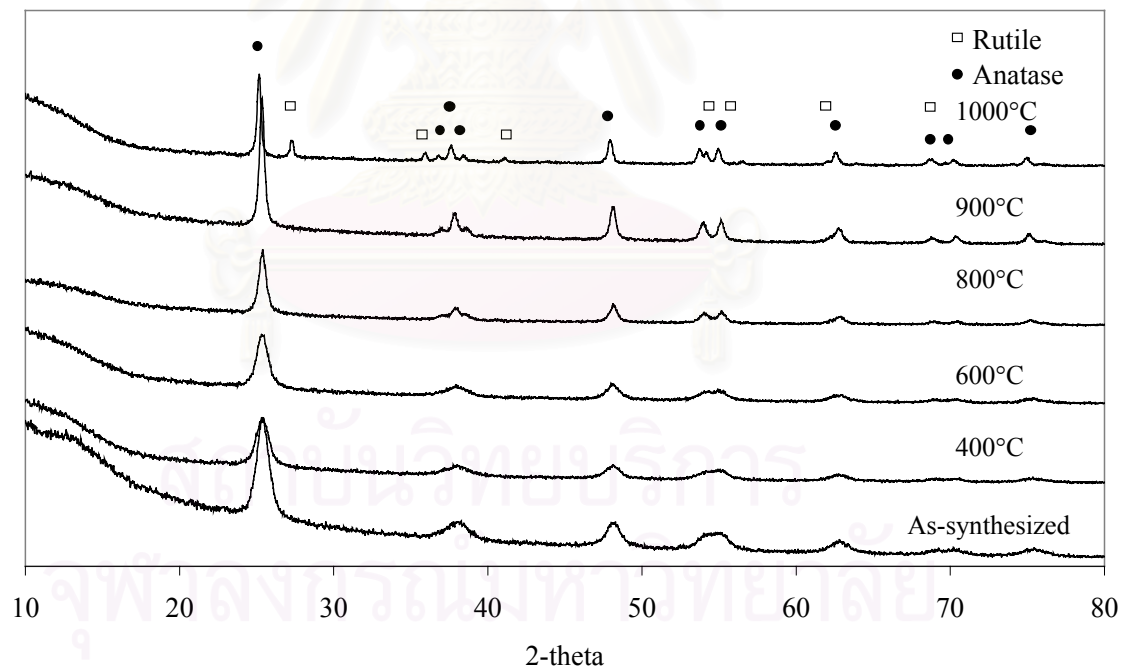


Figure 5.32 XRD pattern of silica modified titanias synthesized in toluene at molar ratio of Si/Ti as 0.08 after calcination in various temperatures. The phase transformation was starting at 1000°C.

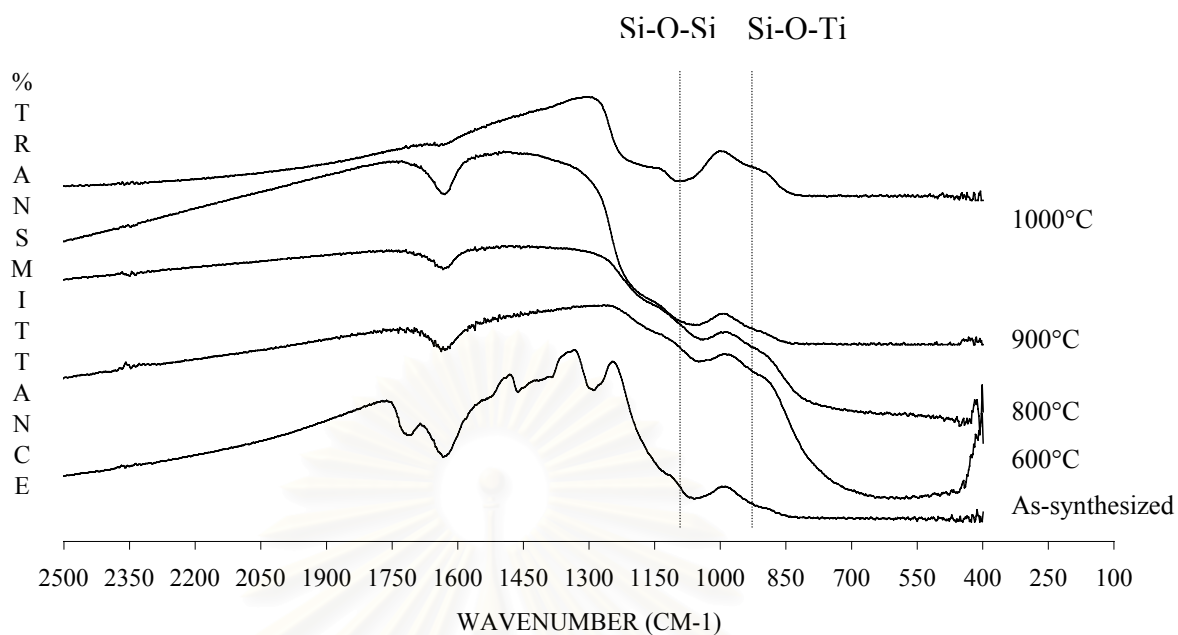


Figure 5.33 FT-IR spectra of silicon modified titania products synthesized in 1,4-BG at molar ratio of Si/Ti as 0.08 after calcination in various temperatures.

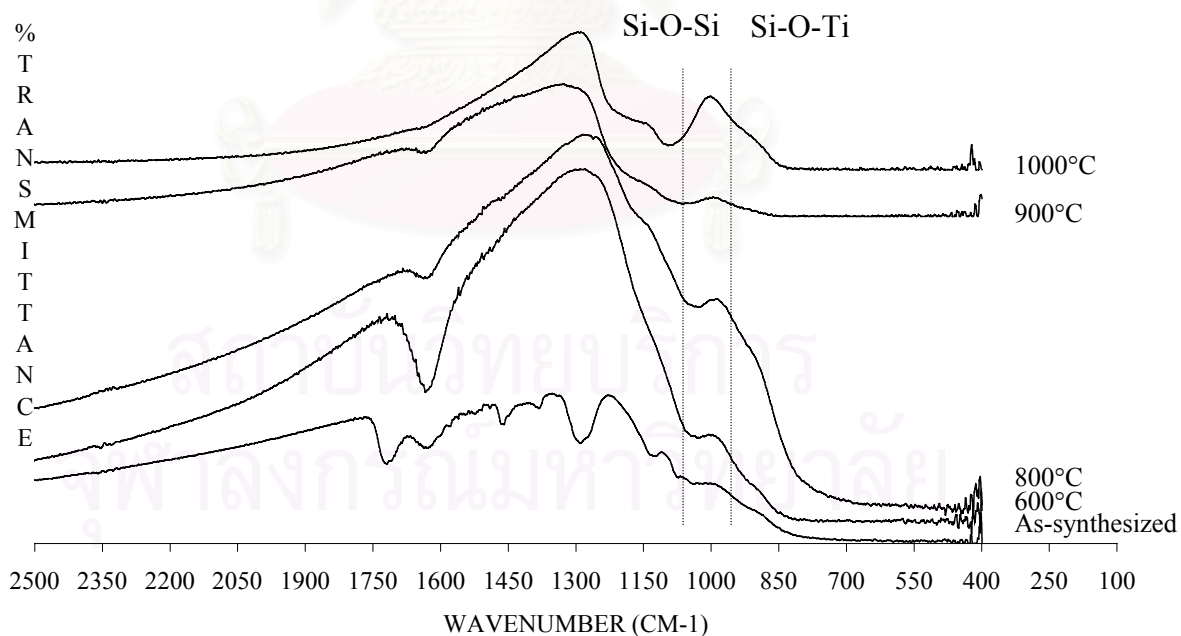


Figure 5.34 FT-IR spectra of silicon modified titania products synthesized in toluene at molar ratio of Si/Ti as 0.08 after calcination in various temperatures.

5.2.2 Effect of aluminium on titania product

Aluminium modified titania products were synthesized in both solvents at 300°C for 2 hrs. XRD pattern of aluminium modified titania products were shown in Figures 5.35 and 5.36. This indicated that the modified titanias were anatase phase without contamination of other titania phase or alumina phase. Table 5.12 shows the crystallite size and surface area of aluminium modified titania products that synthesized in both organic solvents. For this table, in 1,4-BG, the crystallite size slightly decreased with increasing the molar ratio of Al/Ti. On the other hand, the BET surface area slightly increased with increasing the aluminium content. The S_1/S_2 values of aluminium modified titanias that synthesized in 1,4-BG were smaller than the pure titania. This indicated that the aluminium modified titania crystals were aggregated. For the synthesis in toluene, the crystallite sizes did not differ with increasing the Al/Ti molar ratio. The BET surface area, first, are slightly increased to 174 m²/g and slowly decreased with increasing the aluminium content. The S_1/S_2 values were slowly decreased. These indicate that the effect of amounts of aluminium on the structure of titania that the crystals were aggregated with increasing the aluminium contents. SEM morphology of the secondary particle of alumina modified titania product show in Figure 5.37. For 1,4-BG, the secondary particle morphologies did not change. The shape is irregular particle. Alternatively, in toluene, the secondary particles were agglomerated. The particles size were increased with increasing the molar ratio.

Considering S_1/S_2 value of the synthetics in both solvents, the values were decreased with increasing the aluminium content. This indicated that the aluminium doped in the starting material was effecting on the product which the surface area was loss due to the aggregation of the crystals. Comparing the S_1/S_2 of the synthetics in both solvents was found that the aluminium modified titania synthesized in toluene may be contaminated with amorphous phase or the crystal was formed to the free-flow crystal.

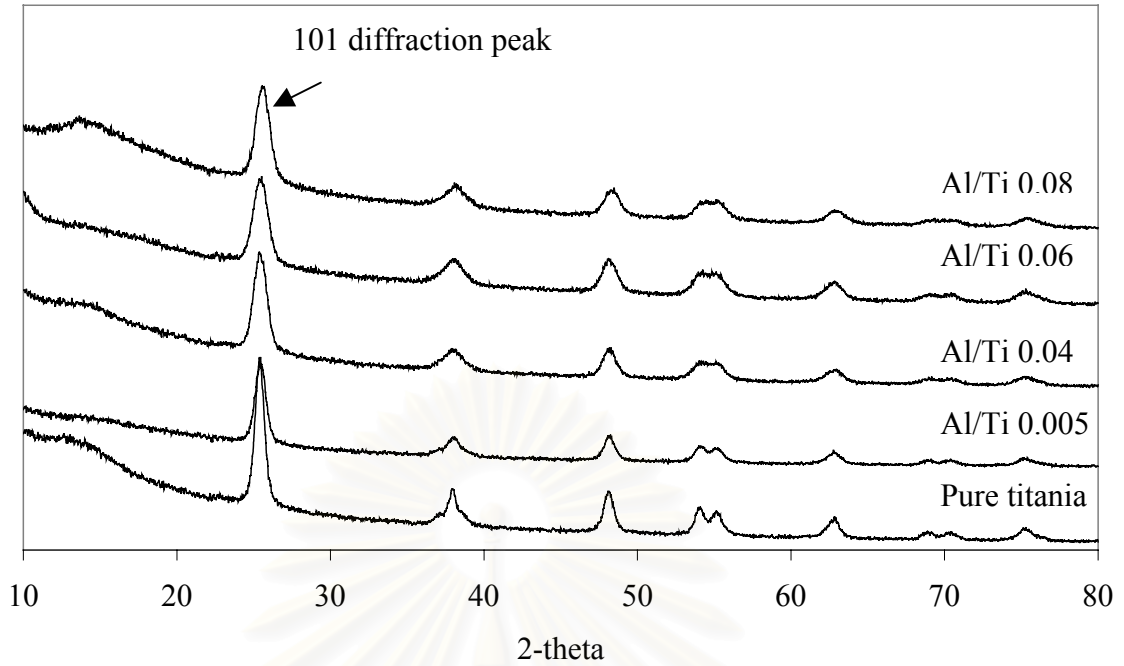


Figure 5.35 XRD patterns of as-synthesized aluminium modified titania products synthesized in 1,4-BG for various aluminium contents in molar ratio of Al/Ti. All as-synthesized were anatase titania without contamination of other phase of titania and silica phase.

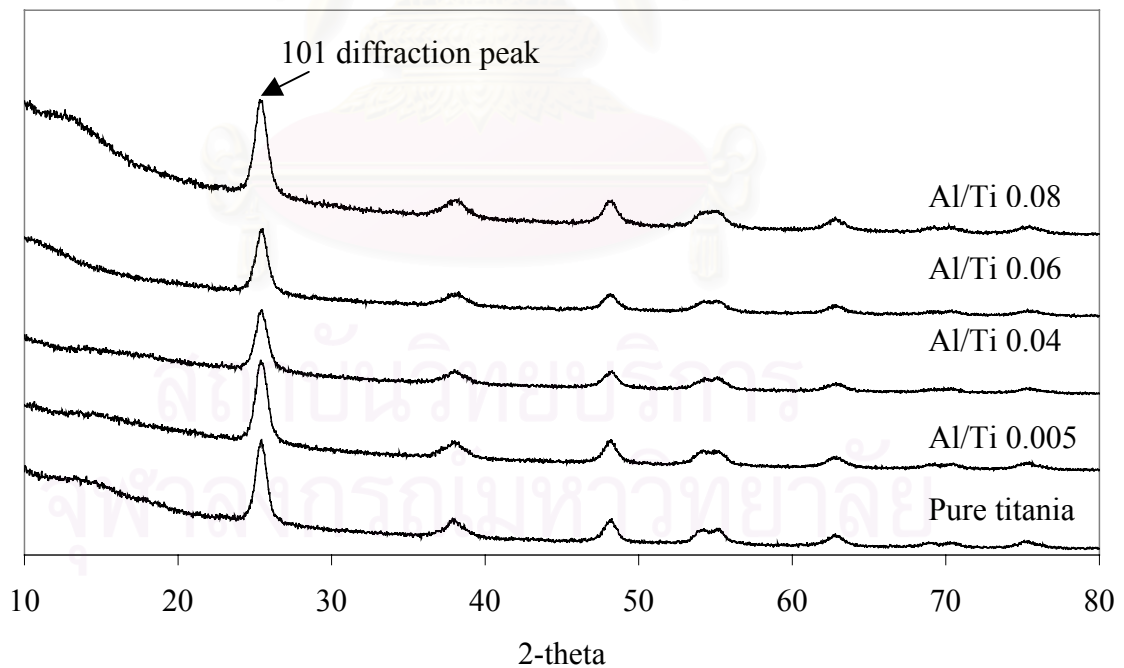
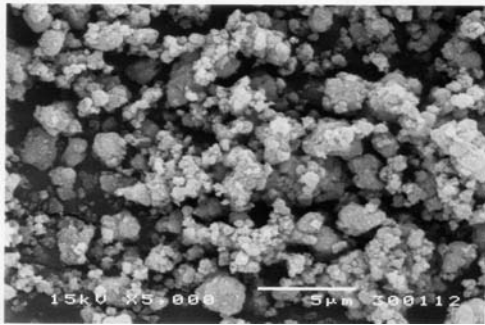
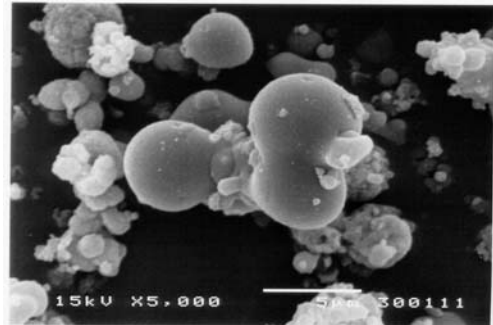


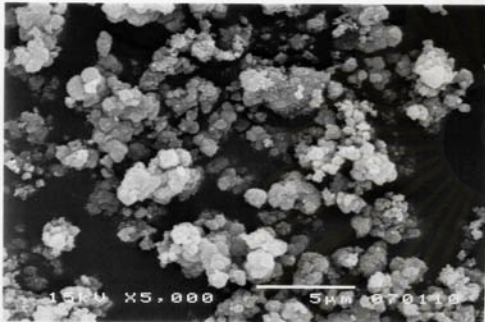
Figure 5.36 XRD patterns of as-synthesized aluminium modified titania products synthesized in toluene for various aluminium contents in molar ratio of Al/Ti. All as-synthesized were anatase titania without contamination of other phase of titania and silica phase.



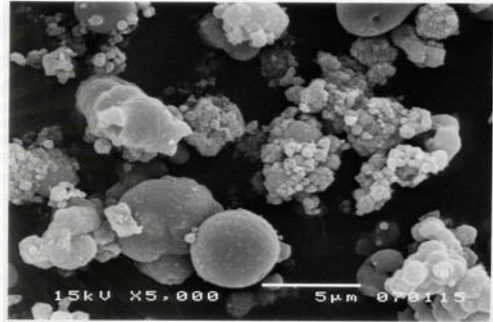
Pure titania, 1,4-BG



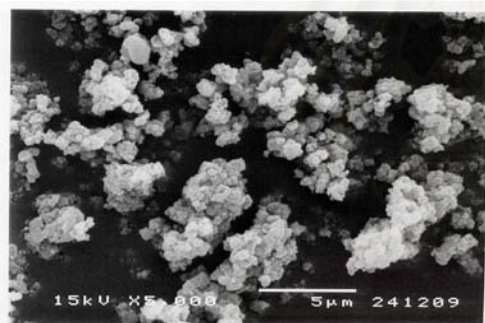
Pure titania, toluene



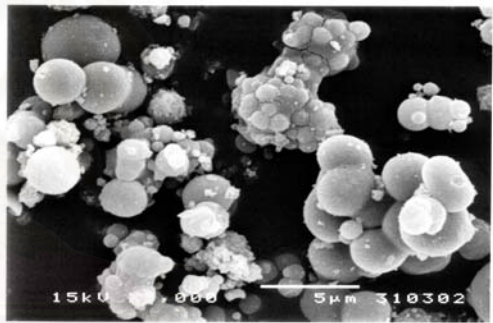
Al/Ti 0.005, 1,4-BG



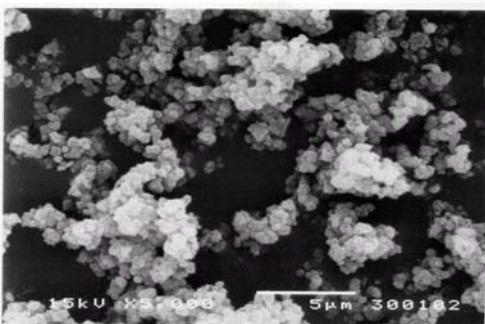
Al/Ti 0.005, toluene



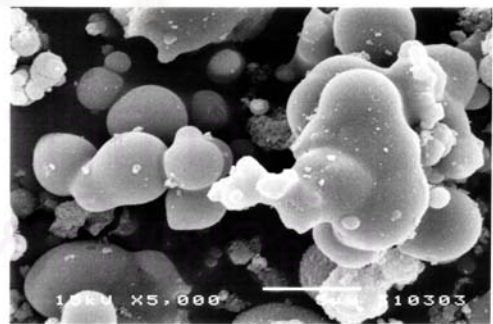
Al/Ti 0.04, 1,4-BG



Al/Ti 0.04, toluene



Al/Ti 0.08, 1,4-BG



Al/Ti 0.08, toluene

Figure 5.37 SEM morphology of aluminium modified titania products synthesized in two solvents of various aluminium contents in molar ratio of Al/Ti. For synthesized in 1,4-BG, the secondary particle were irregular shape and not depended on the content of silicon. On the other hand, for synthesized in toluene, the secondary particles were spherical shape and agglomerated with increasing the amount of aluminium.

Table 5.12 The crystallite sizes and the specific surface areas of aluminium modified titania products that were synthesized in 1,4-BG or toluene for various aluminium contents of molar ratio of Al/Ti.

<i>Al/Ti molar ratio^a</i>	<i>1,4-BG</i>				<i>Toluene</i>			
	<i>Crystallite size (nm)^b</i>	<i>Surface area (m²/g)</i>		<i>S₁/S₂</i>	<i>Crystallite size (nm)^b</i>	<i>Surface area (m²/g)</i>		<i>S₁/S₂</i>
		<i>S₁^c</i>	<i>S₂^d</i>			<i>S₁^c</i>	<i>S₂^d</i>	
0.000	13	110	118	0.9	12	145	128	1.1
0.005	13	116	118	1.0	11	155	140	1.1
0.04	10	121	154	0.8	10	174	154	1.1
0.06	10	125	154	0.8	11	152	140	1.1
0.08	9	138	171	0.8	11	149	140	1.1

^a The titania products synthesized from mixed-reactant (AIP and TNB) in molar ratio (Al/Ti) at 300°C in organic solvents.

^b Crystallite size of anatase titania from the 101 diffraction peak by using Sherrer equation.

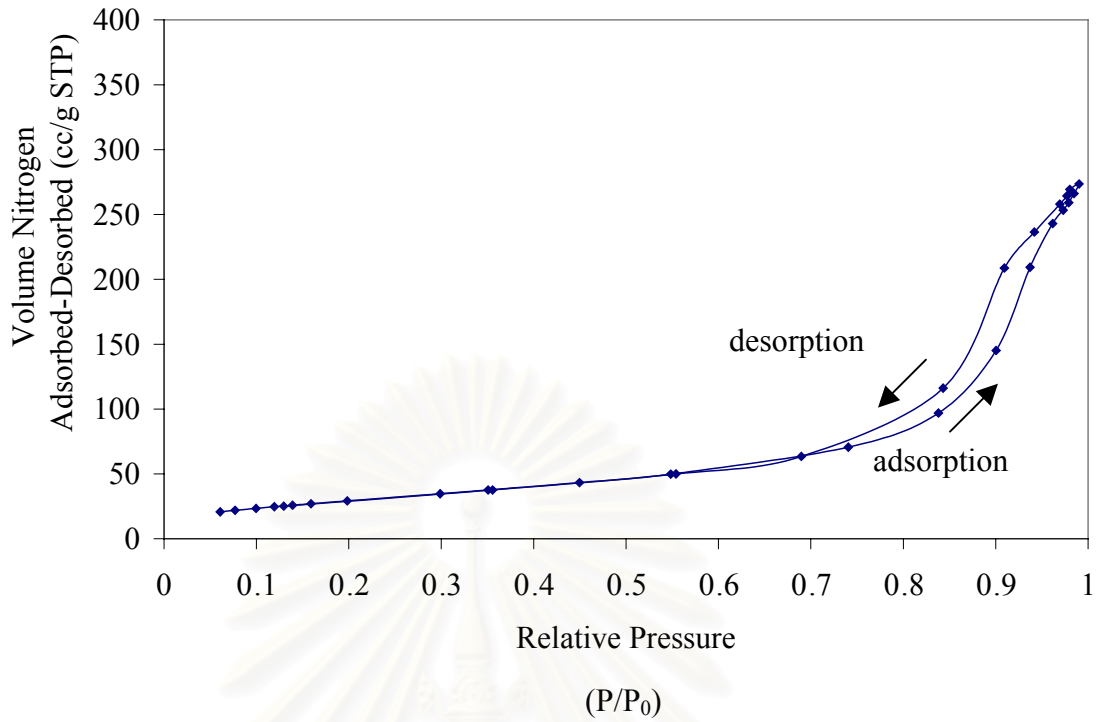
^c Specific BET surface area from BET measurement.

^d Specific surface area calculated from equation of $6/d\rho$ on assumption that the crystal is spherical particle and the density of anatase titania is 3.9 g cm⁻³.

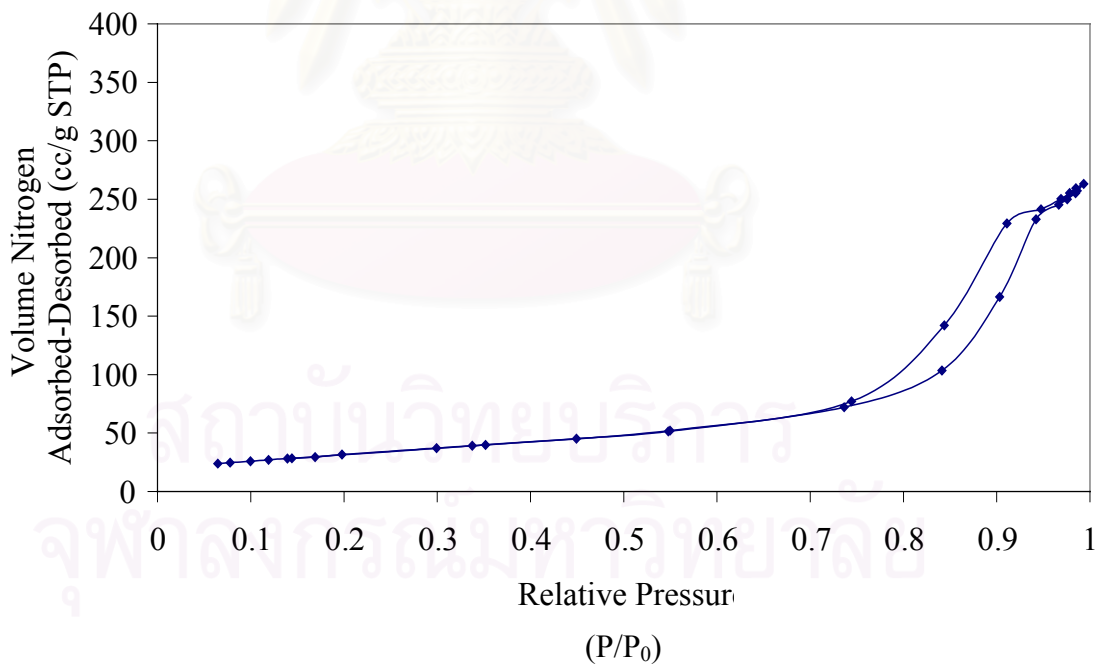
Relative pressure of N₂ adsorption-desorption of modified titanias show in Figure 5.38 and Figure 5.39. The pores of the titania products were mainly microporous and some mesoporous. The pore structures were the open-end pore. The products synthesized in toluene, the pore structures were mostly slit-side pore. On the other hand, the aluminium modified titania synthesized in 1,4-BG, the pore structures were mainly cylinder pore. For this synthetics, the relative pressures of N₂ adsorbed and desorbed did independent on the crystallite sizes which, in pure titania sample, the relative pressure of N₂ adsorbed and desorbed depended on the crystallite size. In addition, the relative pressures of N₂ adsorbed and desorbed did independent on the content of aluminium which doped in the starting material of both synthetics. So that the isotherms were not scarcely change.

Table 5.13 show the pore volume and average pore diameter of aluminium modified titanias synthesized in both solvents. For the synthesis in toluene, the pore volumes were slowly decreased with increasing the content of aluminium. This relate to the crystallite size which the small size has been the small pore volume. For the synthesis in 1,4-BG, the pore volumes were slightly increased with increasing the aluminium content. The synthesis in toluene, the average pore diameter slightly decreased with increasing the aluminium content. This confirmed the modified titania crystals were aggregated. On the other hand, the synthesis in 1,4-BG, the average pore diameters were constant not dependent on the aluminium content, about 16 – 14 nm. Figures 5.40 and 5.41 show the pore size distributions of the aluminium modified titania synthesized in both solvents. For the synthesis in 1,4-BG, the distribution curve was widely curves and the pore volume was decreased with increasing the aluminium content. On the other hand, the synthesis in toluene, the distribution curve was not change but the pore volume decreased with increasing the aluminium content.

Figure 5.42 and 5.43 show weight loss of the aluminium modified titanias that synthesis in both solvents. For increasing the content of aluminium, the weights losses of the products were not difference. These indicated that the contamination of organic moiety in sample had been small amount and not difference.

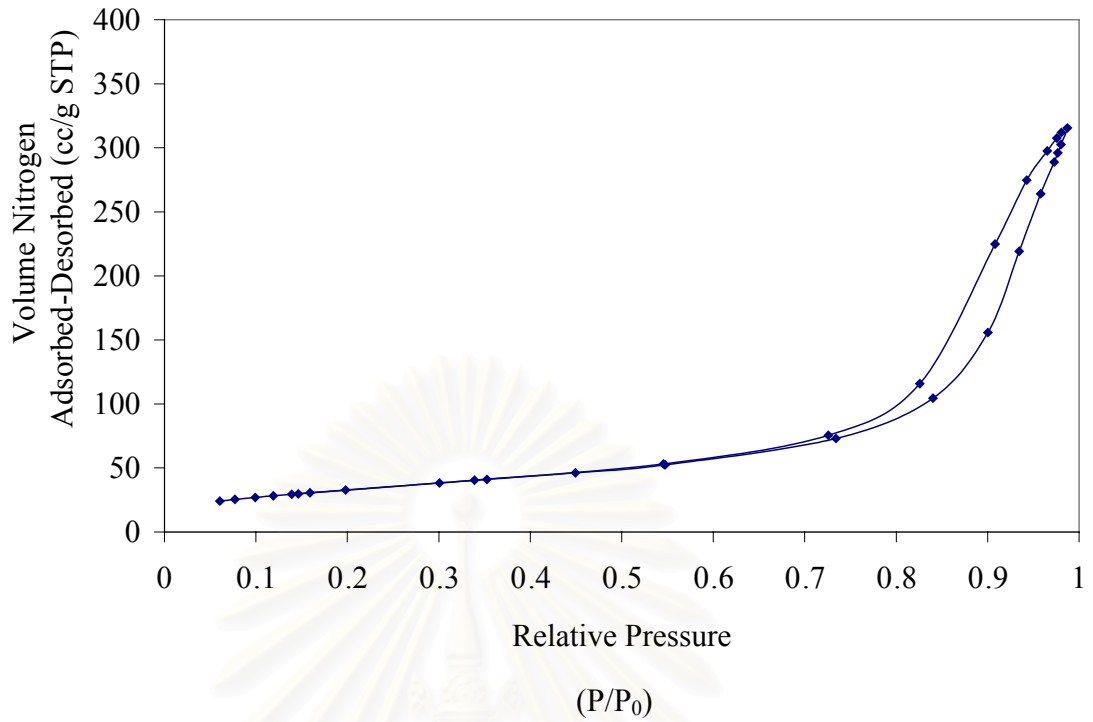


Pure titania, 13 nm, the pore structure is mainly cylindrical pore.

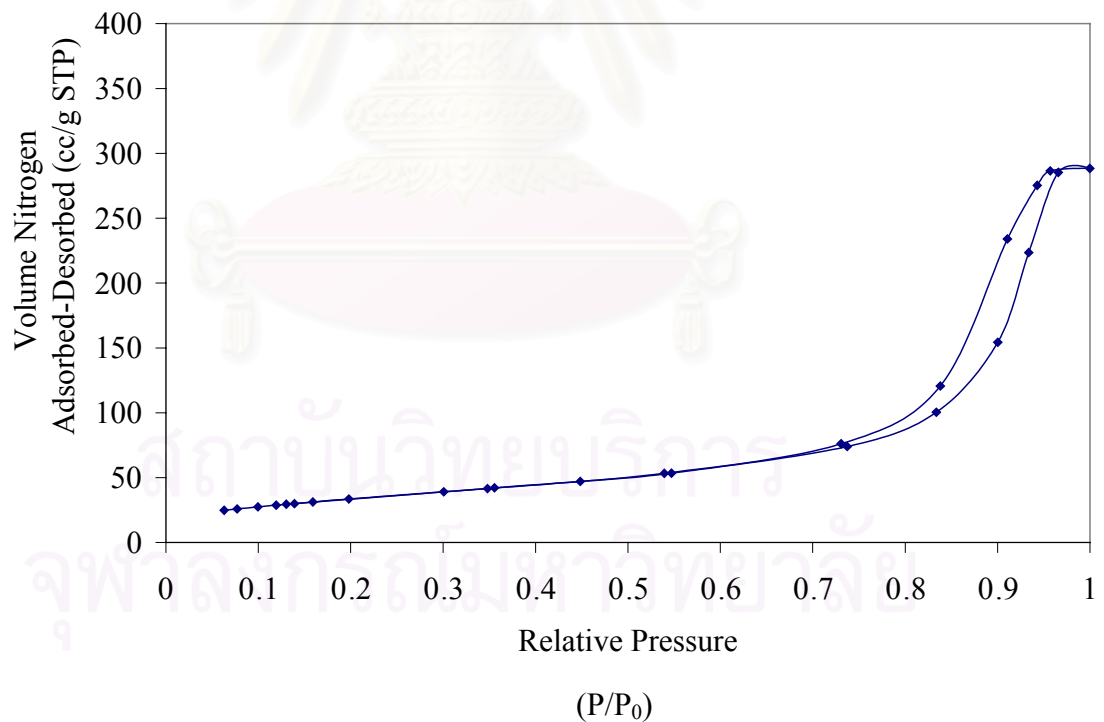


Al/Ti 0.005, 13 nm, the pore structure is mainly cylindrical pore.

Figure 5.38 Relative pressure of N₂ adsorption-desorption of aluminium modified titania product synthesized in 1,4-BG for various molar ratio of Al/Ti and crystallite sizes using BET surface measurement. (see APPENDIX C)

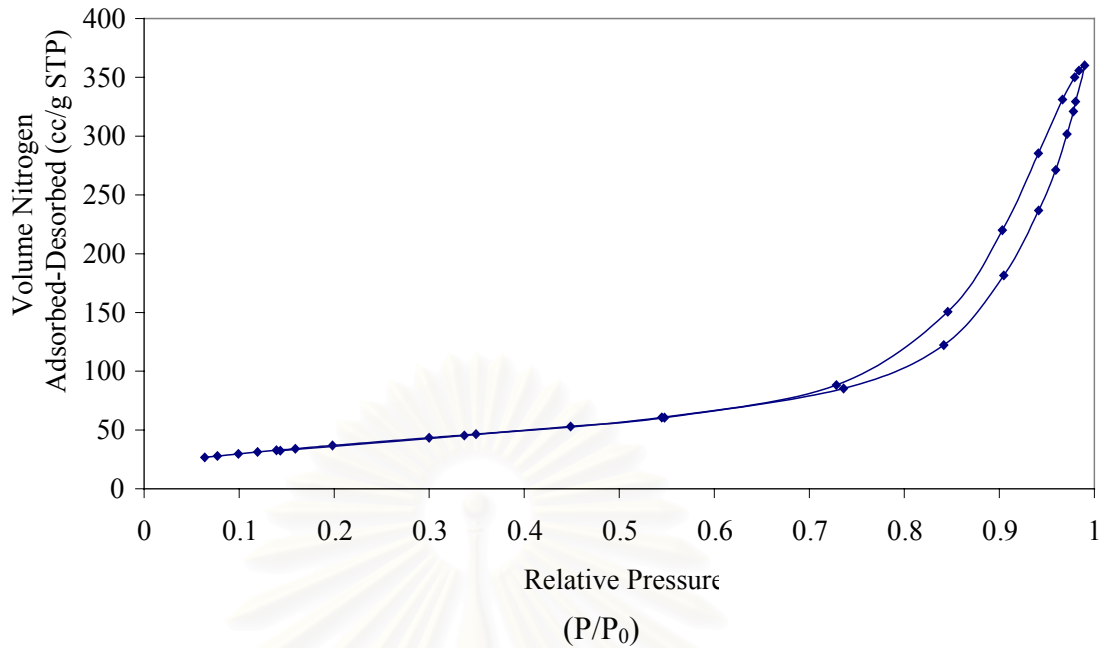


Al/Ti 0.04, 10 nm, the pore structure is mainly cylindrical pore.



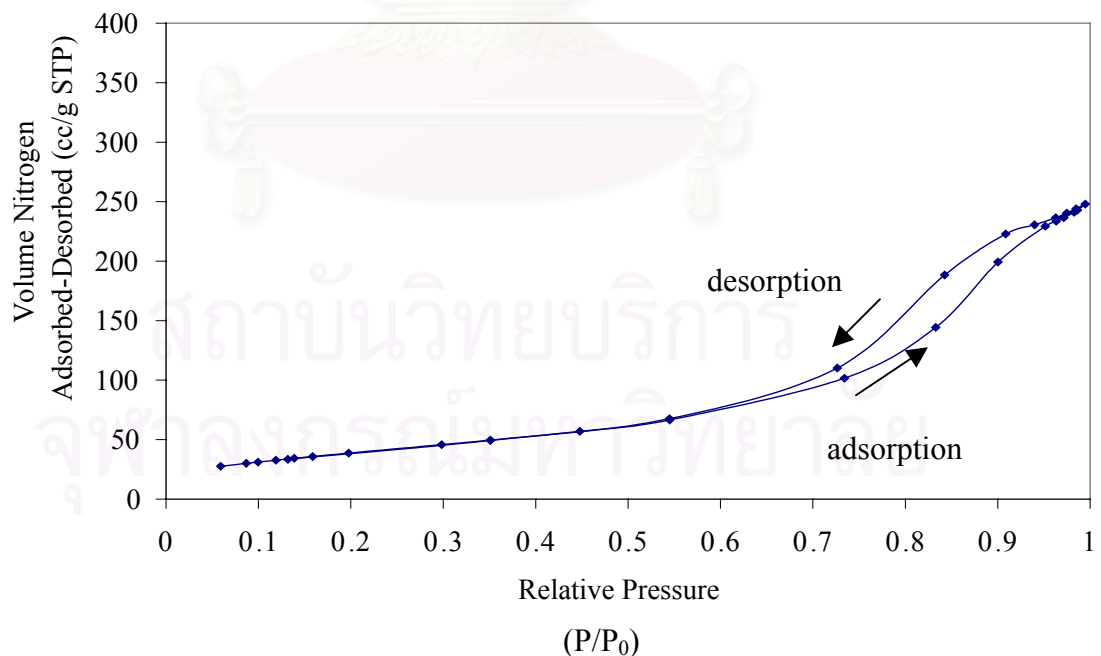
Al/Ti 0.06, 10 nm, the pore structure is mainly cylindrical pore.

Figure 5.38 (cont.) Relative pressure of N₂ adsorption-desorption of aluminium modified titania product synthesized in 1,4-BG for various molar ratio of Al/Ti and crystallite sizes using BET surface measurement.



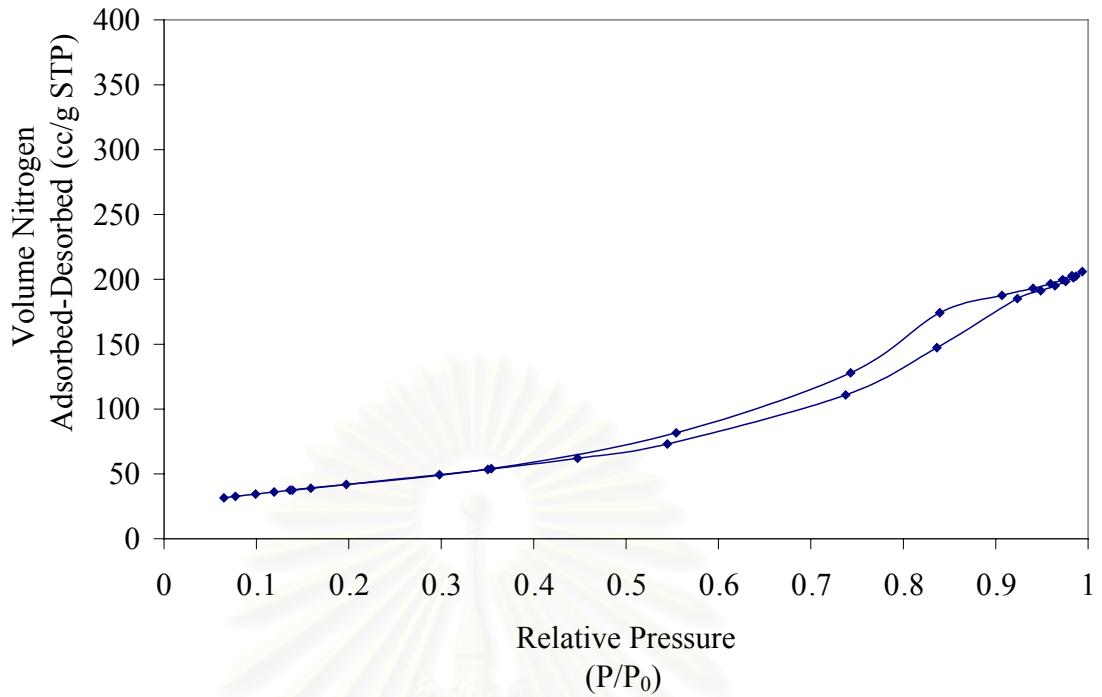
Al/Ti 0.08, 9 nm, the pore structure is mainly cylindrical pore.

Figure 5.38 (cont.) Relative pressure of N₂ adsorption-desorption of aluminium modified titania product synthesized in 1,4-BG for various molar ratio of Al/Ti and crystallite sizes using BET surface measurement.

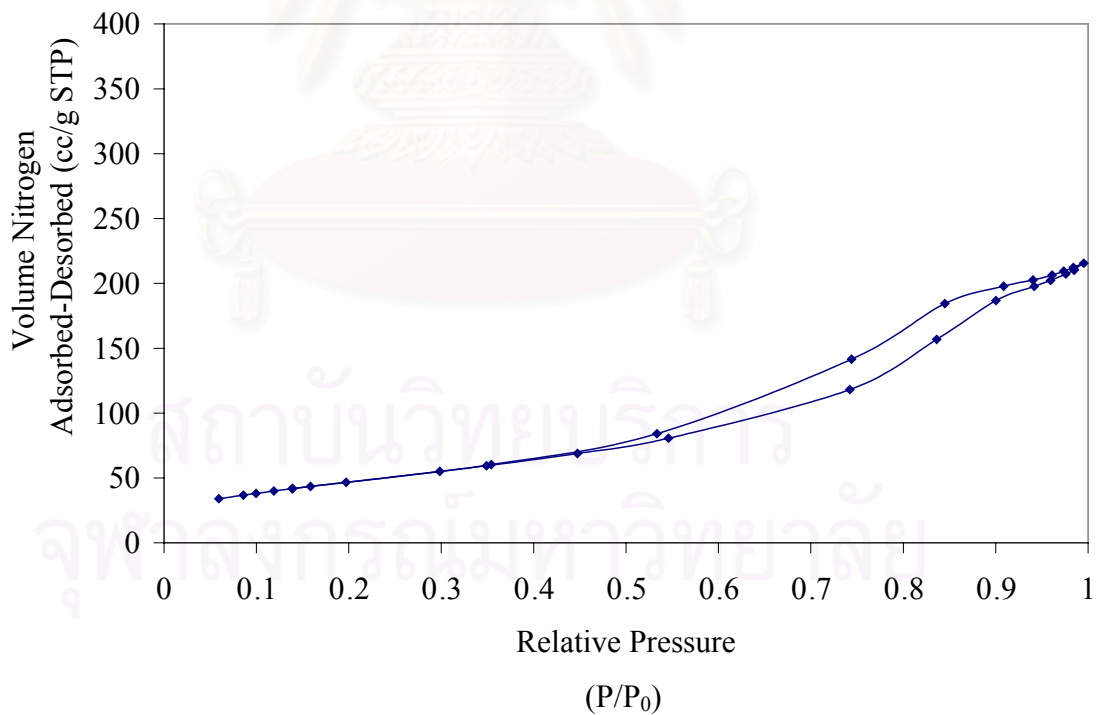


Pure titania, 12 nm, the pore structure is ink bottle pore.

Figure 5.39 Relative pressure of N₂ adsorption-desorption of aluminium modified titania product synthesized in toluene for various molar ratio of Al/Ti and crystallite sizes, from BET surface measurement. (see APPENDIX C)

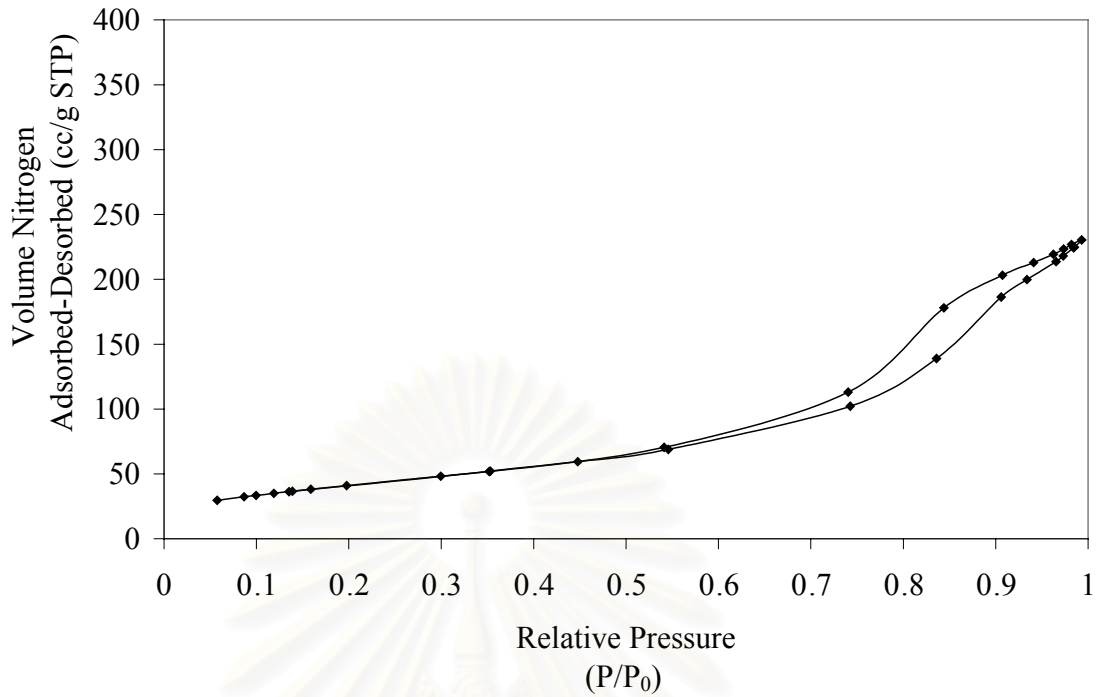


Al/Ti 0.005, 11 nm, the pore structure is ink bottle pore.

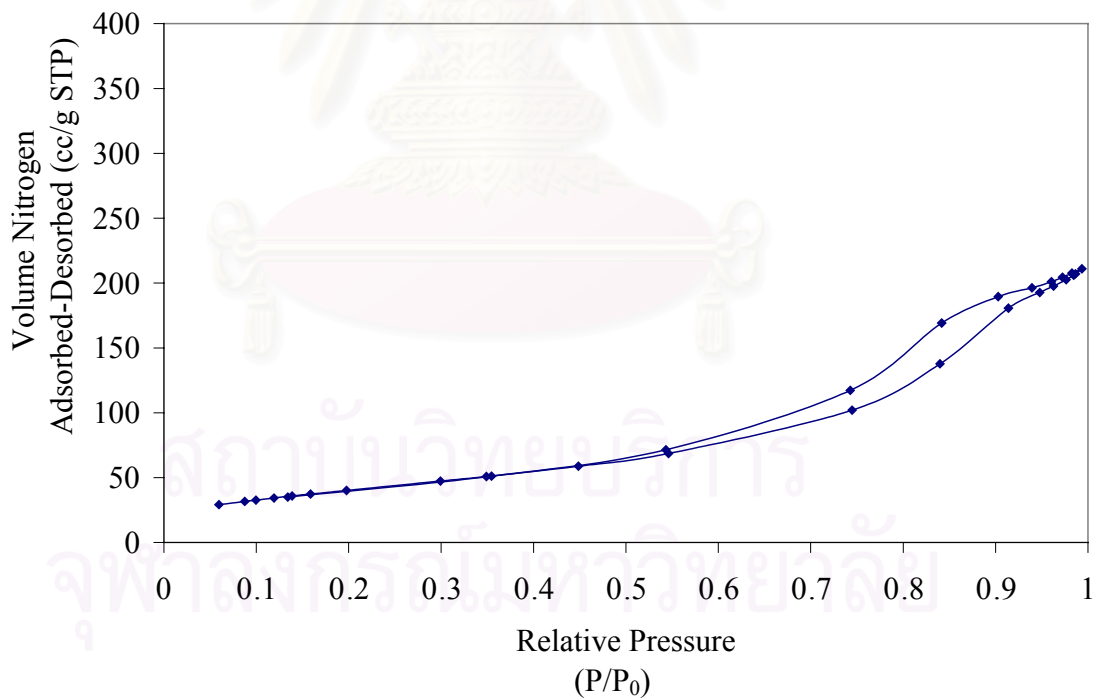


Al/Ti 0.04, 10 nm, the pore structure is ink bottle pore.

Figure 5.39 (cont.) Relative pressure of N₂ adsorption-desorption of aluminium modified titania product synthesized in toluene for various molar ratio of Al/Ti and crystallite sizes, from BET surface measurement.



Al/Ti 0.06, 11 nm, the pore structure is ink bottle pore.



Al/Ti 0.08, 11 nm, the pore structure is ink bottle pore.

Figure 5.39 (cont.) Relative pressure of N₂ adsorption-desorption of aluminium modified titania product synthesized in toluene for various molar ratio of Al/Ti and crystallite sizes, from BET surface measurement.

Table 5.13 Pore volumes and average pore diameters of the aluminium modified titania products synthesized in two solvents.

<i>Al/Ti molar ratio</i>	<i>1,4 Butanediol</i>		<i>Toluene</i>	
	<i>Pore Volume (cc/g)^a</i>	<i>Average pore diameter^b (nm)</i>	<i>Pore Volume (cc/g)^a</i>	<i>Average pore diameter^b (nm)</i>
0.000	0.4	11	0.4	7
0.005	0.4	10	0.3	6
0.040	0.5	12	0.3	5
0.060	0.4	10	0.4	7
0.080	0.6	11	0.3	6

^a BJH cumulative desorption pore volume of pores

^b BJH desorption average pore diameter (4V/A)

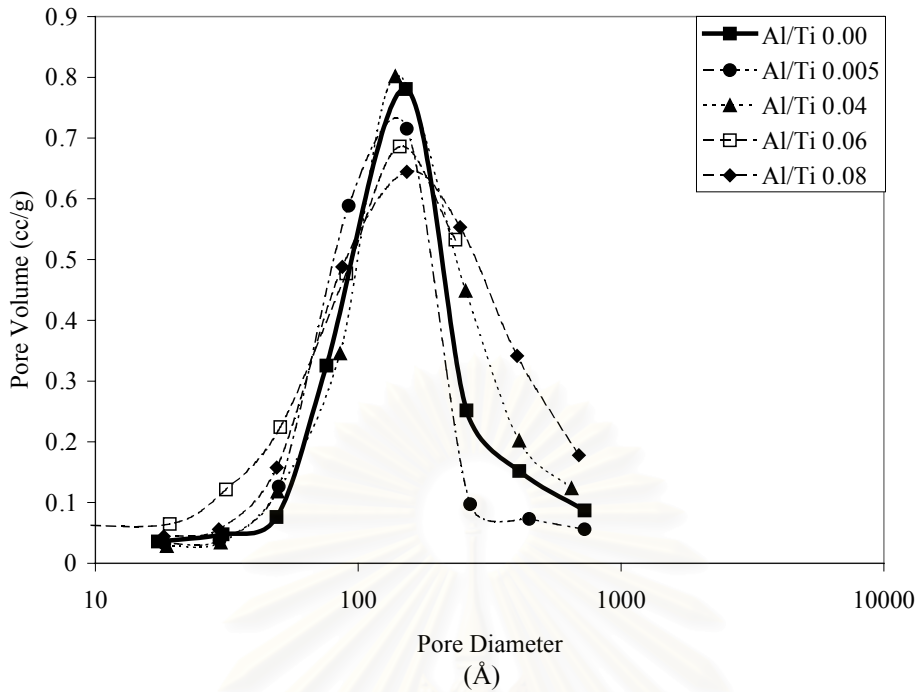


Figure 5.40 Pore size distribution of alumina modified titania products synthesized in 1,4-BG for various contents of alumina.

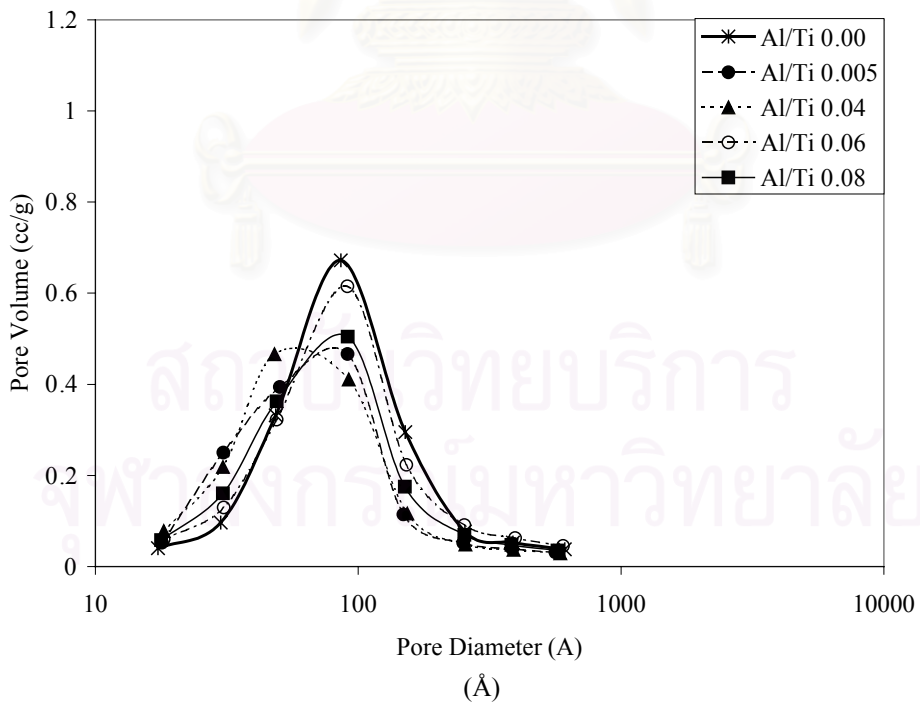
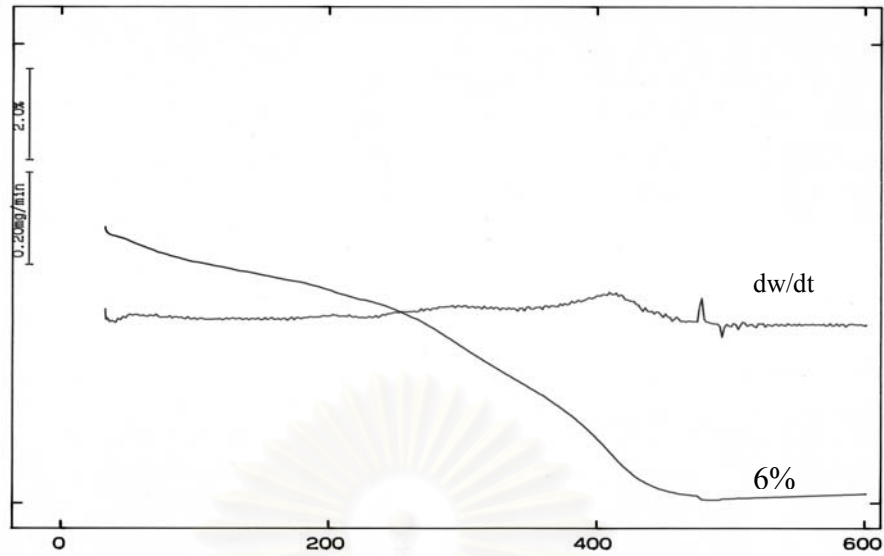
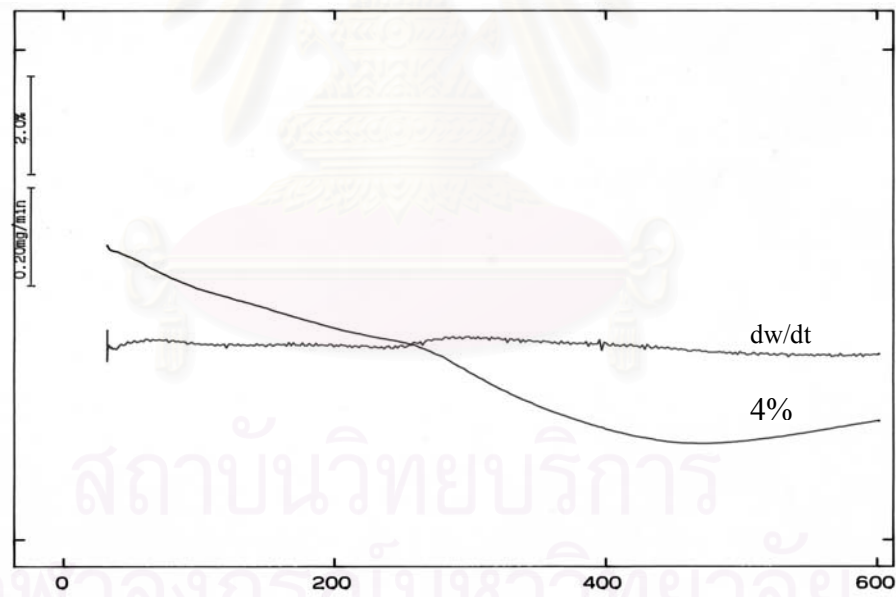


Figure 5.41 Pore size distribution of alumina modified titania products synthesized in toluene for various contents of alumina.



Temperature (°C)

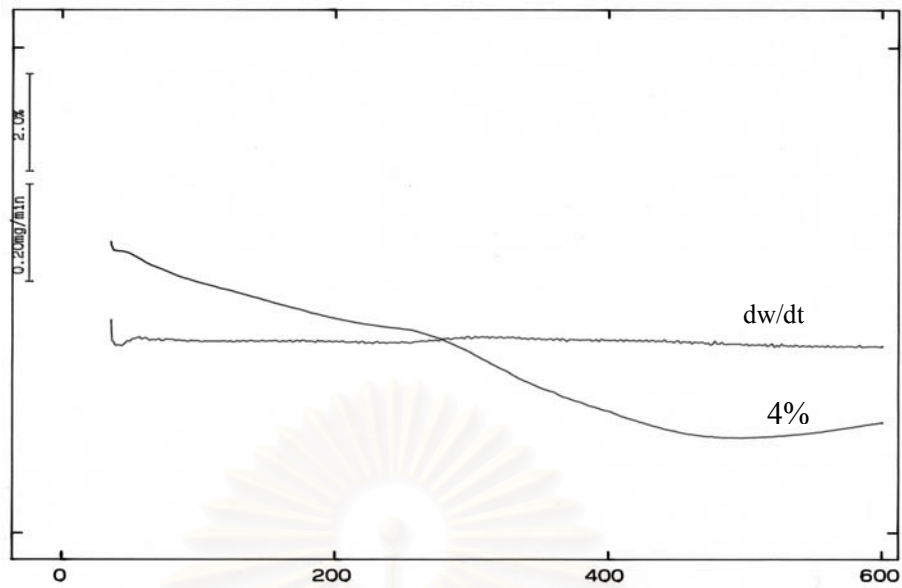
Pure titania



Temperature (°C)

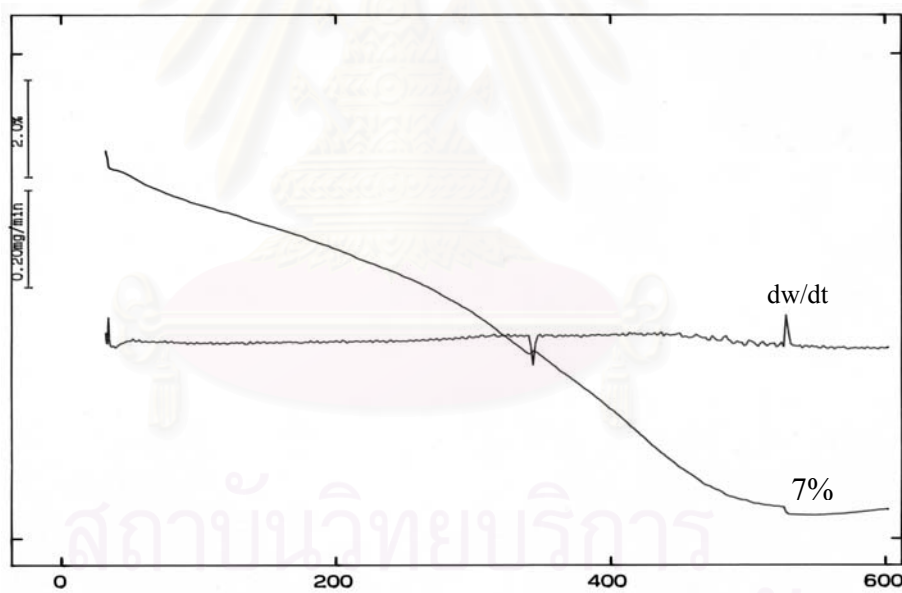
Al/Ti 0.04

Figure 5.42 Weight loss of aluminium modified titania products synthesized in 1,4-BG for various ratios of Al/Ti and weight loss percentages under the calcinations condition.



Temperature (°C)

Al/Ti 0.06



Temperature (°C)

Al/Ti 0.08

Figure 5.42 (cont.) Weight loss of aluminium modified titania products synthesized in 1,4-BG for various ratios of Al/Ti and weight loss percentages under the calcinations condition.

Figure 5.44 and 5.45 show the XRD pattern of aluminium modified titania synthesized in both solvents. The phase transformation of the products synthesized in toluene as anatase to rutile occurred at 900°C. But the synthesis in 1,4-BG, the phase transformation occurred at 1000°C. The phase transformation of aluminium modified titania was occurrence at high temperature than pure titania, synthetics of both solvents. Comparing the phase transformation of the synthesis in both solvents, the aluminium modified titania synthesized in toluene was easily transforming from anatase to rutile than the modified titania synthesized in 1,4-BG. This confirmed that the modified titania synthesized in toluene was aggregation and/or contaminated with amorphous-like phase.

Figure 5.46 and 5.47 show FT-IR spectra of aluminium modified titania synthesized in both solvent after calcination in various temperatures. As-synthesized products, synthetics in both solvent, the spectra show organic compound. For calcination at high temperature, the organic compound was not appearance. Besides, the band of other compound was not appearance assumed that some compound is detected in other range wavenumber or the spectra is overlap on the appearance spectra.

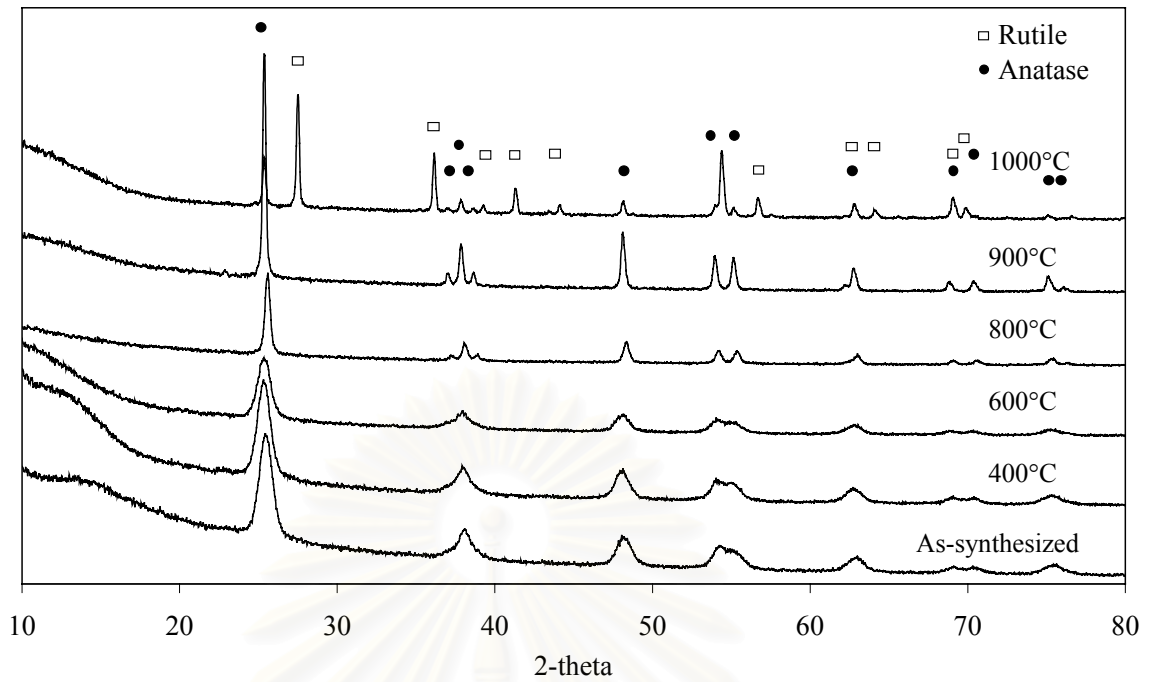


Figure 5.44 XRD pattern of aluminium modified titanias synthesized in 1,4-BG at molar ratio of Al/Ti as 0.08 after calcination in various temperatures. The phase transformation of anatase to rutile occurred at 1000°C.

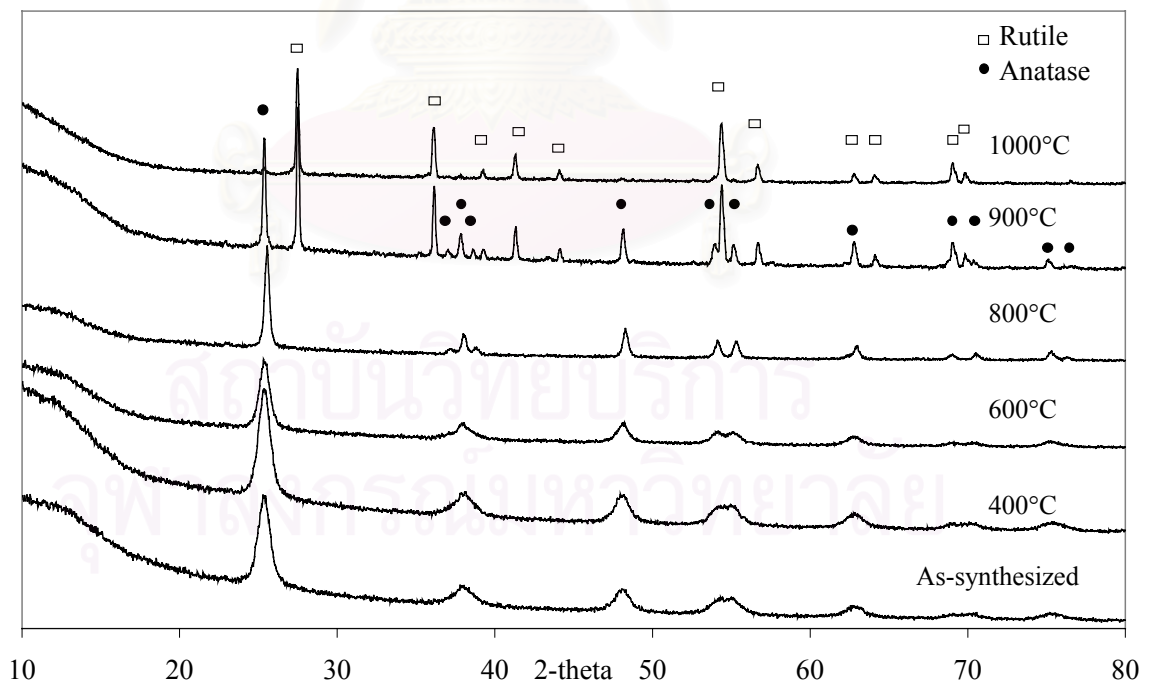


Figure 5.45 XRD pattern of aluminium modified titanias synthesized in toluene at molar ratio of Al/Ti as 0.08 after calcination in various temperatures. The phase transformation of anatase to rutile occurred at 900°C.

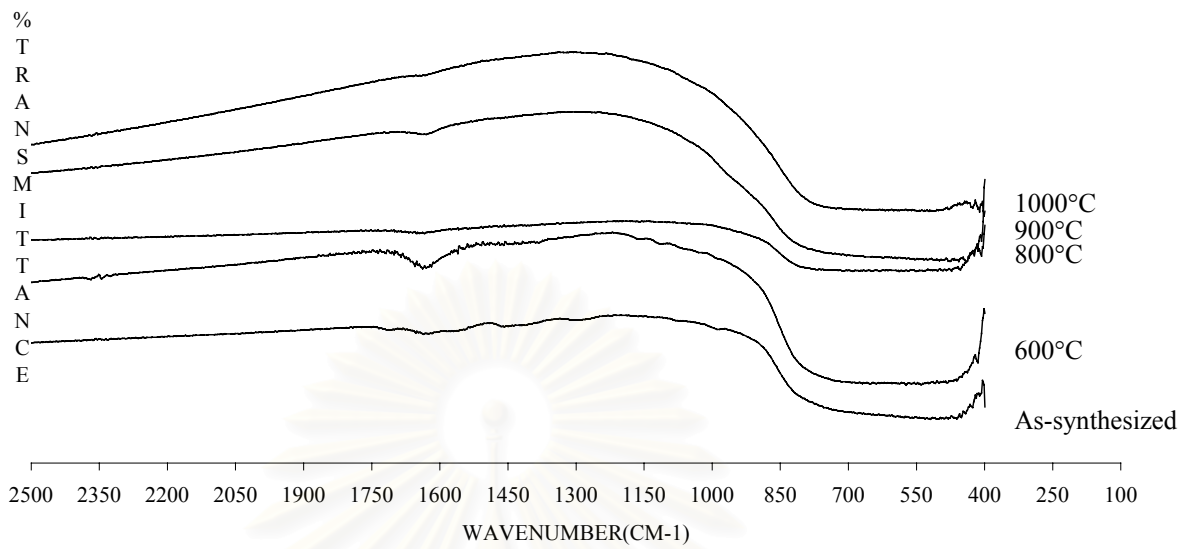


Figure 5.46 FT-IR spectra of aluminium modified titania products synthesized in 1,4-BG at molar ratio of Al/Ti as 0.08 after calcination in various temperature.

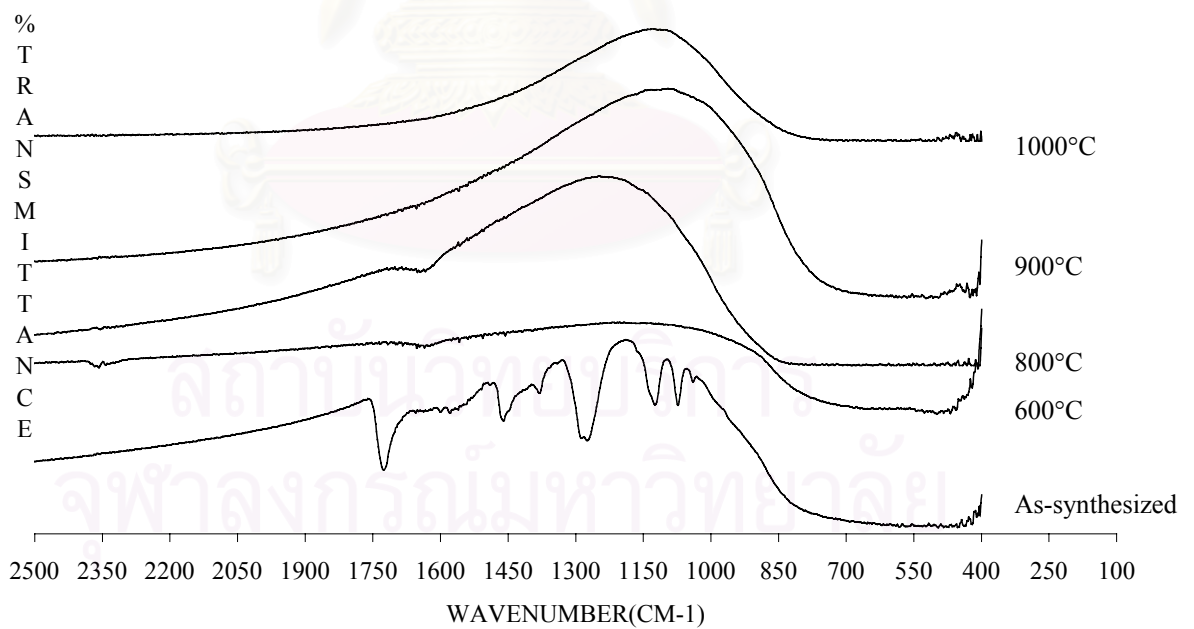


Figure 5.47 FT-IR spectra of aluminium modified titania products synthesized in toluene at molar ratio of Al/Ti as 0.08 after calcination in various temperature.

5.2.3 Effect of phosphorous on titania product

As-synthesized phosphorous modified titania was synthesized in organic solvents, BG or toluene, at 300°C for 2 hrs. The phosphorous modified titania products were prepared in 1,4-BG at the molar ratio of phosphorous and titanium between 0.04 – 0.08. The modified titania products were black-brown powder except the product synthesized in the molar ratio at 0.005 was white powder. For toluene, the phosphorous modified titania products were white powders. XRD patterns of the phosphorous modified titania were shown in Figure 5.48 and 5.49. This identify the phosphorous modified titanias were anatase titania without contamination of other phase.

Figure 5.50 shows the morphology of the titania products that were varied the molar ratio of P/Ti. For 1,4-BG, shape of secondary particle of phosphorous modified titania products were irregular particles and did not change morphology with increasing the content of phosphorous. For toluene, the shape of secondary particle of phosphorous modified titania products were spherical-like particle. The sizes of secondary particles were decreased with increasing the content of phosphorous. This propose that the dielectric constant of the solution was increased due to the increasing of TEPP which the dielectric constant is higher than that, equal 13 at 25°C.

Table 5.14 show the crystallite size and surface area of the phosphorous modified titania products that synthesized in both solvents. For doping the content of phosphorous in molar ratio, the crystallite sizes of modified titania that synthesized in 1,4-BG decreased as smaller than pure titania and were constant about 9 – 10 nm. The surface area of modified titania that synthesized in both solvents, increased to 131 m²/g, 1,4-BG, and 211 m²/g, toluene, at the similar molar ratio as 0.04. On the other hand, for the molar ratio more than as 0.04, the surface areas were decreased with increasing the ratio. S_1/S_2 values of the product that synthesized in 1,4-BG identified the loss of surface area of the phosphorous modified titania which the values were decreased with increasing the content of phosphorous. The loss of surface area was the effect of the content of phosphorous which the products were black-brown powder; it was the effect of contamination of organic moiety on the products.

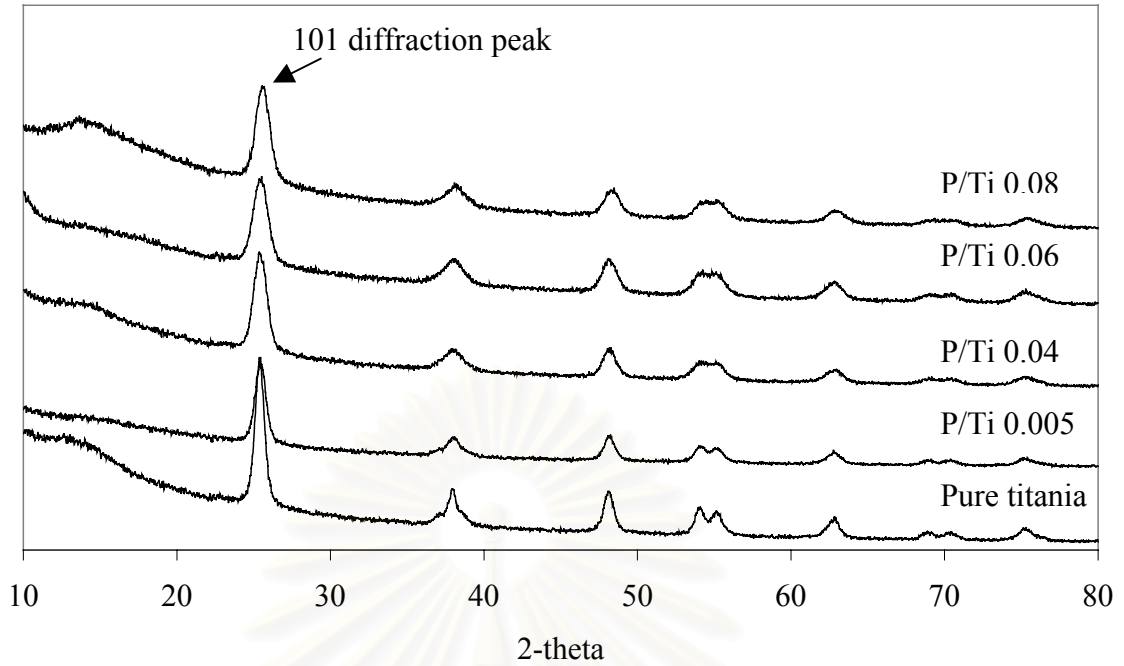


Figure 5.48 XRD patterns of as-synthesized phosphorous modified titania products synthesized in 1,4-BG for various phosphorous contents in molar ratio of P/Ti. All as-synthesized were anatase titania without contamination of other phase of titania and phosphorous phase.

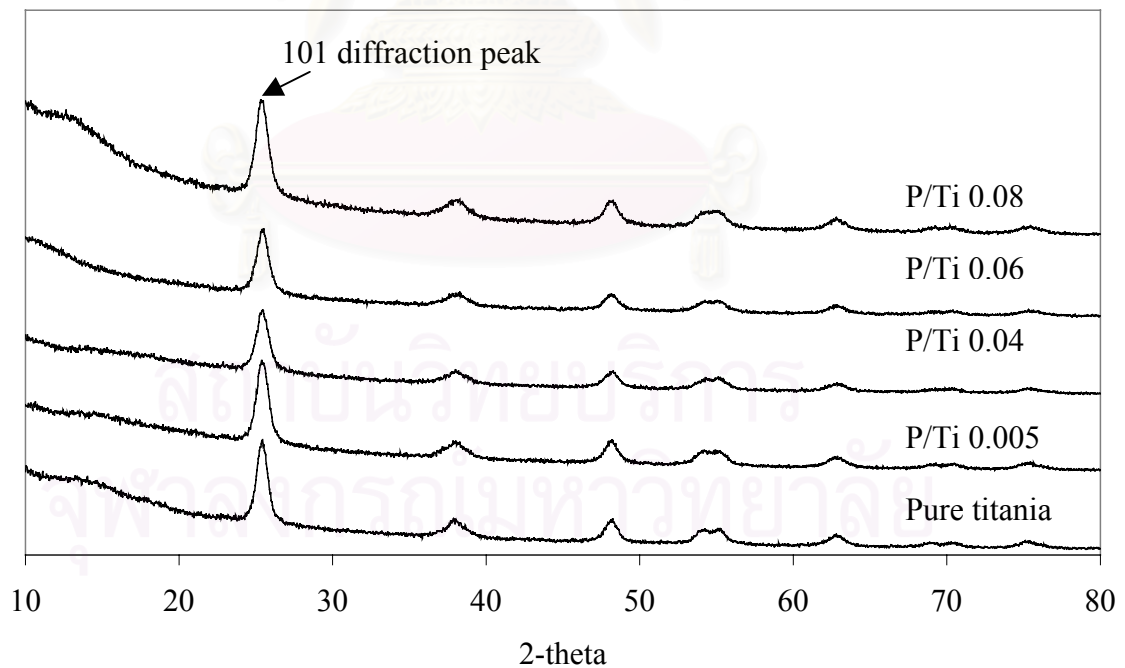
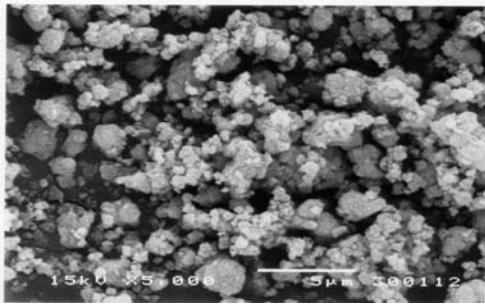
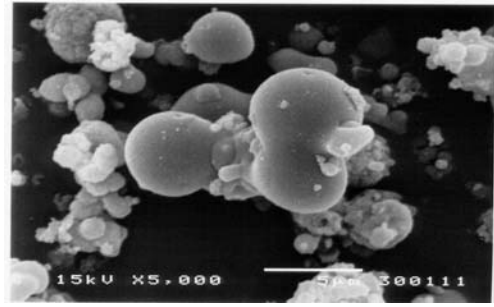


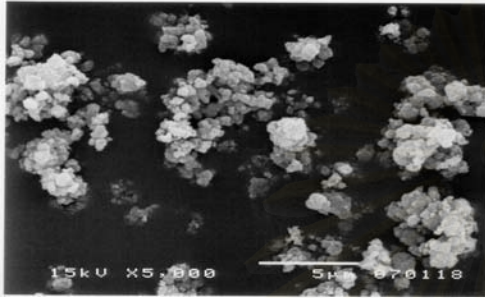
Figure 5.49 XRD patterns of as-synthesized phosphorous modified titania products synthesized in toluene for various phosphorous contents in molar ratio of P/Ti. All as-synthesized were anatase titania without contamination of other phase of titania and phosphorous phase.



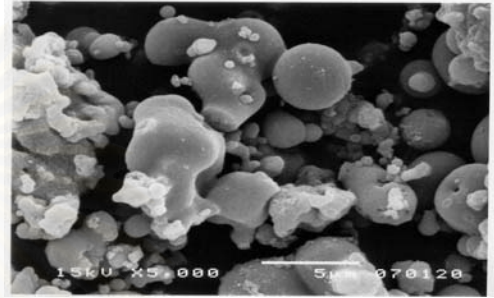
Pure titania, 1,4-BG



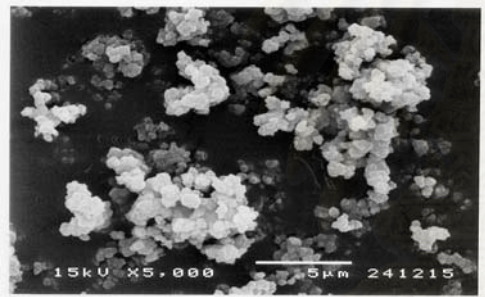
Pure titania, toluene



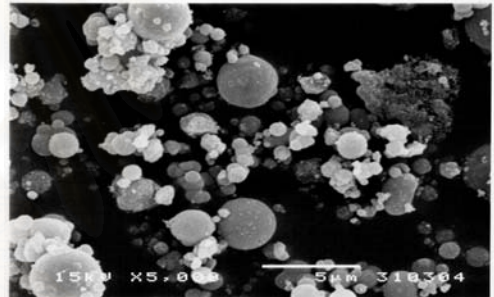
P/Ti 0.005, 1,4-BG



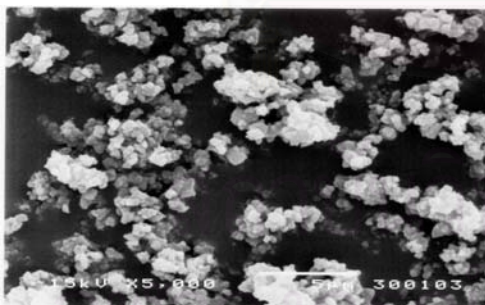
P/Ti 0.005, toluene



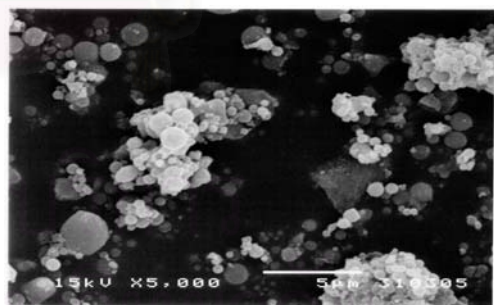
P/Ti 0.04, 1,4-BG



P/Ti 0.04, toluene



P/Ti 0.08, 1,4-BG



P/Ti 0.08, toluene

Figure 5.50 SEM morphology of phosphorous modified titania products synthesized in two solvents of various phosphorous contents in molar ratio of P/Ti. For synthesized in 1,4-BG, the secondary particle were irregular shape and not depended on the content of silicon. On the other hand, for synthesized in toluene, the secondary particles were spherical shape and formed to smaller particle with increasing the Amount of phosphorous.

Table 5.14 The crystallite size and the specific surface area of phosphorous modified titania products that were synthesized in 1,4-BG or toluene for various phosphorous contents of molar ratio of P/Ti.

<i>P/Ti molar ratio^a</i>	<i>1,4-BG</i>				<i>Toluene</i>			
	<i>Crystallite size (nm)^b</i>	<i>Surface area (m²/g)</i>		<i>S₁/S₂^e</i>	<i>Crystallite size (nm)^b</i>	<i>Surface area (m²/g)</i>		<i>S₁/S₂^e</i>
		<i>S₁^c</i>	<i>S₂^d</i>			<i>S₁^c</i>	<i>S₂^d</i>	
0.000	13	110	118	0.9	12	145	128	1.1
0.005	11	122	140	0.9	9	165	171	1.0
0.04	11	131	140	0.9	9	211	171	1.2
0.06	10	122	154	0.8	9	212	171	1.2
0.08	10	65	154	0.4	10	175	154	1.1

^a The titania products synthesized from mixed-reactant (TEPP and TNB) in molar ratio (P/Ti) at 300°C in organic solvents.

^b Crystallite size of anatase titania from the 101 diffraction peak by using Sherrer equation.

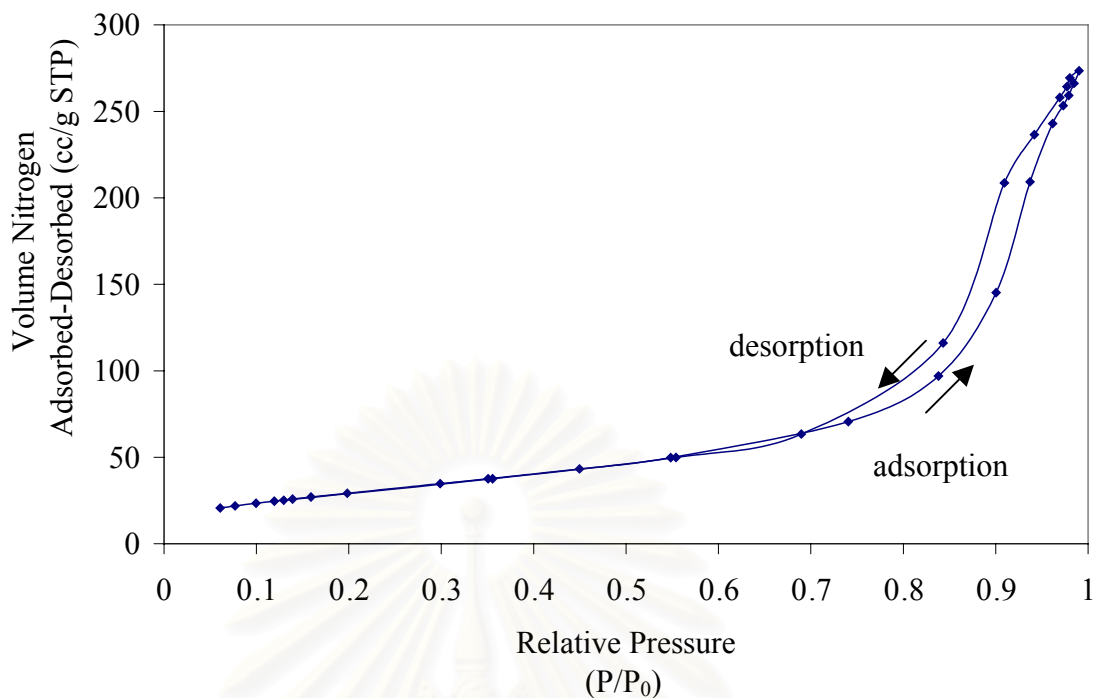
^c Specific BET surface area from BET measurement.

^d Specific surface area calculated from equation of $6/d\rho$ on assumption that the crystal is spherical particle and the density of anatase titania is 3.9 g cm⁻³.

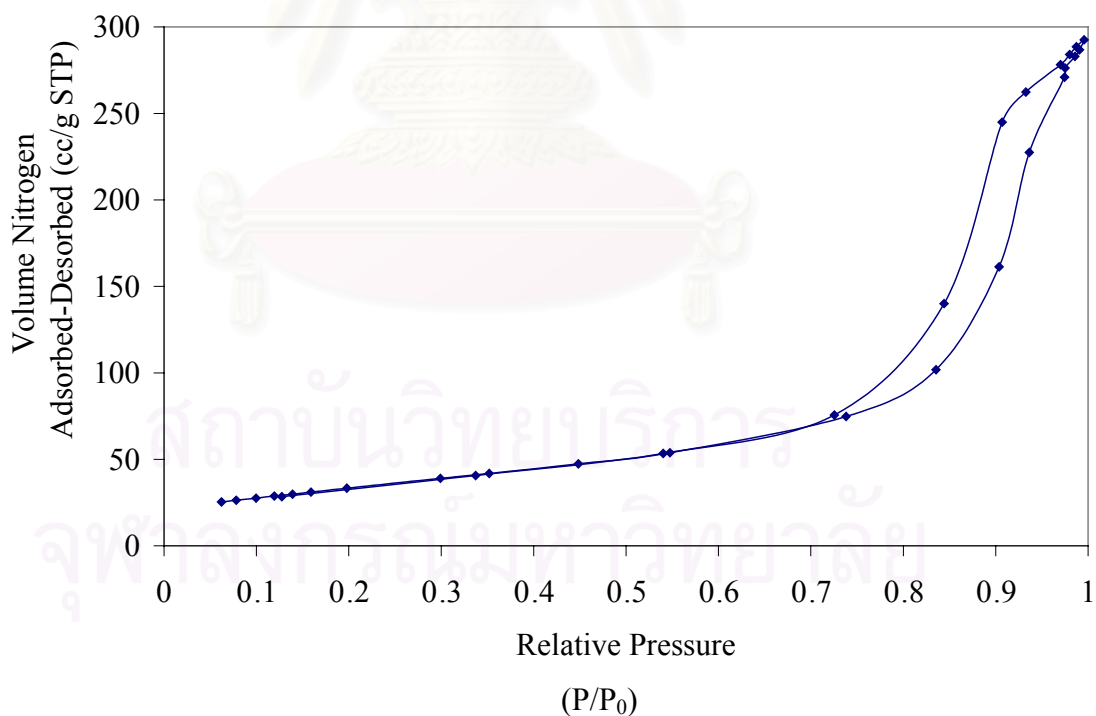
Figures 5.51 and 5.52 show the relative pressure of N₂ adsorption-desorption of phosphorous modified titania products synthesized in both solvents for various the molar ratio of P/Ti. For the synthetic in 1,4-BG, the increasing of molar ratio of phosphorous with TNB affected on the pore structure of the phosphorous modified titania product which the pore structure was changed from the cylinder-like pore to formed the slit-wall pore. On the other hand, the pore structure of the phosphorous modified titania products synthesized in toluene were not changed even the molar ratio increased, the pores structure were mainly slit-wall pore.

Table 5.15 shows the pore volume and average pore diameter of phosphorous modified titania products synthesized in both solvents. The pore volumes were decreased with increasing the amount of phosphorous in the starting material. The average pore diameter of modified titania synthesized in 1,4-BG was slowly decreased with increasing the phosphorous content, but the modified titania synthesized in toluene, the average pore diameter were approximately constant which not depend on the phosphorous content. Figure 5.53 and 5.54 show the pore size distributions of phosphorous modified titania products. The pore diameters were shifted to smaller pore and the distribution curve were broader than pure titania with increasing the amount of phosphorous in the starting material. In addition, the pore volumes were decreased with increasing the amount of phosphorous. These indicate that the phosphorous modified titania products were contaminate with the organic moiety.

Figures 5.55 and 5.56 show the weight loss of the modified titania synthesized in both solvents. In the synthesis in 1,4-BG, the increasing of weight loss were depended on the amount the phosphorous in the starting material. For increasing the phosphorous content, the modified titania products were contaminated with the organic moiety. This confirmed the weight loss that increased with increasing the phosphorous content. On the other hand, the modified titanias synthesized in toluene was low weight loss although the content of phosphorous increased. This indicated that the modified titania products were contaminated with organic moiety which were similarly amount.

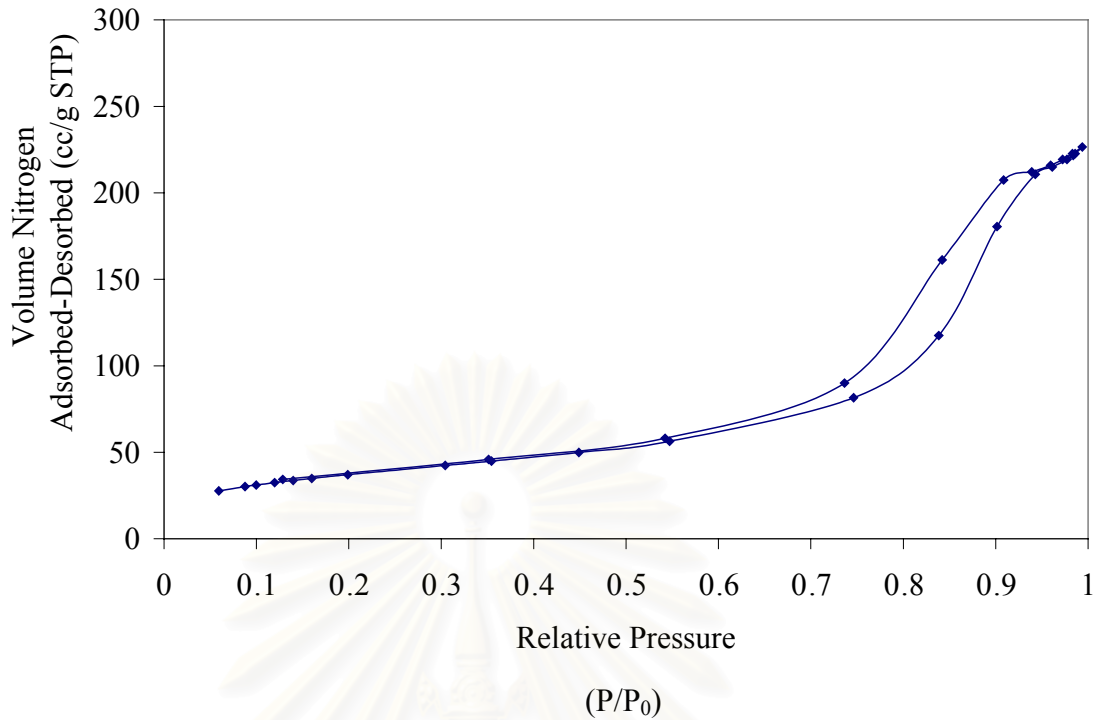


Pure titania, 13 nm, the pore structure is mainly cylindrical pore.

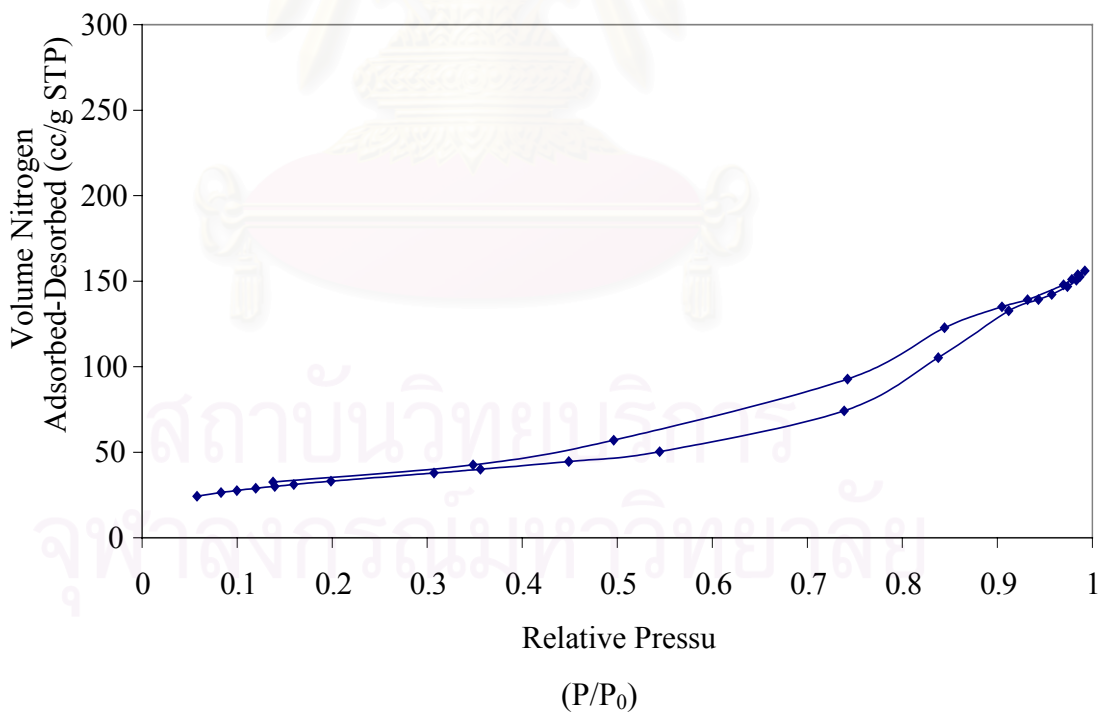


P/Ti 0.005, 11 nm, the pore structure is mainly cylindrical pore.

Figure 5.51 Relative pressure of N₂ adsorption-desorption of phosphorous modified titania products synthesized in 1,4-BG for various molar ratio of P/Ti and the crystallite sizes using BET surface measurement. (see APPENDIX C)

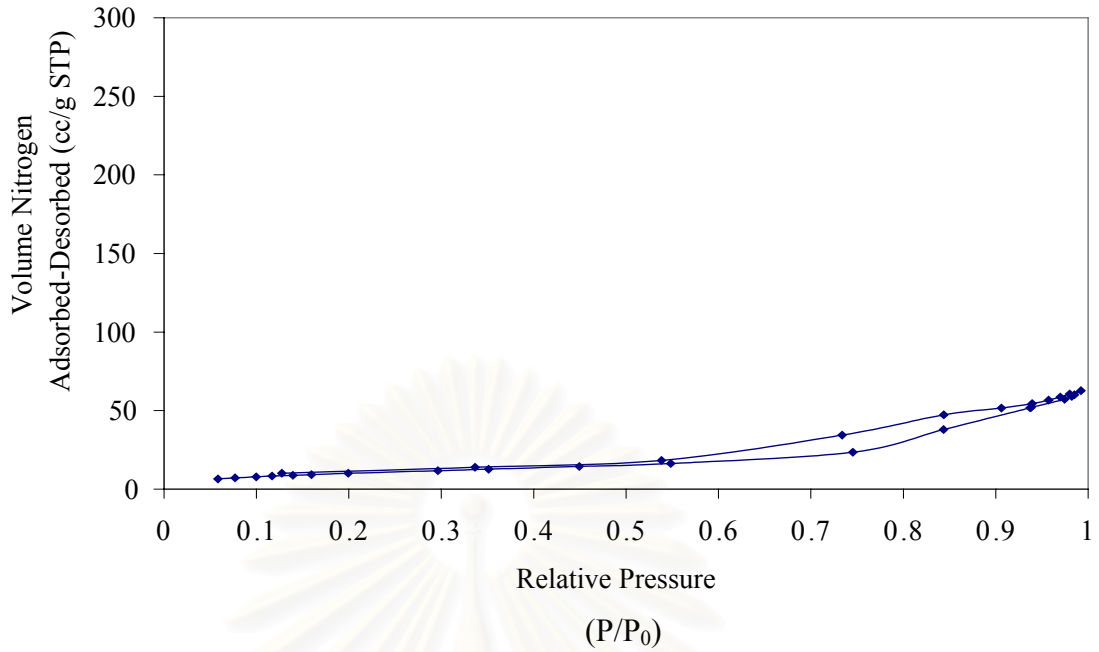


P/Ti 0.04, 11 nm, the pore structure is mainly cylindrical pore.



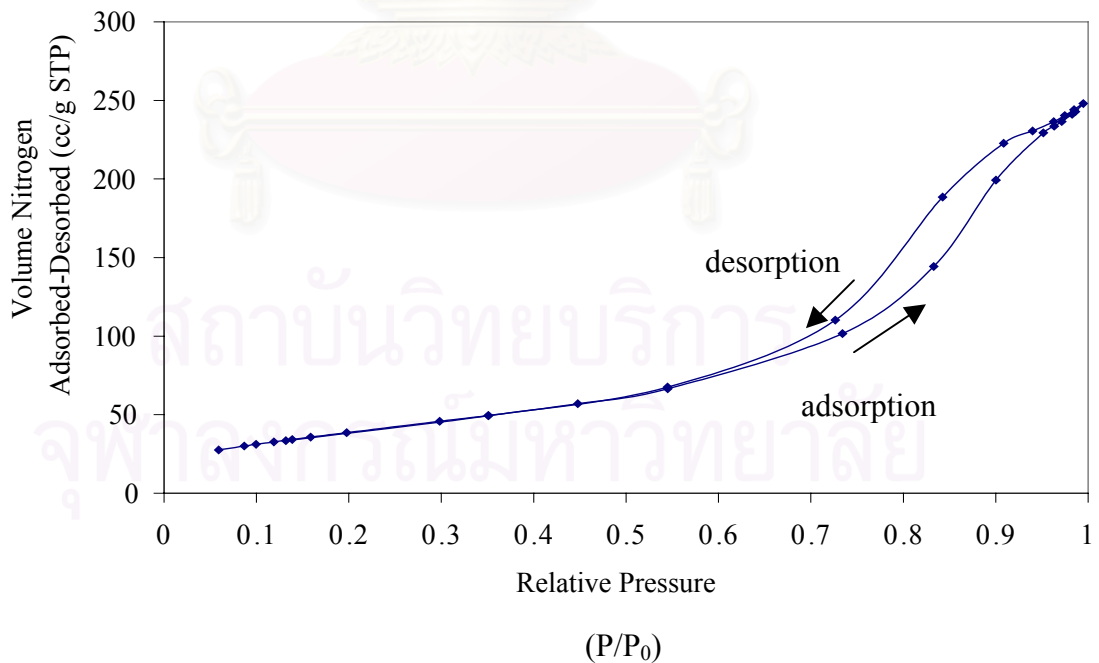
P/Ti 0.06, 10 nm, the pore structure is ink bottle pore.

Figure 5.51 (cont.) Relative pressure of N₂ adsorption-desorption of phosphorous modified titania products synthesized in 1,4-BG for various molar ratio of P/Ti and the crystallite sizes using BET surface measurement.



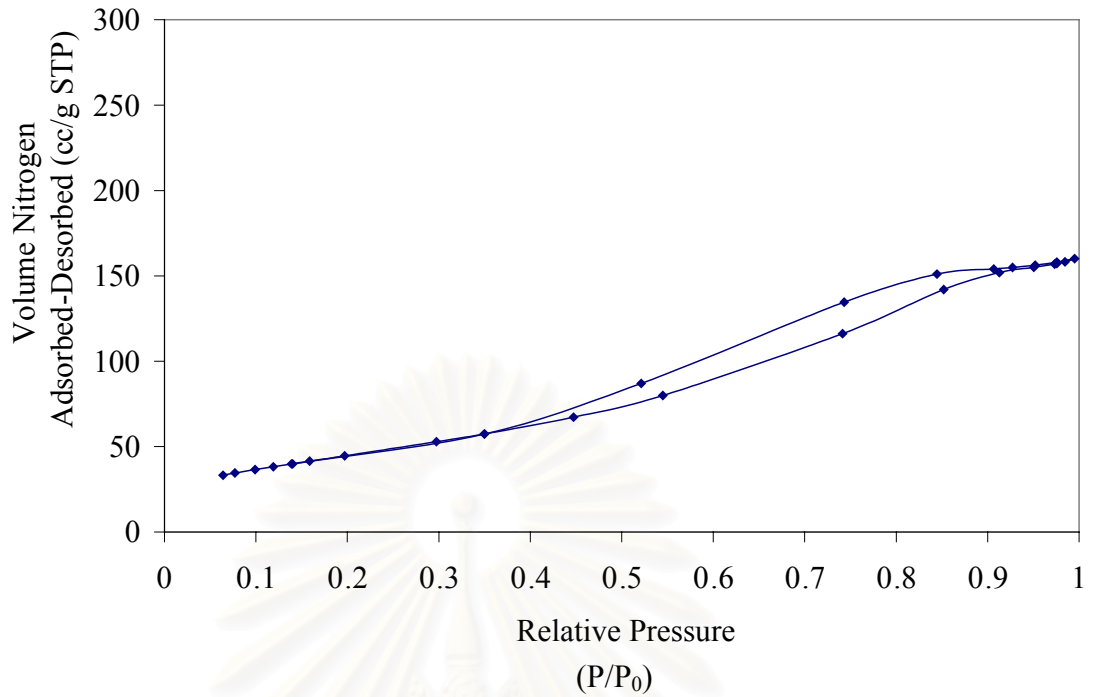
P/Ti 0.08, 10 nm, the pore structure is ink bottle pore.

Figure 5.51 (cont.) Relative pressure of N₂ adsorption-desorption of phosphorous modified titania products synthesized in 1,4-BG for various molar ratio of P/Ti and the crystallite sizes using BET surface measurement.

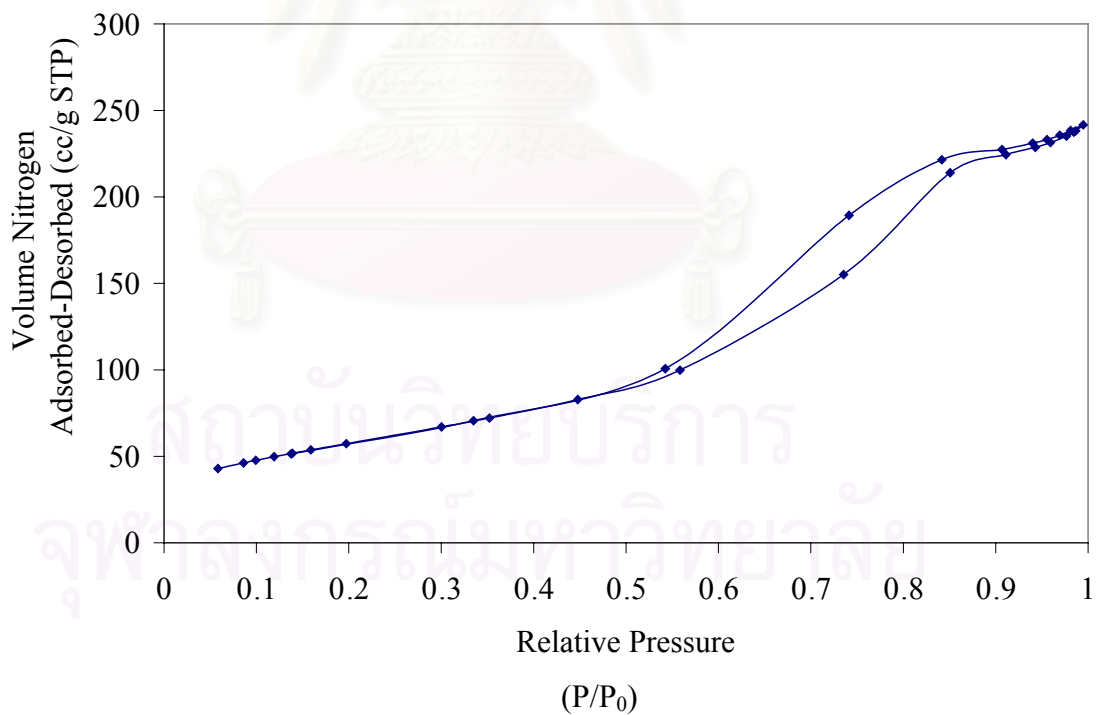


Pure titania, 12 nm, the pore structure is ink bottle pore.

Figure 5.52 Relative pressure of N₂ adsorption-desorption of phosphorous modified titania product synthesized in toluene for various molar ratio of P/Ti and crystallite sizes using BET surface measurement. (see APPENDIX C)

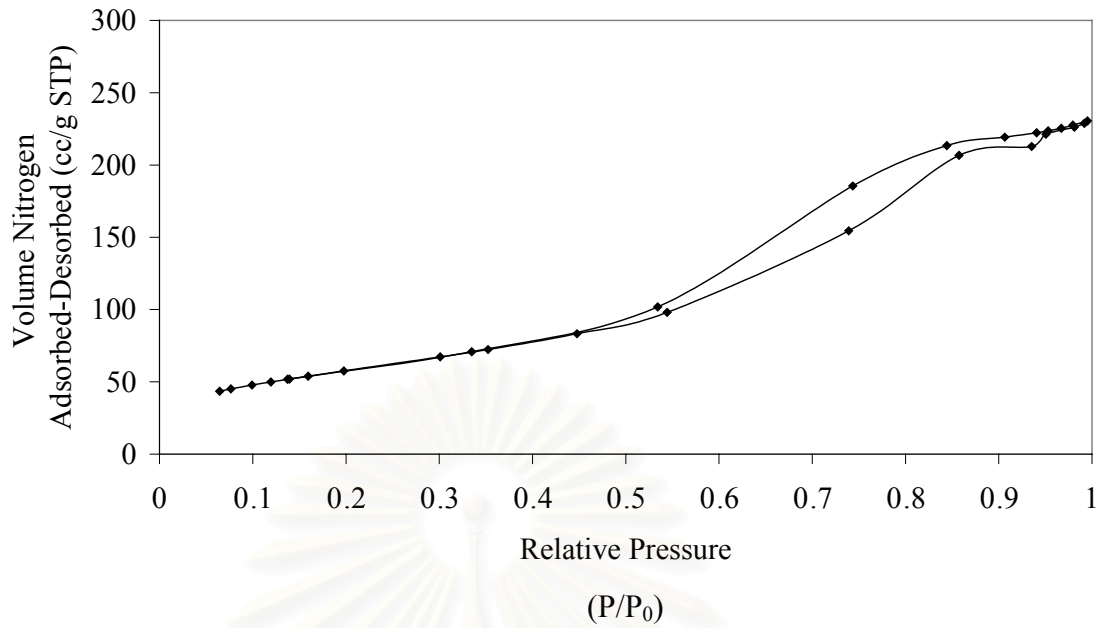


P/Ti 0.005, 9 nm, the pore structure is ink bottle pore.

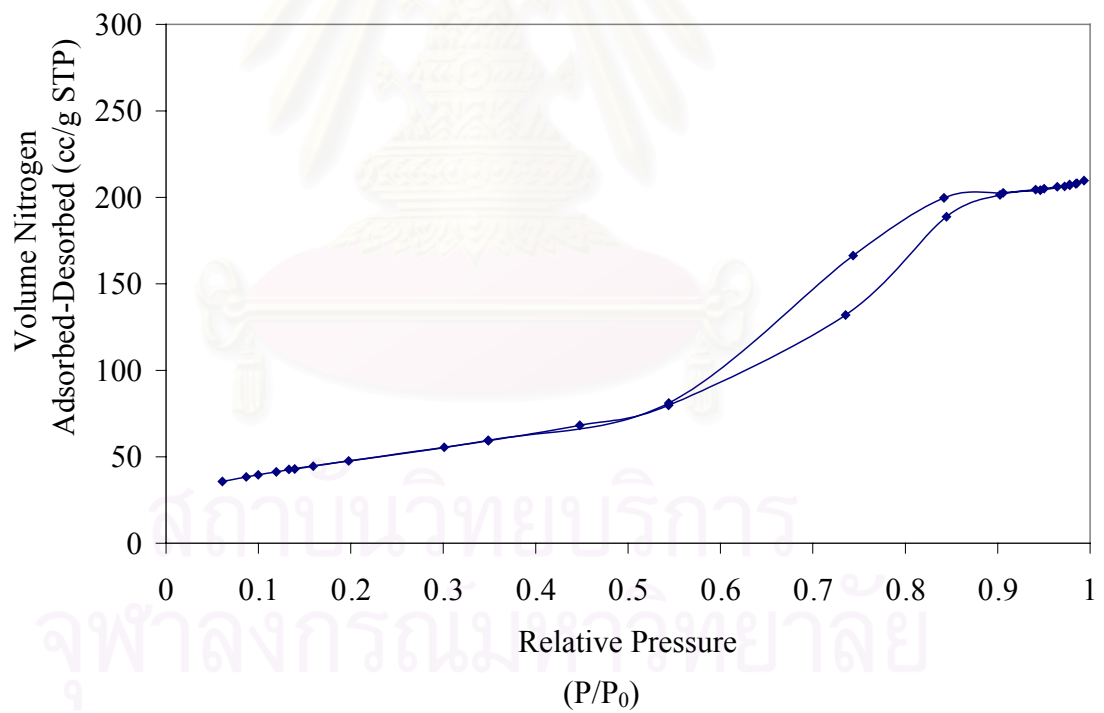


P/Ti 0.04, 9 nm, the pore structure is ink bottle pore.

Figure 5.52 (cont.) Relative pressure of N₂ adsorption-desorption of phosphorous modified titania product synthesized in toluene for various molar ratio of P/Ti and crystallite sizes using BET surface measurement.



P/Ti 0.06, 9 nm, the pore structure is ink bottle pore.



P/Ti 0.08, 10 nm, the pore structure is ink bottle pore.

Figure 5.52 (cont.) Relative pressure of N₂ adsorption-desorption of phosphorous modified titania product synthesized in toluene for various molar ratio of P/Ti and crystallite sizes using BET surface measurement.

Table 5.15 Pore volume and average pore diameter of the phosphorous modified titania products synthesized in two solvents.

<i>P/Ti molar ratio</i>	<i>1,4 Butanediol</i>		<i>Toluene</i>	
	<i>Pore Volume (cc/g)^a</i>	<i>Average pore diameter^b (nm)</i>	<i>Pore Volume (cc/g)^a</i>	<i>Average pore diameter^b (nm)</i>
0.000	0.4	11	0.4	7
0.005	0.4	10	0.3	4
0.040	0.3	8	0.4	5
0.060	0.2	6	0.3	5
0.080	0.1	6	0.3	5

^a BJH cumulative desorption pore volume of pores

^b BJH desorption average pore diameter (4V/A)

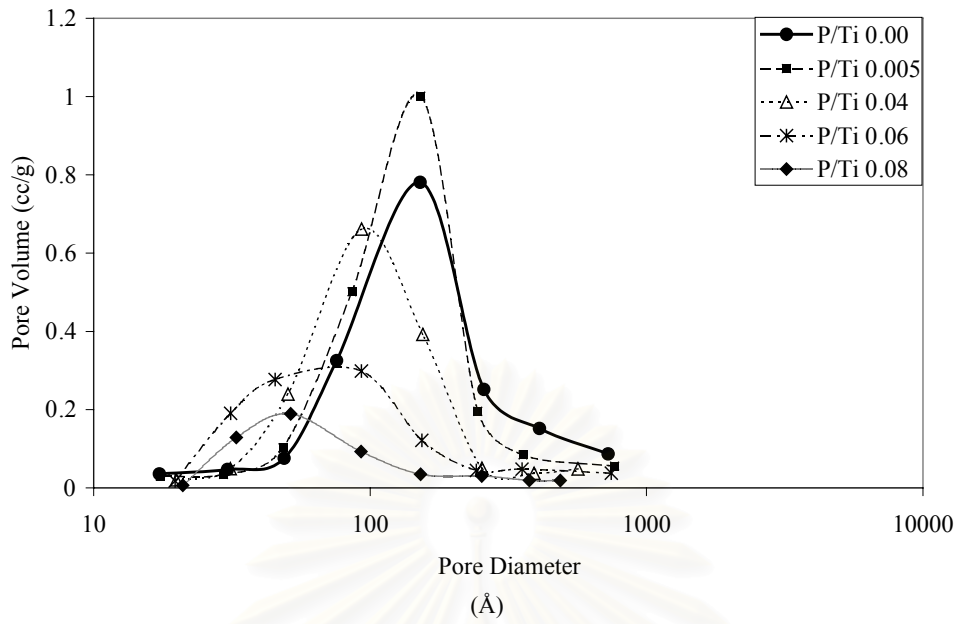


Figure 5.53 Pore size distribution of phosphorous modified titanias synthesized in 1,4-BG for various contents of phosphorous.

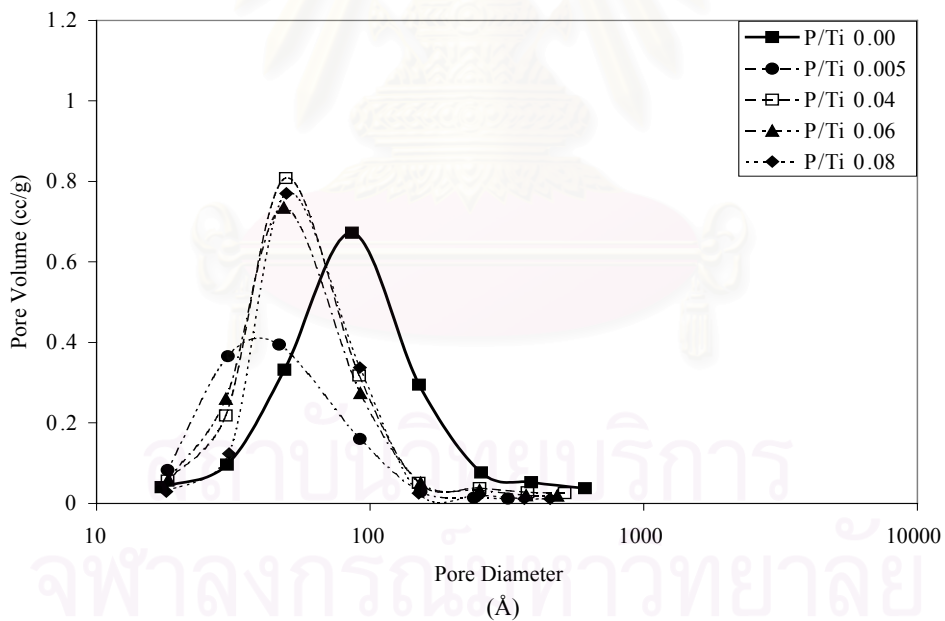
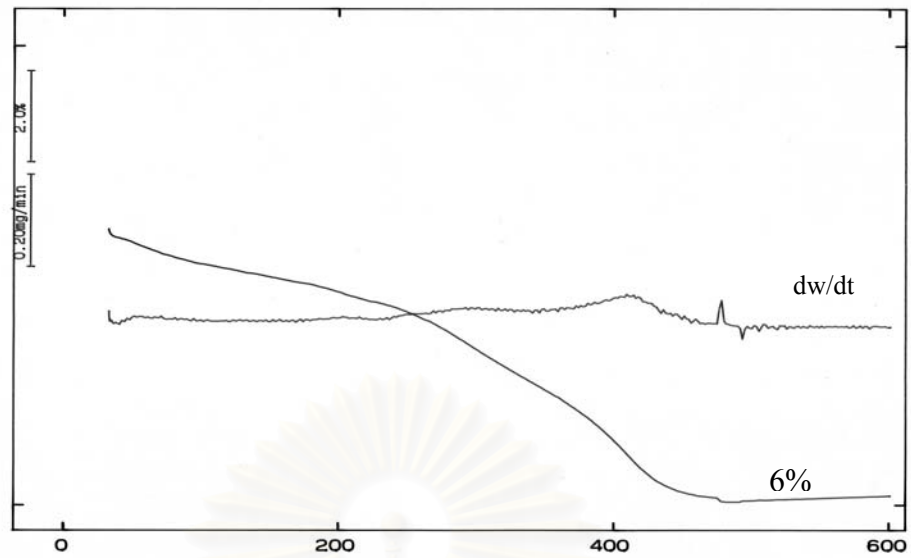
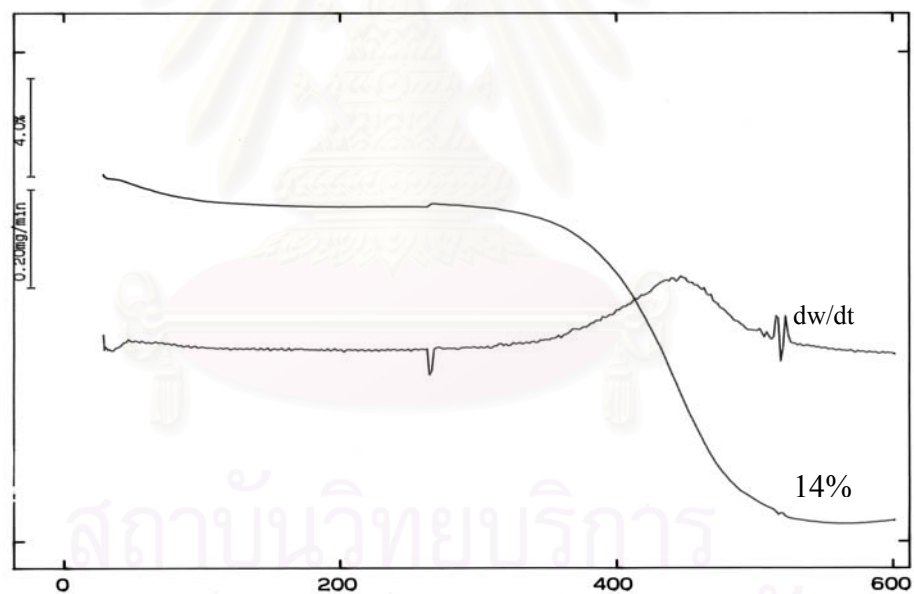


Figure 5.54 Pore size distribution of phosphorous modified titanias synthesized in toluene for various contents of phosphorous.



Temperature (°C)

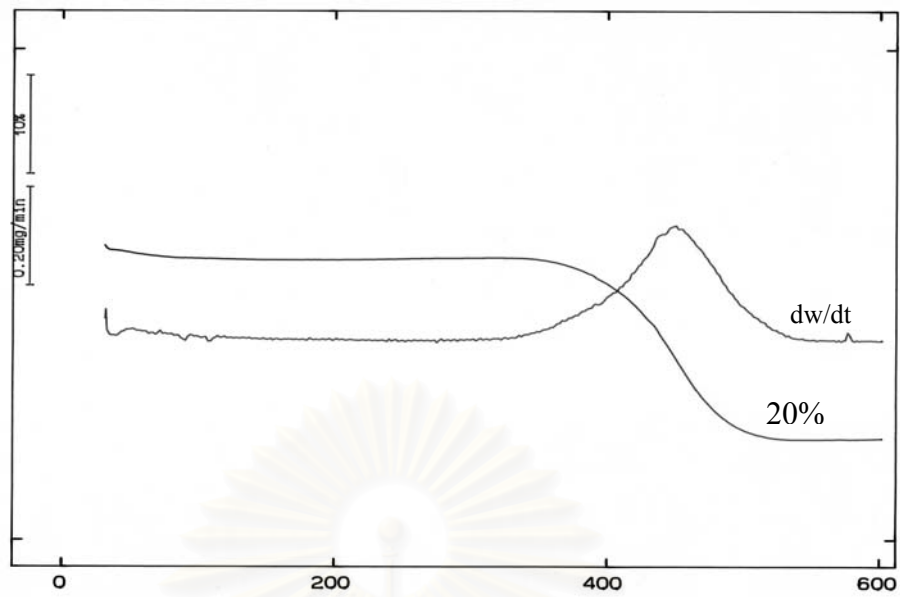
Pure titania



Temperature (°C)

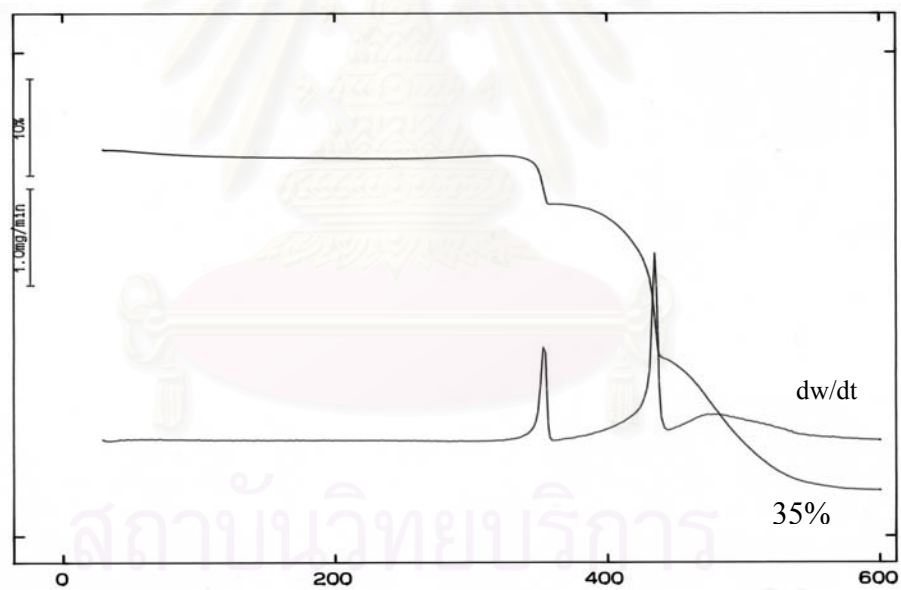
P/Ti 0.04

Figure 5.55 Weight loss of phosphorous modified titania products synthesized in 1,4-BG for various ratios of P/Ti and weight loss percentages under the calcinations condition.



Temperature (°C)

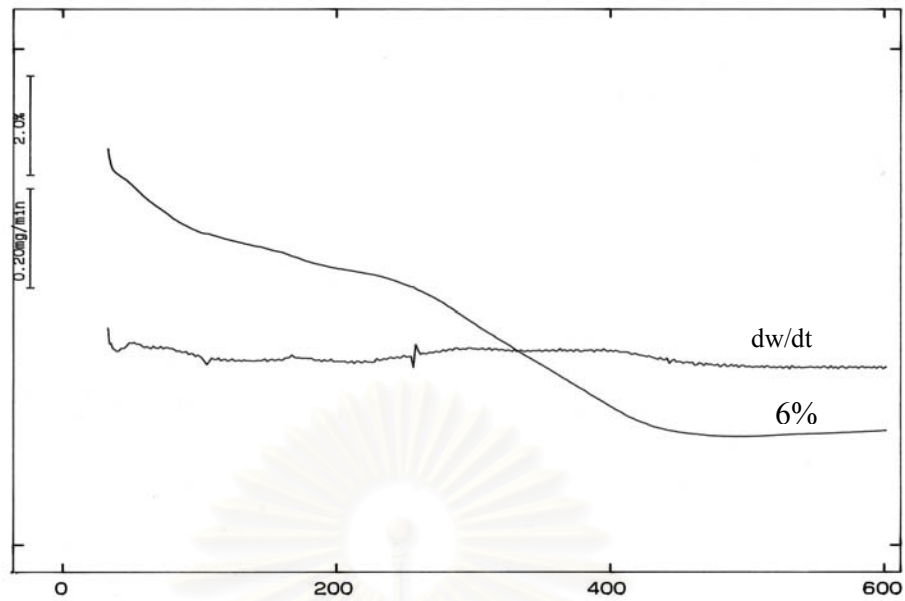
P/Ti 0.06



Temperature (°C)

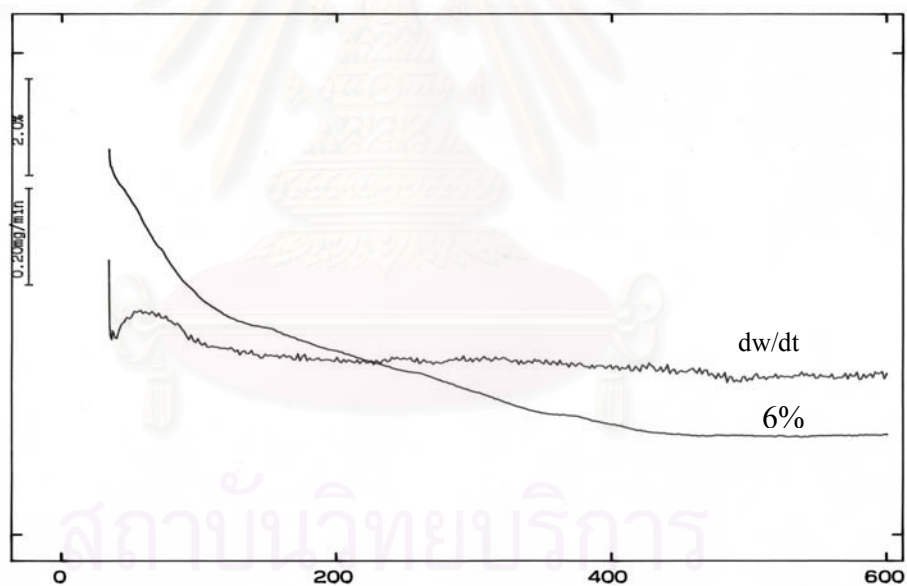
Al/Ti 0.08

Figure 5.55 (cont.) Weight loss of phosphorous modified titania products synthesized in 1,4-BG for various ratios of P/Ti and weight loss percentages under the calcinations condition.



Temperature (°C)

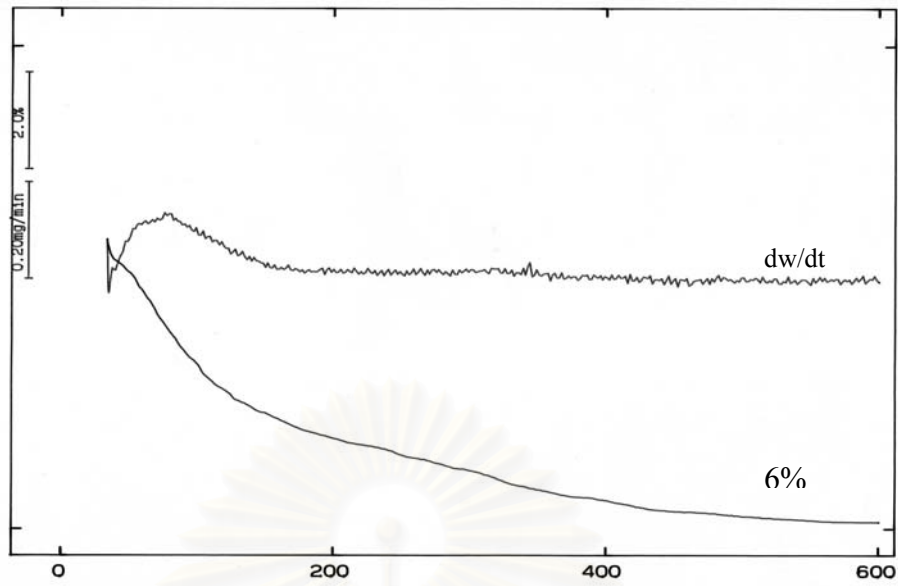
Pure titania



Temperature (°C)

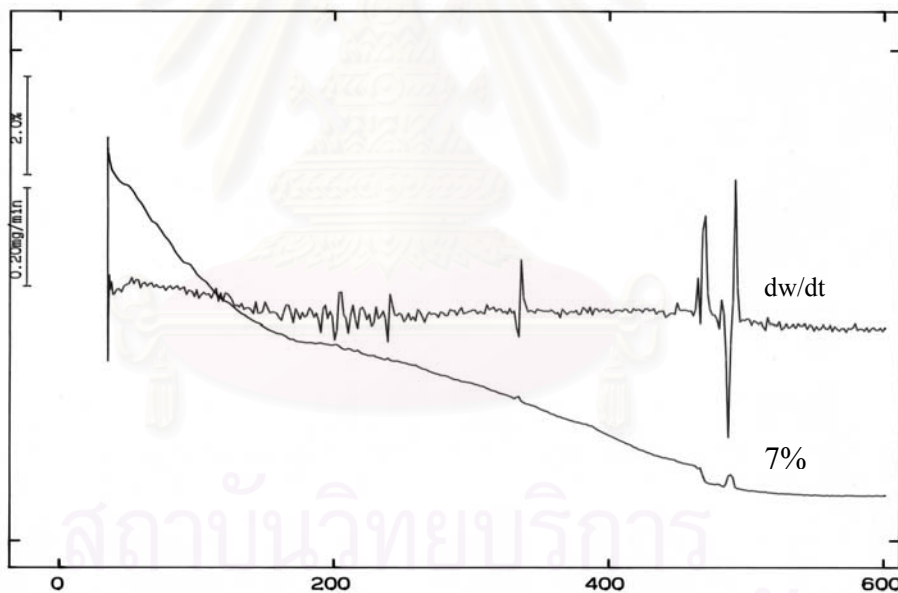
P/Ti 0.04

Figure 5.56 Weight loss of phosphorous modified titania products synthesized in toluene for various ratios of P/Ti and weight loss percentages under the calcinations condition.



Temperature (°C)

P/Ti 0.06



Temperature (°C)

P/Ti 0.08

Figure 5.56 (cont.) Weight loss of phosphorous modified titania products synthesized in toluene for various ratios of P/Ti and weight loss percentages under the calcinations condition.

Figures 5.57 and 5.58 show the XRD pattern of phosphorous modified titania synthesized in both solvents. The phase transformation of the modified titania synthesized in toluene that formed anatase to rutile was occurred at 900°C, which higher than the phase transformation of pure titania. Alternatively, the phosphorous modified titania synthesized in 1,4-BG was transformed from anatase to rutile at 1000°C which higher than pure titania that synthesized in both solvents and modified titania synthesized in toluene. At high temperature, the XRD patterns show intensity of PT compound, in both synthesis solvents. The intensity appeared at > 800°C, in both synthetic solvents (Kohno *et al.*, 2001).

Figures 5.59 and 5.60 show the FT-IR spectra of phosphorous titania products synthesized in two solvents. The spectra band show in range ca. 1350 – 1150 cm⁻¹ indicated the P=O bond, and ca. 970 – 910 cm⁻¹ indicated the P-O-P bond (Dean, 1999). As-synthesized titanias were prepared in both solvents not found the P=O and P-O-P bonds. But at high calcination temperature, at > 800°C, the appearance of P=O and P-O-P bonds were occurring. These confirm the XRD patterns which at >800°C, the PT compound was formed. These propose that P-ion in the product migrate toward the surface of the particle by calcination at high temperature.

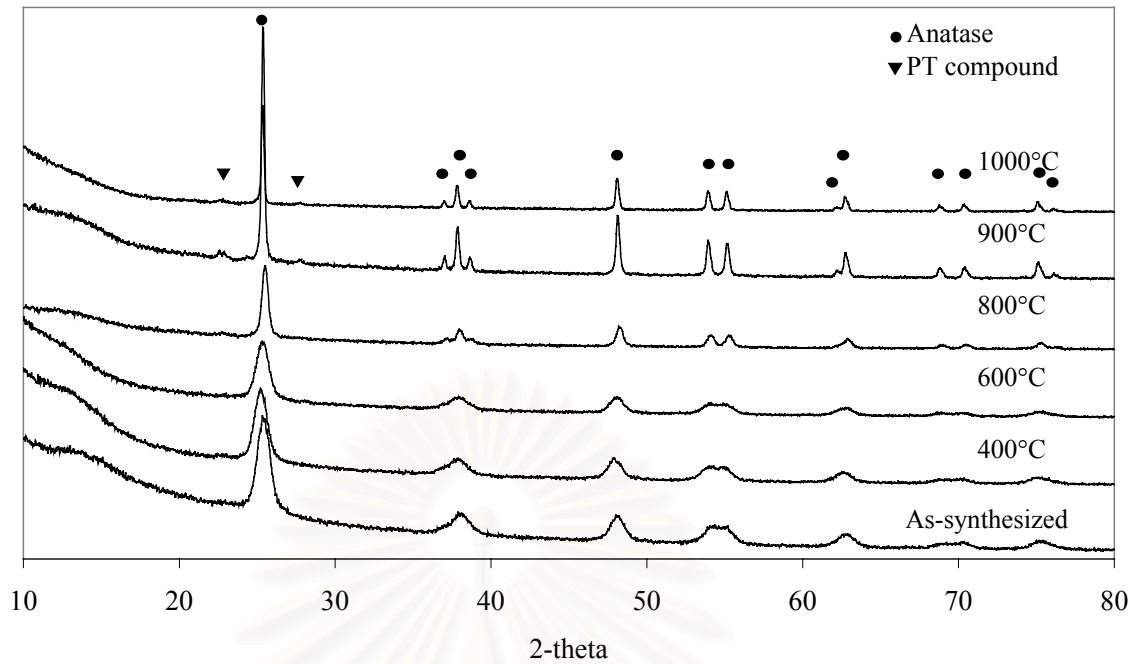


Figure 5.57 XRD pattern of phosphorous modified titanias synthesized in 1,4-BG at molar ration of P/Ti as 0.08 after calcination in various temperatures. The phase transformation of anatase to rutile occurred at high temperature than 1000°C.

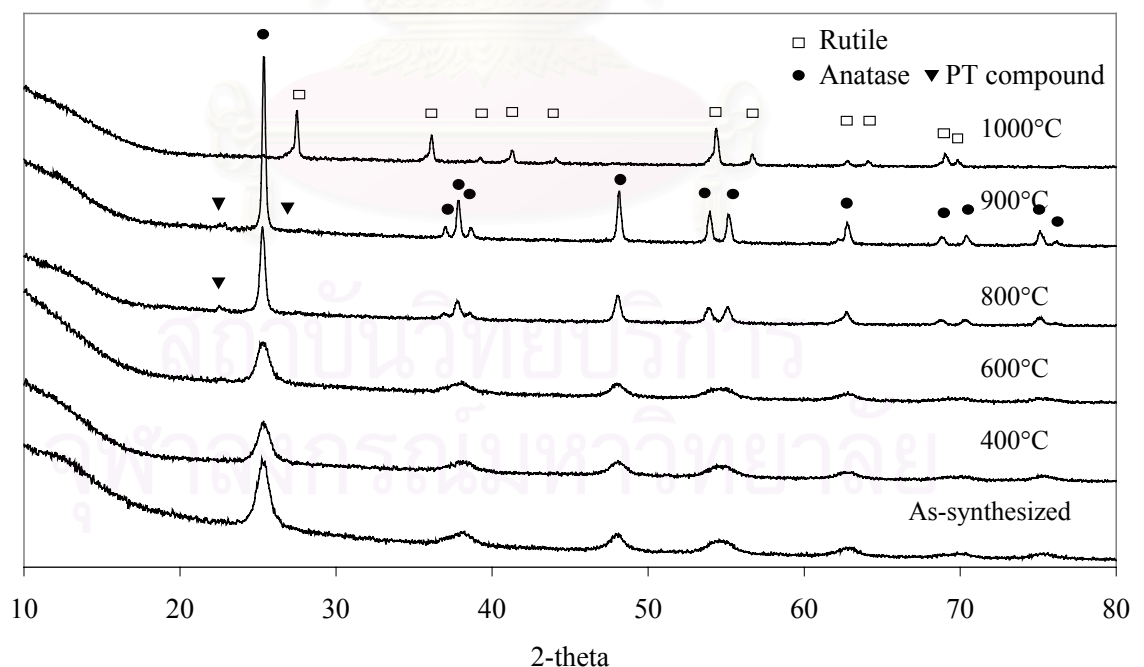


Figure 5.58 XRD pattern of phosphorous modified titanias synthesized in toluene at molar ratio of P/Ti as 0.08 after calcination in various temperatures. The phase transformation of anatase to rutile completely occurred at 1000C.

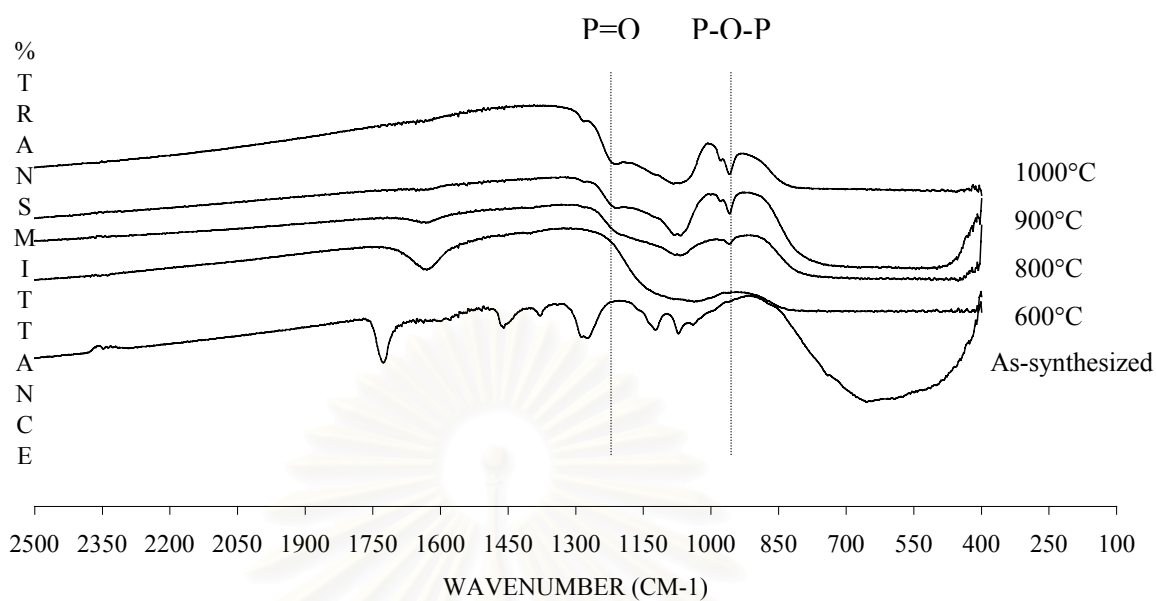


Figure 5.59 FT-IR spectra of phosphorous modified titania products synthesized in 1,4-BG at molar ratio of P/Ti as 0.08 after calcination in various temperatures.

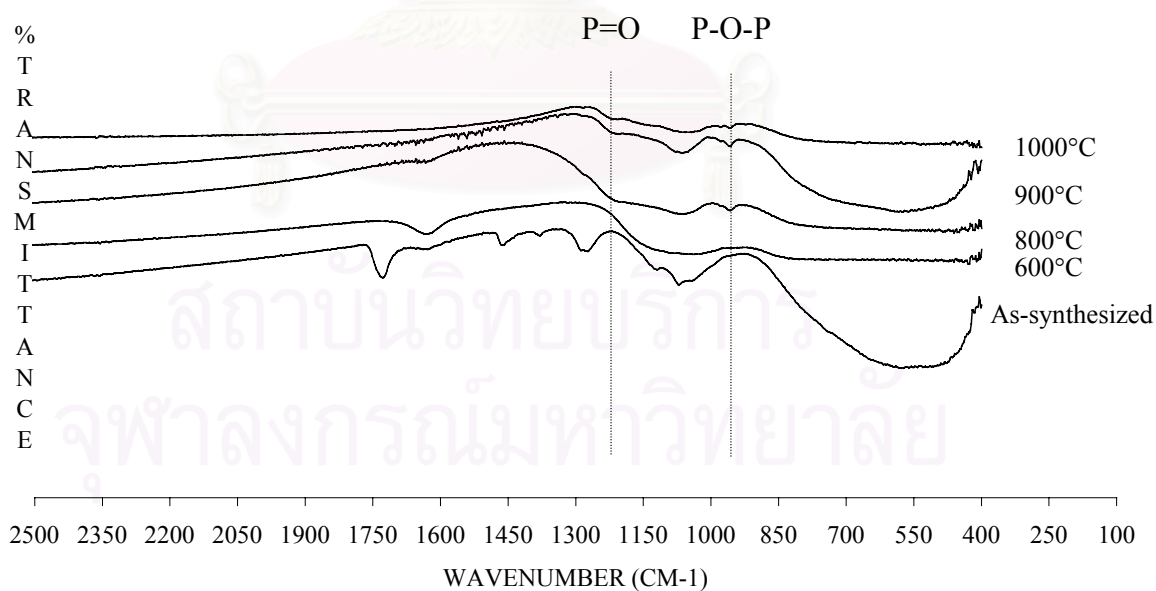


Figure 5.60 FT-IR spectra of phosphorous modified titania products synthesized in toluene at molar ratio of P/Ti as 0.08 after calcination in various temperatures.

Consider about the second element modified titania, XRD pattern of as-synthesized modified titania was not contaminated with other phase of second element. This should be proposed that the present of second element on titania is formed amorphous phase (Yoshinaka *et al.*, 1997). The crystallite size of modified titanias were smaller than the pure titania for both synthesized solvent. For synthesized in 1,4-BG, the crystallite size was decreased with increasing the amount of second element, on the other hand, synthesized in toluene, the crystallite size was different with increasing the amount of second element. These should be proposed that, the synthesized in 1,4-BG, the present of second element in the titania lattice seem to contribute to the deceleration of grain growth of anatase. On the other, synthesized in toluene, the crystal was form via solid state reaction of amorphous so the present of second element is not affected on grain growth of anatase. All of as-synthesized modified titania was affected by these factors.

For the synthesized in toluene, the secondary particle of silicon or aluminium modified titania were agglomerated to formed the large particle with increasing the amount of silicon or aluminium. On the other hand, the secondary particle of phosphorous modified titania was formed smaller spherical shape than pure titania with increasing the amount of phosphorous. This is the effect of dielectric constant of the solution which increase with increasing the amount of phosphorous. Because the dielectric of precursor of phosphorous is higher than toluene so increasing the amount of it, the dielectric of the solution increases.

The pore structure of silicon or aluminum modified titania not changed with increasing the content, both synthesis. On the other hand, the phosphorous modified titania synthesized in 1,4-BG was formed to ink bottle pore and the pore volume of it decreased due to the contamination of organic functional group that increased with increasing the content. The pore size distribution of silicon modified titania synthesized in 1,4-BG was shifted but that synthesized in toluene not changed with increasing the content of silicon. For aluminium modified titania, the pore size distribution of modified titania synthesized in both solvent not changed with increasing the amount of aluminium. The pore size distribution of phosphorous modified titania synthesized in 1,4 BG was significant shifted to small pore and the modified titania synthesized in toluene was slightly shifted to small pore with

increasing the content of phosphorous. These show that the pore structure of modified titania is affected by the mechanism of synthesized modified titania and the kind of second element.

The phase transformation of modified titania synthesized in toluene was start at lower temperature than that synthesized in 1,4-BG which not depend on the kind of second element. These proposed that the phase transformation of modified titania synthesized via the solid state reaction from precipitation amorphous transformed at lower temperature than the modified titania synthesized from directly crystallization process.



สถาบันวิทยบริการ
จุฬาลงกรณ์มหาวิทยาลัย

CHAPTER VI

CONCLUSIONS AND RECOMMENDATION

6.1 Conclusions

The conclusions of the present research are the following:

1. The precipitated product shows the lower stability than crystallization product even if the second element was doped.
2. Titanium (IV) oxide synthesized in toluene proceeds via solid state reaction from precipitated amorphous, whereas that synthesized in 1,4 BG occurs directly through the crystallization process of anatase titania.

6.2 Recommendation for the future studies

From the previous conclusions, the following recommendations for the future studies are proposed.

1. Study of efficiency of titania product that synthesized in both solvents by the oxidation reaction of organic material.
2. Study of the effect of second element bond on the modified titania products.
3. Study of effect of the morphology of secondary particle on the sintering of titania at high temperature.
4. Study of the morphology of secondary particle by the effect of dielectric constant of the solvent. By using the amorphous titania that synthesized in toluene as the starting material of the synthesis in 1,4-BG.
5. Study of the effect of solvent on the pore structure of titania products.
6. Study of the effect of secondary particle shape on the phase transformation.
7. Study of titania synthesized at high temperature than that synthesized in this study.
8. Study of the profile of titania product synthesized in precipitation mechanism versus temperature.

9. Study of the effect of pressure on the titania product at compress-pressure in the reactor
10. Study of the effect of the crystallite size on the pore structure.
11. Study of the phase transformation of amorphous titania synthesized in toluene at non holding time for calcine in various temperature.
12. Study of the titania product that synthesized by used the difference organic solvent in the gab and in the tube.
13. Study of the second element modified titania crystal for the reaction time is more than 4 h and compare the change of crystallite size of the titania synthesized by precipitation mechanism and crystallization.
14. Study of the effect of amount of second element on the pore structure of titania after calcination.
15. Study of the phenomena of the phase transformation of the titania synthesized by the precipitation mechanism.
16. Study of the effect of second element by other kind on the titania product.
17. Study of the other solvent used to synthesized titania and investigate the mechanism phenomena.
18. Study of the effect of the elements that doped in the titania product.
19. Study of the effect of the second element function bond on the efficiency of the titania by the photodecomposition.
20. Study of the organic function bond which is formed when dope TEPP in the starting material for synthesize in 1,4-BG.

REFERENCES

- Ahmed, S. R. Nano-Structure Materials. University of Maryland [Online]. 1999. Available from: <http://www.glue.umd.edu/~srahmed/nanocomposite.html> [2002, October 28]
- Bradley, D. C.; Mehrotra, R. C.; Gaur, D. P. Metal Alkoxides. London, U.K., Academic Press, 1978.
- Bibby D. M.; Dale, M. P. Synthesis of Silica-Sodalite form Non-aqueous Synthesis. Nature (London). 317 (1985): 157 – 158.
- Cheng, H.; Ma, J.; Zhao, Z.; Qi, L. Hydrothermal Preparation of Uniform Nanosize Rutile and Anatase Particle. Chem. Master. 7 (1995): 663 – 671.
- Cruikshack, M. C.; Glasser, L. S. D. A Penta-co-ordinated Aluminate Dimer; X-ray Crystal Structure. J. Chem. Soc., Chem. Commun. (1985): 84 – 85.
- Dagan, G. and Tomkiewicz, M. Preparation and Characterization of TiO₂ Aerogel for Use as Photocatalysis. J. Non-Cryst. Solids 175, 2-3 (1994):294 – 302.
- Del Arco, M.; Holgado, M. J.; Martin, C.; Rives, V. Effect of Thermal Treatments on the Properties of V₂O₅/TiO₂ and MoO₃/TiO₂ System. J. Catal. 99 (1989): 19.
- Dean, J. A. Lange's Handbook of Chemistry. 5 th ed. United State of America: McGraw-Hill, 1999.
- Fox, M. A. and Dulay, M. T. Heterogeneous Photocatalysis. Chem. Rev. 93 (1993): 341 – 357.
- Fujishima, A.; Hashimoto, K.; Watanabe, T. TiO₂ Photocatalysis Fundamental and Applications. 1 st ed. Tokyo: BKC, 1999.
- Gregg, S. J. and Sing, K. S. W. Adsorption, Surface Area And Porosity. 2 nd ed. London: Academic Press (London), 1982.
- Hirano, M.; Nakahara, C.; Ota, K.; Inagaki, M. Direct Formation of Zirconia-Doped Titania with Stable Anatase-Type Structure by Thermal Hydrolysis. J. Am. Ceram. Soc. 85, 5 (2002): 1333 – 1335.
- Herrmann, J-M.; Tahiri, H.; Ait-Icho, Y.; Lassaletta, G.; Gonzalez-Elipe, A. R.; Fernandez, A. Characterization and Photocatalytic Activity in Aqueous Medium of TiO₂ and Ag-TiO₂ Coatings on Quartz. Appl. Catal. B 13 (1997): 219 – 228.

- Hu, L.; Gu, Y.; Gu, J.; Han, J.; Chen, M. Precipitation of Titania Ultrafine Particle via Hydrolysis of Titanium Alkoxides. I. Study of Hydrolysis and Particle Formation. Huadong Huagong Xueyuan Xuebao 16 (1990): 260 – 265.
- Inomata, M.; Miyamoto, A.; Murakami, Y. Promoting Effect of TiO₂ and Al₂O₃ Supports on the Activity of Vanadium Oxide Catalyst for the Oxidation of Benzene Measured in Terms of the Turnover Frequency. J. Chem. Soc., Chem Commun. (1980): 223.
- Inoue, M.; Kominami, H.; Inui, T. Reaction of Aluminium Alkoxides with Various Glycols and the Layer Structure of Their product. J. Chem. Soc. Dalton Trans. (1991): 3331 – 3336.
- Inoue, M.; Otsu, H.; Kominami, H.; Inui, T. Synthesis of Yttrium Aluminate Garnet by the Glycothermal Method. J. Am. Ceram. Soc. 74 (1991): 1452 – 1454.
- Inoue, M.; Otsu, H.; Kominami, H.; Inui, T. Synthesis of Double Oxides Having Spinel Structure (ZnAl₂O₄, ZnGa₂O₄) by Glycothermal Method. Nippon Kagaku Kaishi. (1991): 1036 – 1038.
- Inoue, M.; Kominami, H.; Inui, T. Thermal Transformation of γ -Alumina Formed by Thermal Decomposition of Aluminum Alkoxide in Organic Media. J. Am. Ceram. Soc. 79, 9 (1992): 2597 – 2598.
- Inoue, M.; Nishikawa, T.; Inui, T. Glycothermal Synthesis of Rare Earth Iron Garnets. J. Mater. Res. 13, 4 (1998): 856 – 859.
- Inoue, M.; Nishikawa, T.; Inui, T. Reaction of Rare Earth Acetates with Aluminum Isopropoxide in Ethylene Glycol: Synthesis of The Garnet and Monoclinic Phases of Rare Earth Aluminates. J. Mater. Sci. 33 (1998): 5835 – 5841.
- Iwamoto, S.; Tanakulrungsank, W.; Inoue, M.; Kagawa, K.; Praserttham, P. Synthesis of Large-Surface Area Silica-Modified Titania Ultrafine Particles by The Glycothermal Method. J. Mater. Sci. Lett. 19 (2000): 1439 – 1443.
- Iwamoto, S.; Saito, K.; Inoue, M.; Kagawa, K. Preparation of the Xerogels of Nanocrystalline Titanias by the Removal of the Glycol at the Glycothermal Method and Their Enhanced Photocatalytic Activities. Nano. Lett. 1, 8 (2001): 417 – 421.
- Jones, W.; Tooze, J. F. Eur. Pat. Appl., No. EP 0505022A1, 08.01.92.

- Jung, K.Y.; Park, S.B. Enhanced Photocatalytic Activity of Silica-Embedded Titania Particles Prepared by Sol-Gel Process for the Decomposition of Trichloroethylene. Appl. Catal. B: Environ. 25 (2000): 249 – 256.
- Kaliszewski, M. S.; Heuer, A. H. Alcohol Interaction with Zirconia Powder. J. Am. Ceram. Soc. 73, 6 (1990): 1504 - 1509.
- Kamal, A. M.; Xiong, Y.; Pratisinis, S. E. Synthesis of Titania Powder by Titanium Tetrachloride Oxidation in an Aerosol Flow Reactor. Master. Res. Soc. Symp. Proc 249 (1992): 139 – 144.
- Kamat, P. V. and Dimitrijevic, N. M. Colloidal Semiconductors as Photocatalysts for Solar Energy Conversion. Sol. Energy 44, 2 (1990): 83 – 98.
- Keesmann, I. Hydrothermal Synthesis of Brookite. Z. Anorg. Allg. Chem. 346 (1966): 30 – 43.
- Kin, S. J.; Park, S. D.; Jeong, Y. H.; Park, S. Homogenous Precipitation of TiO₂ Ultrafine Powders from Aqueous TiOCl₂ Solution. J. Am. Ceram. Soc. 82, 4 (1999): 927 – 932.
- Kohno, M.; Furushima, T.; Kominami, H.; Kagawa, K.; Kera, Y. Synthesis of Thermally Stable, Phosphorous-Modified Titanium Oxide Nano-Crystals by Thermal Decomposition of Titanium Alkoxide and Phosphoric Ester in Organic Solvent of High Temperature and High Pressure. J. Ceram. Soc. Japan 109, 4 (2001): 332 – 337.
- Kominami, H.; Kato, J.; Takada, Y.; Doushi, Y.; Ohtani, B. Novel Synthesis of Microcrystalline Titanium (IV) Oxide having High Thermal Stability and Ultra-High Photocatalytic Activity: Thermal Decomposition of Titanium (IV) Alkoxide. Catal. Lett. 46 (1997): 235 – 240.
- Kominami, H.; Kato, J.; Murakami, S.; Kera, Y.; Inoue, M.; Inui, T.; Ohtani, B. Synthesis of Titanium (IV) Oxide of Ultra-High Photocatalytic Activity: High Temperature Hydrolysis of Titanium Alkoxides with Water Liberated Homogeneously from Solvent Alcohols. J. Mol. Catal. A. 144 (1999): 165 – 171.
- Kominami, H.; Kohno, M.; Takada, Y.; Inoue, M.; Inui, T.; Kera, Hydrothermal of Titanium Alkoxide in Organic Solvent at High Temperatures: A New Synthetic Method for Nanosized, Thermally Stable Titanium (IV) Oxide. Ind. Eng. Chem. Res. 38 (1999): 3925-3931.

- Kominami, H.; Onoue, S.-I.; Matsuo, K.; Kera, Y. Synthesis of Microcrystalline Hematite and Magnetite in Organic Solvents and Effect of a small Amount of Water in Solvents. J. Am. Ceram. Soc. 82 (1999): 1937 – 1940.
- Kominami, H.; Inoue, H.; Konishi, S.; Kera, Y. Synthesis of Perovskite-Type Lanthanum Iron Oxide by Glycothermal Reaction of A Lanthanum-Iron Precursor. J. Am. Ceram. Soc. 85, 9 (2002): 2148 – 2150.
- Kondo, M.; Shiozaki, K.; Ooki, R.; Mizutani, N. Crystallization Behavior and Microstructure of Hydrothermally Treated Monodispersed Titanium Dioxide Particles. J. Ceram. Soc. Jpn. 102 (1994): 742.
- Kongwudthiti, S.; Praserttham, P.; Inoue, M.; Tanakulrungsank, W. Synthesis of Large-Surface Area Silica-Modified Zirconia by the Glycothermal Method. J. Mater. Sci. Lett. 21 (2002): 1461 – 1464.
- Kurosaki, A.; Okazaki, S. The Effect of the Addition of Sulfate Ions on the Acidity of TiO₂. Nippon Kagaku Kaishi (1976): 1816.
- Kutty, T. R. N.; Viekanandan, R.; Murugaraj, P. Precipitation of Rutile and Anatase (TiO₂) Fine Powders and their Conversion to MtiO₃ (M= BA, SA, Ca) by the Hydrothermal Method. Mater. Chem. Phys. 19 (1988): 533 – 546.
- Larson, S. A. and Falconer, J. L. Characterization of TiO₂ Photocatalysts Used in Trichloroethene Oxidation. Appl. Catal. B: Env. 4 (1994): 325 – 342.
- Luck, F. A Reviewer of Support Effect on the Activity and Selectivity of Hydrotreating Catalysts. Bull. Soc. Chim. Belg. 100 (1991): 781.
- Mahipal Reddy, B.; Mehdi, S.; Padmanabha Reddy. Dispersion and Thermal Stability of Vanadium Oxide Catalysts Supported on Titania-Silica mixed Oxide. Catal. Lett. 20 (1993): 317 – 327.
- Mariscal, R.; López-Granados, M.; Fierro, J. L. G.; Sotelo, J. L.; Martos, C.; Van Grieken, R. Morphology and Surface Properties of Titania-Silica Hydrophobic Xerogels. Langmuir 16 (2000): 9460 – 9467.
- Martucci, A.; Innocenzi, P.; Traversa, E. Crystallization of Al₂O₃-TiO₂ Sol-Gel Systems. J. Ceram. Soc. Japan. 107, 10 (1999): 891 – 894.
- Matsuda, S.; Kato, A. Titanium Oxide Based Catalysts-a Review. Appl. Catal. 8 (1983): 149.
- McGraw-Hill encyclopedia of science & technology, New York, McGraw-Hill Book, 5 th ed., 1982: 435.

- Montoya, I. A.; Viveros, T.; Domínguez, J.M.; Canales, L.A.; Schifer, I. On the Effect of the Sol-Gel Synthesis Parameters on Textural and Structural Characteristics of TiO₂. Catal. Lett. 15 (1992): 207 – 217.
- Moon, Y. T.; Park, H. K.; Kim, D. K.; Kim, C. H.; Seog, I-S. Precipitation of Monodisperse and Spherical Zirconia Powders by Heating of Alcohol-Aqueous Salt Solution. J. Am. Ceram. Soc. 78, 10 (1995):2690 –2694.
- Musić, S.; Gotić, M.; Ivanda, M.; Popović, S.; Turković, A.; Trojko, R.; Sekulić, A.; Furić, K. Chemical and Microstructural Properties of TiO₂ Synthesized by Sol-Gel Procedure. Mater. Sci. Eng. B 47 (1997): 33 – 40.
- Ogihara, T.; Nakajima, H.; Yanagawa, T.; Ogata, N.; Yoshida, K.; Matsushita, N. Preparation of Monodisperse, Spherical Alumina Powders from Alkoxides. J. Ceram. Soc. 74, 9 (1991): 2263 – 2269.
- Park, H.K.; Kim, D.K.; Kim, C.H. Effect of Solvent on Titania Particle Formation and Morphology in Thermal Hydrolysis of TiCl₄. J. Am. Ceram. Soc. 80, 3 (1997): 743 – 749.
- Popielaski, S. Photocatalysis on Nano-Sized Semiconductors. Rensselaer[Online]. 1998. Available from: [http://www.rpi.edu/locker/25/001225/public_html/New%20Folder/popielarski/\[2002](http://www.rpi.edu/locker/25/001225/public_html/New%20Folder/popielarski/[2002), October 28]
- Readey, M. J.; Lee, R.; Holloran, J. W.; Heuer, A. H. Processing and Sintering of Ultrafine MgO-ZrO₂ and (MgO,Y₂O₃)ZrO₂ Powder. J. Am. Ceram. Soc. 73, 6 (1990): 1499 - 1503.
- Reddy, B. M.; Chowdhury, A.; Reddy, E. P.; Fernández, A. X-Ray Photoelectron Spectroscopy Study of V₂O₅ Dispersion on a Nanosized Al₂O₃-TiO₂ Oxide. Langmuir 17 (2001): 1132 – 1137.
- Sibu, C. P.; Rajesh Kumar, S.; Mukundan, P.; Warriar, K. G. K. Structural Modification and Associated Properties of Lanthanum Oxide Doped Sol-Gel Nanosized Titanium Oxide. Chem. Mater. 14 (2002): 2876 – 2881.
- Sornnarong Theinkeaw. Synthesis of Large-Surface Area Silica Modified Titanium (IV) Oxide Ultra Fine Particles. Master's thesis, Department of Chemical Engineering, Graduated School, Chulalongkorn University, 2000.
- Tadafumi, A.; Kutsuhito, K.; Kunio, A. Rapid and Continuous Hydrothermal Crystallization of Metal Oxide Particles in Supercritical Water. J. Am. Ceram. Soc. 75 (1992): 1019 –1022.

- Takeuchi, M.; Yamashita, H.; Matsuoka, M.; Anpo, M.; Hirao, T.; Itoh, N.; Iwamoto, N. Photocatalytic Decomposition of NO under Visible Light Irradiation on the Cr-Ion-Implanted TiO₂ Thin Film Photocatalyst. Catal. Lett. 67 (2000): 135 – 137.
- West, A. R. Basic solid state chemistry and its application. 1 st ed., Great Britain, John Wiley & Sons, 1997.
- Yanagisawa, K.; Ioku, K.; Yamasaki, N. Formation of Anatase Porous by Hydrothermal Hot-Pressing of Amorphous Titania Spheres. J. Am. Ceram. Soc. 8, 5 (1997): 1303 – 1306.
- Yoshinaka, M.; Hirota, K.; Yamaguchi, O. Formation and Sintering of TiO₂ (Anatase) Solid Solution in the System TiO₂-SiO₂. J. Am. Ceram. Soc. 80, 10 (1997): 2749 – 2753.
- Yin, S.; Inoue, Y.; Uchida, S.; Fujisiro, Y.; Sato, T. Crystallization of titania in liquid media and photochemical properties of crystallized titania. J. Mater. Res. 13, 4 (1998): 844 -847.
- Yang, J.; Mei, S.; Ferreira, M. F. Hydrothermal Synthesis of Nanosized Titania Powders: Influence of Tetraalkyl Ammonium Hydroxides on particle Characteristic. J. Am. Ceram. Soc. 84, 8 (2001): 1696 – 1702.
- Yogarasimhan, S. R. and Rao, C. N. Mechanism of Crystal Structure Transformations. Trans. Faraday Soc. 58 (1962): 1579 – 1589.
- Zaharescu, M.; Crisan, M.; Simionescu, L.; Crisan, D.; Gartner, M. TiO₂-Based Porous Materials obtained from Gels, in Different Experimental Conditions. J. Sol-Gel Sci. 8, 1-3 (1997): 249 – 253.
- Zhang, H.; Finnegan, M.; Banfield, J. F. Preparing Single-Phase Nanocrystalline Anatase from Amorphous Titania with Particle Size Tailed by Temperature. Nano. Lett. 1, 2 (2001): 81 – 85.
- Zzanderna, A. W.; Rao, C. N. R.; Honig, J. M. The Anatase-Rutile Transition. Trans. Faraday Soc. 58 (1958): 1069 – 1073.



APPENDICES

สถาบันวิทยบริการ
จุฬาลงกรณ์มหาวิทยาลัย

APPENDX A

CALCULATION OF CATALYST PREPARATION

Calculation of the second element modified titanias.

In this study, the second element modified titanias were prepared in each organic solvents have different M/Ti molar ratio, M represented as Si, Al and P, M/Ti = 0, 0.005, 0.04, 0.06, 0.08.

1. Titanium (IV) tert-butoxide (TNB, $\text{Ti}[\text{O}(\text{CH}_2)_3\text{CH}_3]_4$) 97% has M.W. of 340.36 g.
2. Tetraethyl orthosilicate (TEOS, $\text{Si}(\text{OC}_2\text{H}_5)_4$) 98% has M.W. of 208.33 g.
3. Aluminium isopropoxide (AIP, $[(\text{CH}_3)_2\text{CHO}]_3\text{Al}$) 98+% has M.W. of 204.25 g
4. Triethyl phosphate (TEPP, $\text{C}_6\text{H}_{15}\text{O}_4\text{P}$) >99% has M.W. of 182.16 g

Example: Calculation of preparation of titania with Si/Ti = 0.04 is shown as follow:

TNB 97% 15 g were used for preparation of all M/Ti molar ratio

TNB 15 g equal pure TNB: 14.55g or 0.04275 mol

TNB 1 mol has Ti 1 mol, so that, Ti has 0.04275 mol

Si/Ti = 0.04;

Si = $0.04 \times 0.04275 = 1.70995 \times 10^{-3}$ mol

Or, Silicon equal 1.70995×10^{-3} mol

TEOS 1 mol has Si 1 mol;

TEOS equal 1.70995×10^{-3} mol or 0.3563 g

For TEOS 98%;

TEOS was used 0.3635 g

APPENDIX B

CALCULATION OF THE CRYSTALLITE SIZE

Calculation of the crystallite size by Debye-Scherrer equation

The crystallite size was calculated from the half-height width of the diffraction peak of XRD pattern using the Debye-Scherrer equation.

From Scherrer equation:

$$D = \frac{K\lambda}{\beta \cos \theta} \quad (\text{B.1})$$

- where
- D = Crystallite size, Å
 - K = Crystallite-shape factor = 0.9
 - λ = X-ray wavelength, 1.5418 Å for CuK α
 - θ = Observed peak angle, degree
 - β = X-ray diffraction broadening, radian

The X-ray diffraction broadening (β) is the pure width of a powder diffraction free of all broadening due to the experimental equipment. Standard α -alumina is used to observe the instrumental broadening since its crystallite size is larger than 2000 Å. The X-ray diffraction broadening (β) can be obtained by using Warren's formula.

From Warren's formula:

$$\beta^2 = B_M^2 - B_S^2 \quad (\text{B.2})$$

$$\beta = \sqrt{B_M^2 - B_S^2}$$

- Where
- B_M = The measured peak width in radians at half peak height.
 - B_S = The corresponding width of a standard material.

Example: Calculation of the crystallite size of titania

$$\begin{aligned} \text{The half-height width of 101 diffraction peak} &= 0.93125^\circ \\ &= 0.01625 \text{ radian} \end{aligned}$$

$$\text{The corresponding half-height width of peak of } \alpha\text{-alumina} = 0.004 \text{ radian}$$

$$\begin{aligned} \text{The pure width} &= \sqrt{B_M^2 - B_S^2} \\ &= \sqrt{0.01625^2 - 0.004^2} \\ &= 0.01577 \text{ radian} \end{aligned}$$

$$B = 0.01577 \text{ radian}$$

$$2\theta = 25.56^\circ$$

$$\theta = 12.78^\circ$$

$$\lambda = 1.5418 \text{ \AA}$$

$$\begin{aligned} \text{The crystallite size} &= \frac{0.9 \times 1.5418}{0.01577 \cos 12.78} = 90.15 \text{ \AA} \\ &= 9 \text{ nm} \end{aligned}$$

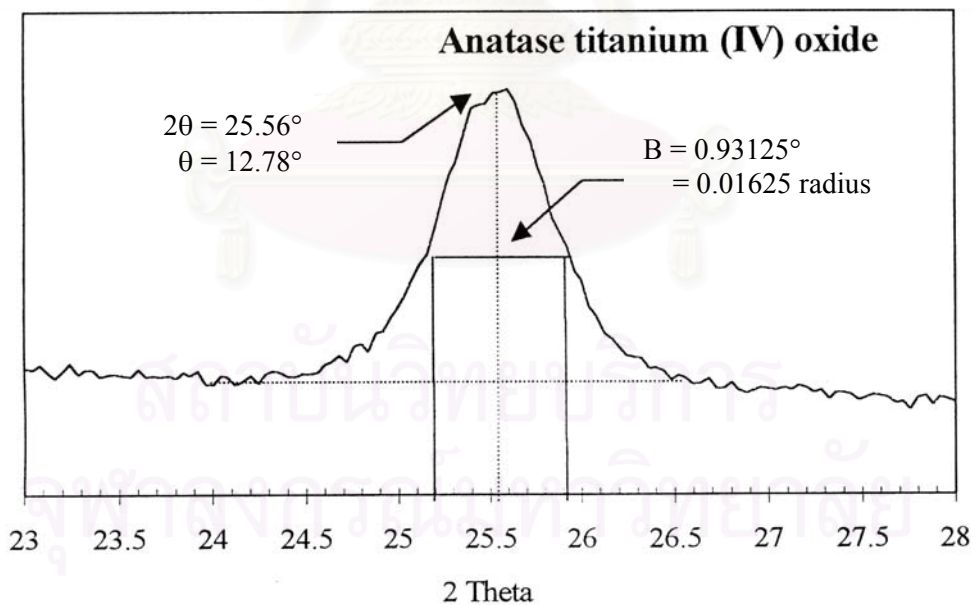


Figure B.1 The 101 diffraction peak of titania for calculation of the crystallite size

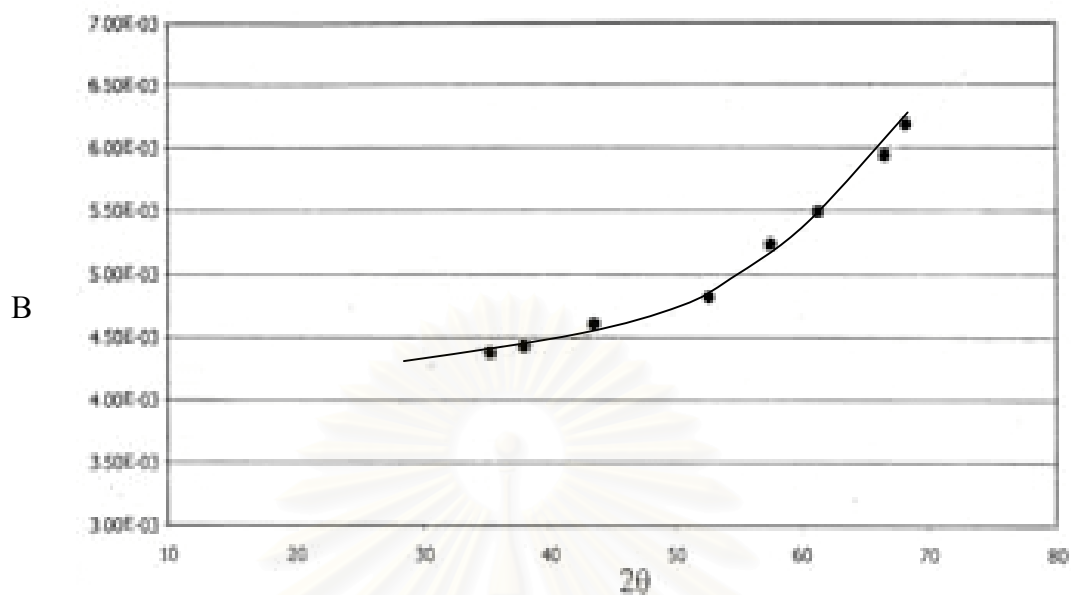


Figure B.2 The plot indicating the value of line broadening due to the equipment. The data were obtained by using α -alumina as standard

สถาบันวิทยบริการ
จุฬาลงกรณ์มหาวิทยาลัย

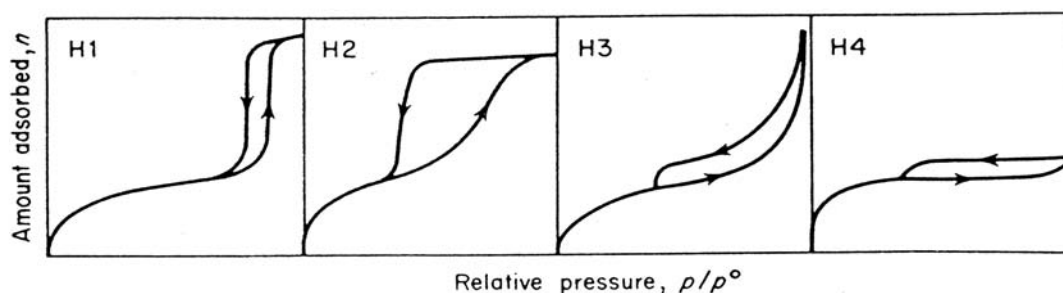
APPENDIX C

ISOTHERM PLOT OF NITROGEN

A manual entitled “Reporting Physisorption Data for Gas/Solid Systems with Special Reference to the Determination of Surface Area and Porosity” has been prepared as a “provisional” publication by Commission I.6 of the International Union of Pure and Applied Chemistry (IUPAC). The purpose of the manual is to draw attention to problems involved in reporting physisorption data and to provide guidance on the evaluation and interpretation of isotherm data.

A new classification of hysteresis loops, as recommended in the IUPAC manual, consist of the four types shown in the Figure below. To avoid confusion with original de Boer classification, the characteristic types are now designated H1, H2, H3 and H4; but it is evident that the first three types correspond to type A, E and B, respectively, in the original classification. It will be noted that H1 and H4 represent extreme types: in the former the adsorption and desorption branches are almost vertical and nearly parallel over an appreciable range of gas uptake, whereas in the latter they are nearly horizontal and parallel over a wide range of relative pressure. Type H2 and H3 may be regarded as intermediate between the two extremes.

As pointed out earlier, certain shapes of hysteresis loops are associated with specific pore structure. Thus, type H1 loops are often obtained with agglomerates or compacts of spheroidal particles of fairly uniform size and array. Some corpuscular systems (e.g. certain silica gels) tend to give H2 loops, but in these cases the distribution of pore size and shape is not well defined. Type H3 and H4 have been obtained with adsorbents having slit-shape pores or plate-like particles (in the case of H3). The type isotherm character associated with H4 is, of course, indicative of microporosity. (Gregg and Sing, 1982)



VITA

Mr. Wachiraphan Payakgul was born on April 15, 1978 in Payao Province, Thailand. He received the Bachelor Degree of Chemical Engineering from Faculty of Engineering, Chulalongkorn University in 2000. He continued his Master's study at Chulalongkorn University in June, 2000.



สถาบันวิทยบริการ
จุฬาลงกรณ์มหาวิทยาลัย